

# **USING SUPERCRITICAL CARBON DIOXIDE AS A TOOL FOR PRESERVING CULTURALLY SIGNIFICANT ITEMS**

**GEORGINA HAMMOND**

A Thesis Submitted to The University of Birmingham for a Degree of  
Doctor of Philosophy

**Department of Chemical Engineering  
University of Birmingham  
May 2017**

UNIVERSITY OF  
BIRMINGHAM

**University of Birmingham Research Archive**

**e-theses repository**

This unpublished thesis/dissertation is copyright of the author and/or third parties. The intellectual property rights of the author or third parties in respect of this work are as defined by The Copyright Designs and Patents Act 1988 or as modified by any successor legislation.

Any use made of information contained in this thesis/dissertation must be in accordance with that legislation and must be properly acknowledged. Further distribution or reproduction in any format is prohibited without the permission of the copyright holder.

## SUMMARY

Conservators treat and repair a huge array of damaged and degrading materials on a regular basis. As such, there are many techniques and protocols in place to deal with these problems successfully, be that via preventative or interventive methods. However, there is need for new and innovative techniques that offer long term stabilisation to materials and objects that are prevalent within museum collections. As an alternative to some of these conservation techniques, hydration with supercritical carbon dioxide was investigated here.

Both modern and historic, hardwood and softwood samples were successfully hydrated using this technique. The addition of a co-solvent (methanol) to the supercritical fluid solvent stream was used as a method to increase the solubility of water in carbon dioxide, and therefore improve levels of hydration. To evaluate the extent of any damage being caused during the supercritical fluid treatment, microstructural and macrostructural analytical techniques were carried out. The supercritical hydration technique allowed historic wood to be hydrated and stabilised. Strength properties were seen to be maintained or improved after the supercritical treatment, providing conservators with a viable method of hydration.

A feasibility study looking at the cleaning and characterisation of historic leather samples was investigated using spectroscopic methods. The sensitivity of Diffuse Reflectance Infrared Fourier Transform spectroscopy on historic leather was explored. Additionally, changes in elemental composition on the surface of the leather were monitored using Scanning Electron Microscopy Energy Dispersive spectroscopy. Cleaning historic leather via a supercritical carbon dioxide solvent stream showed the greatest potential for future work. However, the characterisation of unattributed historic leather is a vast and complex task that would require the expertise of a leather conservator, if the investigation were to be continued.

## PUBLICATIONS

### Conference presentation

Hammond, G. (2016) **“Using supercritical carbon dioxide to hydrate oven dried samples of modern and historic wood with and without the use of a co-solvent”**. Presented at 2<sup>nd</sup> International Conference on Science and Engineering in Arts, Heritage and Archaeology, Oxford.

Hammond, G. (2016) **“Using supercritical carbon dioxide to hydrate oven dried samples of modern and historic wood with and without the use of a co-solvent”**. Presented at MS&T16, Salt Lake City, USA.

Hammond, G. (2016) **“Supercritical Fluids in Conservation”**. Presented at the Getty Research Institute, Los Angeles, USA

### Journal Article

Hammond, G., Cox, P. (2017) **“Using supercritical carbon dioxide, with and without a co-solvent, to hydrate modern and historic wood samples”** Heritage Science, Springer Journal [Accepted March 2017]

## ACKNOWLEDGEMENTS

This thesis has been made possible through the financial support of my company sponsor PJH Partnership Ltd, and the University of Birmingham. I am hugely grateful to them both for their support and trust over the last three years of study.

I would like to thank my supervisors Professor Mark Simmons and Professor Phil Cox for their continued guidance and invaluable knowledge throughout my studies. I am also extremely grateful to Dr Regina Santos who supported my work from the beginning. I would like to make a special mention of Chiralabs Limited, Oxford whose expertise and analytical work has been crucial to the development of this thesis, thank you.

I wish to acknowledge The Ashmolean Museum, Oxford, The Pitt Rivers Museum, Oxford, Birmingham City Art Galleries, Birmingham and The Leather Conservation Centre, Northampton whose conservation departments have given me expert advice over the course of my studies.

Finally, I extend my thanks to my family and friends for their continued support, motivation, encouragement and understanding throughout my studies. I would specifically like to thank Peter, Philippa and Alexander for keeping me sane and Ed for his expert advice and motivation.

# CONTENTS

	<b>Page</b>
Summary.....	I
Acknowledgements.....	II
Contents.....	III
List of figures.....	VIII
List of tables.....	XIV
Abbreviations.....	XVI
 <b>1.0 Literature Review.....</b>	 <b>1</b>
Abstract.....	1
1.1 Introduction to supercritical fluids.....	2
1.1.1 Properties of supercritical fluids.....	3
1.1.2 Supercritical carbon dioxide.....	4
1.1.3 Solvent properties of supercritical carbon dioxide.....	4
1.1.4 Physio-chemical properties of carbon dioxide and methanol systems.....	6
1.1.4.1 Physical properties of carbon dioxide and methanol systems.....	6
1.1.4.2 Critical temperature of pressure in a carbon dioxide and methanol system.....	7
1.2 Uses and applications of supercritical fluids.....	8
1.2.1 Supercritical fluid extraction.....	8
1.2.1.1 SFE and solubility.....	9
1.2.2 Supercritical cleaning with carbon dioxide.....	10
1.2.2.1 Problems with polymeric materials.....	11
1.2.3 Sterilisation with supercritical carbon dioxide.....	11
1.2.4 Impregnation.....	12
1.2.4.1 Classical vs. supercritical fluid impregnation.....	12
1.3. Introduction to art conservation.....	13
1.3.1 Conservation practices and problems.....	14
1.3.1.1 Environmental controls (preventative conservation).....	15
1.3.1.2 Deacidification.....	16
1.3.1.2.1 The Wei T'o Method.....	17

1.3.1.2.2 The Bookkeeper Method.....	18
1.3.1.3 Cleaning and pesticides in museum collections.....	18
1.3.2 Conservation of wood.....	19
1.3.2.1 Waterlogged wood.....	20
1.3.2.2 Dry wood.....	20
1.3.3 Conservation of leather.....	21
1.4 Applications of supercritical carbon dioxide in art conservation.....	21
1.4.1 Cleaning with supercritical carbon dioxide.....	22
1.4.1.1 SFE for the removal of pesticides.....	23
1.4.2 Neutralising and strengthening with supercritical carbon dioxide.....	24
1.5 Material Characterisation: wood.....	26
1.5.1 Cellulose, hemicellulose and lignin.....	26
1.5.2 Hardwood and softwood structures.....	27
1.5.2.1 Softwood.....	28
1.5.2.2 Hardwood.....	28
1.5.2.3 Pits.....	29
1.5.3 Wood strength and stiffness.....	30
1.5.4 Moisture content in wood.....	31
1.5.4.1 Effect of water on the mechanical behaviour of wood.....	33
1.5.5 Transportation processes in wood.....	34
1.5.5.1 Bulk Flow.....	34
1.5.5.2 Diffusion.....	36
1.6 Additional material characterisation: leather.....	37
1.6.1 Vegetable tanning.....	38
1.6.2 Mineral tanning.....	38
1.6.2.1 Alum tanning.....	38
1.6.2.2 Chrome tanning.....	39
1.7 Analytical techniques for wood and leather .....	39
1.7.1 Macrostructural analysis: Three-point bend test .....	39
1.7.2 Microstructure analysis: Microscopy.....	40
1.7.3 Spectroscopic analytical techniques.....	41

1.8 Aims of this work.....	43
<b>2.0 Hydrating wood using supercritical carbon dioxide.....</b>	<b>44</b>
Abstract.....	44
2.1 Introduction.....	45
2.1.1 Solvent streams and the use of methanol as a co-solvent.....	46
2.2 Materials.....	46
2.2.1 Rig components.....	46
2.2.2 Wood preparation and storage .....	46
2.2.2.1 Desiccant based versus nitrogen purged storage solutions for treated wood samples.....	47
2.2.3 Carbon dioxide and methanol.....	47
2.3 Apparatus and methodology.....	48
2.3.1 High pressure equipment and supercritical hydration method.....	48
2.3.1.1 Depressurisation study.....	49
2.3.2 Initial sample characterisation and the preparation of wood samples.....	51
2.3.3 Method for supercritical hydration of oven-dried wood samples using supercritical carbon dioxide.....	54
2.3.3.1 Addition of a separate hydration vessel and sample vessel.....	54
2.3.3.2 Addition of methanol as a co-solvent.....	55
2.3.4 Method for weighing hydrated wood samples.....	56
2.3.5 Methods for the analysis of microstructural studies.....	57
2.3.5.1 Scanning electron microscopy.....	57
2.3.5.2 Light microscopy.....	58
2.3.6 Feasibility studies of wood samples by spectroscopy.....	58
2.3.6.1 ATR-FTIR.....	59
2.3.6.2 DRIFT.....	60
2.3.6.3 FT-NIR Raman.....	60
2.3.7 Three-point bend test for the determination of wood strength.....	60
2.3.8 Statistical analysis techniques.....	64
2.3.9 Sources of error.....	64
2.4 Hydration results and Discussion.....	66

2.4.1 Hydration profiles for wood samples treated with $\text{scCO}_2(\text{PURE})$ and $\text{scCO}_2(\text{MeOH})$ , in the presence of water.....	66
2.4.1.1 Hypotheses.....	66
2.4.1.2 Hydration profile for wood treated with $\text{scCO}_2(\text{PURE})$ in the presence of water...67	
2.4.1.3 Hydration profile for wood treated with $\text{scCO}_2(\text{MeOH})$ in the presence of water...69	
2.4.1.4 Connectivity in wood.....	73
2.4.1.4.1 Epoxy resin for 2-D impregnation.....	77
2.4.1.5 Cellulose, hemicellulose and lignin content.....	78
<b>3.0 Microstructural and macrostructural results and discussion.....</b>	<b>82</b>
3.1 Introduction.....	82
3.2 Microstructural analysis.....	83
3.2.1 Scanning electron microscopy (SEM).....	83
3.2.2 Light microscopy.....	86
3.2.3 Preliminary spectroscopy studies.....	92
3.2.3.1 ATR-FTIR.....	93
3.2.3.2 DRIFT.....	95
3.2.3.3 FT-NIR Raman spectroscopy.....	98
3.2.3.4 DRIFT spectroscopy study.....	99
3.3. Macrostructural analysis.....	107
3.3.1 Macrostructural hypothesis.....	107
3.3.2 Three-point bend test.....	107
3.3.2.1 Bending strength of the wood samples pre- and post $\text{scCO}_2$ treatment.....	113
<b>4.0 A feasibility study for the cleaning and consolidation of historic leather samples with supercritical carbon dioxide.....</b>	<b>122</b>
Abstract.....	122
4.1 Introduction.....	123
4.2 Materials and methods.....	125
4.2.1 Materials .....	125
4.2.2 Leather preparation and characterisation.....	125
4.2.3 Supercritical carbon dioxide treatment.....	126
4.2.4 DRIFT spectroscopy.....	127



4.2.5 SEM-EDS for elemental composition.....	130
4.3 Results and discussion.....	132
4.3.1 Supercritical carbon dioxide treatment.....	132
4.3.2 DRIFT spectroscopy.....	133
4.3.3 SEM-EDS.....	139
4.3.3.1 SEM images.....	139
4.3.3.2 Elemental analysis.....	142
<b>5.0 Overall conclusions and suggestions for future work.....</b>	<b>144</b>
5.1 Overall conclusions.....	144
5.2 Suggestions for future work.....	148
<b>6.0 References.....</b>	<b>151</b>

## LIST OF FIGURES

Figure 1.1. Generic temperature-pressure phase diagram for a pure substance made by author.....	2
Figure 1.2 Illustration of the formation of a homogenous phase.....	3
Figure 1.3. Optimized geometry of CO <sub>2</sub> /EtOH complex.....	5
Figure 1.4. Vapour-liquid equilibria for the CO <sub>2</sub> and MeOH system at 40°C.....	6
Figure 1.5. A graph to show the relationship between calculates values for critical temperature and pressure and the MeOH mole fraction.....	8
Figure 1.6 A basic schematic illustration of a typical scCO <sub>2</sub> extraction rig.....	9
Figure 1.7. Cellulose linear chains of D-glucose linked by β-1,4-glycosidic bonds.....	26
Figure 1.8. The lignin precursors and the most abundant binders in lignin.....	27
Figure 1.9. Diagram showing the three main axes in wood; longitudinal, tangential and radial.....	28
Figure 1.10 Illustration to compare the cellular arrangement in hardwoods and softwoods...	29
Figure 1.11. Diagram showing the common types of pit pair.....	30
Figure 1.12. A graph to represent the relationship between density and Young's Modulus for different wood types with and across the grain.....	31
Figure 1.13. The presence of free and bound water and the respective MC values in the three stages of seasoned to unseasoned timber.....	32
Figure 1.14. The structure and intra - (1) and interchain (2) hydrogen bonding pattern in cellulose.....	33
Figure 1.15. A diagram to show the three main layers of skin: epidermis, dermis and fatty tissue or flesh.....	37
Figure 2.1. A schematic illustration of the supercritical hydration rig as constructed by the author.....	48

Figure 2.2. Diagram to show expected diffusion into wood samples. Shaded areas represent coats of epoxy resin. Arrows represent the expected 2-D diffusion pathway of scCO <sub>2</sub> and water.....	54
Figure 2.3 A diagram showing two different pressure vessel layouts in the oven of the experimental rig.....	55
Figure 2.4. A photograph to show the wood samples mounted on the aluminium stubs using colloidal carbon cement.....	58
Figure 2.5. Illustration to show layout for a three-point bend test, where P is force and L is the distance between the two supports.....	61
Figure 2.6 An example force displacement graph for Maple ( <i>H</i> ).....	62
Figure 2.7 An example force displacement graph for White Oak ( <i>H</i> ) .....	62
Figure 2.8. A mass loss profile for wood samples weighed over 8,064 hours, a Log T (time) scale has been used here to better see the individual data points The wood samples have been treated with scCO <sub>2</sub> (PURE) in the presence of water for 45 minutes.....	67
Figure 2.9. The NMC of wood samples taken at 0 hours, 168 hours, and 504 hours. The wood samples have been treated with scCO <sub>2</sub> (PURE) in the presence of water .....	68
Figure 2.10. NMC of wood samples taken at 0 hours, 168 hours, and 504 hours. The wood samples have been treated with scCO <sub>2</sub> (MeOH) in the presence of water, MeOH has a concentration of 2.5 mol%.....	70
Figure 2.11. NMC of wood samples taken at 0 hours, 168 hours and 504 hours. The wood samples have been treated with scCO <sub>2</sub> (MeOH) in the presence of water, MeOH has a concentration of 5.0 mol%.....	71
Figure 2.12. A comparison of the wood samples mean NMC at 504 hours after different treatment conditions.....	73

Figure 2.13. A comparison of hardwood (angiosperm) and softwood (gymnosperm) pit structure.....	76
Figure 2.14 D-glucose units in a cellulose linear polymer. Circled are the three hydroxyl groups on one D-glucose unit that are free for water sorption in the amorphous region.....	79
Figure 2.15 An illustrative model of the microscopic structure of wood indicating the cellulose, hemicellulose and lignin hierarchy.....	80
Figure 3.1 A SEM image at a magnification of 200x, indicating the damage caused to Maple ( <i>M</i> ) caused by manually splitting the wood samples in preparation for SEM analysis.....	84
Figure 3.2 An annotated SEM image at a magnification of 200 x and a resolution of 20 $\mu\text{m}$ to show the key features of a hardwood structure; vessels, pits and fibres. The White Oak ( <i>M</i> ) sample has been treated with $\text{scCO}_2(\text{PURE})$ .....	85
Figure 3.3 A SEM image at a magnification of 50 x and resolution 100 $\mu\text{m}$ , White Oak ( <i>M</i> ) treated with $\text{scCO}_2(\text{PURE})$ .....	85
Figure 3.4 A SEM image at a magnification of 50 x and resolution 100 $\mu\text{m}$ , of Maple ( <i>M</i> ) treated with $\text{scCO}_2(\text{PURE})$ .....	86
Figure 3.5. Six light microscopy images at a 40 x magnification of a White Oak ( <i>H</i> ) sample...	87
Figure 3.6. Six light microscopy images at a 40 x magnification of a Maple ( <i>H</i> ) sample.....	88
Figure 3.7. Six light microscopy images at a 40 x magnification of a Scots Pine ( <i>H</i> ) sample...	89
Figure 3.8. Six light microscopy images at a 40 x magnification of a Maple ( <i>M</i> ) sample.....	90
Figure 3.9. Six light microscopy images at a 40 x magnification of a Zebrano ( <i>M</i> ) sample.....	91
Figure 3.10. An annotated ATR-FTIR spectra of the untreated Scots Pine ( <i>H</i> ) and treated Scots Pine ( <i>H</i> ) samples.....	94
Figure 3.11. An ATR-FTIR spectra of the untreated Maple ( <i>M</i> ) and the treated Maple ( <i>M</i> ) samples.....	95

Figure 3.12. A DRIFT spectra of the untreated Scots Pine ( <i>H</i> ) and treated Scots Pine ( <i>H</i> ) (magenta spectrum) samples.....	97
Figure 3.13. A DRIFT spectra of untreated Maple ( <i>M</i> ) (blue spectra) and treated Maple ( <i>M</i> ) (magenta spectra) samples.....	97
Figure 3.14. A Raman spectra to show the untreated Scots Pine ( <i>H</i> ) and treated Scots Pine ( <i>H</i> ) samples.....	98
Figure 3.15. A Raman spectra of the untreated Maple ( <i>M</i> ) and treated Maple ( <i>M</i> ) samples...	99
Figure 3.16. DRIFT spectra of the different treated Maple ( <i>M</i> ) samples.....	102
Figure 3.17. DRIFT spectra of the different treated White Oak ( <i>M</i> ) samples.....	102
Figure 3.18. DRIFT spectra of the different treated Zebrano ( <i>M</i> ) samples.....	103
Figure 3.19. DRIFT spectra of the different treated Red Oak ( <i>M</i> ) samples.....	103
Figure 3.20. OH/CH peak areas (around 3460 & 2930cm <sup>-1</sup> respectively) in DRIFT spectra obtained for Maple, White Oak, Zebrano and Red Oak having undergone five different treatments.....	106
Figure 3.21. OH/CH peak areas (around 3460 & 2930cm <sup>-1</sup> respectively) in DRIFT spectra obtained for Maple (blue), White Oak (red), Zebrano (green) and Red Oak (magenta) having undergone the five different treatments.....	107
Figure 3.22. OH/"Cellulose" peak areas (around 3460 & 4020cm <sup>-1</sup> respectively) in DRIFT spectra obtained for Maple (blue), White Oak (red), Zebrano (green) and Red Oak (magenta) having undergone the five different treatments.....	108
Figure 3.23. OH/"Cellulose" peak areas (around 3460 & 4020cm <sup>-1</sup> respectively) in DRIFT spectra obtained for Maple, White Oak, Zebrano and Red Oak having undergone the five different treatments.....	109
Figure 3.24. A comparison of the mean strength values for Maple ( <i>M</i> ) pre and post treatment with scCO <sub>2</sub> (PURE) or scCO <sub>2</sub> (MeOH).....	116
Figure 3.25. A comparison of the mean strength values for White Oak ( <i>M</i> ) samples pre and post treatment with scCO <sub>2</sub> (PURE) or scCO <sub>2</sub> (MeOH).....	116

Figure 3.26. A comparison of the mean strength values for Red Oak ( <i>M</i> ) pre and post treatment with scCO <sub>2</sub> (PURE) or scCO <sub>2</sub> (MeOH).....	117
Figure 3.27. A comparison of the mean strength values for Zebrano ( <i>M</i> ) pre and post treatment with scCO <sub>2</sub> (PURE) or scCO <sub>2</sub> (MeOH).....	177
Figure 3.28. A comparison of the mean strength values for Maple ( <i>H</i> ) samples pre and post treatment with scCO <sub>2</sub> (PURE) or scCO <sub>2</sub> (MeOH).....	118
Figure 3.29. A comparison of the mean strength values for White Oak ( <i>H</i> ) pre and post treatment with scCO <sub>2</sub> (PURE) or scCO <sub>2</sub> (MeOH).....	118
Figure 3.30. A comparison of the mean strength values for Scots Pine ( <i>H</i> ) pre and post treatment with scCO <sub>2</sub> (PURE) or scCO <sub>2</sub> (MeOH).....	119
Figure 3.31. A comparison of the mean strength values for Keruing ( <i>H</i> ) pre and post treatment with scCO <sub>2</sub> (PURE) or scCO <sub>2</sub> (MeOH).....	119
Figure 4.1. A schematic illustration of the supercritical hydration rig as constructed by the author.....	127
Figure 4.2. Two photographs showing the front (coated) and back of the untreated leather sample 1A.....	128
Figure 4.3. Two photographs showing the front (coated) and back of the treated leather sample 1B.....	128
Figure 4.4. Two photographs showing the front (coated) and back of the untreated leather sample 2A.....	129
Figure 4.5. Two photographs showing the front (coated) and back of the treated leather sample 2B.....	129
Figure 4.6. Two photographs showing the front (coated) and back of the untreated leather sample 3A.....	129
Figure 4.7. Two photographs showing the front (coated) and back of the treated leather samples 3B.....	130
Figure 4.8. A photograph of the leather book spine treated with scCO <sub>2</sub> (PURE).....	131

Figure 4.9. DRIFT spectra for the untreated leather sample A: coated side (magenta), matt side (red).....	134
Figure 4.10. DRIFT spectra for the treated leather sample B: coated side (magenta), matt side (red).....	134
Figure 4.11. DRIFT spectra for the treated leather sample C: coated side (magenta), matt side (red).....	135
Figure 4.12. DRIFT spectra for the treated leather sample D: coated side (magenta), matt side (red).....	135
Figure 4.13. DRIFT spectra for the treated leather sample E: coated side (magenta), matt side (red).....	137
Figure 4.14. DRIFT spectra for the treated leather sample F: coated side (magenta), matt side (red).....	138
Figure 4.15. DRIFT spectra of the matt brown sides of different untreated leathers and treated leathers.....	139
Figure 4.16. SEM images of the book spine pre-and post-treatment for three different areas of the spine: damaged tan leather, dark leather, gold embossing.....	141

## LIST OF TABLES

Table 1.1 Typical physiochemical property values of gases, liquids and supercritical fluids...	3
Table 1.2 A table to show the effect on critical temperature and critical pressure with varying MeOH mole fraction in a CO <sub>2</sub> and MeOH system.....	7
Table 1.3. A table to show the key properties associated with both classical and SCF impregnation methods.....	13
Table 1.4 Summary of the professional standards and professional judgement and ethics recommended by Professional Accreditation of Conservators-Restorers and the Institute of Conservation.....	14
Table 1.5 Moisture content values for wood in different conditions.....	32
Table 2.1 The critical temperatures and pressures of a scCO <sub>2</sub> and MeOH system.....	46
Table 2.2. A table to show the observations recorded and the concerns regarding depressurising the scCO <sub>2</sub> system over three time periods.....	50
Table 2.3. Characterisation of individual wood species used in the experimental procedure described in this chapter.....	52
Table 2.4. A table to show the average initial moisture content in historic and modern wood samples before prior to SCF treatment.....	53
Table 2.5. Values used to calculate the dilution factor for 2.5 mol% MeOH in H <sub>2</sub> O.....	56
Table 2.6. A table listing the main sources of error associated with the supercritical hydration treatments, the ways in which these errors were minimised and suggestions for improvements that can be made in the future.....	65
Table 2.7. Characterisation of the wood sample set into ring-porous, diffuse-porous and non-porous.....	75
Table 3.1. Peak area ratios (OH/CH and OH/‘Cellulose’) for five different wood treatment types and four different modern wood types.....	105



Table 3.2. A table to show oven-dried wood samples in decreasing order of mean strength prior to treatment with $\text{scCO}_2(\text{PURE})$ and $\text{scCO}_2(\text{CH}_3\text{OH})$ .....	114
Table 3.3. A table to show the calculated mean bending strength (MOR) values of wood species that have been treated with $\text{scCO}_2(\text{PURE})$ and $\text{scCO}_2(\text{MeOH})$ in comparison to the untreated oven-dried samples.....	114
Table 4.1. Observations made by the author immediately after the leather samples had been treated with $\text{scCO}_2(\text{PURE})$ in the presence of $\text{H}_2\text{O}$ .....	132
Table 4.2. Comparison of SEM-EDS elemental analysis of pre-and post-treatment book spine.....	145

## ABBREVIATIONS

<i>a</i>	width
ABPR	automated back pressure regulator
AMS	accelerated mass spectrometry
ATR	attenuated total reflectance
<i>b</i>	height
BC	before Christ
BPR	back pressure regulator
CaCO <sub>3</sub>	calcium carbonate
CFC's	chloro-fluoro carbons
CH	carbon–hydrogen bond
CO <sub>2</sub>	carbon dioxide
CO	carbon–oxygen bond
DDT	dichloro-piphenyl-trichloro-ethane
DRIFT	diffuse reflectance infrared fourier transform spectroscopy
DT	desiccator tube
E	Young's modulus
EtOH	ethanol
EMC	equilibrium moisture content
FSP	fibre saturation point
FSPL	fibre strength of the proportional limit
FT-NIR	Fourier transform near infrared
FTIR	Fourier transform infrared
GRAS	generally regarded as safe
( <i>H</i> )	historic
H <sub>2</sub> O	water
H <sub>2</sub> SO <sub>4</sub>	sulfuric acid
H <sup>+</sup>	hydrogen positive
HCFC's	hydrochloro-fluoro carbons
HE	refrigerated heat exchanger

ICON	Institute of Conservation
IMC	initial moisture content
IPA	isopropanol
IR	infrared (spectroscopy)
(l)	liquid
L	length
( <i>M</i> )	modern
M0	oven-dried mass
M1a	non-dried mass
M1b	resin mass
MC	moisture content
MeOH	methanol
MMMC	methoxy magnesium methyl carbonate
MgO	magnesium oxide
MOE	modulus of elasticity
MOR	modulus of rupture
MV	micrometering valve
N	newtons
N <sub>2</sub>	nitrogen
NMC	normalised moisture content
NMR	nuclear magnetic resonance
NRV	non-return valve
OH	oxygen-hydrogen bond
P	force
P1, 2, 3	pressure gauge 1, 2, 3
P <sub>c</sub>	critical pressure
PACR	Professional Accreditation of Conservators-Restorers
PEG	polyethylene glycol
PUMP	pneumatic liquid pump
PRV	safety pressure release valve
PTFE	polytetrafluoroethylene
PV1	hydration pressure vessel
PV2	reaction pressure vessel

RH	relative humidity
(s)	solid
SCF	supercritical fluid
scCO <sub>2</sub>	supercritical carbon dioxide
scCO <sub>2</sub> (PURE)	unmodified supercritical carbon dioxide
scCO <sub>2</sub> (CO-SOLVENT)	supercritical carbon dioxide modified with a co-solvent
scCO <sub>2</sub> (EtOH)	supercritical carbon dioxide modified with ethanol
scCO <sub>2</sub> (MeOH)	supercritical carbon dioxide modified with methanol
SEM	scanning electron microscopy
SEM/EDS	scanning electron microscopy with energy dispersive X-ray spectroscopy
SFE	supercritical fluid extraction
SOX	Soxhlet extraction
ssNMR	solid state nuclear magnetic resonance
T <sub>c</sub>	critical temperature
U.H.T	ultra-high temperature
UNESCO	United Nations Educational, Scientific and Cultural Organisation
UV	ultraviolet
V1,2	inlet valve
w	displacement
XRF	X-ray fluorescence
<sup>14</sup> C	carbon-14 isotope
1-D	one dimensional
2-D	two dimensional
3-D	three diemsional



## **1.0 Literature Review**

### **ABSTRACT**

To ensure the long-term survival of culturally significant materials, conservation professionals employ a number of different preventative and interventive techniques. In museums, preventative techniques are typically used to stabilise a range of dry and fragile materials. Although effective, these stabilisation methods do not strengthen the deteriorated materials. As such, there is a need to investigate alternative conservation methods that are able to simultaneously stabilise and strengthen materials that are often complex and intricate in nature.

Supercritical fluid (SCF) applications are widespread across the chemicals industry, mainly for extraction of high-value molecules or materials from complex mixtures or to oxidise waste products. Additionally, SCFs have previously been used to solve a number problems faced by museum collections around the world. Cleaning and deacidification are among the various conservation techniques investigated with the use of SCFs. It is proposed that the hydration of historic materials, via a SCF solvent stream, may be added to the list of techniques suitable for use within a conservation department. The possibility that this technique may stabilise, and strengthen historic materials to a greater degree than conventional conservation methods drives the programme of research described in this thesis.

The first part of this chapter discusses the properties and uses of SCFs and specifically supercritical carbon dioxide (scCO<sub>2</sub>). Applications are highlighted as to why SCFs are expected to be a suitable solvent for applications within art conservation. This is followed by a current state of the art for international conservation practices. Common problems faced by conservation professionals, and the methods they use to solve such issues are then discussed alongside previous applications of scCO<sub>2</sub> in art conservation. Finally, both wood and leather are characterised, with wood being the primary material of focus for the thesis. Methods to assess the microstructural and macrostructural features of both wood and leather are considered and discussed.

## 1.1 Introduction to supercritical fluids

A supercritical fluid (SCF) can be defined as a substance that has a temperature and pressure greater than its critical temperature ( $T_c$ ) and critical pressure ( $P_c$ ) respectively (Subramaniam et al., (1997)). The critical temperature is the highest temperature at which the gas can be converted to a liquid by increasing the pressure. The critical pressure is the highest pressure at which a liquid can be converted to a gas by increasing the liquid temperature. The phenomenon is clearly shown in the phase diagram below (Figure 1.1).

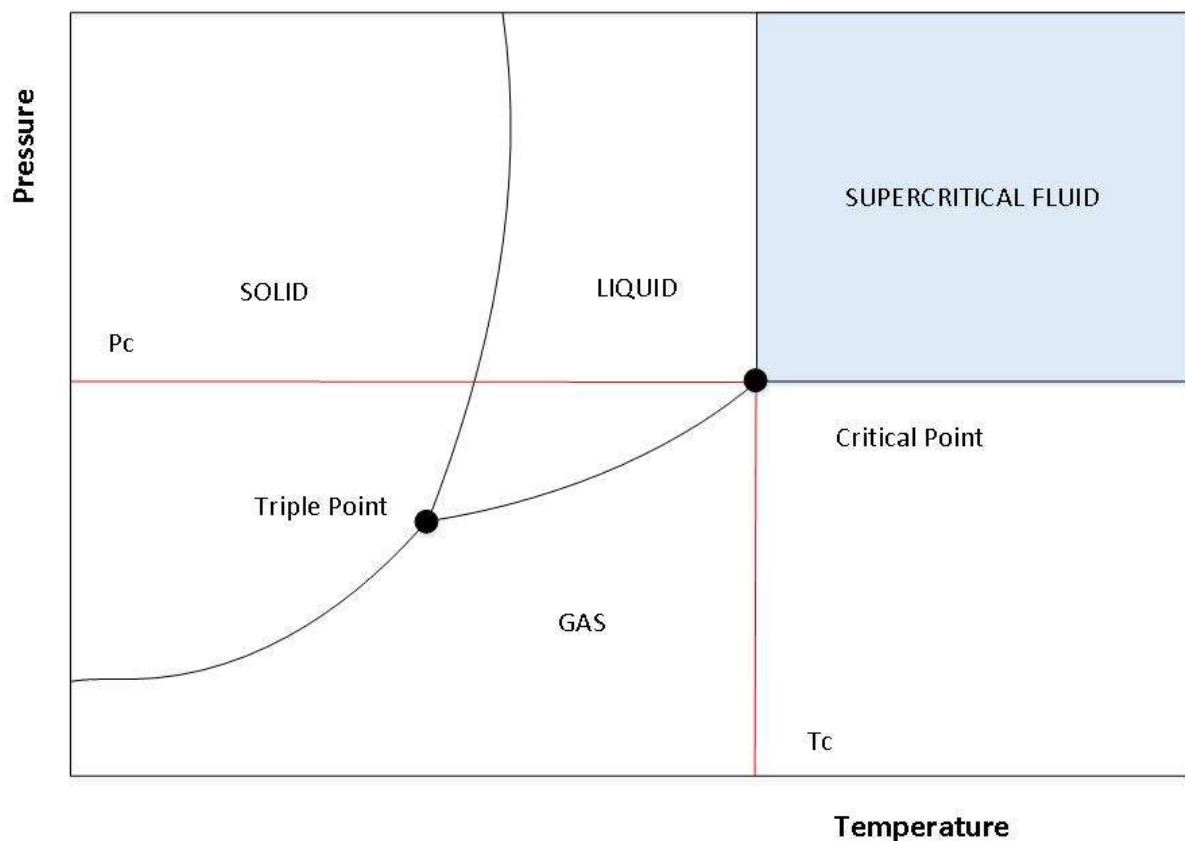


**Figure 1.1. Generic temperature-pressure phase diagram for a pure substance made by author.**

Above the critical point the substance exists as in a single homogenous phase, where it will not condense or evaporate to form a liquid or gas (Taylor, 1996). The disappearance of the distinction between the liquid and the gas phases is illustrated in Figure 1.2 ((i) – (iv)).

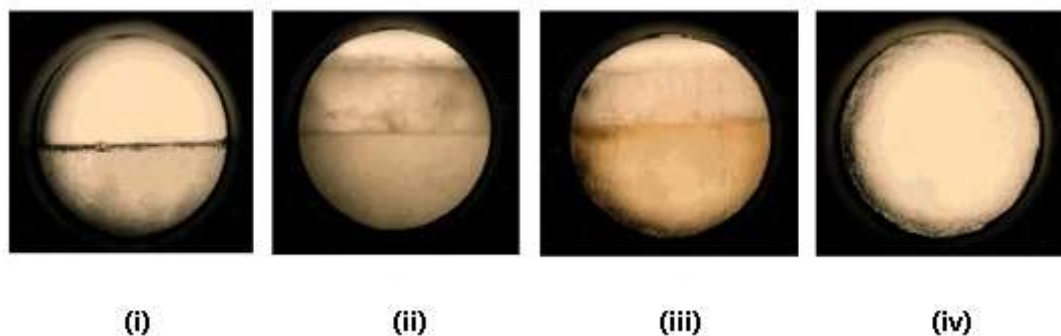


**Figure 1.2 Illustration of the formation of a homogenous phase: (i) The presence of a meniscus shows the two clear phases of a liquid and a gas (ii) The meniscus starts to diminish with increased temperature and pressure (iii) The density difference between the gas and liquid phases is decreasing. The meniscus is still present but severely diminished (iv) Critical temperature and pressure has been reached, therefore the distinct phases of a gas and liquid are no longer visible. One homogenous phase is shown. Adapted from (Oakes et al., 2001)**

### 1.1.1 Properties of supercritical fluids

As mentioned in Section 1.1 SCFs exhibit a number of important characteristics including homogeneity, compressibility and a continuous change from gas-like to liquid-like properties (Clifford, 1999). The physiochemical properties of a SCF are of equal importance as they intermediate to those of a liquid and a gas. Table 1.1 shows some of these properties for a gas, liquid and SCF.

Phases	Density ( $\text{kgm}^{-3}$ )	Viscosity ( $\mu\text{Pa.s}$ )	Diffusivity ( $\text{m}^2\text{s}^{-1}$ )
Gas	1	10	0.001- 0.01
Supercritical Fluid	100-1000	50-100	$1\text{e}^{-5} - 1\text{e}^{-4}$
Liquid	1000	500-1000	$1\text{e}^{-6}$

**Table 1.1 Typical physiochemical property values of gases, liquids and supercritical fluids**

Table 1.1 shows that SCF have liquid-like densities and gas-like viscosities and diffusivities higher than those of a liquid. These properties can be easily controlled by varying the temperature and/or pressure of a system, they are said to be ‘tunable’ especially in the critical region (Figure 1.1) (Baiker, 1999). Due to this ‘tunable’ capability and solvating power of a SCF being functions of density, the system can be changed between liquid and gas in the same critical phase.

The density of a SCF is known to increase with increasing pressure at a constant temperature, and decrease with increasing temperature at constant pressure. As such the fluid is therefore compressible in the critical region. The diffusivity of a SCF decreases with increasing pressure and generally increases with increasing temperature (Tucker and Maddox, 1998). Higher



diffusivity allows for higher mass transfer and reaction rates. This is particularly applicable to carbon dioxide (CO<sub>2</sub>) due to the small size of its molecules, this is discussed later in section 1.1.3. Temperature has a greater effect on SCF viscosities than pressure, however viscosity is also known to increase with pressure (Özcan, 1997).

### **1.1.2 Supercritical carbon dioxide**

Although there are a number of substances that are useful as SCFs, CO<sub>2</sub> is most the most commonly used solvent. CO<sub>2</sub> is non-toxic at low concentrations, non-flammable, inexpensive, inert and recyclable resource. It also holds a generally regarded as safe (GRAS) status (Montanari et al., 1999) and is an environmentally friendly substitute for other organic solvents. Furthermore, CO<sub>2</sub> is a gas at ambient temperature, therefore removing any solvent traces when it returns to ambient conditions. The conditions required for CO<sub>2</sub> to become supercritical are;  $T_c = 31.1^\circ\text{C}$  and  $P_c = 7.38\text{ MPa}$ .

The CO<sub>2</sub> used can be recycled from other existing industrial processes and therefore will have no adverse effects to global warming or the depletion of the ozone layer.

### **1.1.3 Solvent properties of supercritical carbon dioxide**

Pure CO<sub>2</sub> is a non-polar solvent, therefore supercritical carbon dioxide (scCO<sub>2</sub>) is a good solvent for non-polar or very slightly polar organic solutes. It is generally accepted that if a compound dissolves in hexane (short chain hydrocarbon) then it will dissolve in scCO<sub>2</sub>, due to their similar solvating abilities. This rule works well for low molar mass compounds but is not applicable to polymers with negligible vapour pressures (Subramaniam et al., (1997)).

To overcome this problem scCO<sub>2</sub> is commonly modified with polar entrainers to improve its affinity with polar compounds. Mixtures of two substances are known as binary mixtures. Entrainers can be used to increase or decrease polarity, aromaticity and chirality. Different entrainers can be added to CO<sub>2</sub> to provide different characteristics for example aliphatic hydrocarbons decrease polarity, toluene imparts aromaticity and [R]-2-butanol aids chirality (Clifford, 1999). However ethanol (EtOH) or methanol (MeOH) are most commonly entrained to increase polarity, because both have a relatively low molar mass and a critical pressure similar to that of CO<sub>2</sub> (Clifford, 1999, Ekart et al., 1993). These are often added in 5% to 10% volumes but can also be added in up to 50% volumes, a small addition of an entrainer can have a large effect on the characteristics of the solvent.

When scCO<sub>2</sub> is modified with EtOH its solvating power will be higher than that of pure CO<sub>2</sub> (scCO<sub>2(PURE)</sub>). This is largely due to the interactions between the solvent, CO<sub>2</sub> and the co-solvent, EtOH. Lewis acid-base interaction between the electron accepting carbon in CO<sub>2</sub> and the electron donating oxygen in EtOH have been investigated by Lalanne et al (2004). Below Figure 1.3 illustrates the relatively strong specific interaction between OH-CO<sub>2</sub> molecules, these were investigated with vibrational spectroscopy (Lalanne et al., 2004).

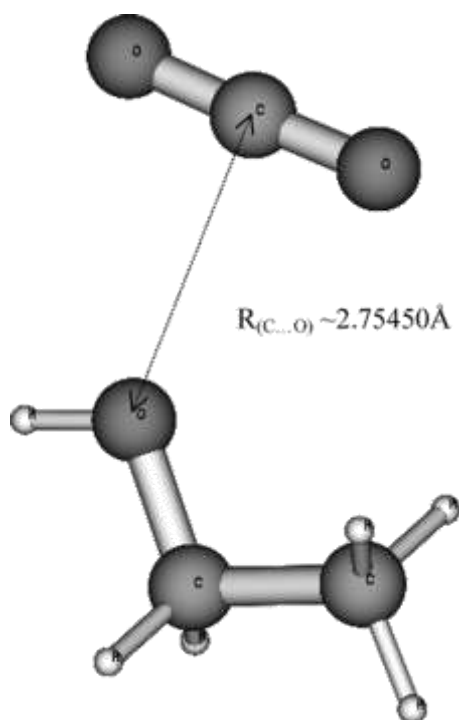


**Figure 1.3. Optimized geometry of CO<sub>2</sub>/EtOH complex (Lalanne et al., 2004)**

Saquin et al. (1998) report that the addition of a co-solvent also increases the density of the SCF solvent (CO<sub>2</sub>), however this is believed to play a minor role in enhancing the solubility's of solutes (Saquin et al., 1998). Instead attention must also be paid to co-solvent and solute interactions. Physical interactions such as dipole-dipole, dipole-induced dipole and induced dipole-induced dipole may occur alongside chemical hydrogen bonding. Hydrogen bonding is known to play a part in the enhanced solubility of solutes in scCO<sub>2(EtOH)</sub>, thus an enhanced solubility of water (H<sub>2</sub>O) in scCO<sub>2(EtOH)</sub> would also be expected due to the increased hydrogen bonding with the co-solvent and water (Foster, 2002). It can be predicted that MeOH will interact in similar way to EtOH as a co-solvent, due to its comparable size and intermolecular bonding.

### 1.1.4 Physio-chemical properties of carbon dioxide and methanol systems

Adding an organic entrainer to a CO<sub>2</sub> system, creates a mixture that has a higher critical temperature and pressure than a pure system. It is important to understand the effect of parameters, such as temperature and pressure, on the mobile phase of the mixture to ensure that experiments are carried out in the correct supercritical phase.

#### 1.1.4.1 Physical properties of carbon dioxide and methanol systems

Figure 1.4 below shows experimental vapour-liquid equilibria data of CO<sub>2</sub> and MeOH mixture system (non-ideal mixture) at 40°C by (Kodama et al., 1998). The figure shows that the CO<sub>2</sub> and MeOH mixture can exist in one phase, liquid, gas or SCF outside the data points, and as two phases, vapour and liquid, shown by the enclosed area from the data points. The liquid and gas region reaches a maximum in pressure at the critical point for a temperature of 40°C. To ensure the mixture is in a single phase it is normal to use a pressure above 10 MPa, thus avoiding the vapour-liquid area.

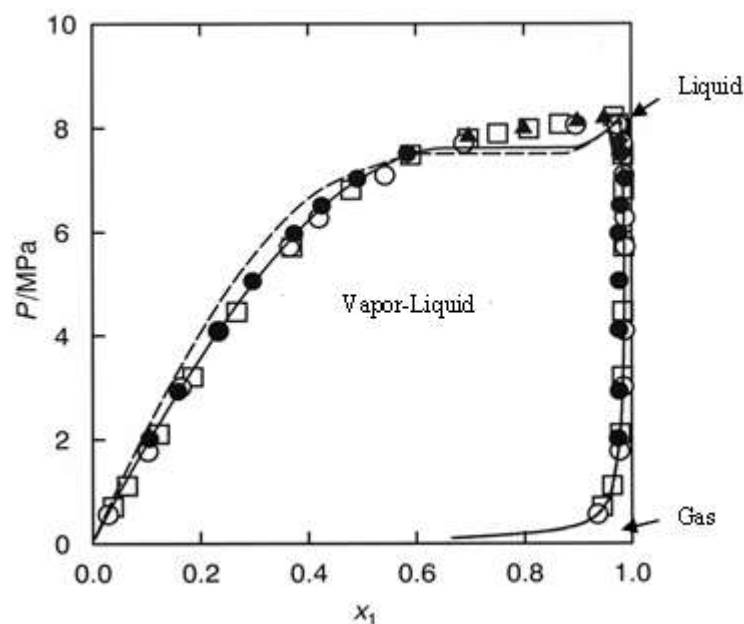


**Figure 1.4. Vapour-liquid equilibria for the CO<sub>2</sub> and MeOH system at 40°C, adapted from (Kodama et al., 1998)**

Increasing the pressure from below the critical pressure with a mixture of critical composition where gas and liquid phases will exist, as seen above, will cause the following to occur. Increasing pressure will cause the liquid to dissolve more CO<sub>2</sub> whilst the gas will solvate more MeOH, the gas will then increase in density more rapidly than the liquid (Clifford, 1999). When the critical point is reached the compositions and densities of the two phases will be identical, or homogenous and hence above the critical pressure only one fluid phase will exist. It should

be said that for a binary mixture the term “supercritical” is more arbitrary than for that of a pure substance.

#### 1.1.4.2 Critical temperature and pressure in a carbon dioxide and methanol system

Computer programmes that have been developed by Saito et al. (1994) can be used alongside equations proposed by Cheuh and Prausnitz (1967), to calculate theoretical values for the critical temperature and critical pressure for different mixtures of CO<sub>2</sub> and organic solvents (Chueh and Prausnitz, 1967) (Saito et al., 1994). Table 1.2 uses such values to demonstrate the relationship between the MeOH mole fraction and the critical parameters. We can see that with an increasing MeOH mole fraction the critical temperature increases at a steady rate whilst the critical pressure increases to a point and then starts to decrease again. This relationship is shown more clearly in Figure 1.5 with the critical pressure exhibiting a maximum value at a MeOH mole fraction of approximately 0.45.

CO <sub>2</sub> Volume Ratio	MeOH Volume Ratio	MeOH Mole Fraction	Critical Temperature (°C)	Critical Pressure (MPa)
100	0	0.00	31.1	7.4
90	10	0.07	51.1	10.5
80	20	0.12	64.9	12.2
70	30	0.20	85.9	14.4
50	50	0.36	124.4	16.5
0	100	1.00	239.5	8.1

**Table 1.2 A table to show the effect on critical temperature and critical pressure with varying MeOH mole fraction in a CO<sub>2</sub> and MeOH system.**

As the pressure increases the density will rapidly increase, this relationship is more distinct as the temperature of the fluid increases. This shows that if the pressure is kept above the critical pressure of the mixture, but the temperature is increased, then the mobile phase will be changed from liquid to gas to supercritical. When the pressure is increased at a higher fluid temperature, the mobile phase will be changed from gas to supercritical.

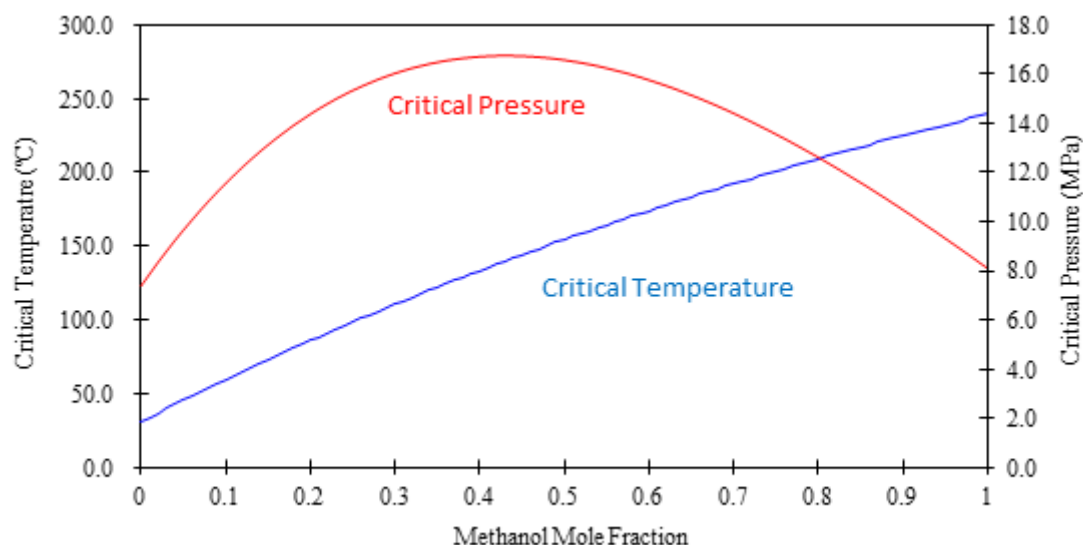


**Figure 1.5.** A graph to show the relationship between calculates values for critical temperature and pressure and the MeOH mole fraction, adapted from JASCO INC Application Notes (Burkhardt, 2012).

## 1.2 Uses and applications of supercritical fluids

Although the phenomena of SCFs was first reported in 1822 by Baron Gaginard de la Tour, the technologies associated with them have only really been developed extensively since the late 1970's (Berche et al., 2009). There are many applications of SCFs, listed below are three of the most common;

- Supercritical Fluid Extraction (SFE)
- Supercritical Fluid Chromatography
- Supercritical Fluid Cleaning

Of these applications SFE is the most developed technology on an international scale.

### 1.2.1 Supercritical fluid extraction

SFE can be used to extract compounds of interest from a more complex compound matrix e.g. vanillin from vanilla pods and caffeine from green coffee beans (Reverchon et al., 1993). SFE is commonly carried out on a solid matrix but is also possible in a liquid. Compared to a traditional SOX extraction system SFE provides a more efficient, environmentally friendly and cost effect method (Snyder et al., 1992).

A typical SFE rig (Figure 1.6) will consist of the following:  $\text{CO}_{2(l)}$  from a cylinder is passed through a chiller to form the more dense  $\text{CO}_{2(l)}$ . The  $\text{CO}_{2(l)}$  then arrives at the mechanised pump

and is pressurised above the critical pressure of CO<sub>2</sub>. This high pressure gas can then be passed through a modifying chamber where the chosen co-solvent e.g. MeOH, will be entrained with the CO<sub>2(g)</sub>. The SCF mix is then sent to the heat exchanger and brought above the critical temperature of CO<sub>2</sub>, the CO<sub>2</sub> is then supercritical. This is then passed through a vessel containing the sample and the extraction takes place. The solutes are then separated out and removed at a lower pressure in a collection reservoir (Sihvonen et al., 1999).

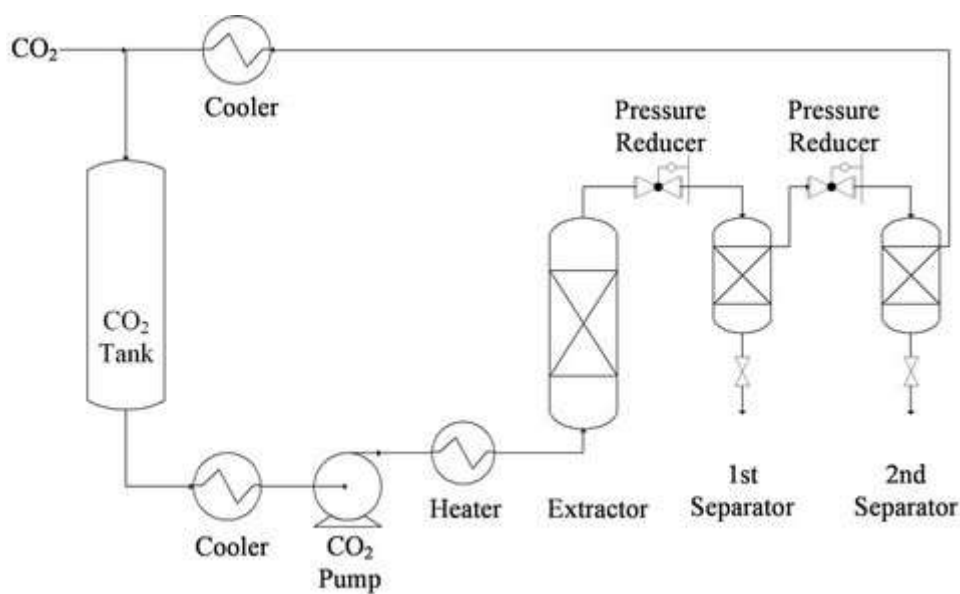


**Figure 1.6 A basic schematic illustration of a typical scCO<sub>2</sub> extraction rig (Liang et al., 2012)**

A SFE system can be set up in one of three ways; in a dynamic method where the SCF continuously flows through the sample and the collection reservoir or in a static method, here the SCF is circulated in a loop with the extraction vessel for a period of time before being released into a trapping vessel. A combination of both these methods can also be used. For SFE the choice of the optimum pressure at which to run the system is a compromise between process yield and operational cost.

### 1.2.1.1 SFE and solubility

Solubility is hugely important in extraction. As previously mentioned in Section 1.1.1 varying the temperature and pressure of the SCF allows for an easily tuneable system with small changes in solubility. It should be noted here that generally SCFs are at their most sensitive around the critical point (Hegg, 2010). Work carried out by Lou et al. (1997) suggests that the effects of temperature on solubility is far more complicated than that of pressure. They found that the effects of temperature depended on not only the temperature and pressure conditions

but also the properties of the solutes and the fluid. Mass transfer mechanisms also play a part in extraction processes (Reverchon, 1997). For example, even though waxes on the surface of a leaf have very low solubility in scCO<sub>2</sub>, it is possible to extract them because they have no affinity with the solid leaf matrix. Therefore, the scCO<sub>2</sub> extraction occurs with minimal mass transfer resistances. In contrast, essential oils that are highly soluble in scCO<sub>2</sub> also exhibit high mass transfer resistances through the solid phase, thus extractions here are controlled by mass transfer mechanisms.

Consideration of the matrix and rates of diffusion are therefore important (Engelhardt and Haas, 1993). Location of the natural materials and the components being extracted should be considered as the solute must be transported relatively rapidly from the interior matrix. The rate at which this occurs depends on the shape and dimensions of the matrix and its diffusion coefficient. Desorption from the matrix site must be allowed to occur, this may be a case of being released from a polymer chain or passage through a cell wall.

scCO<sub>2</sub> behaves as a lipophilic solvent and is good at extracting light oils and also higher molecular weight materials which can include waxes, paraffin's, lipids and resins. As previously mentioned the advantage of using scCO<sub>2</sub> for SFE is that its selectivity and solvent power are adjustable; liquid-like and gas-like properties can be achieved for the extraction of different solutes (Reverchon, 1997). Attention should be paid to the temperature and pressure at which oils are extracted using scCO<sub>2</sub>, as thermal degradation of the oil can occur under extreme conditions.

### **1.2.2 Supercritical cleaning with carbon dioxide**

Both CO<sub>2(l)</sub> and CO<sub>2(s)</sub> are known for their cleaning properties. Snow cleaning systems require a high output velocity and are particularly good at removing a range of particle sizes from material surfaces (Sherman, 2007). Whilst CO<sub>2(l)</sub> operates at a low pressure and can be incorporated in common bulk washer systems with the addition of surfactants. scCO<sub>2</sub> is particularly suited to the precision cleaning of porous intricate parts (Purtell et al., 1993). The technology is able to use the solvent properties of CO<sub>2</sub> alongside the unique properties of SCFs to carry out precision cleaning. The lower surface tension associated with the fluid state allows for scCO<sub>2</sub> to spread along the surface of a sample part more easily than a liquid, whilst also maintaining the ability to dissolve substances that are soluble, which a gas cannot.

Cleaning with scCO<sub>2</sub> uses the same procedure as SFE except the main vessel is replaced with a cleaning vessel which can contain an impeller to promote mixing. The contaminants in liquid

form are then separated off in a separator vessel and CO<sub>2</sub> gas is sent to the chiller to be recycled through the system (Sawan, 1998). It is a closed loop process with only a very small portion of cleaning solution needing to be replaced over time. Drying or rinsing are not required to remove any residual dirt and there is not a waste stream apart from the removed contaminants.

Due to the properties discussed in Section 1.1.3 scCO<sub>2</sub> is particularly suited to removing non-polar, hydrophobic contaminants. Of course, a co-solvent can be added to help aid the removal of polar soils e.g. fingerprints. The process is effective from a technical viewpoint and is superior to other methods when samples are composed of an intricate geometry, or when samples are water and or heat sensitive (Mchardy et al., 1993). It is also advantageous for samples that have very long drying times with aqueous cleaning. However, there are technical limitations to the process and problems with economies of scale.

#### **1.2.2.1 Problems with polymeric materials**

Polymers will absorb CO<sub>2</sub> to a lesser or greater degree depending on their solubility. Polymer solubility is dependent on three key characteristics; morphology, composition and polarity (Lee and Henthorn, 2012). When absorption occurs the polymer viscosity is reduced along with the melting temperature (Woods et al., 2004). Absorption only occurs in the amorphous regions of the polymer, amorphous polymers therefore absorb CO<sub>2</sub> to a greater extent than crystalline polymers (Shieh et al., 1996). These property changes can be advantageous. In the medical industry research into drug delivery systems has focused on the decrease in the glass transition temperature caused by the polymer swelling (Kasturirangan, 2007), this allows for increased diffusion rates which in turn can be used for impregnating small drug molecules into the polymer structure. When the glass transition temperature of a polymer is reduced below the processing temperature it is known as plasticization (Lee and Henthorn, 2012).

Sensitive polymers that undergo extreme polymer swelling and CO<sub>2</sub> dissolution are not suitable for applications of cleaning. However, cleaning at the polymer surface can be suitable for more crystalline polymers that undergo little or no change on interaction with CO<sub>2</sub> (Tomasko et al., 2003).

#### **1.2.3 Sterilisation with scCO<sub>2</sub>**

Perrut (2012) states the growing importance of the use of SCFs and their interactions with microorganisms. The ‘green’ status of scCO<sub>2</sub> provides an interesting alternative to established processes for sterilization, pasteurisation and virus inactivation. Sterilisation is the act of



making some object free of live bacteria or other microorganisms, usually by heat or chemical means. Pasteurisation is the partial sterilization of foods at a temperature that destroys harmful microorganisms without major changes in the chemistry of food (Perrut, 2012). There are three common methods of sterilization used in the medical and pharmaceutical industries today; ethylene oxide exposure,  $\gamma$ -irradiation and steam sterilisation (Dillow et al., 1999). Whilst ultra-high temperature (U.H.T.) is the most common form of pasteurisation in the food industry. These methods are effective but carry disadvantages for thermally and hydrolytically sensitive materials/substances. Sterilisation by scCO<sub>2</sub> provides a route for complete inactivation that is free of organic solvents and irradiation and be carried out at moderate temperatures.

#### **1.2.4 Impregnation**

Impregnation is the process of imbuing or saturating a material or substance with something. Functionalising substances, known as impregnates, are able to chemically or physically bind to a bulk material, or substrate, thereby modifying or enhancing certain characteristic properties of the substrate (Builes and Vega, 2012).

##### **1.2.4.1 Classical vs. supercritical fluid impregnation**

Due to disadvantages associated with liquid and gas phase solutes for impregnates, exploiting SCF properties for impregnation has become of increasing interest. Liquid phase solutes provide slow diffusion rates and long process times, whilst gas phase solutes are hindered by low space yields (Elles and Crim, 2006). SCF solutes however, can deliver deep penetration over short periods of time with low associated temperatures, and can provide the possibility of altering the substrate due to easily tuneable pressures in the critical region (Weidner, 2012) (Table 1.3).

<b>Classical Impregnation</b>	<b>vs.</b>	<b>SCF Impregnation</b>
<ul style="list-style-type: none"> <li>• Low diffusion rates</li> <li>• High operating temperatures</li> <li>• Low depth penetration</li> <li>• Long process times</li> <li>• Need for hazardous solvents</li> <li>• Need for drying procedures</li> </ul>		<ul style="list-style-type: none"> <li>• High rates of diffusion associated with SCF</li> <li>• Low/moderate operating temperatures</li> <li>• Potential for deep penetration</li> <li>• Short contact times</li> <li>• No need for hazardous solvents</li> <li>• No drying procedures</li> </ul>

**Table 1.3. A table to show the key properties associated with both classical and SCF impregnation methods.**

### **1.3 Introduction to art conservation**

Art conservation is a science based discipline dedicated to the preservation of cultural heritage for the benefit of future generations (Price et al., 1996). Conservators are trained in the methods of conservation for different art works of varying material, age and deterioration. These methods can include cleaning, preserving and repairing works of art from deliberate damage or the inevitable decay caused by the effects of time and handling (Viñas, 2005). Conservators often specialise in specific types of art work, including but not limited to, painting, paper, textiles, photographs, sculpture, furniture and ethnographic objects. Specific guidelines are dictated by international centres of conservation as shown by Table 1.4. The guidelines that are particularly relevant to the nature of this study are highlighted in bold.

Conservation can be preventative or take direct action on an object in order to stabilise or retard further degradation. Whilst restoration involves work carried out on an already severely damaged object in order to bring back some of the original historic and aesthetic values relevant to object and its environment (Letellier and Eppich, 2015).

<i>Professional Standards</i>	<i>Professional Judgement &amp; Ethics</i>
<p><u>1. Assessment of cultural heritage -</u> Assessing and reporting on condition, environment and threats, assessing risks, identifying any problems to be solved.</p> <p><b><u>2. Conservation options and strategies -</u></b> <b>Identifying and evaluating options; courses of action for conservation measures.</b></p> <p><u>3. Conservation measures -</u> Advising on, developing policy for and implementing conservation measures; planning to minimise the effects of disasters and emergencies; maintaining conservation records</p> <p><u>4. Organisation and management -</u> Managing projects and workflow; client/internal and external relations; health and safety; security; records and reports</p> <p><b><u>5. Professional development -</u></b> <b>Maintaining up-to-date practice; extending and communicating knowledge; promoting conservation and the care of cultural heritage</b></p>	<p>i. Understanding principles and practice</p> <p>ii. Conversance with guidelines</p> <p>iii. Understanding the wider contexts of conservation</p> <p>iv. Critical thinking, analysis and synthesis</p> <p><b>v. Openness to alternative methods and approaches</b></p> <p>vi. Understanding the ethical basis of the profession</p> <p>vii. Observing code of ethics and practice</p> <p>viii. Observing legal requirements</p> <p>ix. Responsibility for the care of cultural heritage</p> <p>x. Responsible and ethical dealings with others</p> <p>xi. Respect for the cultural, historic and spiritual context of objects</p> <p>xii. Handling value-conflicts and ethical dilemmas</p> <p><b>xiii. Understanding and acting within the limits of own knowledge and competence</b></p>

**Table 1.4 Summary of the professional standards and professional judgement and ethics recommended by Professional Accreditation of Conservators-Restorers (PACR) and the Institute of Conservation (ICON), taken from (Icon, 2014)**

### **1.3.1 Conservation practices and problems**

There is an ongoing debate between artists and conservation professionals. Many are concerned about the methods used to restore valuable artworks, believing that the preservation techniques not only devalue the work but harm the original integrity of the work. Conversely many think that these practices are essential to the long term survival of irreplaceable and historic works (Viñas, 2005). Both sides state strong arguments that are unlikely to be solved soon. It can be said that conservation work destroys the authenticity of the artwork, however it is also true that

if it weren't for skilled conservation methods artworks would be unlikely to survive for future generations to enjoy.

Each different material, be it paper or paint, requires a different technique for conservation. In practice, most techniques are relatively simple following standard procedures according to the media. However, they require a very high level of patience and care with some conservation projects taking years to complete. All materials require a controlled environment for optimum conservation, with humidity control being the most vital. However light exposure, air pollution and changes in temperature must also be controlled within strict guidelines.

Art conservators are faced with a number of different problems for different media on a daily basis. However, there are problems that occur more commonly than others and pose larger threats to the survival of cultural heritage. Highlighted below are three specific areas that warrant a large amount of the conservator's time, they include; environmental (atmospheric) controls, deacidification of media and the presence and removal of pesticides in museum collections.

#### **1.3.1.1 Environmental controls (preventative conservation)**

A major part of preventative conservation is maintaining and controlling the environmental and atmospheric conditions within a museum or gallery space. Unfortunately, it is often found that the need to display and promote cultural heritage to the general public has a direct negative effect on the stability of the collections. Commonly, it is the needs of the visitors that are catered for and not the works within the museum. This can result in the collections being housed in environmental conditions that may cause long term detrimental problems (Blades et al., 2000). Consequently, a number of studies have been carried out across European museums recording and collecting environmental data to find the key factors which cause degradation.

Camuffo et al. (2001) investigated microclimate, gaseous and particle air pollution and biological contamination in four museums across Europe. Variations in temperature and humidity are known to directly affect factors associated with preventative conservation. Across all four museums it was found that building structure, air conditioning or vent systems, heating, exchange of outside air and visitor numbers all played a part in temperature and humidity imbalance (Camuffo et al., 2001).

Humidity is defined as the amount of moisture or water vapour in the air. An increase in humidity will cause hygroscopic materials to absorb water causing dimensional changes and

internal stress, whilst a decrease in humidity causes shrinkage (Brown and Rose, 1996). If these variations persist long term, then changes in dimensions of a material will have an adverse cumulative effect. Non-hygroscopic materials are sensitive to variations in temperature; continual raising and lowering of temperature causes changes in their visco-elastic properties, therefore reducing the materials ability to return to their original structural integrity under controlled conditions (Placet et al., 2008). This is a particular problem for paintings as the possibility of the cracking and flaking of paint increases dramatically.

The discovery and subsequent public access to the Palaeolithic cave paintings at Lascaux in the 1940's, provides a harsh lesson in the fragility of media in a disturbed microclimate. Now a United Nations Education, Scientific and Cultural Organisation (UNESCO) world heritage site, the cave paintings show some of the oldest prehistoric art in the western world. Left in peace since around 15000 BC the paintings were found in near perfect condition. However, they were soon to become victims of their own fame, with the markings almost disappearing from site just some twenty years after their opening to the public. A number of factors including changes in air circulation, light and approximately 1,200 visitors per day caused a damaging change in the established equilibrium resulting in extensive mould and fungus growth (Bastian et al., 2010). After being closed for a number of years, it has now been established that the original environmental conditions can once again be restored in the cave interior (Brunet et al., 2000). Here the decision to completely stop public access has been vital to the survival of the Lascaux paintings, mass tourism meant that the irreplaceable works were very nearly lost forever.

It seems that conservators face an ongoing difficult decision between the comfort and interests of museum visitors or the long term survival of cultural heritage (Kerschner, 1992). Certainly, many museums compromise the necessary stable conditions essential to the long term conservation of cultural heritage over the daily needs of mass tourism. Attention must be paid to the microclimates established within a museum walls and the factors needed to maintain that.

#### **1.3.1.2 Deacidification**

Acidification of different media is a major problem in all areas of art conservation, with the acidification of cellulose fibres in paper and canvas being the most prevalent. Throughout history, paper in various forms and structure, has been used for the dissemination of cultural

heritage (Baty, 2010). Paper deacidification therefore represents a fundamental process within conservation.

An increase in demand and the invention of the printing press in mid-nineteenth century saw a dramatic change in the way paper was produced. The birth of the printing press saw linen and hempen based paper replaced with the more convenient and industrially efficient wood pulp paper (Baglioni et al., 2013). Unfortunately, this media was more chemically reactive to hydrolytic degradation as well as thermal and oxidative degradation.

Hydrolysis in paper, under stable conditions, is usually a slow process that causes the yellowing of paper and loss of mechanical strength. However, the hydrolytic process can be catalysed by acidic pH levels due to the increase in available hydrogen positive ( $H^+$ ) ions, causing increased cellulose depolymerisation and subsequent aging of the cellulose fibres (Arney et al., 1979). Paper degradation is termed as an ‘autocatalytic’ process (Giorgi et al., 2002). This is due to the main components of paper, including lignin, hemicellulose and hydrolysed cellulose being oxidised by acidic products added during the papermaking process. The oxidation of these materials produces acidic by-products that continue to catalyse the degradation process. Increased temperature and moisture will also increase the rate of hydrolysis. These degradation processes shorten the average chain length of a fibre therefore damaging the mechanical strength. Giorgi et al (2002) estimate that the breaking of 0.5 – 1.0% of bonds in the cellulosic fibrils virtually leads to the complete loss of fibre strength.

In general a successful deacidification process should neutralize the acidic paper and produce thermodynamically stable by-products that are able to act as a alkaline reservoir (Giorgi et al., 2002). There are currently two main deacidification techniques in conservation; the Wei T’o Method and The Bookkeeper Method (Porck, 1996).

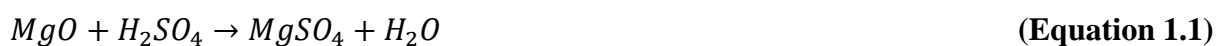
#### **1.3.1.2.1 The Wei T’o Method**

Used for mass deacidification of books, the Wei T’o method uses the effective agent methoxy magnesium methyl carbonate (MMMC) in a solvent mixture of MeOH and hydrochloro-fluoro carbons (HCFC’s). HCFC’s have replaced previously used chloro-fluoro carbons (CFC’s) which are harmful and known to cause depletion in the ozone layer. The books for deacidification have to be preselected so that books with certain inks, adhesives and synthetic bookbinding’s are excluded due to risk from MeOH. The books are dried prior to treatment to decrease the water content from about 6% to 0.5%. The books are then impregnated under

pressure with MMMC. The magnesium compounds formed neutralise the acid and build an alkaline reserve.

#### **1.3.1.2.2 The Bookkeeper Method**

The Bookkeeper Method uses the magnesium oxide (MgO) in a solvent of perfluoro heptane. Prior to treatment books or sheets of paper are placed in a cylinder and brought to equalised pressures. The deacidification suspension is then pumped in causing the deposition of highly reactive, sub-micron sized particles of MgO. These particles have high surface area and are held to the paper by electrostatic forces, they will neutralise any acid present in the paper texture e.g. sulphuric acid (H<sub>2</sub>SO<sub>4</sub>). Any unreacted MgO forms an acid reserve. In the presence of sulphuric acid, the following reaction will occur:



Although there are established methods for deacidification in paper and cellulose based materials, due to the enormity of the task there is a need to develop mass deacidification methods that work on an unselective basis. Currently a number of books and cellulose material varieties are not suitable for deacidification treatment due to a certain level of risk (Arney et al., 1979). The use of nano-technologies is one particular route that may prove fruitful to conservators in the future (Baglioni et al., 2013, Giorgi et al., 2005).

#### **1.3.1.3 Cleaning and pesticides in museum collections**

Collections and museum objects are often routinely cleaned as part of conservation procedures. However, it has recently become apparent that in many cases more extensive cleaning is necessary to remove the presence of harmful pesticides. In the past, to prevent pest infestations, the use of pesticides in museum storage areas and on collections has been extensive. It is known that since the eighteenth century the application of pesticides in museums has been liberal and mismanaged, resulting in a lack of or very incomplete records (Krug and Hahn, 2013). Collections and staff are at potential risk due to the toxic nature of many of the well-known chemicals and heavy metals in standard pesticides.

Chlorine, lead, arsenic and mercury are found in pesticides. These chemicals and elements are often volatile or semi-volatile and will accumulate in the air or dust particles. Due to the lack

of records the amounts or types of pesticides used are not known. This is a major problem for museums worldwide. In America the National Museum of American Indian Act in 1989 and the Native American Graves and Repatriation Act in 1990 encouraged the return of objects to their native communities with information of treatments applied (Madden et al., 2010). This in part led to the need to recognise and record the pesticides used. However, there is no standardised methodology in place to measure residues and simple question such as what degree of removal is sufficient, remain unanswered.

Although Integrated Pest Management is now state-of-the-art worldwide, the problem remains with the recognition and removal of pesticides, with no standardised guidelines. Early insecticide analysis using gas chromatography on 118 samples from the Danish National Museum Ethnological Department showed the presence of naphthalene, dichloro-diphenyl-trichloro-ethane (DDT) and methoxychlor (Glastrup, 1987). Whilst analysis carried out by Kigawa et al (2011) found that fumigation under standard museum conditions caused chemical alterations to proteins such as muscle, animal glue and silk. They also found residues of bromine and iodine left in glue and silk (Kigawa et al., 2011). X-Ray fluorescence (XRF) results from the textiles at the German Historical Museum Collections found the presence of lead and chlorine in high quantities with mercury and arsenic in smaller amounts (Krug and Hahn, 2013).

Clearly there is a need to remove these substances from museum collections. However, there is a lack of effective methods for the removal of harmful substances that are embedded in the matrix of items. In current practise conservators are primarily concerned with cleaning the surfaces of materials and removing dust from museum storage and facilities (Tello and Unger, 2010). These methods of cleaning are not enough to remove embedded substances. An effective decontamination method needs to be established to successfully and permanently remove poisonous substances.

### **1.3.2 Conservation of wood**

In general, the conservation methods applied to wood all depend on the circumstances in which it was found or kept, and what state it is in. Dry, wet and waterlogged wood all present conservators with different challenges. The moisture content of the wood collected dictates the conservation method that will be applied; at the extremes the wood will either be dry or



waterlogged with the fibre saturation point of the wood providing the distinction point (Unger et al., 2001). Dry wood is most susceptible to attack by pests and microorganisms and is also more at risk to changes in its environment. Although waterlogged wood is considered the more sensitive of the two having been weakened by water, it is the most commonly found of the historic wood types due to the anaerobic environment in which it is submerged (Haake, 2014).

#### **1.3.2.1 Waterlogged wood**

In waterlogged wood, water-soluble starches and sugars are the first to be leached from the wood structure along with tannins and mineral salts. Over time, hydrolysis will also cause the cellulose in the cells walls to break down leaving only lignin to support the wood structure. Water replaces the degraded wood materials which provides some stability in the structure (Christensen et al., 2006). Consequently, wood from waterlogged, archaeological sites is always treated immediately or stored in water to stop the wood structure from undergoing shrinking or extreme warping (Kaye, 1995).

Following the correct storage, the treatment of large waterlogged wood items is well established. The process commonly proceeds in two key steps; a consolidant material is added to help retain mechanical strength in the structure, whilst the excess water needs to be removed from the wood, avoiding shrinkage and distortion (Grattan and Clarke, 1987). This procedure was followed after the excavation of Henry VIII's flagship, the Mary Rose, in 1982. For 12 years conservators in Portsmouth sprayed fresh water onto the ship structure to remove the salt and to stop the wood from drying out, whilst the following 19 years were spent spraying the structure with Polyethylene Glycol (PEG) to displace excess water (Björdal and Nilsson, 2001). PEG has been used as a consolidant on large waterlogged items for several years, however the process is time consuming, irreversible and expensive. The conservators on the Mary Rose have therefore sought to develop an alternative to PEG that is more time efficient in its application and has antibacterial properties that make separate applications of antibacterial preservatives redundant (Walsh et al., 2014). Freeze-drying combined with a solution of PEG is the most favoured method for the conservation of smaller waterlogged items. However, it is also an expensive treatment and is limited by the size of the freeze-chamber (Hamilton, 1999).

#### **1.3.2.2 Dry wood**

Dry wood exposed to insect activity and environments of fluctuating humidity is at the highest risk of degradation. In galleries or museums maintaining and controlling a stable environment is a key factor in the preservation of wooden items. However, for wood that has that has been

buried at terrestrial sites or exposed to the environment, attack by microorganisms, including fungi and bacteria, is the most prevalent form of degradation. It has been found that some woods are at a greater advantage than others with oak, cedar, redwood, juniper and cypress wood having a higher tolerance to decay than pine, birch, beech (Zabel and Morrell, 1992). As discussed in Section 1.2.3 most microorganisms require oxygen and moisture to thrive in an environment, a lack of either of these conditions will severely hinder their growth (Perrut, 2012). Therefore conservators often place wood in an oxygen purged environment, impeding the colonisation of aerobic organisms (Blanchette, 2000). Boric acid can also be used by conservators as it kills most common insects (Haake, 2014).

### **1.3.3 Conservation of leather**

Of all the materials to be found in a museum collection, leather is one of the most complex to conserve. ‘Leather’ as a category of material cannot be considered as a single material, but more as an indication of many sources from which the material may have originated (Waterer, 1971); leather can be made from almost any animal hide and processed in many different ways (Dirksen, 1997). The manufacturing of leather as a product has changed and developed over time, however it is the application of different tanning processes (vegetable or mineral) (Section 1.6) that cause the most problems for conservators.

The conservation of leather is usually approached in one of two ways; via either an interventive or preventative method, depending on whether the item requires more urgent or passive conservation (Haines, 1991a). In recent times there has been a move away from the traditional interventive methods of conservation that can include the application of dressings and treatments, towards methods of preventative conservation (Dirksen, 1997). Here preventative conservation is concerned with the appropriate storage conditions for leather varieties, rather than the addition of waxes or resins that can cause oxidation and biological deterioration. As such temperature, humidity and light exposure should all be controlled by conservators, as well as providing a physical support for the leather items to avoid cracking, splitting and general loss of structure (Alcántara, 2002).

## **1.4 Applications of supercritical carbon dioxide in art conservation**

The application of scCO<sub>2</sub> within art conservation has not been extensive, this is probably due to the high costs associated with the specialist equipment required for scCO<sub>2</sub> and the relatively low research funding found in most conservation departments across the world. However, when scCO<sub>2</sub> has been used in a conservation capacity the results have been very encouraging.

scCO<sub>2</sub> has been known to be used in the restoration of paper, wood, stone, textiles and various ethnographic materials (Sousa et al., 2007). Cleaning, including the removal of pesticides, and deacidification are two of the most widely investigated applications in conservation.

#### **1.4.1 Cleaning with supercritical carbon dioxide**

Sousa et al. (2007) carried out some very interesting work on the cleaning of heavily deteriorated and soiled eighteenth century textiles using liquid and scCO<sub>2</sub> as a solvent stream. The addition of co-solvents to the solvent stream including scCO<sub>2</sub> with isopropanol (IPA), and scCO<sub>2</sub> with IPA and water were investigated. Commonly, with textiles such as these, a wet cleaning method would be employed in the restoration process. However, this can be ineffective at dirt removal and cause problems such as shrinkage. The dry-cleaning properties of scCO<sub>2</sub>, as discussed in section 1.2.2 are well known attributes of the fluid and can be used for the delicate cleaning of textiles as a replacement to contemporary wet cleaning practices.

The dirt extracted from the textiles by Sousa et al. (2007) was evaluated through weight loss and colour variation. Through various degradation processes the textiles had lost mechanical strength, mechanical properties were therefore also investigated with optical microscopy in longitudinal cross sections. It was found that scCO<sub>2</sub> with IPA as a co-solvent actually increased the percentage of dirt found on the surface of the material, this is probably due to the high diffusivity of the fluid causing particles to migrate to the surface without being extracted. The higher density CO<sub>2(l)</sub> was more successful at removal of dirt from the surface, water as a co-solvent was also found to have a very positive effect. A two-step process was found to be the most effective process for dirt extraction. Firstly, pure scCO<sub>2</sub> is used, removing 50 - 70% of dirt and roughly 25 - 35% in extremely soiled areas. Secondly, CO<sub>2(l)</sub> is used, removing up to 50% of dirt from extremely soiled areas. The addition of co-solvents helps to promote the extraction of polar particles from the surface, this removes a further 20% of the dirt. Analysis showed that the fibre and texture of the material was not physically damaged and there was no loss of material, this is obviously of primary importance to conservators.

The addition of a co-solvent in scCO<sub>2</sub> is commonly used to increase the solubility of CO<sub>2</sub> (Section 1.1.4). Recently scCO<sub>2(co-solvent)</sub> mixtures have been used for the removal of organic materials from archaeological artefacts for radiocarbon dating. Currently harsh acid-base treatments are used to remove contaminating organic matter from archaeological objects in preparation for <sup>14</sup>C dating with accelerator mass spectroscopy (AMS). Unremoved contaminants can interfere with the AMS reading and cause an inaccurate determination of age.

Rowe et al. (2013) employed a simple SFE process with  $\text{scCO}_2(\text{MeOH})$  to remove the organic contaminants prior to plasma oxidation and AMS. Initially, wood and charcoal samples were extracted. Comparison between these SFE samples and the acid-base pre-treatments found equivalent  $^{14}\text{C}$  results. Russian textiles along with Russian and Egyptian mummy gauzes were also treated. A gas chromatography/mass spectroscopy carried out on these extractions found traces of beeswax, coconut oil, frankincense, glycerol, humic acids (Rowe et al., 2013). This is not unexpected given that  $\text{scCO}_2$  is known to be particularly good at extracting fat and lipid based materials (Section 1.2.2). This method to pre-treat samples before  $^{14}\text{C}$  dating shows great promise as a method where conservation is of interest. Coupled with non-destructive plasma oxidation it provides a viable alternative to harsh acid-base treatments (Rowe et al., 2013).

#### **1.4.1.1 SFE for the Removal of Pesticides**

Tello (2006) in her thesis used SFE with  $\text{CO}_2$  to clean a range of ethnographic objects of varying media, followed by SFE for the removal of heavy metals and pesticides. There are currently no set procedures for the removal of heavy metals and pesticides within museum collections, methods are therefore wide ranging, inefficient and in some cases can present health hazards. Dry and wet cleaning procedures dominate the current removal practices with methods including vacuum extraction, freeze drying procedures and the use of ultrasonic waves (Tello, 2006). For the removal of the poisonous substances from the selected samples Tello (2006) slightly altered her experimental conditions from the SFE cleaning conditions. Using a 10L vessel the pressure was increased from 25 MPa to 35 MPa along with the extraction time from 3 to 7 hours, whilst the flow rate was decreased from  $20 \text{ kg h}^{-1}$  to  $2 \text{ kg h}^{-1}$ . The temperature remained constant at  $40^\circ\text{C}$ , remaining just above the  $T_c$  for  $\text{CO}_2$ . The addition of modifiers was also assessed; 95% EtOH was used as a co-solvent and trimercaptotriazine was sometimes added to EtOH to form chelates; these were to try and aid the removal of arsenic and mercury.

It was determined that pesticides and heavy metals can be removed from the ethnological materials and objects via SFE with a solvent stream of  $\text{scCO}_2$ . Levels of chlorine containing compounds such as DDT and lindane can all be reduced significantly, as can the heavy metal mercury. It was also found that even with the addition of entrainers, the levels of arsenic were not affected. Visually all the materials remained unaffected, with the exception of a piece of caribou fur that was subject to drying and de-greasing, thus reducing its stability.

Kang et al. (2004) focused on pesticide reduction in wood using  $\text{scCO}_2$ , with special attention paid to colour retention in the material. A much shorter extraction period of 30 minutes under

45°C and 30 MPa was used to assess the removal of DDT from wood species. scCO<sub>2</sub> was found to remove 60% of DDT from wood coated with pigments that would commonly be found on wooden icons. Overall, there was a minimal impact on the colour quality of pigments (Kang et al., 2004). Zimmt et al (2009) used scCO<sub>2</sub> with acetone as a co-solvent for the removal of commercial Diazonion solution, a pesticide in chrome tanned leather. Here it was found that extraction with pure scCO<sub>2</sub> resulted in 50% pesticide removal, whilst the addition of acetone resulted in no detectable pesticide residue (Zimmt et al., 2010). From a conservation viewpoint, it is important to note that in all of these studies scCO<sub>2</sub> was used as a solvent stream for the extraction of pesticides without harming fragile materials.

Clearly, several factors affect the extent of pesticide removal from a chosen material. Consideration must be paid to the non-polarity of CO<sub>2</sub> and the poisonous substance, solubility of substance in CO<sub>2</sub> and the structure of the matrix of the object/material. For example, scCO<sub>2</sub> is particularly good at removing chlorine-based pesticides, these like CO<sub>2</sub> tend to be non-polar and are therefore soluble in CO<sub>2</sub> (Section 1.1.3). Wet cleaning procedures are unable to remove these non-polar substances due to the high polarity of water. Diffusion of the pesticides into the material matrix is also influential. Some matrices are in general easier to penetrate than others, for example leather and plant fibres are easier to penetrate than calcium or keratin based substances. Initially easy penetration allows the pesticide to diffuse deep into the matrix, however it also allows for easy diffusivity of scCO<sub>2</sub>; aiding the extraction of pesticides. Interestingly, Tello (2006) suggests that the thickness of material may play a part in decontamination, with thicker materials such as fur and leather responding much better to extraction than thinner blades of grass or horse hair. This is perhaps something to consider when determining extraction conditions.

#### **1.4.2 Neutralising and strengthening with supercritical carbon dioxide**

Neutralising and strengthening treatments for aged acidic paper are some of the most important methods in conservation, they are used on a regular basis and help to restore yellowing paper with diminished mechanical properties. Although there are established methods for deacidification and strengthening within conservation, they are not without their problems. Some treatments are known to actually damage paper strength, whilst others that require a gas phase treatment that can only be carried out in industrial settings which increases costs (Selli et al., 2000). Using scCO<sub>2</sub> as a solvent stream provides a low cost, non-toxic alternative that does not cause further deterioration of inks, bindings or adhesives.

Selli et al. (2000) carried out a cleaning treatment on wood pulp paper under supercritical conditions with CO<sub>2</sub> for 30 minutes. This was followed by a deacidification treatment with scCO<sub>2</sub> and calcium carbonate (CaCO<sub>3</sub>). Due to the high diffusivity and low viscosity of the fluid, CaCO<sub>3</sub> is distributed across the whole vector, neutralising acidic ions and acting as an alkaline reservoir. Analysis of kinetic equations have shown that an alkaline reservoir significantly reduces the rate of degradation over time (Selli et al., 2000). Treatments were then carried out on artificially aged acidic paper samples under similar conditions but with the addition of an EtOH co-solvent and 40 wt.-% of either Catechol (1,2-dihydroxybenzene) or PEG 400. Under mechanical tests these samples were shown to have improved strength after the addition of Catechol, PEG 400 showed no improvements. It has been suggested that Catechol forms strong hydrogen bonds with the cellulose chains in the paper creating a stronger cross-linked structure (Arshid et al., 1956).

Research carried out by Francais et al. (1998) looks at a mass deacidification and strengthening process that consists of three key processes; extraction, impregnation and stripping. Extraction of the degradation products using scCO<sub>2</sub> and EtOH is followed by impregnation of a basic organometallic agent. The best results were found using methyl-ethyl magnesium carbonate with scCO<sub>2</sub> and EtOH, neutralising papers with a pH over 7.0 and creating a significant alkaline reserve. It should be said that the basic extraction not only reduced odorous components, biological contamination and yellowing colour agents, but also showed significant moisture reduction with slight deacidification and increased mechanical strength. There was also no adverse effect on the paper, printing inks, or covers with only the disappearance of hand written inks. These are all important observations to note in the context of conservation. Extraction was followed by a strengthening treatment which was carried out via the impregnation of silicon-derived and cellulose-derived polymers, concluding that a mixture of strengthening agents would perhaps produce the best results. Stripping with scCO<sub>2</sub> and EtOH was used to remove any unreacted agents, with a final treatment of pure scCO<sub>2</sub> to eliminate any EtOH residues.

## 1.5 Material Characterisation: Wood

### 1.5.1 Cellulose, hemicellulose and lignin

Wood is a non-homogenous, porous solid composed mainly of three constituents; cellulose, hemicellulose and lignin. Cellulose provides the skeleton of the wood structure, hemicellulose the matrix and lignin binds the cells together providing rigidity for the cell (Sahle-Demessie, 1994). Cellulose consists of linear chains made of D-glucose linked  $\beta$ -1,4-glycosidic bonds forming polymer chains that are stiff and straight (Figure 1.7). Cellulose polymers are known to have both, highly crystalline and amorphous regions. Hemicelluloses are carbohydrate polymers with random and amorphous structures located within the cellulose and between the crystalline cellulose and lignin (Yang et al., 2007). Hydrogen bonding exists between cellulose and lignin, as well as the cellulose and hemicellulose.

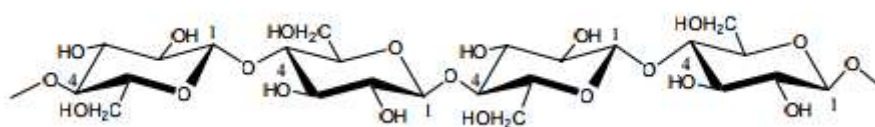


**Figure 1.7. Cellulose linear chains of D-glucose linked by  $\beta$ -1,4-glycosidic bonds (Benabid and Zouai, 2016)**

Lignin occurs uniquely in vascular plants and serves several vital functions including bonding cellulose and hemicellulose together, cross-linking carbohydrates, and providing mechanical strength and biodefence to plants. Lignin also provides the hydrophobic surface that allows plants to transport water to heights greater than 100 metres (Novaes et al., 2010). Wang (2016) defines lignin as an amorphous, polyphenolic material arising from an enzyme mediated dehydrogenative polymerisation of three phenylpropanoid monomers; conniferyl, synapyl and p-coumaryl alcohols (Figure 1.8).

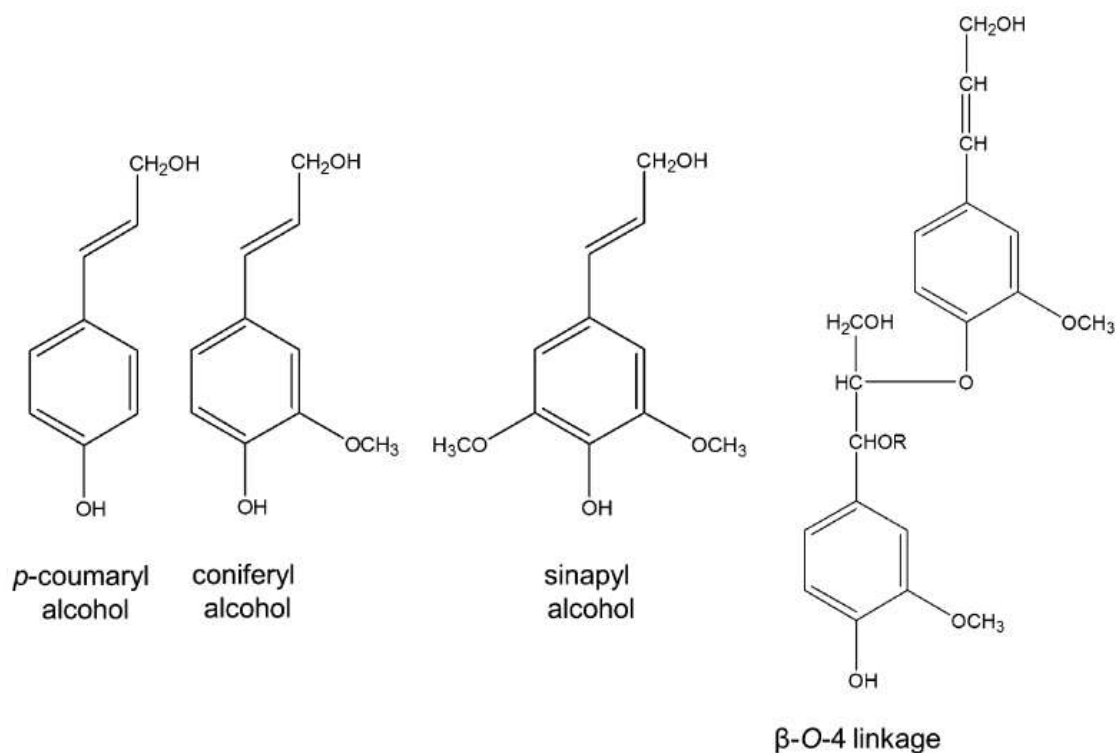


**Figure 1.8. The lignin precursors and the most abundant binders in lignin (Santos et al., 2012)**

Viscoelastic properties of wood are due to the amorphous polymer structure of lignin. Lignin demonstrates both areas of elasticity and areas of viscosity, with the elastic regions responding immediately to strain and the viscous areas responding more slowly. Viscoelastic properties are often advantageous causing the wood to bend under strain rather than snap, with the lignin matrix dissipating energy through the structure.

In general softwood contains 26 – 32% lignin, temperate hardwood structures contain 20 – 25% whilst tropical hardwood structures can contain in excess of 30% lignin. Evidence has shown that softwood lignin varies little between species, however it has been suggested that the structure of hardwood lignin may vary greatly between species (Santos et al., 2012).

### 1.5.2 Hardwood and softwood structures

The anisotropic nature of wood means that it is described in three co-ordinate directions; radial, tangential and longitudinal (Figure. 1.9).



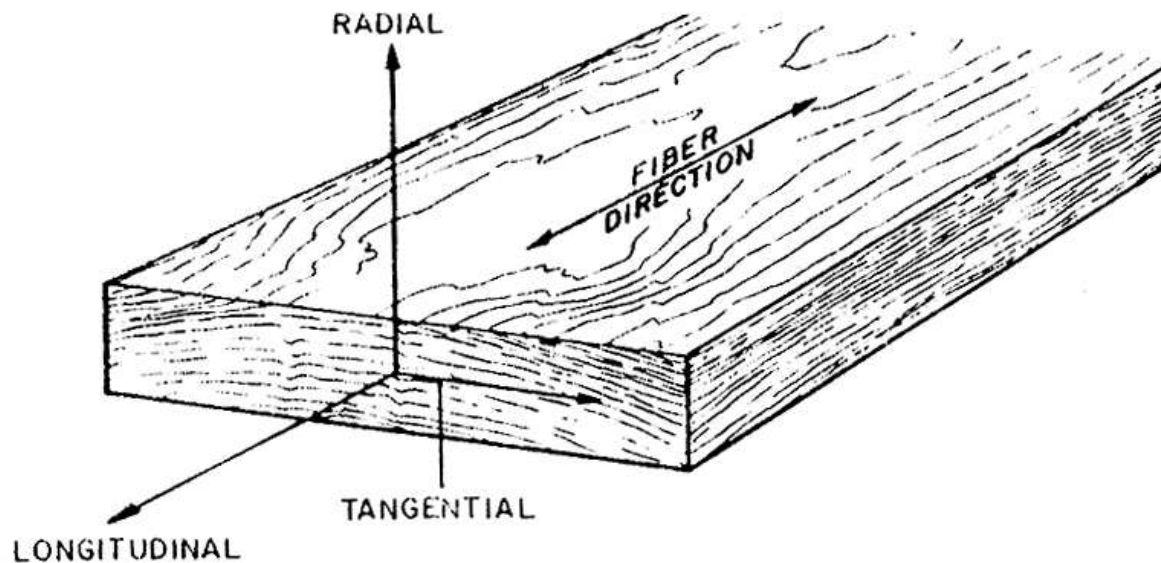


**Figure 1.9. Diagram showing the three main axes in wood; longitudinal, tangential and radial. With respect to grain direction and growth rings, taken from (Bergman, 2010)**

Wood species can be characterised by their macroscopic characteristics and are classified into two distinct groups; gymnosperms also known as softwoods and angiosperms also known as hardwoods. However the structure and permeability of wood can be complex to understand due to the presence of early and late wood, sapwood and heartwood within the species (Eriksson et al., 1990).

#### **1.5.2.1 Softwood**

Softwoods have a simpler structure than hardwood (Figure 1.10). For most softwoods over 90% of the wood is composed of vertical cells called tracheids, these longitudinal cells control fluid conduction through the wood (Stamm, 1964). The cell cavity of the tracheid is called the lumen and adjoining each tracheid are openings known as pits (Section 1.5.2.3). Pits in softwoods consist of minute membrane pores which can be easily blocked by debris, thus affecting fluid penetration (Section 1.5.6). In the horizontal plane, bands of ray parenchyma cells are orientated from the pith of the tree to the bark. Around 1% of softwood is made up of resin canals.

#### **1.5.2.2 Hardwood**

Hardwood structures have two main types of cells in the vertical plane; vessels (pores) which are joined together one on top of another and carry sap upwards, and bulky tracheids that are made up of thick cell walls which provide strength in the vertical plane (Figure 1.10) (Stamm, 1964). These vessels can be arranged in one of two ways, ring-porous or diffuse-porous. In

ring-porous hardwoods the vessels are large in the early wood and small and evenly distributed in the latewood. Diffuse-porous hardwoods are composed of medium sized, evenly distributed vessels throughout. When the vessels dry up they are called tyloses. Some hardwoods have impenetrable tyloses and some have none, so are easily penetrable (Rowell, 2012). Longitudinal parenchyma are thin walled cells that store food for wood, in some domestic hardwoods up to 24% volume can be parenchyma. Horizontal rays are much more abundant in hardwoods than in softwoods. Hardwood rays have two different cell types; procumbent and upright cells. Procumbent cells are square or rectangular and arranged horizontally, whilst upright cells lie along the axis parallel to the grain and are located on the upper or lower ray margins.

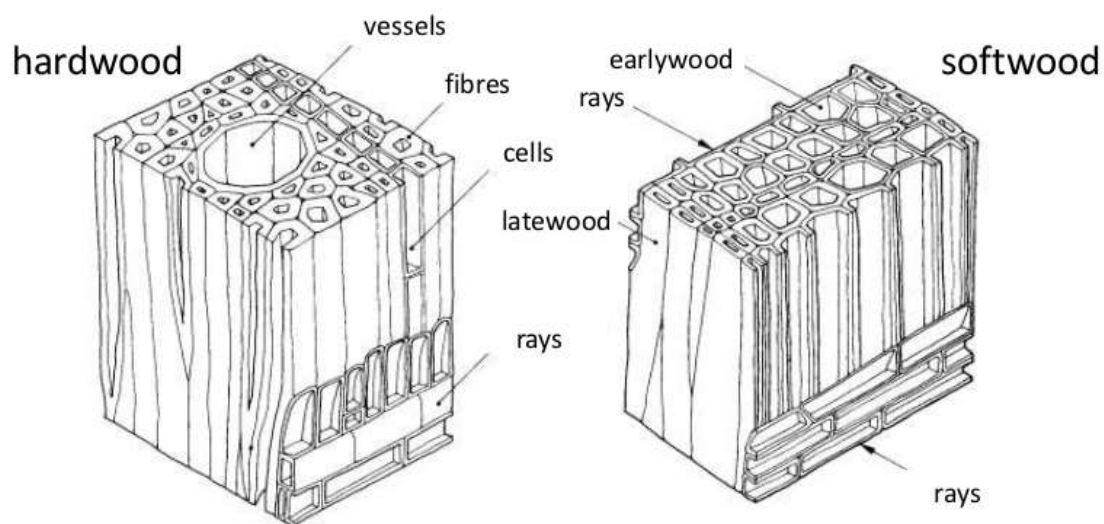


**Figure 1.10 Illustration to compare the cellular arrangement in hardwoods and softwoods. Taken from (Bergman, 2010).**

Many hardwoods are deciduous species. Temperate hardwoods tend to be dormant in winter, as the temperature falls in the autumn the trees will lose their leaves. Tropical hardwoods however will only lose their leaves in response to seasonal or sporadic periods of drought.

### 1.5.2.3 Pits

In both soft and hardwood flow between the longitudinal conductive cells is controlled by pits (Ahmed and Chun, 2011). The two main types of pits are called simple and bordered. All pits consist of a pit cavity and pit membrane. Pit cavity width can vary; in simple pits it is usually constant, in bordered pits the cavity wall narrows towards the cell lumen. The pit membrane is made up of the primary wall and middle lamella. Pits commonly occur in pit-pairs, as the walls of adjoin cells are layered on top of each other. Two simple pits are a simple pit-pair, two

bordered pits are a bordered pit-pair and a pairing of a simple and a bordered pit is called a semi-bordered pit (Rowell, 2012).

In softwood bordered pits, the membrane has a central thickened disk called a torus. Aspiration of this pit can occur through lateral displacement of the membrane, this usually occurs when a wood is dried or when sapwood is transformed into heartwood. Permeability of aspirated pits depends on membrane area, the type of material that has covered the membrane and how firmly the torus is seated. In unaspirated pits permeability is a function of porosity, thickness and membrane area.

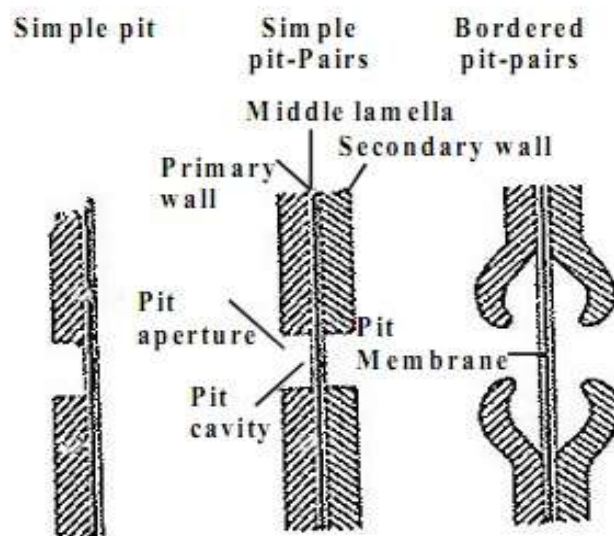


**Figure 1.11. Diagram showing the common types of pit pair (from left to right) A: Simple pit. B: A simple pit-pair. C: Softwood bordered pit pair where the border is raised above the level of the surrounding wall and the membrane has a torus. Reproduced from (Meylan and Butterfield, 1972).**

### 1.5.3 Wood strength and stiffness

Wood is found to be reasonably stiff, this is due to the composite nature of the material. As discussed in Section 1.5.1 wood is made up of cellulose fibrils, hemicellulose and lignin. The cellulose fibrils bind the lignin and hemicellulose together providing strength within the wood structure. The fibrils have a Young's Modulus (E) value of 100 GPa with lignin and hemicellulose only around 6 GPa (Greer, 2008). As expected the cell walls within the wood have a much higher elasticity than the wood itself. Hence less force is needed to split with the grain, separating the weaker lignin and hemicellulose, whilst a greater force is needed to split the strong cellulose against the grain.

Modulus of Elasticity (MOE) refers to Young's Modulus and is a number that measures an object or substance's resistance to being elastically deformed as a force is applied to it. MOE of wood is made weaker by spaces between the cell walls being filled by air or water even though the cellulose fibrils have a high Young's Modulus. Modulus of Rupture (MOR) or bending strength is defined as the stress in a material just before it yields in a flexure test. MOR can be used to measure a wood species overall strength, unlike MOE, which measure's the woods deflection but not its overall strength. Young's Modulus is strongly correlated to density as shown in Figure 1.12. Typically, a very stiff (or very strong) material has a high value of Young's Modulus and a high density, hence as the density of the material increases so does the stiffness. Wood types have very different densities depending on the different specimens. For example, Balsa is a very low density wood at about  $100 \text{ kgm}^{-3}$  whist Oak can have a density of up to about  $1000 \text{ kgm}^{-3}$ .

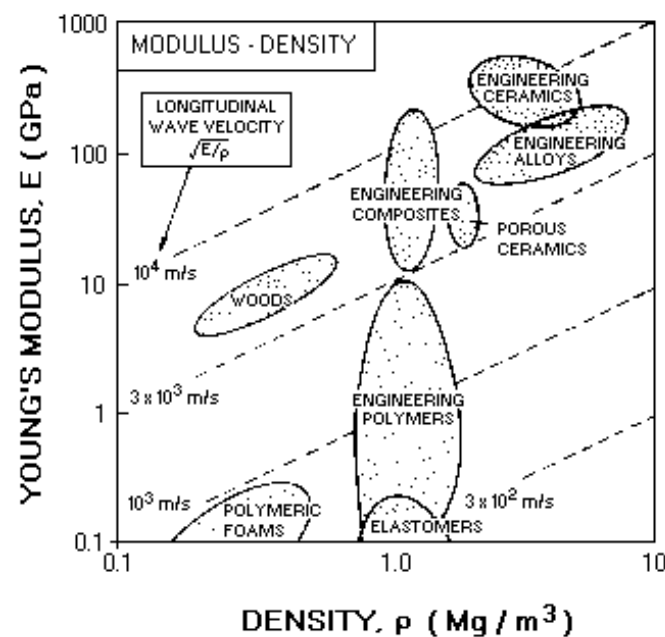


**Figure 1.12. A graph to represent the relationship between density and Young's Modulus for different wood types with and across the grain. Reproduced from (Walters et al., 2010)**

### 1.5.4 Moisture content in wood

Wood is a hygroscopic material. Hygroscopic materials absorb and retain moisture from the air; high levels of humidity lead to high levels of moisture being absorbed by the wood structure. Water molecules are attracted to the free hydroxyl sites on the cellulose polymer chain resulting in a monomolecular layer of water held in place by strong hydrogen bonds. The pushing apart of the cellulose by the water molecules is the beginning of the wood structure

starting to swell. The measure of water in wood is described by the Moisture Content (MC). MC is a percentage measure of how much water is in wood relative to the wood itself (Simpson, 1993) this is expressed in Equation 1.2 below (Eckelman, 1994);

$$MC = \left( \frac{\text{wet weight} - \text{dry weight}}{\text{dry weight}} \right) \times 100 \quad \text{(Equation 1.2)}$$

Equilibrium moisture content (EMC) occurs when the MC of the wood is stabilised and there is no difference in the vapour pressure between the wood and local air. EMC in hygroscopic materials is reached when the surrounding environment has a temperature and relative humidity that are stable.

Wood Condition	MC (%)
Dry Wood	$\leq 19$
Stabilised Wood – INDOOR	8 – 14
Stabilised Wood – OUTDOOR	12 – 18
Fibre Saturation	28

**Table 1.5 Moisture content values for wood in different conditions. Values taken from (Reeb, 1995)**

When a wood becomes saturated, and reaches a MC of about 28% there are two types of water known to be present in the wood structure; free and bound water. Water held in the cell walls is known as bound water, this is where water will be held initially when the wood absorbs moisture. Once the fibres within the cell wall become saturated water will be absorbed and held in the cell cavities, this is free water. The presence of free water can be destructive and lead to decay as the water is accessible within the wood structure. Therefore, usually decay only starts to occur once the MC of wood goes beyond the fibre saturation point (FSP).

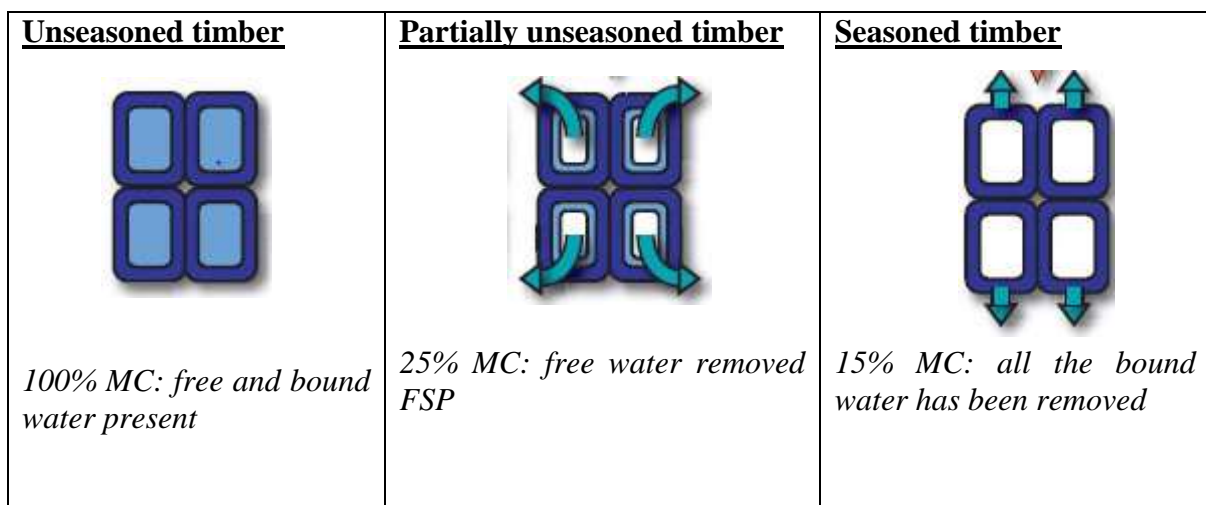


**Figure 1.13. The presence of free and bound water and the respective MC values in the three stages of seasoned to unseasoned timber. Drawn by author.**

Changes in MC can also cause wood to shrink and swell, this only occurs below the fibre saturation point with shrinkage commonly taking place between 28 – 19% MC. Changes in the presence of bound water in the cell walls directly effects dimensional changes in wood, however free water has no effect as it is only present above a MC of 28%. Shrinkage is known to take place mainly the tangential plane of the wood, with only half as much occurring in the perpendicular plane. Repetitive shrinking and swelling can cause ‘checks’ or cracks to develop tangential to the wood rings, causing permanent structural damage.

#### 1.5.4.1 Effect of water on the mechanical behaviour of wood

Increased water content in wood lowers the stiffness and strength of the wood structure. When wood is saturated the cell walls fill with water, which causes them to soften and change in dimension. The cellulose fibrils that make up the cell wall have both a crystalline and amorphous matrix composed of a series of polymer chains. These polymer chains have strong hydrogen bonds between the cellulose-cellulose chains. However, cellulose-water bonds are more preferential due to water being a small highly polar molecule, thus cellulose-cellulose bonds are broken to form cellulose-water bonds. The hydrogen bond linkage in cellulose is show in Figure 1.14.

The broken cellulose bonds cause the softening of the cell walls, making the fibrils easier to stretch, in turn reducing stiffness. The strength of wood is also reduced as wood becomes saturated and water fills the cells walls, the walls expand, increasing in surface area and reducing the number of cellulose fibrils per unit area (Greer, 2008).

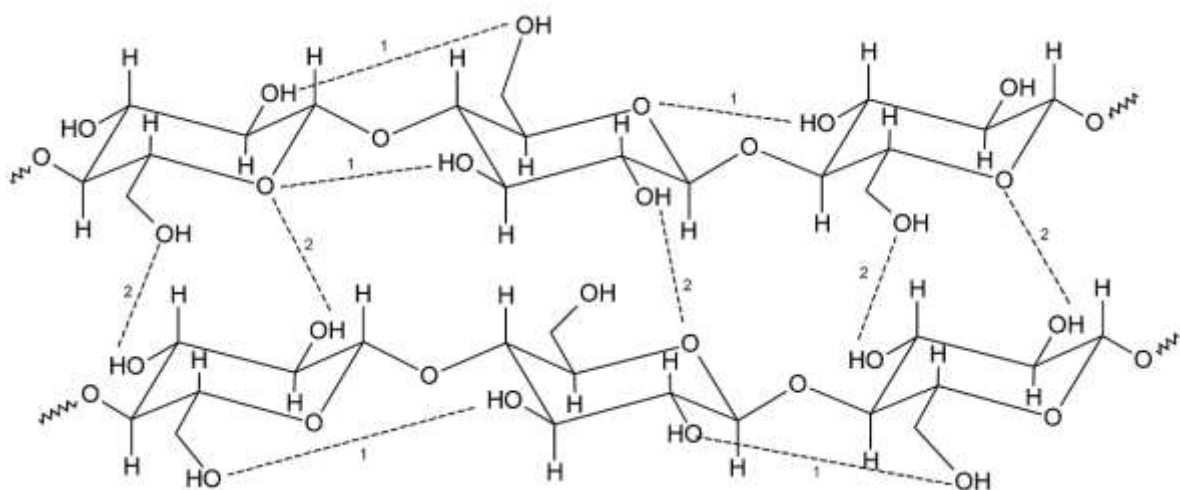


**Figure 1.14. The structure and intra - (1) and interchain (2) hydrogen bonding pattern in cellulose (Baptista et al., 2013)**

### 1.5.5 Transportation processes in wood

The transport of fluids through wood can be divided into two types; bulk flow and diffusion.

#### 1.5.5.1 Bulk flow

Bulk flow is the flow of fluids through the interconnected voids of wood structure under the influence of a static or capillary pressure gradient e.g. the impregnation of wood with monomers for in-situ polymerization or the pressure treatment of wood with biocides to prevent decay. The extent of bulk flow of a fluid through a wood is determined by permeability (Siau, 1984).

Discussing the relationship between porosity and permeability can help us greater understand bulk flow through wood. Porosity is a measure of how much of a material is open space, whilst permeability is a measure of the ease with which a fluid can move through a porous material. A material therefore has to be porous to be permeable, however for permeability to exist the spaces in the material must be connected by free unblocked openings, hence not all porous materials are permeable (Hoadley, 2000). The permeability of wood will therefore also depend on the distribution of pit pairs and the number of cell walls that must be traversed. As mentioned in Sections 1.5.2.1 and 1.5.2.2 the structure of wood not only varies greatly between species and specimens of the same species, but between one growth ring to the next (Stamm, 1964). It is therefore acknowledged that fine measurements of both permeability and porosity in porous solids are difficult to calculate.

Darcy's Law is commonly used to describe liquid flow through porous media, however it can also be used to help understand the flow of fluids through wood (Cussler, 2009):

$$\text{Conductivity} = \frac{\text{Flux}}{\text{Gradient}} \quad \text{(Equation 1.3)}$$

Here conductivity is permeability. Darcy's Law makes a number of assumptions some of which are not applicable to wood. Nonetheless it is still useful to utilise Darcy's Law for looking at flow rate and pressure gradient. The main assumptions of Darcy's Law are (Siau, 1984):

- I. Flow through the media is viscous and linear. Applied pressure differential is therefore directly proportional to linear velocity and volumetric flow.
- II. The fluid is homogenous and incompressible.
- III. The porous medium is homogenous.
- IV. There is no interaction between the fluid and the substrate

V. Permeability is independent of length of the specimen and flow direction.

Accordingly, when applying Darcy's Law to wood the following assumptions should be addressed (Siau, 1984); I – viscous flow generally occurs when capillary openings are small, as they are in wood. For this there is a relatively high viscous drag because of the high ratio of surface area to volume. Under these conditions the high flow velocities necessary for turbulence are improbable. However, non-linear flow can occur at relatively low velocities where fluid moves from a large to a small capillary, such as a tracheid lumen to a pit opening. II – liquids are essentially incompressible, but the compressibility of gases must be taken into consideration. III and IV – wood has a very complex and non-homogenous structure especially in the case of hardwoods. When water flows through wood there are hydrogen bonding forces exerted by the hydroxyl sorption sites on the cell wall surface. Therefore, the permeability of wood to water and aqueous solutions is lowered in comparison to non-polar liquids of the same viscosity.

Darcy's Law for liquids:

$$K = \left( \frac{Flux}{Gradient} \right) = \left( \frac{\frac{Q}{A}}{\frac{\Delta P}{\mu L}} \right) = \frac{QL\mu}{A\Delta P}$$

**(Equation 1.4)**

Where K is permeability (m<sup>2</sup>), Q is volumetric flow rate (m<sup>3</sup>s<sup>-1</sup>), L is the length of the specimen in the flow direction (m),  $\mu$  is the viscosity of the liquid (Pa·s), A is the cross-sectional area of the specimen perpendicular to the flow direction (m<sup>2</sup>) and  $\Delta P$  is the pressure differential (Pa).

Due to the high penetration ability of SCF solvents compared to that of liquids, SCF impregnation for the delivery of aqueous solutions e.g. biocides, into wood and wood composites has become an area of great interest, with developments into commercial scale practices. scCO<sub>2</sub> is able to overcome pit impermeability which poses a limitation to effective biocide treatment in heartwood (Acda et al., 2001). It has been shown that SCF treatments are able to completely impregnate Douglas-fir heartwood, which have previously been resistant to fluid treatments (Morrell et al., 1993).

Wood will not equilibrate instantaneously when being pressurised by a fluid, a pressure differential will occur between the surface of the wood and the interior. The development of this differential is dependent on pressurisation, venting rates and the structural geometry of the



wood (Lenth and Kamke, 2007). Permeability is therefore directly related to pressure development. To some extent the differential can be controlled by adjustments in pressurisation and venting rates, therefore avoiding excessive pressure differentials and decreasing the chances of permanent damage to the wood structure (Schneider et al., 2006). However, the inclusion of a co-solvent makes the relationship more complex.

#### **1.5.5.2 Diffusion**

Diffusion through wood can be subdivided into two types; inter-gas diffusion which includes the transfer of water vapour through the air in the lumens of the cells and bound water diffusion which takes place within the cell walls of the wood. Examples of diffusion in wood include the air drying or kiln drying of wood and in the interior of woodwork or furniture in response to seasonal changes in relative humidity.

The movement of biocides into wood during SCF impregnation is also dependent on diffusion. The rate of diffusion is controlled by many factors including the chemical and physical interaction between each component part; wood, biocide and CO<sub>2</sub>. An understanding of each of these relationships and the condition effects upon them is crucial in being able to create a diffusion model to describe and predict impregnation (Lucas et al., 2007). Unfortunately, there has been limited success in the development of such models that are accurately able to predict the total retention figures and distribution of biocides in wood under supercritical conditions. Sahle-Demessie (1994) based a model for predicting retention and biocide distribution on 1-D compressible flow through porous media controlled by measurable fluid and wood characteristics. However, no attention was paid to adsorption and desorption interactions and their subsequent effect on the model. Kang et al. (2006) used the Egners solution method and experimental data to calculate a diffusion co-efficient in 1-D diffusion, however the co-efficients were found to be unusually high as the concentration gradients approached zero. Lucas et al. (2007) were able to create a two-parameter model that made accurate retention predictions. However, decanal, the biocide used has an extremely high solubility in scCO<sub>2</sub> compared to other biocides, and is capable of both physical and chemical reactions with lignocellulosic material.

This relationship between the lignocellulose and the high pressure scCO<sub>2</sub> is of importance, but not greatly understood (Kjellow and Henriksen, 2009). The structure of wood mainly consists of amorphous polymers. Sorption of scCO<sub>2</sub> into a synthetic polymer matrix can cause swelling

and affect the physical and mechanical properties of the polymer (Von Schnitzler and Eggers, 1999) (Section 1.2.2.1).

### 1.6. Additional material characterisation: leather

Leather encompasses a vast material category, as a product is can be made from the skin of any animal and can be manufactured in many ways (Guldbeck, 1969). The most common skins used for leather production include cattle, sheep, goats, pig and horse. The skin of any of these animals is made up of three main layers; the top layer or epidermis which provides waterproofing and a barrier to infection, the corium or dermis is the thickest layer and provides tensile strength and elasticity to the skin, and finally the bottom layer which is mainly consisted of flesh (Demeroukas and Ritchie, 2015) (Figure1.15). The correct handling of the corium layer in skin produces a durable and flexible leather, a tanner's main job is to preserve the corium from putrefaction. The corium *"is made up of collagen fibres, which in turn are composed of helically-twisted protein biopolymers, chemically linked to one another to allow for strength and flexibility"*(Storch, 1987). It is important to remember, especially when considering the conservation of leather products, that each species of animal will have a slightly different collagen composition in its skin, therefore giving the leather a unique appearance.

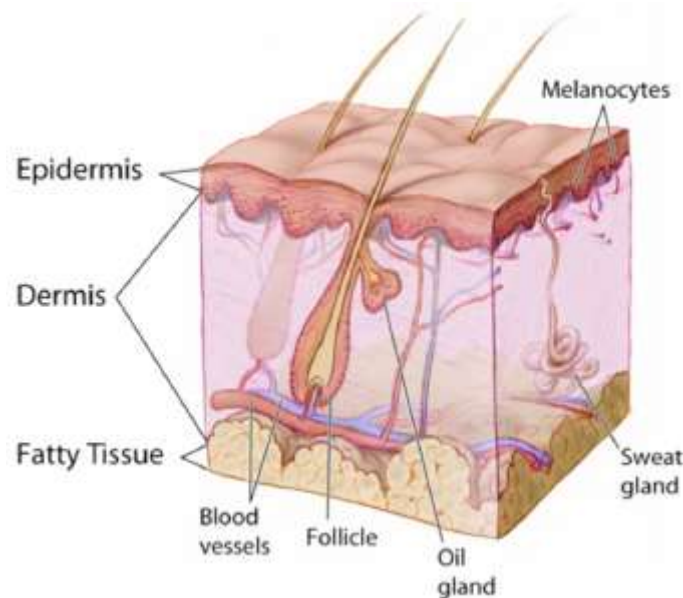


**Figure 1.15. A diagram to show the three main layers of skin: epidermis, dermis and fatty tissue or flesh. Reproduced from (John. F, 2015)**

The manufacture of leather has changed greatly over the last 50 years with the development of faster tanning processes. Traditionally leather was manufactured via vegetable or alum tanning, the processes of which are outlined below. From 1884 onwards, chrome tanning was developed

and revolutionised leather production with much shorter tanning times, today, 80% of leather is produced via chrome tanning methods (Dirksen, 1997). Despite these different methods, the preparation for tanning all follow the same process which involves the following steps; soaking → fleshing → liming/dehairing → de-liming → bating → pickling. The removal of hair and the epidermis of the hide allows the tanning solution to infiltrate the collagen fibres, the flesh layer is also cut away leaving just the corium for conversion to leather.

### **1.6.1 Vegetable tanning**

Vegetable tanning is the most traditional form of tanning for leather production. This process uses tannins derived from plant sources such as extracts from bark and wood of trees e.g. oak. The tannin molecules bind to the collagen fibrils and separate them, this stops the fibrils from shrinking and sticking together and create a tough and durable leather that has a natural colour varying from pale to reddish brown.

However, vegetable tanning is not without its disadvantages. The process is very slow and can take up to two years, some tannins have also been found to produce leathers that are more susceptible to degradation by red rot (Van Soest et al., 1984). This is especially the case with leathers that were produced between 1850 – 1900. During this time,  $\text{H}_2\text{SO}_4$  was added to the preparation process as a more effective method of hair removal, consequently all the calcium salts which made the up protective enzymes known as ‘non-tans’, were also removed (Haines, 1991b). Although the addition of  $\text{H}_2\text{SO}_4$  gave the leather a higher quality finish desired by manufacturers, it also left the leather more much more susceptible to deterioration by red rot.

### **1.6.2 Mineral tanning**

#### **1.6.2.1 Alum tanning**

Alum tanning is the more traditional of the two mineral tanning methods outlined here, it follows a simple method called thawing that requires inexpensive chemicals. A chosen animal skin, typically pig or goat, is steeped in a warm solution of potash alum and salt for 10 to 15 minutes, egg yolk and flour may also be added at this point to enhance the leathers pliability and softness (Barlee, 2001). The leather is then removed and dried over a period of weeks. Leather produced by the thawing process is white in colour, soft and resistant to many microorganisms. It should be noted that the thawing process is not permanent and can be reversed by submerging the leather in water.

### **1.6.2.2 Chrome tanning**

Chrome tanning has been used from around the early 1880's onwards and is distinct from vegetable tanning in its efficiency of leather production. Leather hides must be placed in acid baths prior to the addition of chromium (III) sulphates, this ensures that the chromium complexes are small enough to fit between the fibre and residues of the collagen fibrils (Sreeram and Ramasami, 2003). The pH of the solution is then raised after a sufficient level of penetration of chromium has been reached, this is the basification step. Chrome tanned skins are naturally blue in colour (wet blue) but can be surfaced dyed to a variety of colours; the leather is also typically hard-wearing, waterproof and supple.

The main disadvantages associated with chrome-tanning are its related environmental concerns. The poor exhaustion levels of chromium salts have led researchers in America to believe that there would be an economical loss of \$100 million per annum, due to material loss (Sundar et al., 2002). Guidelines have been set for permissible levels of chromium in wastewater, however the high cost of treatment systems for chromium waste removal have rendered better management in tanneries a priority (Suresh et al., 2001b).

## **1.7 Analytical techniques for wood and leather**

### **1.7.1 Macrostructural analysis: Three-point bend test**

The three-point bending test is a popular method for determining the MOR and hence the strength of wood. In this test a specimen with a rectangular or flat cross-section is placed on two parallel supporting pins. The loading force is applied in the middle by means of a loading pin; the test requires very basic sample preparation and is simple to carry out. Motlagh et al. (2010) used the three-point bending test to evaluate the load capacity, ultimate strength, MOR and the mode of failures of Iranian historic wood samples that were reinforced with carbon fibre polymers. Samples were prepared as per ASTM D-143 (2006) standards. Samples such as these are said to be clear and homogenous and they are void of any defects such as knots or cracks which are common in unprepared wood samples (Motlagh et al., 2012).

Although the three-point bending test and the four-point bending test seem very similar in procedure and sample preparation they do have some distinct differences in application (Mujika, 2006). The four-point bending test is thought to be the more reliable of the two mechanical tests for measuring tensile stress, this is supported by Weibull statistical analysis (Junior et al., 2008). The selection of a mechanical test is important, especially if you are

dealing with very brittle materials such as ceramics. Hence the three-point bending test is recommended for homogenous samples like plastic, whilst the four-point bending test is more suitable for non-homogenous, composite materials (Belouettar et al., 2009). The three-point bend test is ideal for the specific isolation of stress on a material, whereas the four-point bending test produces peak stresses across a larger region of the test specimen, therefore causing greater exposure to possible defects or failures in a sample.

### **1.7.2 Microstructure analysis: Microscopy**

Wood properties at a macroscopic scale are in part determined by the structure at a microscopic scale. Light microscopy provides a simple and effective way of looking at wood morphology with minimal sample preparation. For conservation purposes species determination is a key step when assessing wooden artefacts. Light microscopy can provide identification of the wood species as well as information for evaluating the samples chemical, physical and mechanical properties (Mizuno et al., 2010, Čufar et al., 2014). Ultraviolet (UV) microscopy is convenient for the study of lignin compounds. This type of microscopy is able to exploit the characteristic  $\pi$ - $\pi^*$  transitions of the aromatic moieties in lignin that cause a higher level of UV absorption than lignin found in carbohydrates (Łucejko et al., 2015); Li et al. (2014) used UV microscopy to determine the state of lignin preservation in historic Chinese bamboo samples.

Scanning Electron Microscopy (SEM) can also be used for looking at the surface morphology of wood. Visual information about the sub microscopic level in wood which consists of microfibrils embedded in an interfibrillar matrix can also be determined. In SEM, after an electron beam is scanned across the surface of a prepared sample, signals caused by the excitation of secondary electrons are detected and mapped to produce images. For these images to be successful the samples must be carefully prepared. Typically, solid bulk samples are mounted on holders or stubs using a conductive tape or adhesive. Non-conductive samples such as wood, are then coated in a thin layer of electrically conducting material e.g. gold or gold/palladium alloy, via low vacuum sputter-coating. This coating enhances the emission of secondary electrons, allowing for more detailed mapping and thus more clarity in the SEM images produced.

By comparing known degradation effects on wood, sometimes known as ‘degradation signatures’, it is possible to observe and classify types of bacterial and fungal attacks on wood via SEM (Blanchette, 2000). SEM is commonly used alongside other analytical procedures to help clarify types of degradation in wood and interpret chemical results. Light and electron

microscopy were used in conjunction to determine major forms of microbial decay in waterlogged wood found in Sweden (Björdal and Nilsson, 2001). SEM has also been used for the analysis of chrome tanned leather to study grain surface and fibre bundles (Suresh et al., 2001a, Krishnamoorthy et al., 2012).

SEM with Energy Dispersive X-ray spectroscopy or SEM/EDS is used for surface elemental analysis of solid materials. During SEM, interactions between the primary beam and the atoms in the test sample cause shell-transitions which result in the emission of an X-ray. The energy characteristic of the X-ray can be detected and characterised which allows for EDS analysis (Fandrich et al., 2007). SEM/EDS can provide quantitative analysis of elemental compositions with a sampling depth of 1 to 2 microns, as such it has been used to look at the level of penetration of water-based chemicals in wood cell walls (Wallström and Lindberg, 1999). Alongside other spectroscopic and micro-analysis techniques SEM/EDS has also been used for the characterisation of historic leather samples; seven separate paint layers and individual pigment grains were identified on a post-Byzantine icon of St Nicolas painted on a leather support (Ganitis et al., 2004) using Raman spectroscopy and SEM/EDS. The same combination of analytical techniques were used successfully to determine the palette used on seventeenth century illuminated pages and a leather screen (Chaplin et al., 2010).

### **1.7.3 Spectroscopic analytical techniques**

Fourier Transform Infra-Red (FTIR) spectroscopy is the most regularly used spectroscopic technique when analysing wood samples. This is probably due to laboratories more commonly having FTIR rather than Raman spectrometers. FTIR is suitable for wood analysis therefore labs do not need to invest in new equipment for this type of study. Additionally, extra care may need to be taken with analysis by Raman spectroscopy due to possible heat damage to the samples caused by high power lasers. Qualitative and quantitative analysis of wood samples by FTIR has been used by Chen et al (2010). Multivariant calibration models were used to separate samples into hardwoods and softwoods with quantities of lignin, cellulose and hemicellulose also being identified (Chen et al., 2010). FTIR has also been used successfully to look at rot deterioration caused by fungi in wood. Changes in spectral bands associated with lignin and carbohydrates were able to indicate the level of decay over time in different wood species (Pandey and Pitman, 2003). Thermogravimetric analysis alongside FTIR (TG-FTIR) has been used to help understand the pyrolysis mechanism of lignin (Liu et al., 2008). Due to its advantageous properties this method of online gas analysis has been widely adopted to look

at the kinetics and mechanisms associated with biomass. Attenuated Total Reflectance FTIR (ATR-FTIR) has been used to quantitatively distinguish degradation differences in historic and sound elm wood (Pizzo et al., 2015) .

Raman spectroscopy uses the inelastic scattering of monochromatic light from a laser in the visible, near infrared or near ultraviolet range. Interactions between the laser light and molecular vibrations or excitations in the system, result in energy of the laser photons being shifted up or down. The shift in energy can provide information about the vibrational modes in the system. As such Raman spectroscopy can be used in science conservation and cultural heritage as it provides a non-destructive qualitative and quantitative analysis of organic materials at a chemical level (Łucejko et al., 2015). Despite this there are few examples of Raman being used for conservation analysis, Petrou et al (2009) and Marengo et al (2003) provide some of the few examples of the analysis of Neolithic and sixteenth century wood via FT-Raman. Information on the chemical composition of wood and pulp fibres provided by Raman spectra are of interest in industry, especially when related to changes due to processing. However Raman spectra of the lignin constituents within wood can be extremely complex to interpret, as such much work has been done around lignin, their models and lignin model compounds to further understand the spectra produced (Agarwal, 2008).

Although Diffuse Reflectance Infrared Fourier Transform (DRIFT) spectroscopy is suitable for opaque materials such as wood, the technique can introduce anomalies into the IR spectrum of wood (Ferraz et al., 2000). These anomalies occur because of a scattering effect due to the irregular surface of wood, nevertheless it is possible to reduce this effect and produce high quality spectra by using granular size samples and a solution of potassium bromide (Michell, 1994) or for solid wood surfaces, the roughness and structure of the cut must be identical (Pandey and Theagarajan, 1997). Baldock et al (2002) used a combination of DRIFT and solid-state  $^{13}\text{C}$  nuclear magnetic resonance (NMR) to assess the chemical composition of char after the incomplete combustion of vegetation. NMR is a powerful analytical tool for determining the chemical characterisation of natural materials such as wood (Bardet et al., 2004). The water content of wood is a common measure of degradation within archaeological wood samples. Bardet et al (2004) used ssNMR to give an illustration of the water content of archaeological wood as an indication of the state of degradation, however it was noted that it was still difficult to determine the structural properties of historic waterlogged wood.

## 1.8 Aims of this work

Although there are established methods used by conservators to help hydrate dry and brittle materials in museum collections, none are ideal. Therefore a need exists to explore alternative hydration techniques. Given that SCFs have been used successfully in various areas of art conservation, the overall objective of this work was to explore whether similar methods could be applied to the hydration of wood.

More specifically, the main aims of this work were to;

- Design, construct and optimise process equipment for supercritical hydration, using scCO<sub>2</sub> as the fluid of choice, and additionally to investigate co-solvent addition and changes in experimental process parameters.
- Investigate supercritical hydration as a method for the addition of water to wood samples, including historic and modern, hardwood and softwood.
- Assess, via microstructural and macrostructural analytical techniques, the extent of any damage caused during the supercritical hydration treatments. It is hoped that assurance can then be made to conservation professionals as to the suitability of this technique.
- Investigate the potential of the supercritical hydration mechanism to maintain or increase the MOR of the wood samples.
- Present findings to conservation professionals at cultural heritage conferences and symposiums to assess the suitability of the supercritical hydration technique as a standalone, or collaborative method in art conservation. Compare this novel process with conventional methods of wood hydration used in conservation departments.
- Finally, in a feasibility study to investigate other historic media, assess the additional applications of scCO<sub>2</sub> technology for use in conservation departments.



## Chapter 2: Hydrating Wood Using Supercritical Carbon Dioxide

### ABSTRACT

The use of supercritical carbon dioxide ( $\text{scCO}_2$ ) in the presence of water ( $\text{H}_2\text{O}$ ) to drive the absorption of water into oven dried, rectangular samples of historical and modern, hardwood and soft wood (Scots Pine, Maple, White Oak, Red Oak, Zebrano, Keruing) (length = 0.06 m, width = 0.01 m and height = 0.01 m) samples were investigated. All experiments were carried out at  $50^\circ\text{C}$  under 20 MPa of pressure for 45 minutes. Additionally, the effect of the co-solvent, methanol ( $\text{MeOH}$ ), on the hydration levels of the wood samples was investigated. Comparison of these results allowed a mechanism for the supercritical hydration of wood samples to be suggested.

A range of conditions were then chosen to hydrate the wood samples that could then undergo a selection of microstructural studies (using Light Microscopy, Scanning Electron Microscopy and Diffuse Reflectance Infrared Fourier Transform spectroscopy) and further analysis of sample properties including hydration via mass measurement and strength via the three-point bend test. All samples were compared to oven-dried untreated samples.

The historic and modern wood samples hydrated with  $\text{scCO}_2$  all gained in mass after treatment. Increasing the concentration of the co-solvent,  $\text{MeOH}$  ( $\text{scCO}_{2(\text{MeOH})}$ ), improved the levels of hydration; increased mass gain and a higher stable mass gain over time was recorded for all wood samples. Wood type was found to have more of an influence than wood age upon water absorption and retention, with hardwood samples being the most responsive to the supercritical treatment. The type and/or relative quantity of water absorbed by the hydrated wood samples was the most difficult property to deduce. As such, speculative conclusions have been made from the collaborative analysis techniques carried out.

## 2.1 Introduction

The presence of dry and fragile materials such as wood, leather and paper is not unusual within museum collections. A variety of established methods are used by conservation professionals to help stabilise and preserve these materials for continued public enjoyment (Richmond, 2009). These approaches, although effective, do not always seek to strengthen the materials but simply stabilise them. Previous research has shown that there may be a role for SCFs and more specifically  $\text{scCO}_2$ , within existing conservation practices. These have included the deacidification of books and paper and the removal of harmful pesticides from ethnographic objects and other fragile museum artefacts (Français et al., 1997, Tello, 2006).

The wide application of uses and the differing structural properties of both hardwood and softwood species means that wood is a material found in many guises within museum collections. From picture frames to canoes, tables to bow and arrows, wooden objects and treenware take many forms and thus provide conservators with many problems. Due to the hygroscopic nature of wood it is often found in a fragile state which requires preventative conservation methods, usually in the form of environmental controls, to preserve the wood as well as possible. Development of a safe and effective interventive hydration method for wooden artefacts and objects may therefore be of use to conservation professionals. Hydration with  $\text{scCO}_2$ , in the presence of water may provide an alternative route for the prevention of future damage to the wood stability and structure.

The wood samples discussed in this thesis were oven-dried to a constant mass to within  $\pm 0.001\text{g}$ , to simulate dried out wood that may be found in museum collections. Discussion of the effect of different moisture contents in wood can be found in Section 1.5.6. Once the supercritical hydration treatment had been achieved the properties and microstructure of the wood samples were studied in detail. This is the main area of research in this chapter: the external and internal structure of (treated and untreated) historic and modern wood samples, as well as hydration, strength, and visual properties. Supercritical hydration with the co-solvent, MeOH, showed some benefits over supercritical hydration without a co-solvent.

### 2.1.1 Solvent systems and the use of methanol as a co-solvent

Hydration of wood using both pure  $\text{scCO}_2$  ( $\text{scCO}_{2(\text{PURE})}$ ) and  $\text{scCO}_2$  modified with MeOH ( $\text{scCO}_{2(\text{MeOH})}$ ), in the presence of water, was carried out. The critical point of  $\text{scCO}_{2(\text{PURE})}$  is known to be 31.1°C and 7.38 MPa (Kumar et al., 1987). As discussed in Section 1.1.4, when a co-solvent is added into the solvent stream and a binary solvent mixture is produced, the critical point will be altered. The critical point of the binary solvent mixture will determine whether the system exists in a single phase or in a vapour-liquid equilibrium under the chosen conditions. For the experimental conditions discussed in this chapter to remain constant, it was ensured that the system was in the single phase, supercritical region for all treatment procedures. Phase diagrams and Table 2.1 below were consulted to ensure the correct conditions were maintained.

MeOH mole fraction	Tc (°C)	Pc (MPa)
0.00	31.1	7.4
0.07	51.1	10.5
0.12	64.9	12.2
0.20	85.9	14.4
0.36	124.4	16.5
1.00	240.0	8.0

**Table 2.1 The critical temperatures and pressures of a  $\text{scCO}_2$  and MeOH system. The critical temperatures and pressures increase with increasing MeOH concentration.**

## 2.2 Materials

### 2.2.1 Rig components

The high-pressure rig was constructed from 316 stainless steel rated to 45 MPa at 200°C, connected by stainless steel Swagelok fittings (Swagelok, Manchester, UK). The rig vessels with volumes of 5 mL and 25 mL are also rated to 45 MPa at 200°C. Details of further rig components and experimental set up is found in Section 2.3.

### 2.2.2 Wood Preparation and storage

Modern hardwood samples were collected from SL Hardwoods (Croydon, UK), whilst historical hard and softwood samples were collected from Oxford Violins (Oxford, UK) and Oxford Wood Recycling Ltd (Abingdon, UK). All the wood samples were kept under ambient conditions until they underwent oven drying.

### **2.2.2.1 Desiccant based versus nitrogen purged storage solutions for treated wood samples**

There are two main storage techniques used when looking to achieve low humidity atmospheres for storage within a desiccator; desiccant based or nitrogen (N<sub>2</sub>) purged storage. Desiccant based storage techniques commonly consist of a desiccator chamber containing a naturally hygroscopic material e.g. silica gel, which absorbs moisture from the ambient air within the chamber, thus reducing the humidity. This is a simple and economic solution for storage however it does not give a precise control on humidity and the removal of moisture from the environment is a passive process which is slow in achieving a dry environment. Frequently removing the wood samples from the chamber will reintroduce moisture, once again increasing the amount of time taken to create a low relative humidity atmosphere. Nitrogen purged storage provides an alternative solution that is more time efficient. The introduction of nitrogen gas from an external source into a chamber effectively replaces a humid atmosphere, containing water, with an inert, dry atmosphere containing N<sub>2</sub>. The treated wood samples in the experimental procedure outlined in this chapter are weighed at regular intervals over an extended period. The rapid recovery time of the N<sub>2</sub> purged storage technique which reduces the exposure of the wood samples to moisture, is therefore the most appropriate method of storage for this experimental procedure.

Treated wood samples were kept in N<sub>2</sub> sealed containers that were purged with N<sub>2</sub> every time the samples were removed for weighing, therefore limiting the exposure to ambient conditions in the lab. The N<sub>2</sub> sealed containers were stored in a cupboard in the lab in which the rig was set up, internal lab conditions were monitored over the duration of the experiments. A control was also set up whereby one untreated (oven-dried) and three treated wood samples (scCO<sub>2</sub>(PURE) and scCO<sub>2</sub>(MeOH) with MeOH at 2.5 mol% and 5.0 mol%) were kept in a low humidity dessicator chamber with silica gel over a 48-week period. The results of this controlled test can be found in the Appendix (Appendix 1).

### **2.2.3 Carbon dioxide and methanol**

CO<sub>2</sub> (liquid withdrawal) was supplied by Air Liquide (Paris, France). Absolute MeOH (99.9% pure) was supplied by Fisher Scientific (Loughborough, UK) and was of Analar grade.

## 2.3 Apparatus and methodology

### 2.3.1 High pressure equipment and supercritical hydration method

The experimental rig, constructed by the author, for carrying out supercritical hydration experiments is shown in Figure 2.1.

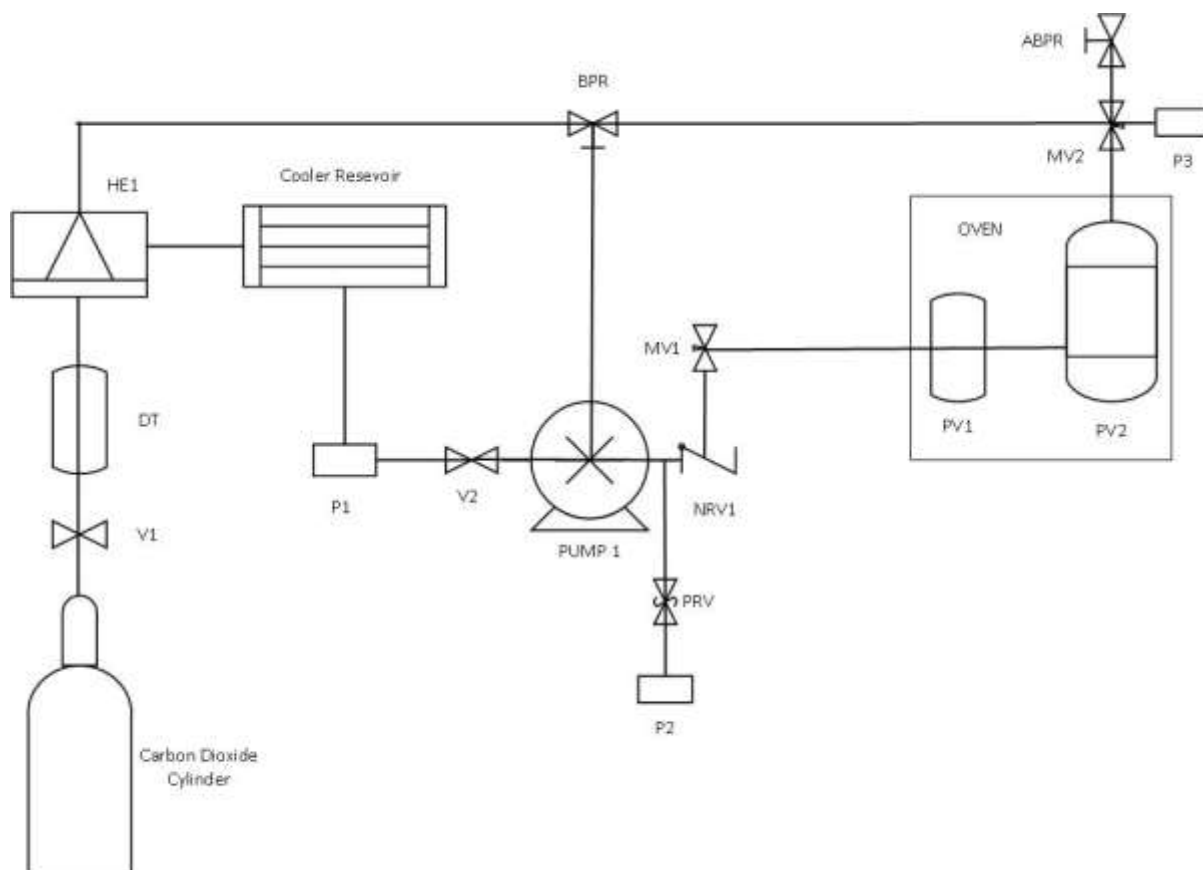


**Figure 2.1.** A schematic illustration of the supercritical hydration rig as constructed by the author. Key: V1 = CO<sub>2</sub> inlet valve; DT = dessicator tube; HE1 = refrigerated heat exchanger (cooling); P1,2,3 = pressure gauges; V2 = pump inlet valve; PUMP1 = pneumatic liquid CO<sub>2</sub> pump; PRV = safety pressure release valve; NRV1 = non-return valve; MV1,2 = micrometering valves, PV1 = hydration pressure vessel, PV2 = reaction pressure vessel; ABPR = automated back pressure regulator; BPR = back pressure relief valve.

The rig, seen in Figure 2.1, can be separated into three separate sections; supercritical fluid delivery, supercritical hydration, and depressurisation.

### ***Supercritical Fluid Delivery***

This section delivered CO<sub>2</sub> at the correct pressure to the hydration section. Liquid CO<sub>2</sub> was supplied by a 50 kg cylinder released by the valve (V1). CO<sub>2(l)</sub> was withdrawn and passed through a refrigerated heat exchanger coil in a liquid state to allow efficient pumping and avoid cavitation effects in the pump. The refrigerated heat exchanger coil was chilled by a continuous flow of coolant fluid from the recirculation bath, maintained below -10°C by the refrigeration unit (Stuart SRC4). The cooled CO<sub>2(l)</sub> was compressed to the desired pressure using a Thar high pressure P-series pump. The pressure and flow rate was monitored and set by the Thar Instruments Process Suite. CO<sub>2(l)</sub> leaving the pump passed through a non-return valve (NRV1) into the oven.

### ***Supercritical Hydration***

CO<sub>2(l)</sub> was delivered into the hydration section at a controlled pressure and was heated to a desired temperature before passing over the material which was being hydrated. The compressed CO<sub>2(l)</sub> entered the oven (Genlab MINO/50) which was set to 50°C, and passed through the 5 mL hydration vessel and the 25 mL vessel containing the chosen samples as scCO<sub>2</sub>. The system was held at static pressure for 45 minutes.

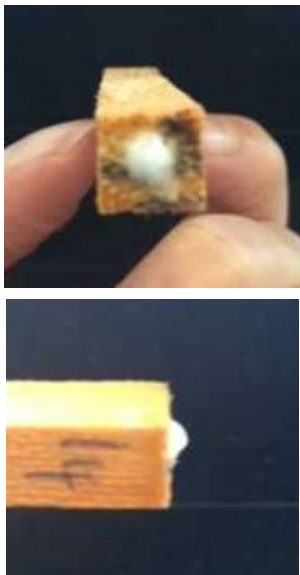
### ***Depressurisation***

Following the required hydrating period for the experiment the system was depressurised. To depressurise the system, the pump was turned off and the valve (MV1) was closed to hold the chilled CO<sub>2(l)</sub> for the next run. The exit valve (MV2) was opened further to allow for depressurisation over 45 minutes. A hair dryer was used to stop the CO<sub>2(g)</sub> freezing and blocking the exit valve when venting to atmospheric pressure. The CO<sub>2(g)</sub> was vented into a fume hood. CO<sub>2(g)</sub> was not recycled at this point.

#### **2.3.1.1 Depressurisation study**

To assess the most suitable rate of depressurisation for the system a selection of wood samples underwent treatment with scCO<sub>2</sub> and were depressurised over three different time periods. It was decided that the historic Scots Pine samples would be the most suitable for the study as they appeared to be the most fragile of the sample set and were the only softwood species. Post-

treatment samples were depressurised from 20 MPa to 0 MPa over 5, 45 and 90 minutes which were deemed fast, medium, and slow timescales respectively.

Rate of depressurisation (min)	Observations	Concerns
5	<p>Fractured samples</p> <p>Foaming at either end of the samples through epoxy resin layers (see photographs below)</p>  <p>Samples have reduced in mass</p>	<ul style="list-style-type: none"> <li>• Sample damage</li> <li>• Unsafe</li> <li>• Possible extraction</li> </ul>
45	<p>Visually samples seem unharmed by the treatment</p> <p>Samples have gained in mass</p>	<ul style="list-style-type: none"> <li>• N/A</li> </ul>
90	<p>Visually samples seem unharmed by treatment</p> <p>Samples have gained in mass</p>	<ul style="list-style-type: none"> <li>• Time consuming</li> </ul>

**Table 2.2. A table to show the observations recorded and the concerns regarding depressurising the scCO<sub>2</sub> system over three time periods.**

Depressurisation over 5 minutes gave some concerning results; it was observed that a possible extraction had taken place, highlighted by the photograph in Table 2.2, and there was also some structural damage to the samples. Although both times of 45 and 90 minutes gave no major

cause for concern regarding sample damage, it was thought that a time of 90 minutes may impede the number of experiments which could be completed within the available time. As a safe compromise, 45 minutes was selected as a suitable depressurisation rate that should, if performed correctly, cause no undue damage to the historic or modern wood samples subjected to the scCO<sub>2</sub> treatment.

### **2.3.2 Initial sample characterisation and the preparation of wood samples**

Wood samples were collected and characterised into historic (*H*) (>100 years since being cut) and modern (*M*) (<100 years since being cut) and then sub-categorised into hardwoods and softwoods. Hardwood species included Maple (*H/M*), White Oak (*H/M*), Red Oak (*M*), Zebrano (*M*) and Keruing (*H*). Scots Pine (*H*) was the only softwood species used. Table 2.3 below describes the key properties of the different species in the sample set. Grain type and texture are also described as they may be significant when analysing individual supercritical hydration levels in Section 2.4. It has been assumed that the wood samples have been taken from the heartwood of the tree rather than the sapwood, unless severe inconsistencies arise. The heartwood is the preferred cut for woodworking and construction as it is stronger and less susceptible to shrinkage and fungal attack. To deduce whether the wood samples consist mainly of earlywood or latewood, the age of the specific tree from which the samples originate would need to be known. As this information is not known it has been assumed that the wood samples consist equally of early and latewood, unless severe inconsistencies arise.



Wood Species	Properties	Grain Type/Texture
<b>Tropical Hardwood</b>		
<b>Zebrano</b> (Zebrawood) <i>Microberlinia brazzavillensis</i>	<b>Av. Dried Weight:</b> 805 kgm <sup>-3</sup> <b>Specific Gravity</b> (Basic, 12% MC): 0.67, 0.81 <b>MOR:</b> 122.8 MPa <b>MOE:</b> 16.37 GPa	Grain is usually wavy or interlocked with a coarse texture and open pores. Endgrain is diffuse-porous with medium pores in no specific arrangement.
<b>Keruing</b> (Apitong) <i>Dipterocarpus spp</i>	<b>Av. Dried Weight:</b> 745 kgm <sup>-3</sup> <b>Specific Gravity</b> (Basic, 12% MC): 0.59, 0.74 <b>MOR:</b> 115.2 MPa <b>MOE:</b> 15.81 GPa	Grain is generally straight to interlocked. Endgrain is diffuse-porous with very large pores in no specific arrangement.
<b>Temperate Hardwood</b>		
<b>Maple</b> (Hard Maple, Sugar Maple) <i>Acer saccharum</i>	<b>Av. Dried Weight:</b> 745 kgm <sup>-3</sup> <b>Specific Gravity</b> (Basic, 12% MC): 0.59, 0.74 <b>MOR:</b> 115.2 MPa <b>MOE:</b> 15.81 GPa	Grain is generally straight but may be wavy, Endgrain is diffuse-porous with small pores that are uniformly spaced.
<b>White Oak</b> (e.g. European Oak, English Oak) <i>Quercus alba</i>	<b>Av. Dried Weight:</b> 755 kgm <sup>-3</sup> <b>Specific Gravity</b> (Basic, 12% MC): 0.60, 0.75 <b>MOR:</b> 102.3 MPa <b>MOE:</b> 12.15 GPa	Grain is straight with a coarse, uneven structure. Ring-porous with 2-4 rows of solitary earlywood pores and numerous small latewood pores in radial arrangement.
<b>Red Oak</b> (e.g. Willow Oak) <i>Quercus rubra</i>	<b>Av. Dried Weight:</b> 700 kgm <sup>-3</sup> <b>Specific Gravity</b> (Basic, 12% MC): 0.56, 0.70 <b>MOR:</b> 99.2 MPa <b>MOE:</b> 12.14 GPa	Grain is straight with a coarse, uneven structure. Large, open pores
<b>Softwood</b>		
<b>Scots Pine</b> <i>Pinus sylvestris</i>	<b>Av. Dried Weight:</b> 550 kgm <sup>-3</sup> <b>Specific Gravity</b> (Basic, 12% MC): 0.39, 0.55 <b>MOR:</b> 83.3 MPa <b>MOE:</b> 10.08 GPa	Grain is straight with a medium, even texture. Medium sized resin canals, numerous and evenly distributed

**Table 2.3. Characterisation of individual wood species used in the experimental procedure described in this chapter. Species include Zebrano, Keruing, Maple, White Oak, Red Oak and Scots Pine. MOE is described here as the ratio of tensile stress to tensile strain. MOR is described here as the ratio of the rupture's bending moment to the beam's section modulus.**

Samples were kept under atmospheric conditions until they were cut with a precision high-speed table circular saw into rectangular pieces (length = 0.06 m, width = 0.01 m, height = 0.01 m). They were then lightly sanded to remove any debris from cutting. Each sample was then weighed, with the mass recorded being taken as the non-dried mass (M<sub>0</sub>). Samples were oven

dried at 70°C in the presence of anhydrous sodium sulphate to within a constant mass of  $\pm 0.001$  g, this mass was recorded as the oven dried mass ( $M_{1a}$ ). The initial moisture content (IMC) for the wood samples was taken to be:

$$IMC = (M_0 - M_{1a}) \times 100 \quad \text{(Equation 2.1)}$$

Typical IMC for stabilised wood indoors is found to be between 8.0% w/w and 14.0% w/w (Reeb, 1995), with modern wood having a higher MC than historic wood. The average IMC for historical and modern wood samples is shown in Table 2.4 below. The IMC on average for the historic woods was found to be around 7.7% w/w and for the modern woods around 9.0 % w/w. It is to be expected that the historic samples have a lower IMC given that they will have received a certain amount of damage over the years and will have been exposed to a variety of atmospheric conditions causing the wood to dry out.

Sample Type	Wood Species	Average Initial Moisture Content (% w/w)
Historic ( <i>H</i> )	Maple	8.0
	White Oak	7.2
	Scots Pine	7.1
	Keruing	8.3
Modern ( <i>M</i> )	Maple	9.7
	White Oak	8.6
	Red Oak	8.8
	Zebrano	8.8

**Table 2.4. A table to show the average initial moisture content in historic and modern wood samples before prior to SCF treatment.**

To be sure that the mass that is being lost from the wood samples could be claimed to be water weight a second method was carried out as a comparison. Wood samples were dried over the drying agent, anhydrous sodium sulphate, at room temperature and pressure until a constant weight was reached. This method confirmed that the weight lost from the wood during the oven dried method could be assumed to be water, with other volatile matter being insignificant. The oven dried method was chosen as the preferred method for establishing MC throughout the experimental procedure, due to its speed and ease.

Two coats of epoxy resin were painted on the ends of each sample to allow 2-D diffusion (Figure 2.2) rather than 3-D diffusion into the samples (Acda et al., 2001, Muin and Tsunoda, 2003). The resin was allowed to dry and the samples were re-weighed, this mass was recorded

as the oven dried + resin mass (M1b). Samples were then kept in N<sub>2</sub> sealed containers until they were needed for the hydration experiments, these samples were weighed at regular intervals in order to establish that a constant mass was being maintained.

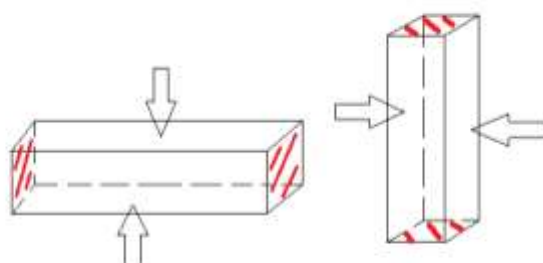


**Figure 2.2. Diagram to show expected diffusion into wood samples. Shaded areas represent coats of epoxy resin. Arrows represent the expected 2-D diffusion pathway of scCO<sub>2</sub> and water.**

### **2.3.3 Method for supercritical hydration of oven dried wood samples using supercritical carbon dioxide**

Preliminary hydration experiments were carried out in a single 70 mL pressure vessel. Cellulose tissue saturated with water was placed in the vessel linearly with two samples of wood, the vessel was then sealed. The tissue mass was recorded pre-and post-saturation. The oven temperature was set to 50°C and chilled CO<sub>2(l)</sub> was introduced to the system and pumped to pressure. All system valves were open during pumping, apart from the exit valve which was closed until depressurisation. The rig was set up to be a static system, pressure was held at 20 MPa for 45 minutes. Several experiments with both hardwood and softwood samples were carried out with this rig following this procedure.

#### **2.3.3.1 Addition of a separate hydration vessel and sample vessel**

It was found that higher levels of hydration were achieved if two separate pressure vessels were used in series with each other in the oven, rather than a single larger vessel (Figure 2.3). One 5 mL vessel was introduced as the hydration cell which held the cellulose tissue saturated with distilled water and one 25 mL vessel was introduced in series containing two wood samples. This rig layout was used for the duration of the hydration experiments, it is represented in Figure 2.1. The tissue mass was recorded pre-and post-saturation with distilled water, placed in the 5 mL vessel and sealed. If a co-solvent (MeOH) was used it was added at this point with

water to the cellulose tissue with a pipette. Two wood samples were placed linearly in the 25 mL vessel and sealed. Samples of the eight different wood species were carried out in quintuplets.

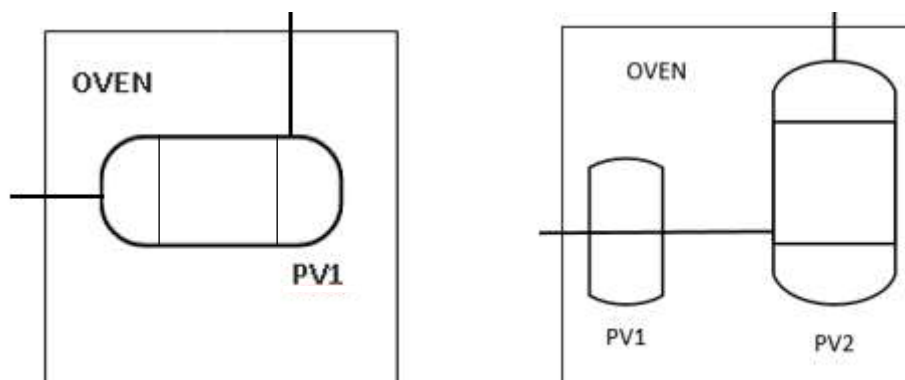


**Figure 2.3 A diagram showing two different pressure vessel layouts in the oven of the experimental rig; single vessel hydration (PV1) and dual vessel hydration which uses a separate hydration cell (PV1, PV2).**

The temperature of the oven was set to 50°C and recorded. A separate temperature probe (K Type thermocouple) with a digital monitor (TC305K Digital handheld thermometer) was used to ensure that the temperature remained constant for the duration of the experiment (Appendix 2). The CO<sub>2(l)</sub> was chilled to -10°C by the chiller unit and was introduced into the system by opening V2. All the system valves were opened apart from the exit (MV2) valve which remained closed until depressurisation. Once conditions had stabilised the samples were held at static pressure for 45 minutes. The pump was then turned off and valve (MV1) was closed to hold the chilled CO<sub>2(l)</sub> for the next run. The exit valve was manually opened slightly and with care to allow the system to depressurise slowly over 45 minutes in-order to avoid any damage to the samples. It was deemed safe to unseal the vessel when the pressure gauge (P3) read zero bar. The samples could then be immediately removed from the vessel to be weighed and stored in N<sub>2</sub> sealed containers.

### 2.3.3.2 Addition of methanol as a co-solvent

The reactions between scCO<sub>2</sub> and MeOH as a co-solvent are detailed in Section 1.1.4 (Chapter 1). Initial experiments showed that higher levels of hydration were achieved with higher concentrations of co-solvent in the scCO<sub>2</sub> solvent stream. This is due to the favourable increase in the solubility of water in scCO<sub>2</sub> with the addition of polar MeOH. However, adding a co-

solvent to a SCF alters the parameters of the critical point at which the fluid becomes supercritical, hence the addition of MeOH increases the  $T_c$  and  $P_c$  of the system. To avoid thermal damage to the samples it was preferred that the temperature of the oven was kept at or below 50°C. Concentrations of 2.5 mol% and 5.0 mol% were used as this allowed experiments to be carried out at ~50°C whilst also increasing hydration levels compared to 0.0 mol%. Concentrations of 10.0 mol% require a critical temperature and pressured of around 51°C and 10 MPa respectively, therefore concentrations were kept below this level.

The following table was used to calculate the volume ratio of MeOH to H<sub>2</sub>O (dilution factor) used in each experiment for the differing mole ratios. For example, to make a 2.5 mol% solution of MeOH<sub>(aq)</sub>:

	<b>MeOH</b>	<b>H<sub>2</sub>O</b>
<b>Vol (cm<sup>3</sup>)</b>	1.00	17.4
<b>Density (gcm<sup>-3</sup>)*</b>	0.792	1.00
<b>Mass (g)</b>	0.792	17.4
<b>Molar mass (gmol<sup>-1</sup>)</b>	32.0	18.0
<b>Moles</b>	0.0248	0.965
<b>Ratio</b>	1	39

**Table 2.5. Values used to calculate the dilution factor for 2.5 mol% MeOH in H<sub>2</sub>O. \*The SI unit of density is kgm<sup>-3</sup>, gcm<sup>-3</sup> has been used here as a convenient unit to allow for ease of calculation with figures to similar decimal places.**

Therefore, for 2.5 mol% the dilution factor is 17.4 MeOH/H<sub>2</sub>O. The co-solvent solution was used to saturate the cellulose tissue in the hydration cell. The tissue was saturated and replaced for each treatment.

### 2.3.4 Method for weighing hydrated wood samples

The percentage change in mass of each sample was calculated using the following equation:

$$\text{Percentage change in mass} = \left( \frac{M2 - M1b}{M1b} \right) \times 100 \quad \text{(Equation 2.2)}$$

Where M1b is the oven dried mass and M2 is the mass post SCF treatment. This value was known as the normalised moisture content (NMC) of the wood sample; the value is ‘normalised’ by the sample mass giving a percentage. This calculation was carried out immediately after depressurisation, continuing at regular time intervals until a constant mass

was reached, it was assumed that any mass gained during the treatment was due to water addition to the sample. For the duration of the time post-SCF treatment the samples were kept in individual, nitrogen sealed vials to maintain a dry environment. The vials were kept at lab temperature and pressure. All experiments (each involving two wood samples) were carried out in quintuplets. The mean values from each of the individual experiments were combined and an overall mean  $\pm$ one standard error of the mean calculated.

### **2.3.5 Methods for the analysis of microstructural studies**

#### **2.3.5.1 Scanning Electron Microscopy (SEM)**

Scanning Electron Microscopy (SEM) was used to study the internal microstructure of untreated samples and samples one week post-treatment. It was hoped that SEM would provide a visual aid as to whether the samples were being damaged internally by the moderate temperature and high pressure of the SCF treatment. The samples were fractured along the grain as carefully as possible to minimise further damage to the structure of the wood. Flat, square fragments of the wood samples approximately  $0.01 \times 0.01$  m were mounted on aluminium stubs (Figure 2.4). Colloidal carbon cement was placed on the base of the stub and up the side of the sample. The carbon cement ensured the non-conductive wood was made conductive for the SEM treatment. The stubs were left to dry and then coated in gold (Au) prior to visualisation in a Hitachi S- 4300 field emission scanning electron microscope at Oxford University (Oxford, UK). The images used in this study were taken at 50 x and 200 x magnification, additional images are found in the Appendix (Appendix 3).



**Figure 2.4.** A photograph to show the wood samples mounted on the aluminium stubs using colloidal carbon cement.

Turkulin (2004) states that “*microscopic observations cannot quantify the degradation process*” (Turkulin, 2004), in respect to photo degradation; therefore it may be difficult to assess damage to the sample through SEM alone. However, if SEM is combined and corroborated with other microscopic evidence, such as light microscopy, then conclusions as to potential damage caused by the scCO<sub>2</sub> treatments may be made.

#### **2.3.5.2 Light microscopy**

Pictures of treated and heat damaged wood samples and pictures of the wood cuts were taken using a digital camera Olympus C5050.V Microscopic analysis of the wood samples was achieved using a trinocular microscope (*ca.* 10 x – 40 x magnification) with a Nikon digital camera attached, employing reflected lighting as appropriate. The images used in this study were to 40 x magnification. Light microscopy was carried out at Chiralabs Limited (Oxford, UK).

#### **2.3.6 Feasibility studies of wood samples by spectroscopy**

Three different types of vibrational spectroscopy techniques were investigated; Attenuated Total Reflectance-Fourier Transform Infrared (ATR-FTIR), Diffuse Reflectance Infrared

Fourier Transform (DRIFT) and Fourier Transform Near Infrared Raman spectroscopy (FT-NIR Raman). The aim was to investigate which spectroscopic technique provides the best information about treated and untreated wood samples. Prior to this some preliminary studies had been performed using ATR-FTIR on treated and untreated samples. From these studies, it was agreed that in principle it may be possible to identify a degree of water content and other constituents of the wood. This would be with regards to a relative scale and with the limitation that these studies were carried out on the surface of the wood. All spectroscopic analysis was carried out at Chiralabs Limited (Oxford, UK) (Lindon et al., 2016).

On an infrared (IR) spectrum each trough is caused by energy being absorbed from a particular frequency of IR radiation to excite bonds in the molecule to a higher level of vibration. Some of the troughs produced can be easily assigned to particular bonds e.g. OH group. However, the fingerprint region on the right-hand side of a spectrum usually at around  $1800\text{ cm}^{-1}$  to  $400\text{ cm}^{-1}$ , can contain a very complicated series of absorptions that can be difficult to identify. The fingerprint region is still important because each compound produces a different pattern of troughs in this part of the spectrum.

#### **2.3.6.1 ATR-FTIR**

ATR is ideal for strongly absorbing or thick samples which can produce intense peaks when measured by transmission, it was therefore deemed suitable to try in the feasibility study on the treated and untreated wood samples. Furthermore, the samples can be analysed in their natural state without grinding or the addition of heat. For this ATR-FTIR spectroscopy technique each wood sample was placed on a FTIR Diamond ATR crystal and the surface was analysed in-situ. Untreated and treated Scots Pine (*H*) and Maple (*M*) samples were analysed.

In ATR-FTIR spectroscopy an infrared red (IR) beam is directed at a certain angle onto an optically dense crystal with a high refractive index. This internal reflectance creates an evanescent wave. In regions of the IR spectrum where the wood samples absorb energy, the evanescent wave will be attenuated. This attenuated beam then returns to the crystal and exits via the opposite end, where it is directed to a detector in the IR spectrometer. An IR spectrum is then generated from the detected attenuated IR beam.



### **2.3.6.2 DRIFT**

Initially DRIFT spectroscopy was carried out on Scots Pine (*H*) and Maple (*M*) samples. Each sample was presented by placing the holder of a Diffuse Reflectance optics attachment such that a rough flat face was illuminated. This technique can be applied to freshly sectioned portions of wood, either with or across the grain, allowing the probing of the internal levels of constituents compared to those on the established outer surfaces. DRIFT spectroscopy uses IR radiation which interacts with the wood samples and IR transparent matrix causing the light to diffuse or scatter, as it moves throughout the wood sample. An output mirror then directs this scattered energy to the detector in the spectrometer to generate a spectrum.

In the primary study, DRIFT was found to give the most feature-rich spectra and was therefore deemed suitable for further analysis of wood samples. For the second study using DRIFT twenty wood samples were analysed, with some trends being identified.

### **2.3.6.3 FT-NIR Raman Spectroscopy**

To minimise any heat damage to the wood samples being tested, a near-infrared (NIR) laser was used in the Raman spectroscopy technique. The technique depends on the scattering of light. The wood sample is illuminated with a monochromatic laser beam which interacts with the molecules of the wood samples and originates a scattered light. A small amount of the scattered light will have a different frequency to that of the incident light and this is used to construct a Raman spectrum (Bumbrah and Sharma, 2016). Raman spectra tend to have a large number of scattered lines because molecules exist in a number of rotational and vibrational states therefore giving off a number of different corresponding frequencies.

Scots Pine (*H*) and Maple (*M*) samples were analysed using this method. In each case the sample was presented by placing in a bespoke holder of a FT-Raman spectrometer.

### **2.3.7 Three Point Bend Test for the determination of wood strength**

A simple three-point bend test was used to determine Young's Modulus (*E*) of different wood samples. Bending strength or Modulus of Rupture (MOR), can also be determined as a function of *E*. A selection of wood samples was collected to test the possible adverse effects of the SCF

treatments on the mechanical properties of the wood. Treated and untreated samples were selected in order to be able to make direct comparisons between the mechanical properties. For each treatment three samples of wood were selected, and the three-point bend test was carried out in triplicate. The untreated wood was oven dried to a constant mass and kept in sealed nitrogen containers until use. The testing was carried out using a Bose Electroforce 5500 mechanical tester (Bose / TA Instruments, Minnesota, USA) and WinTest 7 software (Bose) in the Biochemistry Department at University of Birmingham. All the wood samples were tested at 504 hours (3 weeks) after treatment, once the wood samples had achieved a stabilised NMC. Thus, the MC of the wood samples tested will have been relatively low and will have varied between each wood sample and species.

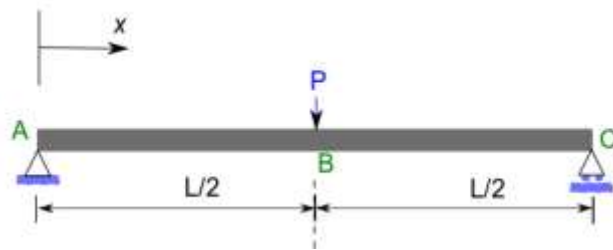


**Figure 2.5. Illustration to show layout for a three-point bend test, where  $P$  is force and  $L$  is the distance between the two supports. Figure adapted from (Brancheriau et al., 2002)**

The wood samples being tested had previously been cut into consistent rectangular beams prior to SCF treatment. The width ( $a$ ) and height ( $b$ ) of the wood samples were measured and the samples were placed in the apparatus with the height of the wood orientated vertically. The distance ( $L$ ) between the two supports was measured. A force ( $P$ ) was applied up to 200 N over 40 seconds. In order to make accurate assumptions about the samples elastic properties it is important that the wood does not become permanently deformed i.e. the beam does not return to its original shape after deflection. The force applied was therefore added incrementally and could be stopped at any time. For each treatment type, force ( $P$ ) and displacement ( $w$ ) values were recorded perpendicular to the grain for the three wood samples for each of the wood sample set. The triplicate values were averaged to give a mean value representative of the woods structure.

Force, displacement curves were plotted using the WinTest 7 software. A gradient ( $\delta P/\delta w$ ) was recorded in the elastic region (linear) of the graph for each test. Figure 2.6 and Figure 2.7 are both examples of the force displacement graphs produced during testing.

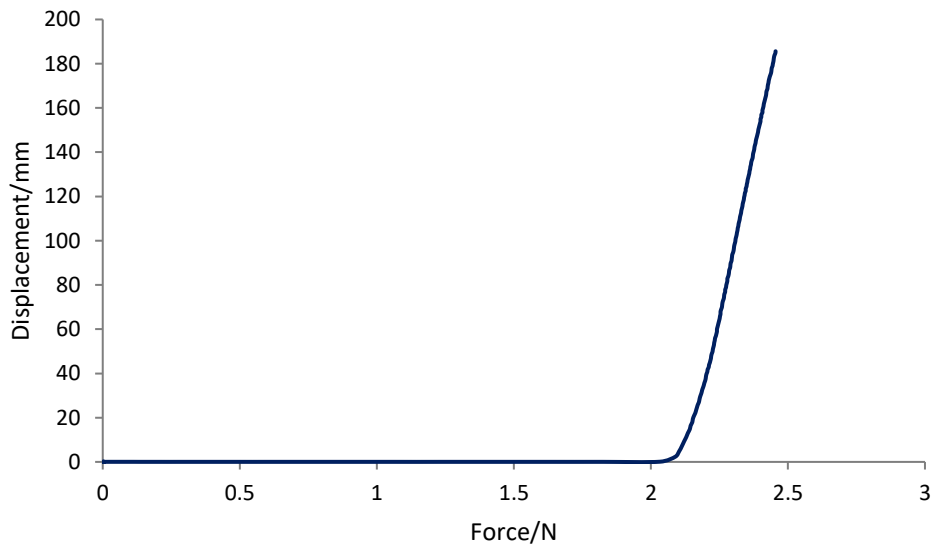


**Figure 2.6. An example force displacement graph for Maple (*H*)**

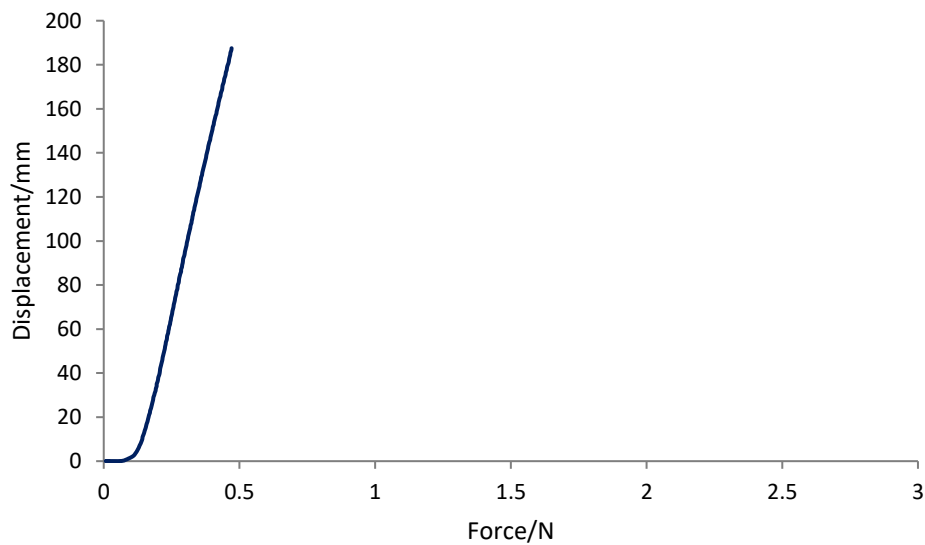


**Figure 2.7. An example force displacement graph for White Oak (*H*)**

Deflection at the centre of the beam is:

$$w_o = \frac{PL^3}{48EI}$$

**(Equation 2.3)**

I is the second moment of area defined by:

$$I = \frac{a^3b}{12}$$

**(Equation 2.4)**

However, because the gradient is equal to  $\delta P/\delta w$  it is possible to rearrange equations (2.3) and (2.4), so the gradient of the line equals:

$$\frac{\delta P}{\delta w} = \frac{48EI}{L^3}$$

**(Equation 2.5)**

Equation 2.5 can be rearranged to solve for Young's Modulus (E);

$$E = \frac{\left(\frac{\delta P}{\delta w}\right)L^3}{48I}$$

**(Equation 2.6)**

The bending strength (MOR) of the wood can be found using the Equation 2.6 where  $m$  is equal to the gradient of the graph and  $g$  is the gravitational constant.

$$Strength = \frac{3mgL}{2ab^2}$$

**(Equation 2.7)**

Using these equations, values for E and MOR can be collected for the different wood samples. The advantage of using equation (2.5) instead of equation (2.3) to estimate E means that it is possible to deal with experimental error by using the best line of fit to find the gradient ( $\delta P/\delta w$ ).

### **2.3.8 Statistical analysis techniques**

The effects of the experimental conditions on the overall mean moisture contents were statistically examined. The Student t Test was used to examine for differences where experiments were paired for comparison. The null hypothesis stated that the SCF treatment with either  $\text{scCO}_2(\text{PURE})$  or modified  $\text{scCO}_2$  has no effect on the moisture content of an oven-dried wood sample. The chosen level of significance,  $\alpha$ , for all tests was 0.05. The Student t Test was also used to statistically examine the effects of the supercritical hydration treatments on the bending strength of the sample set. The null hypothesis stated that the supercritical hydration treatment has no effect on the MOR of the oven-dried wood samples. Again, the level of significance,  $\alpha$ , for all tests was 0.05.

### **2.3.9 Sources of Error**

The main sources of error associated with the methods and materials for the supercritical hydration treatments are presented in Table 2.6 below. Errors were minimised where possible within the experimental procedure, however improvements have been suggested which should be considered for future work.

Sources of Error	Precautions Taken	Future Improvements
Natural variability of wood	Care was taken to choose wood samples that had little or no defects e.g. splits, knots, discolouring.	Taking wood samples of the same species from the same larger sample rather than smaller off cuts would ensure more consistencies through the individual samples.
Cutting wood to size	Individual wood samples were all cut to size using the same method.	Cutting wood samples to a larger, more manageable size may reduce the errors in cutting.
Leaks in the rig	<p>The rig was constructed by the author and required many modifications due to leaks.</p> <p>PTFE tape was applied where it was safe. New fittings were bought where tape would not be sufficient.</p>	Construct the rig with new fittings to minimise leaks. However, this can be extremely costly.
Small batch runs	<p>The pressure vessel containing the wood samples was 25 mL and could only hold two wood samples at maximum capacity.</p> <p>An average of 5 runs per day were carried out in two week blocks. The experimental work was carried out in bulk so that consistency was maintained between the separate runs.</p>	<p>Scale up the pressure vessel containing the wood samples. 2000 mL and 20,000 mL pressure vessels are available to use via the authors company sponsor.</p> <p>Use of these larger vessels would require modifications to the rig to enable efficient cooling and heating of CO<sub>2</sub>.</p>

**Table 2.6. A table listing the main sources of error associated with the supercritical hydration treatments, the ways in which these errors were minimised and suggestions for improvements that can be made in the future.**

## 2.4. Hydration results and discussion

In this section the hydration profiles for treatments with  $\text{scCO}_2(\text{PURE})$  and  $\text{scCO}_2(\text{MeOH})$ , in the presence of water are presented and debated. The concentration of MeOH was varied to best establish the most feasible method for the supercritical hydration. With conservation methods in mind and due to the variance in the wood samples age and physical properties, it is important to look at the samples performance post treatment, on an individual basis. Therefore, material characteristics determined by the wood samples age, type and species are individually discussed to help determine the key factors affecting the hydration levels achieved by the different woods.

Chapter 3 will discuss additional analytical techniques which were used to determine any changes to the microstructural and macrostructural properties of the samples set pre and post treatment with  $\text{scCO}_2$ .

### 2.4.1. Hydration profiles for wood samples treated with $\text{scCO}_2(\text{PURE})$ and $\text{scCO}_2(\text{MeOH})$ , in the presence of water

#### 2.4.1.1. Hypotheses

Four main hypotheses were made before the wood sample set were subject to supercritical hydration, with and without a co-solvent (MeOH).

- Due to the low solubility of water in  $\text{scCO}_2$  the hydration levels (NMC) achieved by all wood samples were expected to be low at around 1- 2% at a constant mass.
- The use of the co-solvent, MeOH, will give higher levels of NMC than the  $\text{scCO}_2$  treatments without a co-solvent. Additionally, levels of NMC across the wood sample set will also increase with the increase of MeOH from 2.5 mol% to 5.0 mol%.
- A difference in the NMC of the modern and historic wood samples at a constant mass was expected with historic samples achieving a lower NMC at a constant mass than the modern wood samples, irrespective of the presence of MeOH.
- Due to the differences in pore and pit arrangement in hardwoods and softwoods, it was expected that the softwood sample, Scots Pine (*H*), would achieve lower NMC levels than the temperate hardwood samples, irrespective of the presence of MeOH.

### 2.4.1.2 Hydration profile for wood treated with $\text{scCO}_2(\text{PURE})$ in the presence of water

A mass loss profile for wood samples treated with  $\text{scCO}_2(\text{PURE})$  in the presence of water is presented in Figure 2.8. A hydration profile is presented in Figure 2.9 which utilises the data obtained in Figure 2.8.

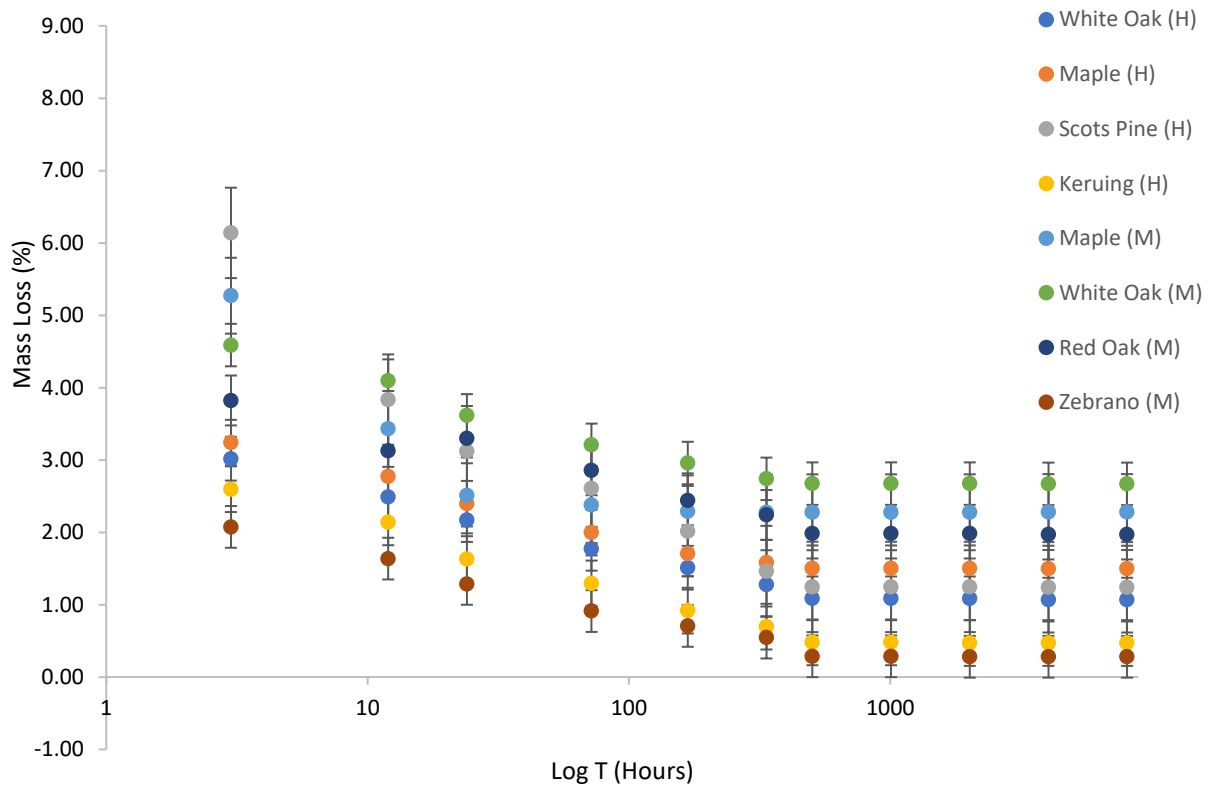


**Figure 2.8.** A mass loss profile for wood samples weighed over 8,064 hours (48 weeks), a Log T (time) scale has been used here to better see the individual data points The wood samples have been treated with  $\text{scCO}_2(\text{PURE})$  in the presence of water for 45 minutes. Each point represents the overall mean from five independent sets of measurements  $\pm$  one standard error of the mean. The same mass loss profile without a Log T scale is presented in the Appendix (Appendix 3, Figure 1)



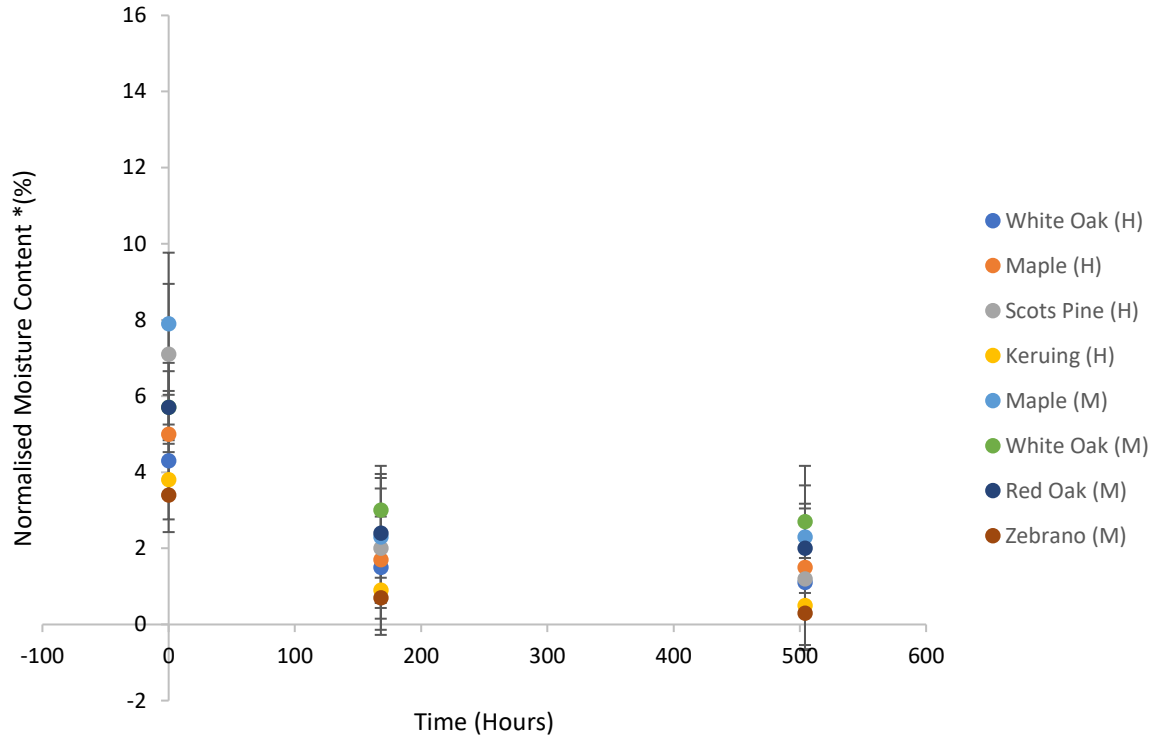


**Figure 2.9.** The NMC of wood samples taken at 0 hours, 168 hours (1 week) and 504 hours (3 weeks). The wood samples have been treated with  $\text{scCO}_2(\text{PURE})$  in the presence of water. Each point represents the overall mean from five independent sets of measurements  $\pm$  one standard error of the mean. \*Normalised moisture content is expressed here as the percentage change in mass due to water in respect to the oven dried mass of the wood sample.

At 504 hours, or three weeks, all the wood samples had stabilised at a constant mass. Hydration profiles presented in this chapter use data up to and including the 504 hours (at which all wood samples had stabilised), but do not after that time. However, all the samples were continually weighed at regular intervals over a 48-week (8,064 hours) period as seen in Figure 2.8. The wood samples treated with  $\text{scCO}_2(\text{PURE})$  have shown an increased MC post treatment (Figure 2.8, Figure 2.9). An average stabilised NMC (at 504 hours) of approximately 1.5% for both the historic and modern wood samples was achieved. Thus, showing that hydration with  $\text{scCO}_2(\text{PURE})$  in the presence of water was possible, if very low. Understandably, due to the very low levels of hydration, none of the NMC recorded for  $\text{scCO}_2(\text{PURE})$  treatment were significant in comparison to untreated wood samples.

In Figure 2.8 at 504 hours the hardwood samples White Oak (*M*), Maple (*M*) and Red Oak (*M*) have retained the highest mean percentage mass increase at approximately 2.5%. Keruing (*H*) and Zebrano (*M*), the tropical hardwoods, have achieved the lowest mass increase at

approximately 0.5%. Maple (*H*), Scots Pine (*H*) and White Oak (*H*) all have a mass increase of approximately 1.5%. The only softwood in the sample set, Scots Pine (*H*), had the second highest percentage mass increase of approximately 7.7% at 0 hours, however this dropped off rapidly to finish at approximately 1.3%. This profile and the hydration profile (Figure 2.9.) indicate that the age of the wood, rather than the type of the wood (hardwood or softwood), is the influencing factor in determining the level of hydration retained by the wood samples. In this instance, it seems that the hardwoods; White Oak (*M*), Maple (*M*) and Red Oak (*M*) have been able to form cellulose-water bonds with greater ease than the tropical hardwood and softwood samples. Both Keruing (*M*) and Zebrano (*H*) have responded very poorly to  $\text{scCO}_2(\text{PURE})$  treatment. The complex nature of tropical hardwood structures makes it difficult to assign this poor response to just one factor, however likely explanations are suggested in Section 2.4.1.4 and Section 2.4.1.5 below.

#### **2.4.1.3 Hydration profile for wood treated with $\text{scCO}_2(\text{MeOH})$ in the presence of water**

The addition of the co-solvent, MeOH, was clearly seen to increase the overall NMC for both the historic and modern wood samples (Figure 2.10, Figure 2.11). Statistically the treatment using 5.0 mol% MeOH, as a co-solvent, gave the highest number of significant results, followed by 2.5 mol% MeOH and then  $\text{scCO}_2(\text{PURE})$ . For 5.0 mol% MeOH, the stabilised NMC after 504 hours for all wood samples was above 4%. As discussed in Section 1.1.3 (Chapter 1) when  $\text{scCO}_2$  is modified with a polar co-solvent such as MeOH, the solvating power of  $\text{scCO}_2$  with other polar compounds e.g. water, is significantly increased (Lalanne et al., 2004). This solvent stream of  $\text{scCO}_2(\text{MeOH})$  and water is known as a binary mixture (Clifford, 1999) and will improve the affinity of  $\text{scCO}_2$  with water. Therefore, the increased levels of NMC in the wood samples were expected. However, it should be noted that hydrating with  $\text{scCO}_2(\text{PURE})$  was also possible although the samples only achieved a maximum NMC at constant mass of approximately 2.7%.

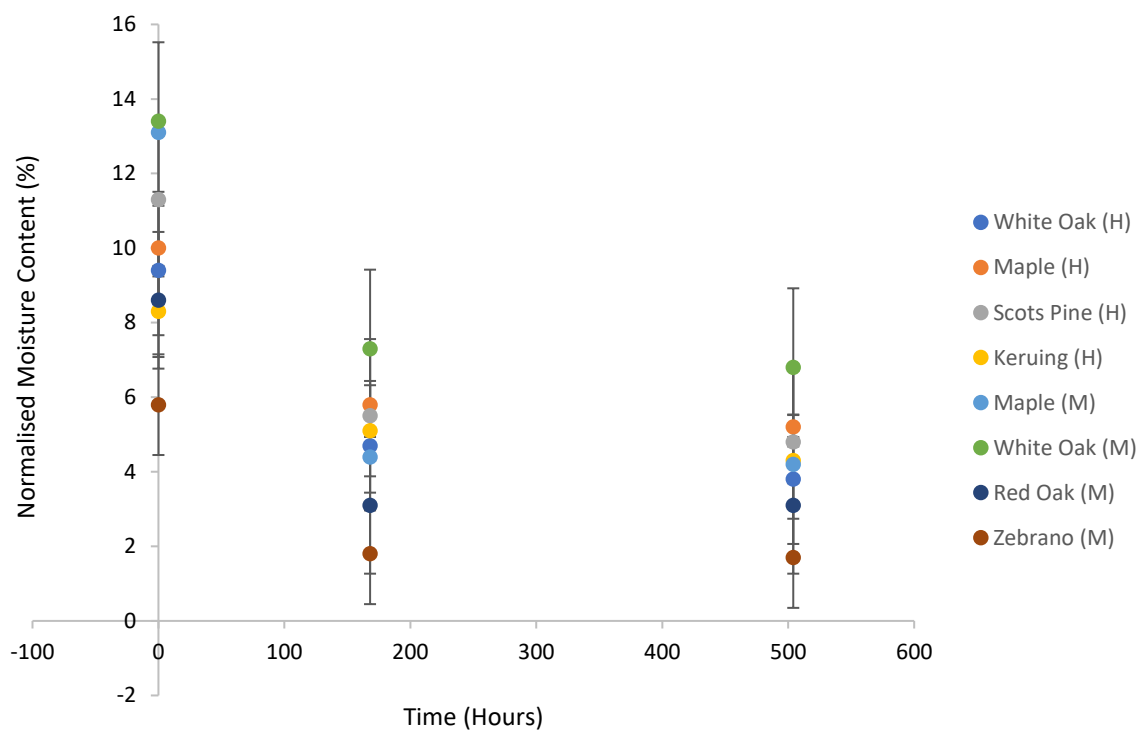


**Figure 2.10. NMC of wood samples taken at 0 hours, 168 hours (1 week) and 504 hours (3 weeks). The wood samples have been treated with  $\text{scCO}_2(\text{MeOH})$  in the presence of water, MeOH has a concentration of 2.5 mol%. Each point represents the overall mean from five independent sets of measurements  $\pm$  one standard error of the mean.**

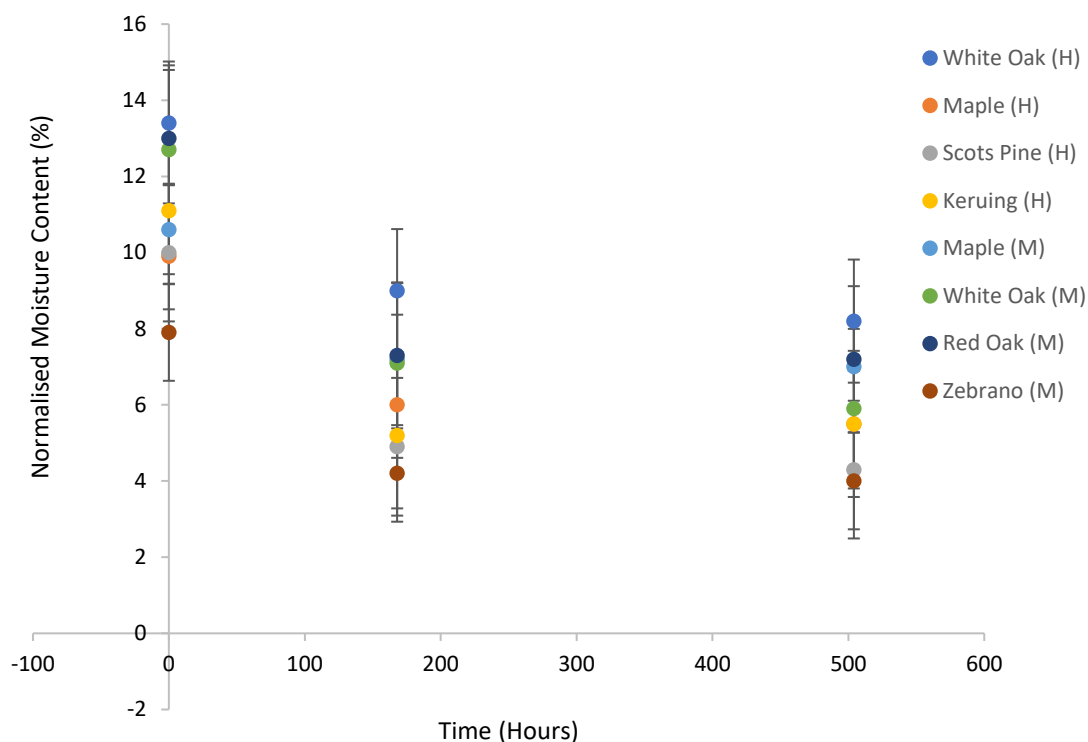


**Figure 2.11. NMC of wood samples taken at 0 hours, 168 hours (1 week) and 504 hours (3 weeks). The wood samples have been treated with  $\text{scCO}_2(\text{MeOH})$  in the presence of water, MeOH has a concentration of 5.0 mol%. Each point represents the overall mean from five independent sets of measurements  $\pm$  one standard error of the mean.**

Figure 2.10 presents the NMC of the wood samples treated with 2.5 mol% MeOH. White Oak (*M*) is shown to have the highest NMC at 0 hours and 504 hours, at 13.4% and 6.8% respectively. White Oak (*M*) also held the highest mean NMC at 504 hours without the use of a co-solvent (Figure 2.9). Maple (*H*) and Scots Pine (*H*) are shown here to have a high mean NMC at 0 hours, however, both wood samples had a steady loss of moisture over time and stabilise at a mean NMC of approximately 5%. The use of a co-solvent seems to have helped the Scots Pine (*H*) samples retain a higher NMC over time. Previously, without the use of a co-solvent Scots Pine (*H*) gained a high initial NMC at 0 hours but was unable to maintain the increase in MC over time. Conversely, Maple (*M*) has not responded in the same way with the use of a co-solvent 2.5 mol%; its high initial NMC of 13.1% fell to 5.2% at 504 hours. Without the use of a co-solvent Maple (*M*) was also unable to retain a high initial NMC of 7.9%. The Keruing (*H*) has performed surprisingly well with the addition of MeOH, especially in comparison to its counterpart, Zebrano (*M*), which has consistently retained the lowest NMC with and without the use of a co-solvent.

White Oak (*H*), shown in Figure 2.11, had the highest initial retention at zero hours at 13.4% and the highest mean NMC of 8.2% at 504 hours. Red Oak (*M*) and Maple (*M*) both had a high mean NMC of approximately 7% at 504 hours. Yet, Maple (*M*) had a better retention level than Red Oak (*M*) which drops from a high initial NMC of 13%. Again Keruing (*H*) performed well with an initial retention of 11.1% dropping to 5.5%, just below that of White Oak (*M*) at 5.9% at 500 hours. Of the hardwoods, White/Red Oak and Maple both historic and modern, seem to have responded well to the SCF treatment, especially the Oak samples which consistently gained a high stabilised NMC. This suggests the treatment is suitable for both historic and modern wood samples even with the highest percentage co-solvent. White Oak (*H*) and Red Oak (*M*) gave significant results at 0, 168 and 504 hours when treated with 5.0 mol% MeOH. The mechanical analysis carried out will assess whether the SCF treatment is in turn unfavourably affecting the integrity of the wood samples. The NMC of the tropical hardwood Zebrano (*M*) increased with the use of a co-solvent, however it is shown to be the poorest of all the tested wood types at retaining water over time.

Zebrano (*M*) gave no significant results at 504 hours with any of the supercritical treatment types. Due to this low ability to retain increased levels of moisture, it could be suggested that Zebrano (*M*) is one of the wood samples that is not suitable for SCF impregnation of this type. Scots Pine (*H*) also provides an interesting series of responses to the SCF treatment, especially with the addition of a co-solvent. With 2.5 mol% MeOH, Scots Pine (*H*) retains a 5.2% NMC at 504 hours. Comparable to its response with the  $\text{scCO}_2(\text{PURE})$ , Scots Pine (*H*) had a high uptake initially but was unable to retain a significant NMC at 504 hours. With 5.0 mol% MeOH, Scots Pine (*H*) had a lower uptake initially than 2.5 mol% MeOH at 0 hours and had a sharp drop in retention between 0 hours and 168 hours. This resulted in Scots Pine (*H*) only just managing a slightly higher NMC than the worst performing wood, Zebrano (*M*) at 4.3% and 4% at 504 hours respectively. Additionally, Scots Pine (*H*) gave no significant results under any of the supercritical treatments.

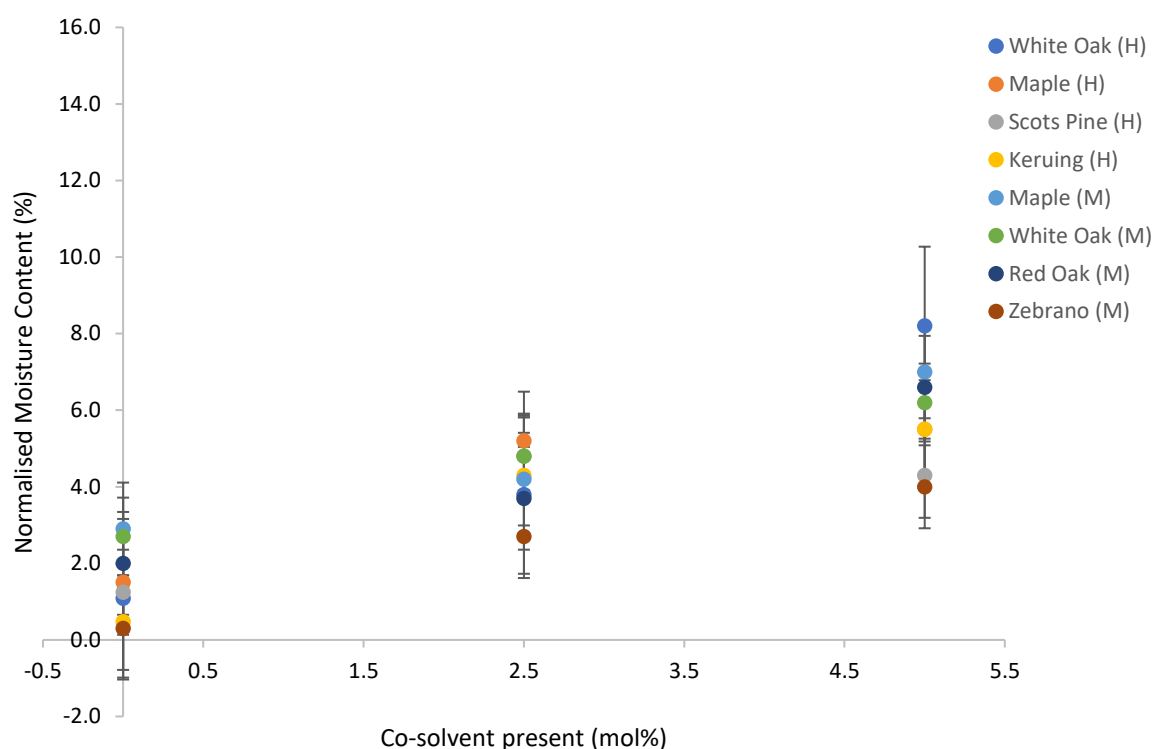


**Figure 2.12. A comparison of the wood samples mean NMC at 504 hours (3 weeks) after different treatment conditions. Each point represents the overall mean from five independent sets of measurements  $\pm$  one standard error of the mean.**

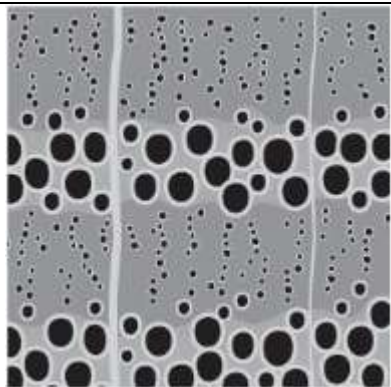
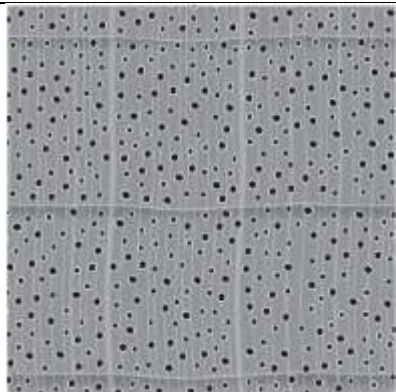
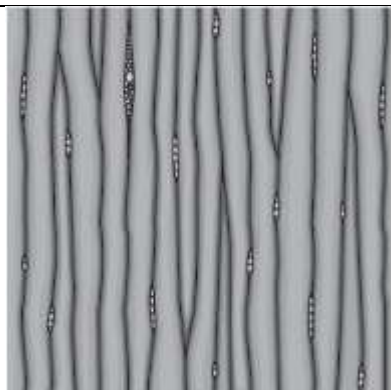
#### 2.4.1.4 Connectivity in wood

The differing connectivity of the hardwood and softwood structures is also likely to influence the level of impregnation and penetration of water into the wood matrix. As discussed in Section 1.5.3 (Chapter 1), pits are the main pathways for liquid flow between longitudinal conductive cells in wood and pit arrangement is distinct between hardwoods and softwoods (Ahmed and Chun, 2011).

For hardwoods, longitudinal flow is conducted by vessels and wood fibre; however, vessel flow is preferential to wood fibre, and thus vessel rather than fibre characteristics are directly related to flow (Sano and Jansen, 2006). Vessel diameter and length, inter-vessel pit size and number are all influential to flow, with the size, number and distribution of vessels affecting the appearance or uniformity of hardwoods. For radial penetration, flow is influenced by ray parenchyma lumen diameter and length, and end wall pit number and diameter. Whereas for softwoods, longitudinal flow is the responsibility of vertical cells called tracheids that make up 90% of the wood structure and the adjoining bordered pits. Ray parenchyma cells are also influential in the radial penetration of softwoods. As described later in this Section, the

relationship between vessel diameter and length and inter-vessel pit size and number are complex and extensive. Differences can be found between species and even positions in the structure within the same species. Therefore, attempts have been made to draw feasible conclusions from the hydration data collected and known properties of the individual wood samples.

Hardwoods, because of the presence of vessels (which when cut across the end grain are referred to as pores), are called “porous” woods. The lack of these vessels in softwoods means that they are referred to as “non-porous”. Table 2.7 below further classifies White Oak, Red Oak, Maple, Keruing, Zebrano and Scots Pine and expands on the initial characterisation made in Table 2.3 in Section 2.3.2.

Pore Arrangement	Characteristics
	<p><b><u>Ring Porous</u></b></p> <p><i>e.g. White Oak and Red Oak</i></p> <p>The largest pores are found in the earlywood, those in the latewood are more evenly distributed and uniform in size with a smaller diameter. These woods have open-grain structures.</p>
	<p><b><u>Diffuse Porous</u></b></p> <p><i>e.g. Maple, Keruing and Zebrano</i></p> <p>Pores, especially in temperate hardwoods, are small in diameter and distributed evenly across the early and latewood. Some tropical hardwoods have larger pore diameters to adapt to more extreme climate conditions. These woods have a closed-grain structure.</p>
	<p><b><u>Non-porous</u></b></p> <p><i>e.g. Scots Pine</i></p> <p>Softwoods have tracheid cells rather than vessel cells. Different softwoods can have different growth-ring characteristics. Scots Pine is characterised as a yellow pine. In yellow pine, the rings are clearly visible and behaviour is similar to that of ring-porous woods.</p>

**Table 2.7. Characterisation of the wood sample set into ring-porous, diffuse-porous and non-porous. Illustrations adapted from (Hoadley, 2000)**

It has previously been reported that diffuse-porous wood has a higher permeability than ring-porous wood and that softwoods have a lower permeability than hardwoods; density was said to not be related to permeability (Bao et al., 1999). Evidence from the hydration profiles shown in Figure 2.12 support the statement that permeability in softwoods is lower than that in hardwoods; Scots Pine (*H*) consistently retained low levels of NMC. On the other hand, both ring-porous woods White Oak (*M/H*) and Red Oak (*M*) both achieved some of the highest levels of stabilised NMC whilst Zebrano (*M*) and Keruing (*H*), both diffuse-porous woods, consistently achieved the lowest. In Table 2.7 above it can be clearly seen that the diffuse-



wood woods (Maple (*M/H*), Keruing (*H*) and Zebrano (*M*)) have an even distribution of small diameter vessels whilst ring-porous woods (White Oak (*M/H*), Red Oak (*M*)) have a combination of small and large diameter vessels spread between the early and latewood. Therefore, the composition of the Zebrano (*M*), Keruing (*H*) and Maple (*M/H*) samples could affect the levels of hydration achieved via supercritical treatment. For example: a high composition of earlywood consisting of large vessel diameters would be expected to give greater levels of impregnation in comparison to a high composition of latewood and small diameter vessels. Earlywood permeability can be many times higher than of that in latewood (Domec and Gartner, 2002); this could go some way to explaining why there is variability between wood samples from the same species.

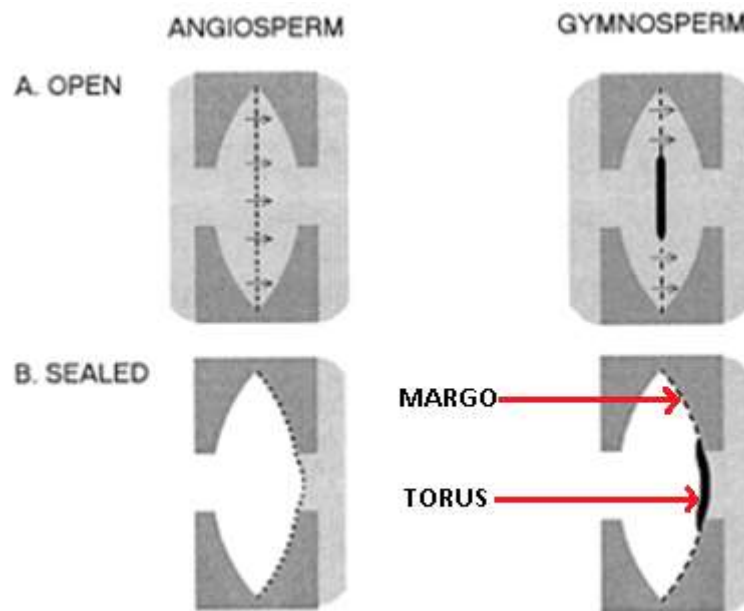


**Figure 2.13. A comparison of hardwood (angiosperm) and softwood (gymnosperm) pit structure. Illustration adapted from (Hacke et al., 2004).**

The conclusions made by Bao et al (1999) do not take into consideration the effect on permeability with the increasing age of a wood sample. It would be expected that the small diameter vessels in ring-porous wood would be more susceptible to blockage over time, leading to lower levels of permeability. Pits are found in both porous and non-porous woods are also susceptible to damage over time. Despite hardwoods having a more complex cellular structure than softwoods, their inter-vessel pitting is less specialised (Hacke et al., 2004). Figure 2.13 compares the difference in hardwood (angiosperm) and softwood (gymnosperm) pit structure and highlights clear differences. Where inter-vessel pit membranes are generally homogenous in porosity and thickness, the margo-torus pit membrane in inter-tracheid is not. The margo

provides a thin and porous membrane allowing for water flow and preventing air movement, with the thick torus providing the final barrier to air movement. The inter-vessel pits do not have a torus, and thus sealing the pit depends completely on capillary forces, these pores are therefore smaller in size than the softwood margo (Côté, 1963). Thus, even though the hardwood pits may be more susceptible to blockage due to their small size, the thick torus found in softwoods can cause similar problems. Aspiration is common among softwoods, this is where the torus seals one of the pit apertures, subsequently blocking the pathway through the pit (Shusheng et al., 1994). This can make non-porous woods such as Scots Pine (*H*) difficult to impregnate with preservatives, therefore the impregnation of water into the non-porous matrix may also be hindered.

Although softwoods have larger pores in the margo membrane relative to the narrow hardwood pores. The conductivity of these pits may be limited by shorter lumen lengths found in the softwood tracheid's, which may jeopardise overall wood conductivity. Due to the lumen's being longer in hardwood structures any direct effects of small pores in the pit membrane are redundant. Consequently, if with time several softwood pits became blocked or damaged, the overall effect on conductivity may be greater than that felt by hardwood samples subjected to the same damage.

#### **2.4.1.4.1 Epoxy resin for 2-D impregnation**

As stated in Section 2.3.2, two coats of epoxy resin were painted on either end of every wood sample treated with scCO<sub>2</sub>. Epoxy resin was applied because of the understanding that it would limit the diffusion of scCO<sub>2</sub> and water to a 2-D interface. An almost identical procedure had been successfully employed by Acda et al. (2001) for the SCF impregnation of various wood samples with a biocide.

However, the levels of hydration achieved by all the wood samples treated with scCO<sub>2</sub> may have been limited by the application of epoxy resin. Although, longitudinal diffusion into the wood will have still been possible, the resin will have blocked some of the longitudinal pathways into the wood sample, possibly limiting the maximum hydration levels possible in the individual wood species. This may be especially relevant in the hardwood samples as it has been stated that longitudinal permeability can be up to 10 – 15 times higher than radial permeability (Panshin and Zeeuw, 1980). Therefore, in future work it may be interesting to measure difference in hydration levels achieved by 3-D diffusion, in comparison to 2-D

diffusion and see if the hardwood achieved greater increases in moisture content relative to softwood.

The ratio of side grain to end grain should also be considered at this point as this will vary between ring-porous, diffuse-porous and non-porous wood types. Obviously, the application of epoxy resin will limit some of, if not all the end grain features of the wood samples and their ability to absorb water. Therefore, the side grain of the wood sample may have an influencing factor in the overall water absorption of the wood sample. The primary cell types in both hardwoods and softwoods are orientated along the grain, through which movement is quite rapid. Across the grain however, paths for movement are much more limited. Here the water must “*move through the relatively small pit openings between axial cells, or along the transversely orientated ray cells*”(Walker, 2006), thus the movement fluids across the grain is dependent on the size, number and condition of the pit opening. It is known that the ray cells in Pine species have large opening between cells, therefore allowing a greater ease of movement across the grain than woods with small openings. This evidence suggests that the Scots Pine (*H*) sample may be less impeded in water absorption than the other hardwood samples with smaller openings between cells.

#### **2.4.1.5 Cellulose, hemicellulose and lignin content**

Although the structure and composition of cell walls in wood varies hugely, cellulose ( $(C_6H_{10}O_5)_n$ ) composition accounts for approximately 35 – 50% of dry weight (Chen, 2014). Cellulose is extremely hygroscopic and is therefore known to absorb rather than dissolve large quantities of water. In the water sorption process the hydrogen bonds between the cellulose molecules are replaced by several new hydrogen bonds between the cellulose and water molecules, with some cellulose-cellulose hydrogen bonds remaining (Pettersen, 1984). The free hydroxyls found in the amorphous section of the cellulose polymer are high in density and held in a set position, hydroxyls in the crystalline region of cellulose are too compact within the polymer chain for water molecules to penetrate (Howsmon, 1949). When water is absorbed onto the amorphous hydroxyls, swelling occurs and the water absorbed is known as bound water. It is expected (Section 1.5.6, Chapter 1) that the water absorbed by the wood samples treated with  $scCO_2$  will be bound water, free water is formed only when the cell walls are saturated and the water absorbed fills the cell cavities. The possible presence of bound water is discussed later in the DRIFT spectroscopy study (Section 3.2.3.4, Chapter 3).

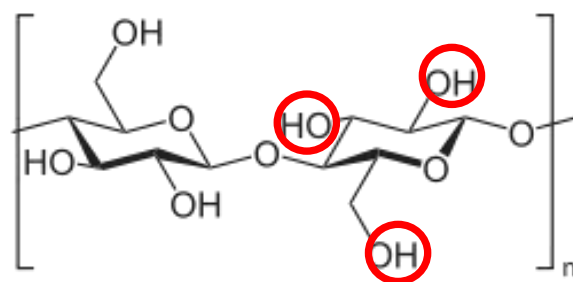


**Figure 2.14 D-glucose units in a cellulose linear polymer. Circled are the three hydroxyl groups on one D-glucose unit that are free for water sorption in the amorphous region.**

Cellulose, and its ability to absorb water in the cell wall, therefore has a significant effect on the levels of hydration achieved by wood. The availability of the hydroxyl sites on the amorphous cellulose structure is also of significance. Figure 2.14 highlights the three available hydroxyl groups on each D-glucose unit of cellulose. In this instance, historic samples may be at a disadvantage in achieving high NMC, damage to the cell wall over time may cause integral damage to the cellulose polymer chain and the hydroxyl groups, therefore hindering ability to absorb water.

The bonding between cellulose, hemicellulose and lignin should also be considered at this point as there may be factors that inhibit the ability of a wood species to absorb water into the cell wall. Despite considerable research in recent years into the relationship and interactions between wood polymers, the knowledge in this field remains incomplete (Srndovic, 2011), though it is known that these polymer structures are arranged hierarchically in the wood cell walls. Hemicellulose influences the pattern of aggregation of the cellulose microfibrils and provides the pattern for lignin assembly. Consequently, hemicellulose mainly interacts with the cellulose fibrils forming non-covalently bonded hydrogen bonds, whilst hemicellulose and lignin form covalent bonds (Srndovic, 2011, Kerr and Goring, 1975). A model of the fibrillar formations of cellulose embedded in the amorphous matrix of hemicellulose and lignin is illustrated in Figure 2.15. Cellulose fibrils dictate the orientation of both hemicellulose and lignin, although less is known about lignin orientation except that it can differ between hard and softwood species. As indicated in Figure 2.15 hemicellulose is orientated in parallel with the cellulose fibrils. Some of the hemicellulose will extend into the matrix and covalently bond with lignin but the majority will coat, and be attached to the cellulose fibril.

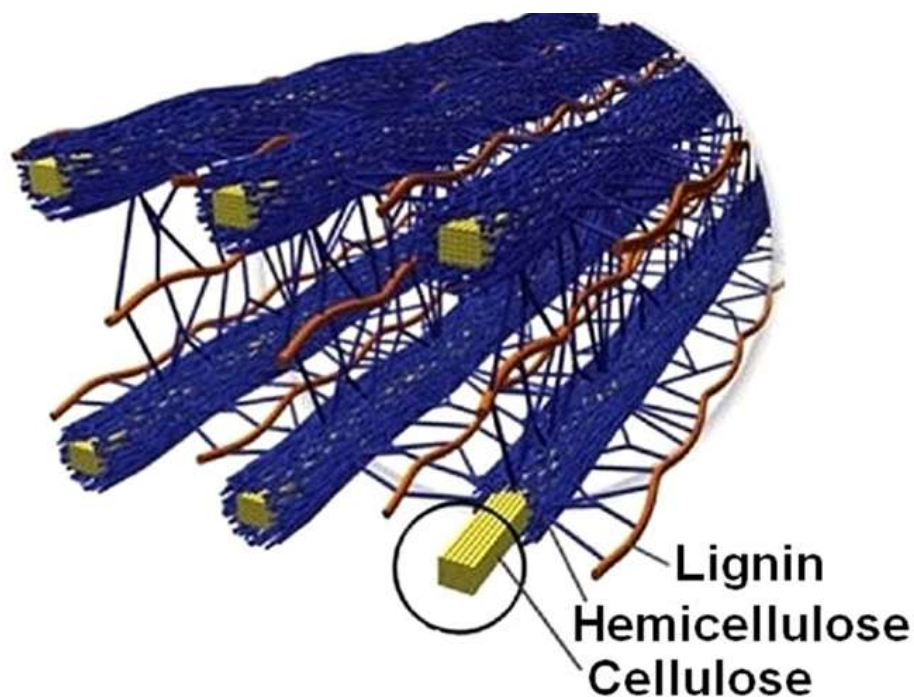


**Figure 2.15 An illustrative model of the microscopic structure of wood indicating the cellulose, hemicellulose and lignin hierarchy. Illustration taken from (Ilnicka and Lukaszewicz, 2015).**

Some assumptions may be drawn about how the hierarchy, bonding and orientation of cellulose, hemicellulose and lignin may affect the ability of historic and modern, hardwood and softwood to absorb water. It may be assumed that due to the lack of conclusive investigations into the relationship between these complex plant-based polymers (Yang et al., 2006), that we are unable to make specialised distinctions between the different wood species and their water sorption mechanics. However, it may be possible to draw some conclusions from the damage to the historic samples through abiotic and/or biodeterioration, and the subsequent damage to the cellulose fibrils and surrounding matrix.

The historic wood samples used in this work are classified as dry rather than waterlogged wood. It is expected that they will have been subjected to one or both following deteriorative processes (Blanchette et al., 1991):

- Biodeterioration – rot caused by insects and/or pests, this may not be visually identified but can cause the decomposition and eventually the complete mechanical failure of wood structures.
- Abiotic deterioration – caused by long exposure to changing weather conditions and hence constantly changing factors of light, heat, moisture, pollutants and general wear

and tear. Heat exposure below 100°C can cause depolymerisation in the wood structure.

Although Maple (*H*) and White Oak (*H*) consistently achieved high levels of stabilised NMC, Scots Pine (*H*) and Keruing (*H*) achieved some of the lowest NMC out of the whole sample set. It should be said that the Scots Pine (*H*) sample was the most visibly aged of the historic wood samples, and it is therefore unsurprising that it achieved low levels of NMC. As described above it is most likely that abiotic deterioration has occurred over 100+ years causing some depolymerisation and breakdown of the woody fibres. As a tropical hardwood, Keruing (*H*), may have a greater natural resistance to deteriorative processes as it is more durable than the softwood, Scots Pine (*H*). Although it is unknown whether the historic wood samples were taken from the heartwood or sapwood of the tree, it is interesting that White Oak (*H*) achieved consistently high levels of NMC alongside White Oak (*M*). White Oak is known to be a species whose heartwood is naturally resistant to decay, whereas pine species are known to be naturally slightly or completely non-resistant to decay (Knapic et al., 2006).

As stated in Section 1.5.5.1 (Chapter 1), one of the primary functions of lignin is to bind cellulose and hemicellulose together. Softwoods are known to consist of 26% - 32% lignin and tropical hardwoods around 30% lignin, whilst temperate hardwoods are composed of approximately 20% - 25% lignin (Santos et al., 2012). The lower composition of lignin found in temperate hardwood could be a factor in the woods ability to absorb water. If there is less lignin to bind the hemicellulose and cellulose together, then there may be a higher availability of hydroxyl sites on the cellulose chain free to absorb water via hydrogen bonding. Therefore, assumptions can be made between the inconsistent hydration results of both Scots Pine (*H*) and Zebrano (*M*) and the lower percentage of lignin present in their softwood and tropical hardwood structures. Consequently, there seems to be a negative correlation between the percentage composition of lignin known to be in the wood structure and the stabilised NMC achieved by the treated wood samples, as indicated by the hydration profiles for both Zebrano (*M*) and Scots Pine (*H*). A study by Huang et al. (2016) found that in both hardwoods and softwoods hemicellulose rather than cellulose changed in conjunction with lignin structure and amount (Huang et al., 2016) Therefore, it could be the case that with higher quantities of lignin, there are less free hydroxyl sites on the amorphous cellulose because of changes made to the hemicellulose via lignin interactions.

## **Chapter 3: Microstructural and Macrostructural Results and Discussion**

### **3.1 Introduction**

This chapter looks at the microstructural and macrostructural properties of the wood sample set via imaging, spectroscopic and mechanical analysis. By corroborating and combining the analytical techniques the author can look to answer two key questions. Primarily, does the applied supercritical treatment cause any damage to the internal and/or external structure of the wood samples and secondly, what type of water (bound or free), if any, is being absorbed into the wood structure?

DRIFT spectroscopy encompasses the bulk of the spectroscopic studies carried out for this study. It was found that DRIFT spectroscopy gave the most feature rich spectra and was therefore deemed the most suitable spectroscopic technique for the analysis of the wood sample set, pre-and post-treatment. Attention is paid to the ratios calculated for OH/CH and OH/“Cellulose” peak areas in the hope that a greater level of understanding may be achieved as regards the relationship between wood species, treatment type and levels of water absorbance. Additional microscopic and macroscopic techniques were carried out to further diagnose this complex relationship to varying degrees of success. SEM and light microscopy were looked at in conjunction with one another to try and establish any pre-existing damage and damage that may have been caused during supercritical hydration. These imaging techniques were also used to further characterise the wood sample set. Analysis of the MOR of the wood samples post-treatment were most encouraging and provided valuable information that may help to establish future work with scCO<sub>2</sub>.

## 3.2 Microstructural analysis

### 3.2.1 Scanning electron microscopy (SEM)

It was hoped that SEM images would help us to monitor any changes in the internal structure of the wood samples that may be caused during the SCF treatments. The wood samples underwent SEM before and after treatment with  $\text{scCO}_2(\text{PURE})$  to be able to make structural comparisons. However, several issues were raised after a review of the method for sample preparation and on analysis of the SEM images. The main issues raised included the following:

- It would be interesting to analyse the internal matrix of the wood samples rather than the external surface. The wood samples therefore had to be split with a high level of force causing additional damage to the structure.
- It was assumed that the historic samples may have lost some mechanical strength over time. Therefore, due to the level of force applied to split the wood samples, the historic samples may have been at a greater disadvantage than the modern wood samples in being able to show the true extent of any damage caused by the  $\text{scCO}_2$  treatment.
- The SEM analysis required samples to be placed in a vacuum, therefore drying out any samples that had been previously treated with  $\text{scCO}_2(\text{PURE})$ .

Considering the issues outlined above, it was decided that only the four modern wood samples; Maple (*M*), White Oak (*M*), Red Oak (*M*) and Zebrano (*M*), would be prepared and processed for SEM imagery. All the samples undergoing SEM had been oven-dried prior to preparation as this was a standard experimental procedure for both the treated and untreated samples. Experts would suggest that this is not best practise of wood preparation for SEM, and oven-dried samples would not normally be suitable for the analysis as some level of damage will be induced by the oven-drying method. However, it was assumed that the induced damage would be consistent among all wood samples as they had all been subject to the same drying conditions. The oven dried samples were therefore prepared for SEM. The preparation of the samples required a natural “fracture” to provide a cross-section of the wood. This type of fracture was difficult to achieve as the  $0.06 \times 0.01 \times 0.01$  m wood samples had initially been selected for their uniformity and therefore lack of fracture or damage. Thus, to induce a fracture the samples were clamped and a force was applied until it was possible to break the samples by hand along the grain. This type of force would have most likely have caused damage to the internal structure of the wood (Figure 2.13), which in turn could lead to disingenuous conclusions when looking for structural changes in the wood samples. It should also be noted



that due to the variability in density in the wood samples, the force applied to cause fracture was inconsistent.

It became clear that comparison between the images produced by SEM would be difficult to compare in isolation. Figure 3.1 illustrates the damage caused to the wood fibres around the area that the force was applied to split the samples. However, some of the SEM images were more successful than others and it was possible to see some of the main features common to hardwood structures on the 200 x magnification images (Figure 3.2). It was hard to make direct comparisons between identical wood species due to the damage induced in the preparation of samples.

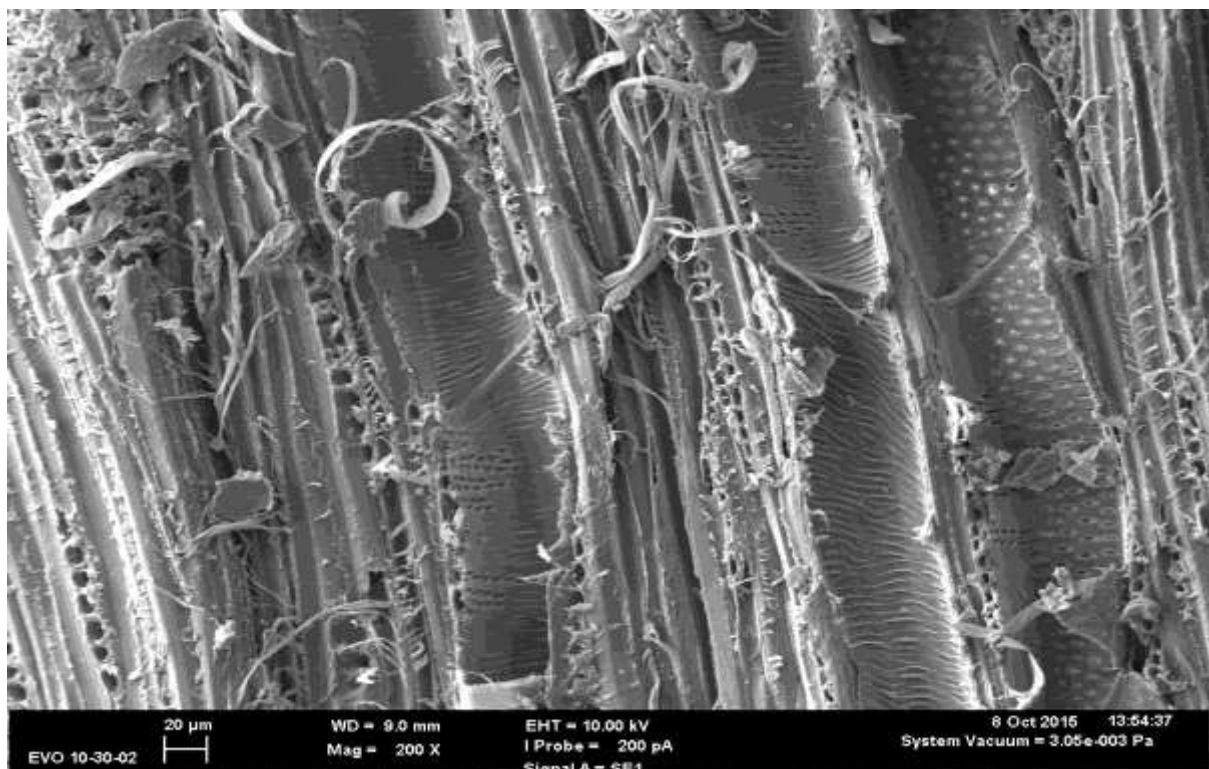


**Figure 3.1** A SEM image at a magnification of 200x, indicating the damage caused to Maple (*M*) caused by manually splitting the wood samples in preparation for SEM analysis.

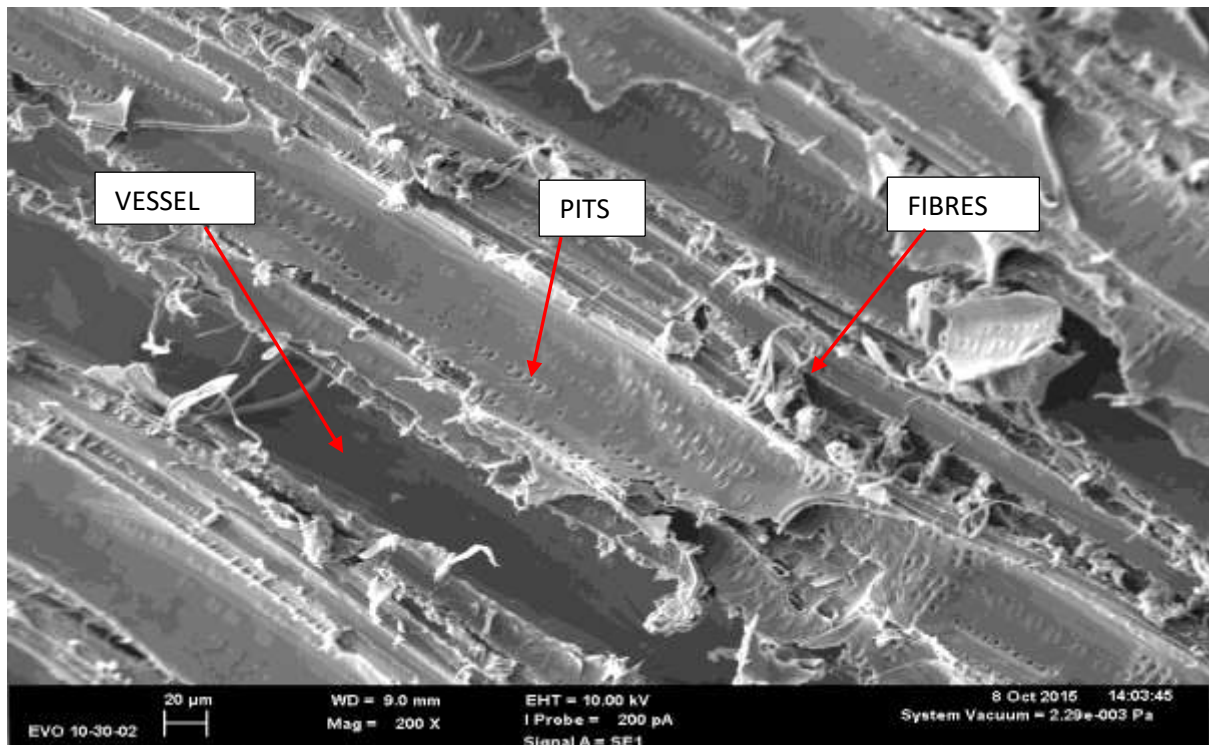


**Figure 3.2** An annotated SEM image at a magnification of 200 x and a resolution of 20  $\mu\text{m}$  to show the key features of a hardwood structure; vessels, pits and fibres. The White Oak (*M*) sample has been treated with  $\text{scCO}_2(\text{PURE})$ .

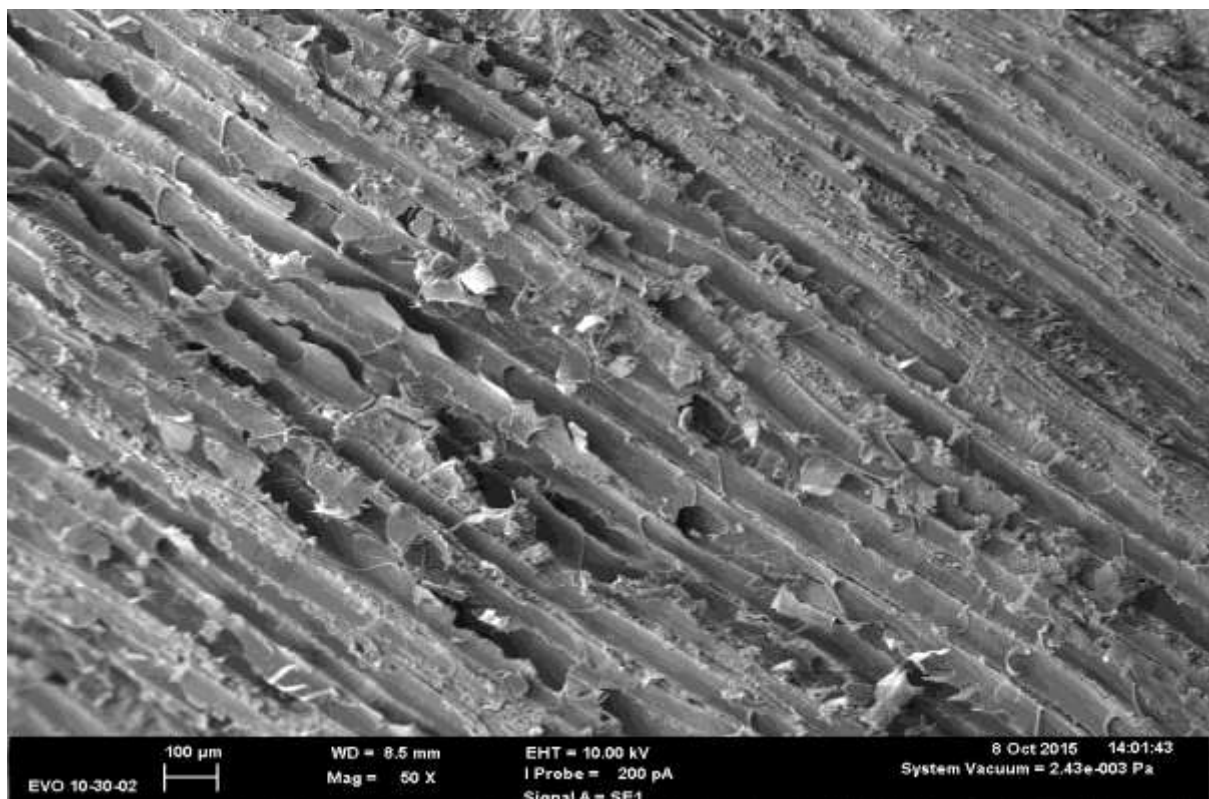


**Figure 3.3** A SEM image at a magnification of 50 x and resolution 100  $\mu\text{m}$ , White Oak (*M*) treated with  $\text{scCO}_2(\text{PURE})$ .

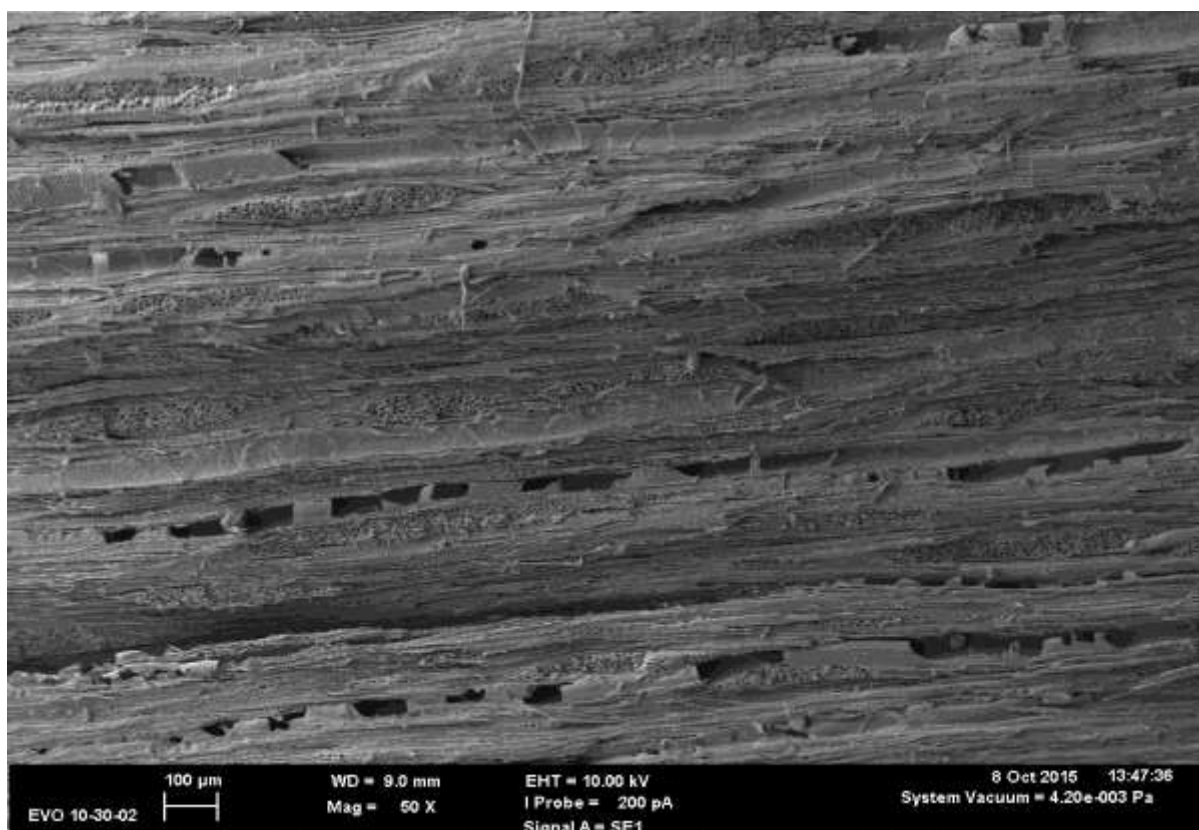


**Figure 3.4** A SEM image at a magnification of 50 x and resolution 100  $\mu$ m, of Maple (*M*) treated with scCO<sub>2</sub>(PURE).

The SEM images were successful in part; several clear, readable high resolution images of four different modern wood samples were produced (Figure 3.3 and Figure 3.4). These images in isolation may not provide much useful evidence of any damage caused to the internal wood structure of the wood samples. However, it may be that these images in collaboration with the images produced by light microscopy on the surface and interior of the wood samples can provide a better understanding of the microstructure of the wood samples before and after SCF treatment.

### 3.2.2 Light Microscopy

Light microscopy was carried out on the internal and external surfaces of three historic wood and two modern samples, before and after they were treated with scCO<sub>2</sub>(PURE). The three historic wood samples were White Oak (*H*), Maple (*H*) and Scots Pine (*H*) and the two modern wood samples were Maple (*M*) and Zebrano (*M*). Light microscopy images of heat damaged samples are also presented. White Oak (*H*), Maple (*H*), Scots Pine (*H*), Maple (*M*) and Zebrano (*M*) were all subject to heat damage after the oven setting was placed at 80°C rather than 40°C for

a treatment with  $\text{scCO}_2(\text{PURE})$ . All images were taken at a magnification of 40 x, with and across the grain of the wood sample. Original sized images are found in the Appendix (Appendix 5).

**White Oak (*H*)**

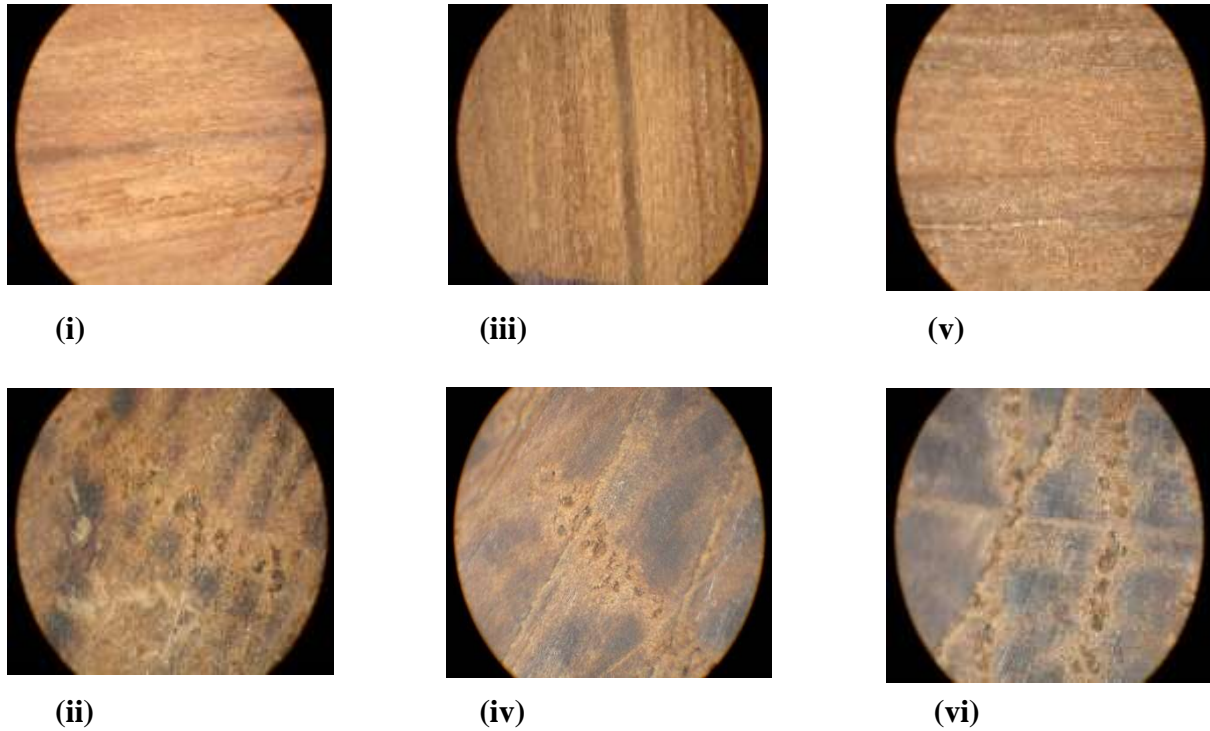


**Figure 3.5. Six light microscopy images at a 40 x magnification of a White Oak (*H*) sample; (i) untreated exterior, (ii) untreated interior, (iii) treated exterior, (iv) treated interior (v) treated and heat damaged exterior (vi) treated and heat damaged.**



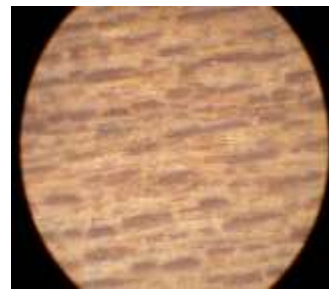
**Maple (*H*)**



**(i)**



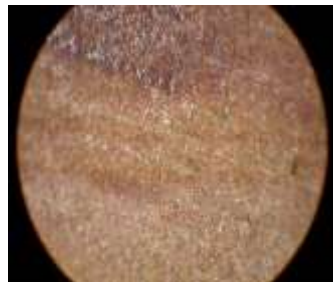
**(iii)**



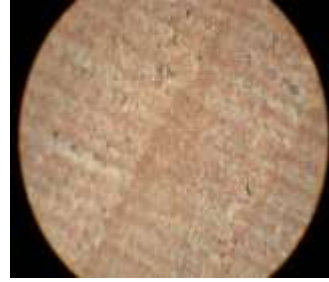
**(v)**



**(ii)**



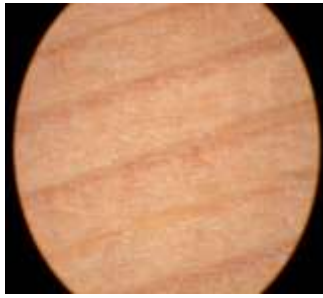
**(iv)**



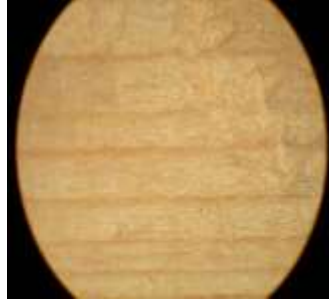
**(vi)**

**Figure 3.6. Six light microscopy images at a 40 x magnification of a Maple (*H*) sample; (i) untreated exterior, (ii) untreated interior, (iii) treated exterior, (iv) treated interior (v) treated and heat damaged exterior (vi) treated and heat damaged.**

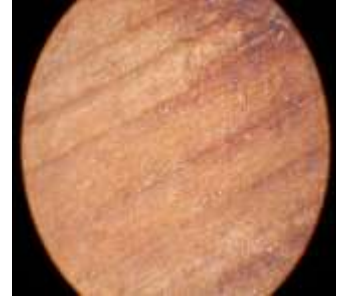
**Scots Pine (*H*)**



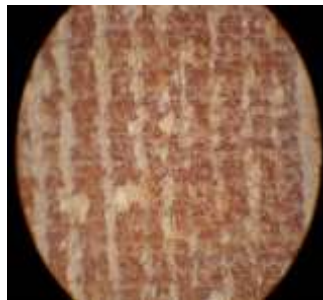
**(i)**



**(iii)**



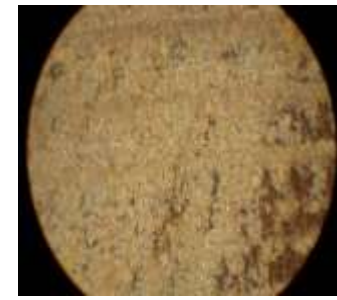
**(v)**



**(ii)**



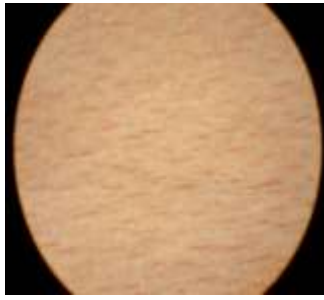
**(iv)**



**(vi)**

**Figure 3.7. Six light microscopy images at a 40 x magnification of a Scots Pine (*H*) sample; (i) untreated exterior, (ii) untreated interior, (iii) treated exterior, (iv) treated interior (v) treated and heat damaged exterior (vi) treated and heat damaged.**

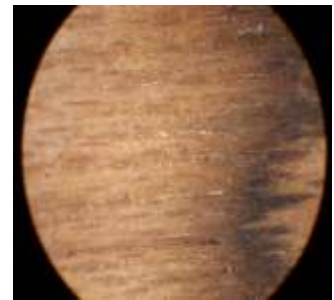
**Maple (*M*)**



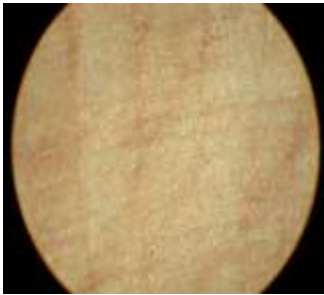
**(i)**



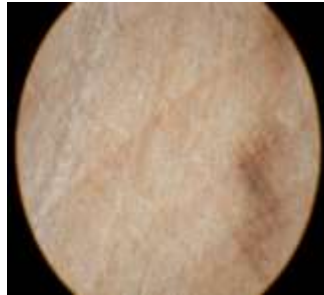
**(iii)**



**(v)**



**(ii)**



**(iv)**



**(vi)**

**Figure 3.8. Six light microscopy images at a 40 x magnification of a Maple (*M*) sample;(i) untreated exterior, (ii) untreated interior, (iii) treated exterior, (iv) treated interior (v) treated and heat damaged exterior (vi) treated and heat damaged.**

### **Zebrano (*M*)**

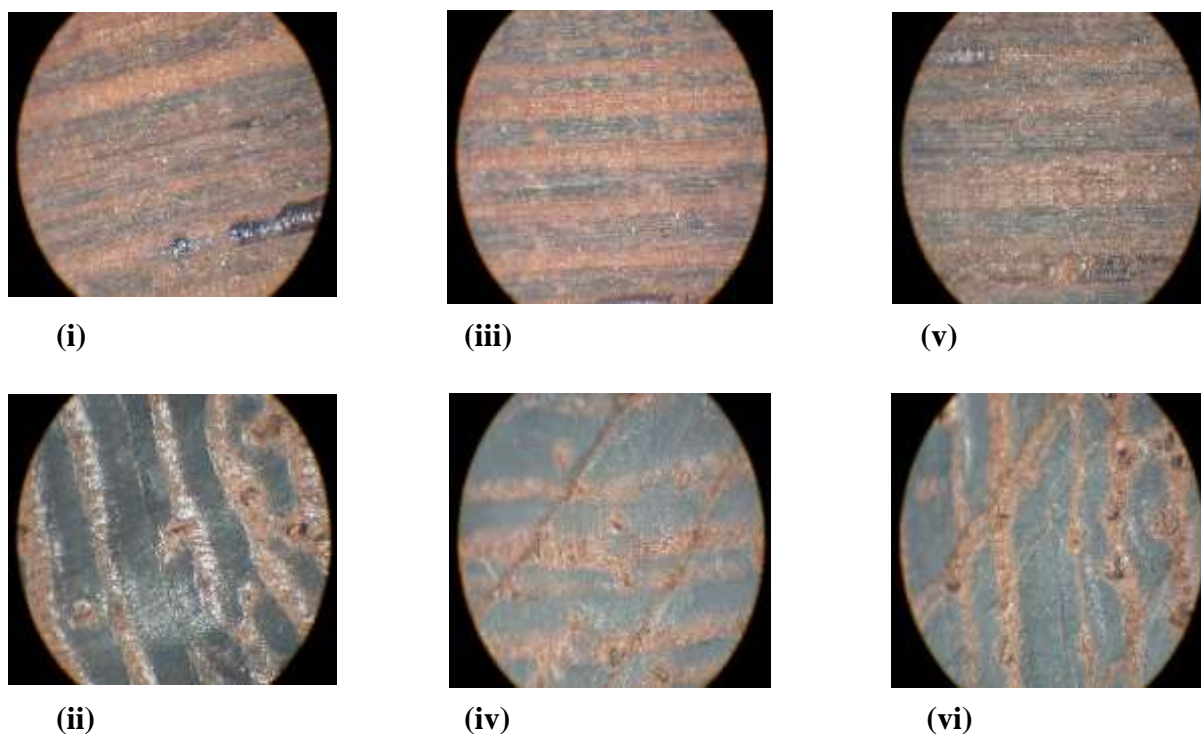


**Figure 3.9. Six light microscopy images at a 40 x magnification of a Zebrano (*M*) sample; (i) untreated exterior, (ii) untreated interior, (iii) treated exterior, (iv) treated interior (v) treated and heat damaged exterior (vi) treated and heat damaged.**

The images produced by light microscopy of the six historic and modern wood samples are very interesting. It was encouraging to see that on both the interior and exterior of the six wood samples analysed, there are no significant differences in appearance pre-and post-treatment with  $\text{scCO}_2(\text{PURE})$ . Not only does this suggest that the wood samples are not being damaged by the supercritical treatment, but they are also visually unchanged. A conservator would need to be strongly assured of this information before they carried out a treatment on any wooden object. The microscopy images also confirm and provide further insight to the characterisation and structure of the different wood species. The images are only taken at a magnitude of 40 x, however some main characteristic features can still be seen. On both the tangential exterior surfaces of the Maple (*H/M*) samples an even distribution of ray flecks can be seen (Figure 3.6, Figure 3.8), confirming the diffuse-porous composition of the hardwood (Table 2.5). In the three interior images of White Oak (*H*) (Figure 3.5), the large earlywood pores associated with a ring-porous structure, are clearly visible. For Scots Pine (*H*) the medium sized resin canals can be seen in the interior image of the treated sample, whilst the medium, open structure and straight grain typically associated with Scots Pine (*H*) can be seen on all the exterior images (Figure 3.7). Finally, the interior images of Zebrano (*M*) identify medium sized pores in no



specific arrangement and a wavy grain distribution (Figure 3.9). Although SEM images were not useful for assessing any possible damage caused by the supercritical treatment, they can still be looked at in collaboration with light microscopy images which may provide further wood character evidence.

It is useful to compare the images taken pre and post treatment to the images of the samples that were subject to heat damage in the oven during a treatment with  $\text{scCO}_2(\text{PURE})$ . The exterior of the heat damaged samples of Maple (*M/H*), Pine (*H*) and Zebrano (*M*) are darker in colour to their respected untreated and treated samples. It is likely that the colour change seen on the damaged samples has been caused by the wood fibres starting to char in the oven. The interior image of the damaged Scots Pine (*H*) sample shows the migration of the natural resin in the structure, caused by the increased heat of the oven. It is encouraging that this migration is not seen in the untreated or treated Scot Pine (*H*) sample, however the presence of this natural resin within the softwood structure may be a consideration as to why Scots Pine (*H*) samples consistently achieved low levels of NMC.

### **3.2.3 Preliminary spectroscopy studies**

Feasibility studies for spectroscopic techniques were carried out to see whether in principle it may be possible to quantify the degree of water content and other constituents of wood present in a treated sample and untreated sample. Accepting the limitation that the analyses were performed on the surface of the wood and therefore would be on a relative scale. It would be expected that the interior constitution of the samples may differ from the exterior. For these feasibility studies Scots Pine (*H*) and Maple (*M*) samples were treated with  $\text{scCO}_2(\text{PURE})$ , these were known as the ‘treated’ samples. Samples that had been oven-dried to a constant mass were also tested, these were known as the ‘untreated’ wood samples. The spectroscopic techniques used were Attenuated Total Reflectance- Fourier Transform Infrared (ATR-FTIR), Diffuse Reflectance Infrared Fourier Transform (DRIFT) and Fourier Transform Near Infrared Raman spectroscopy (FT-NIR Raman). Methods were followed as per Section 2.3.6. The spectra of each method were analysed to see which gave the most information rich description for the wood samples provided (Lindon et al., 2016). These were then looked at separately within a more detailed study (Section 3.2.3.4).

### 3.2.3.1 ATR-FTIR

#### *Scots Pine (H)*

The ATR-FTIR spectra for treated and untreated Scots Pine (*H*) samples is shown in Figure 3.10 below, the spectrum has been annotated to highlight the main bands and vibrations associated with the wood samples. The broad band observed around  $3200\text{ cm}^{-1}$ , associated with OH stretches, is similar for the treated sample compared to the untreated sample. This band derives from a series of hydroxyl containing species, including water; variation in the proportions of these species will give an apparent shift in the band maximum. In principle, it may represent the nature of binding for water, as different proportions of the contributing species will change the overall peak position and shape. No shift in the band position suggests that there is little or no difference in water content between the two samples. The biggest peaks observed in the region  $1150 - 1050\text{ cm}^{-1}$  are due to CO stretching vibrations of cellulose and hemicellulose (Lindon et al., 2016). The areas of the peaks at around  $3360\text{ cm}^{-1}$  and  $2930\text{ cm}^{-1}$  can broadly be thought of as proportional to the amount of hydroxyl OH (i.e. including water) and CH groups respectively (Lindon et al., 2016). Likewise, the area of the peaks in the  $1150 - 1050\text{ cm}^{-1}$  band are indicative of the amount of cellulose (Lindon et al., 2016). Areas of other peaks may represent degree of treatment or the quantity of cellulose, hemicellulose and lignin present. Therefore, in theory, it may be possible to quantify the degree of water content and other constituents of the wood, at least on a relative scale. It is found that for this spectrum, the OH/CH area ratio appears approximately the same for the two samples.

#### *Maple (M)*

The ATR-FTIR spectra for treated and untreated Maple (*M*) samples is shown in Figure 3.11 below. The broad band observed around  $3200\text{ cm}^{-1}$ , associated with OH stretches, is slightly shifted towards lower wavenumbers for the treated sample compared to the untreated one. Although this shift is very small, it is spectroscopically real. Again, this band derives from a series of hydroxyl containing species, including water; variation in the proportions of these species gives an apparent shift in the band maximum and may represent the nature of binding for water. The biggest peaks observed in the region  $1150 - 1050\text{ cm}^{-1}$  are due to CO stretching vibrations of cellulose and hemicellulose, as such it could be suggested that if these peaks are very similar for each sample then the supercritical hydration treatment is causing no damage. For this study these largest vibrations are not of particular use when we are looking to quantify

the water present in the samples, however they could be useful if individual characterisation of the wood species were required.

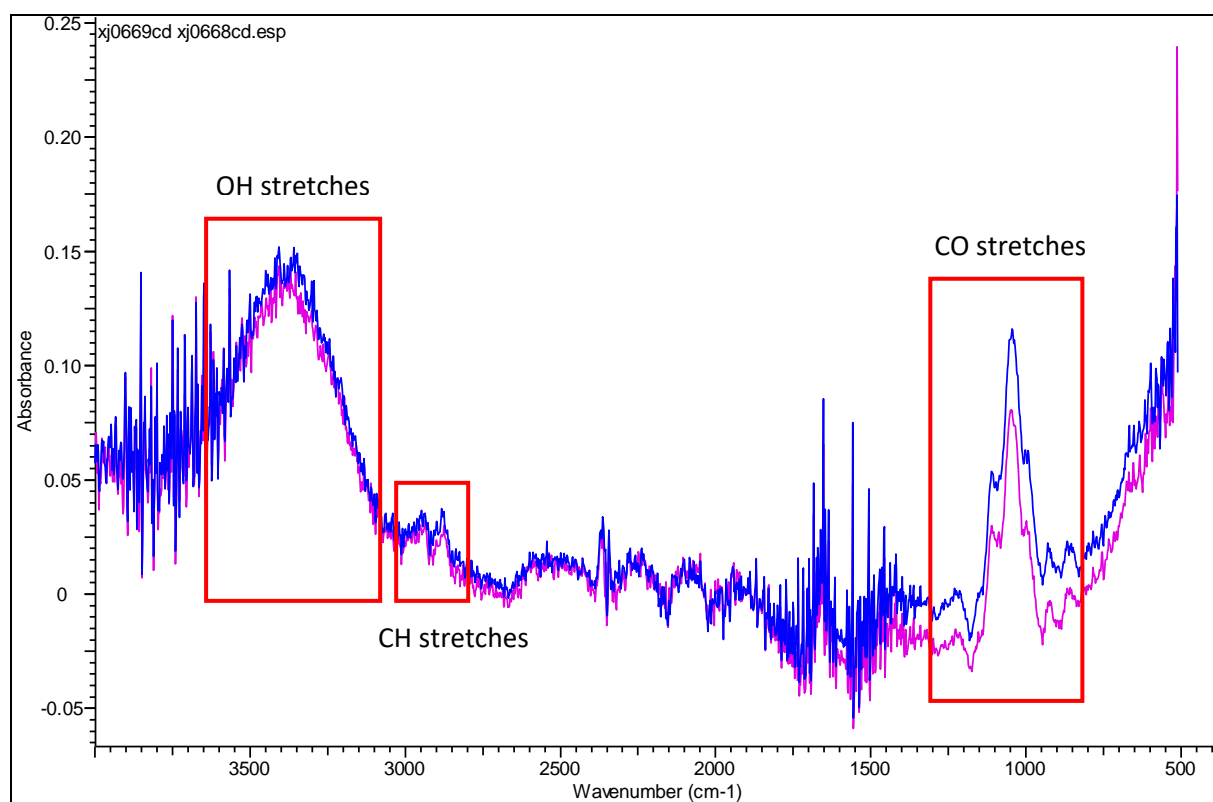


**Figure 3.10.** An annotated ATR-FTIR spectra of the untreated Scots Pine (*H*) (blue spectrum) and treated Scots Pine (*H*) (magenta spectrum) samples.

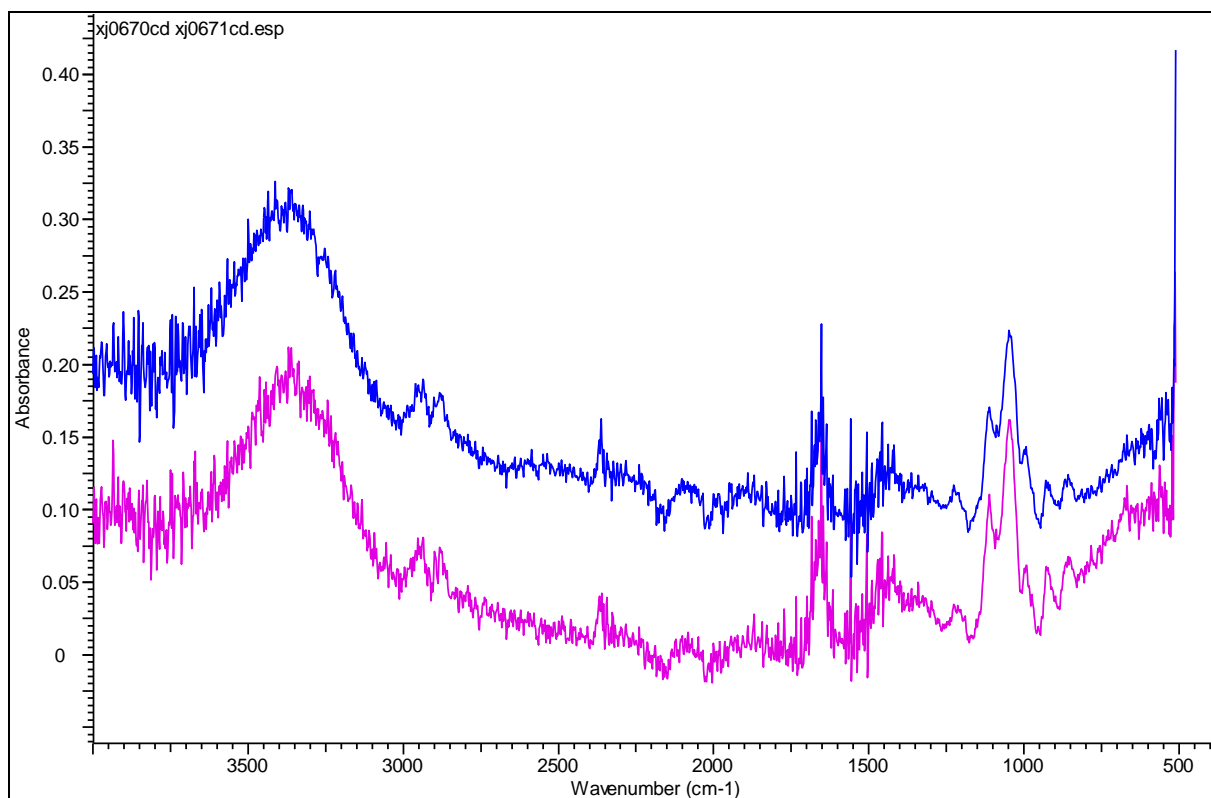


**Figure 3.11. An ATR-FTIR spectra of the untreated Maple (*M*) (blue spectrum) and the treated Maple (*M*) (magenta spectrum) samples.**

### 3.2.3.2 DRIFT

#### *Scots Pine (H)*

The DRIFT spectra for treated and untreated Scots Pine (*H*) samples are shown in Figure 3.12 below, the spectrum has been annotated to highlight the main bands and vibrations associated with the wood samples. Compared to the ATR-FTIR spectra, it can be seen that the DRIFT spectra are more information rich. The diffuse reflectance approach seems therefore more promising for future analysis. Interestingly, features in the 3600 - 5000  $\text{cm}^{-1}$  region have become apparent. The spectra of both the treated and untreated Scots Pine (*H*) samples look very similar to each other. There are no significant differences that are apparent other than a general wavelength independent shift associated with the overall reflectivity of the surface.

#### *Maple (M)*

The DRIFT spectra for treated and untreated Maple (*M*) samples are shown in Figure 3.13 below. Similarly, to the Scots Pine (*H*) spectrum (Figure 2.17), it can be seen that the DRIFT spectra are more spectral feature-rich than the comparative ATR-FTIR produced spectra. The DRIFT spectra of both the treated and untreated Maple (*M*) samples look similar, however

some differences are observed. Notably, the broad band observed around  $3200\text{ cm}^{-1}$ , associated with OH stretches, is slightly shifted towards lower wavenumbers for the treated sample compared to the untreated one. The cellulose derived bands on the two spectra are also significantly different.

A subtle difference in cellulose associated bands may be an indication as to the type of wood being tested. Maple (*M*) is a hardwood and Scots Pine (*H*) is a softwood, hence both wood samples are composed of different quantities of cellulose that are arranged in different formations with hemicellulose and lignin. Consequently, with the correct interpretation of the fingerprint region (Section 2.3.6, Chapter 2) observed with DRIFT spectroscopy, detailed characterisation of the wood species treated in this chapter may be possible in collaboration with other micro-structural analytical techniques. In theory, it is possible to subtract one spectrum from another i.e. Scots Pine (*H*) blue spectrum can be subtracted from the Scots Pine (*H*) magenta spectrum (Figure 3.12). Any differences in the two spectra where features have been lost or grown would be apparent on an otherwise straight line. However, it is important to remember that all the surfaces of all the individual wood samples would have shown some natural variability and therefore reflectivity. These natural differences could be confused for real changes in samples that were not actually applicable.

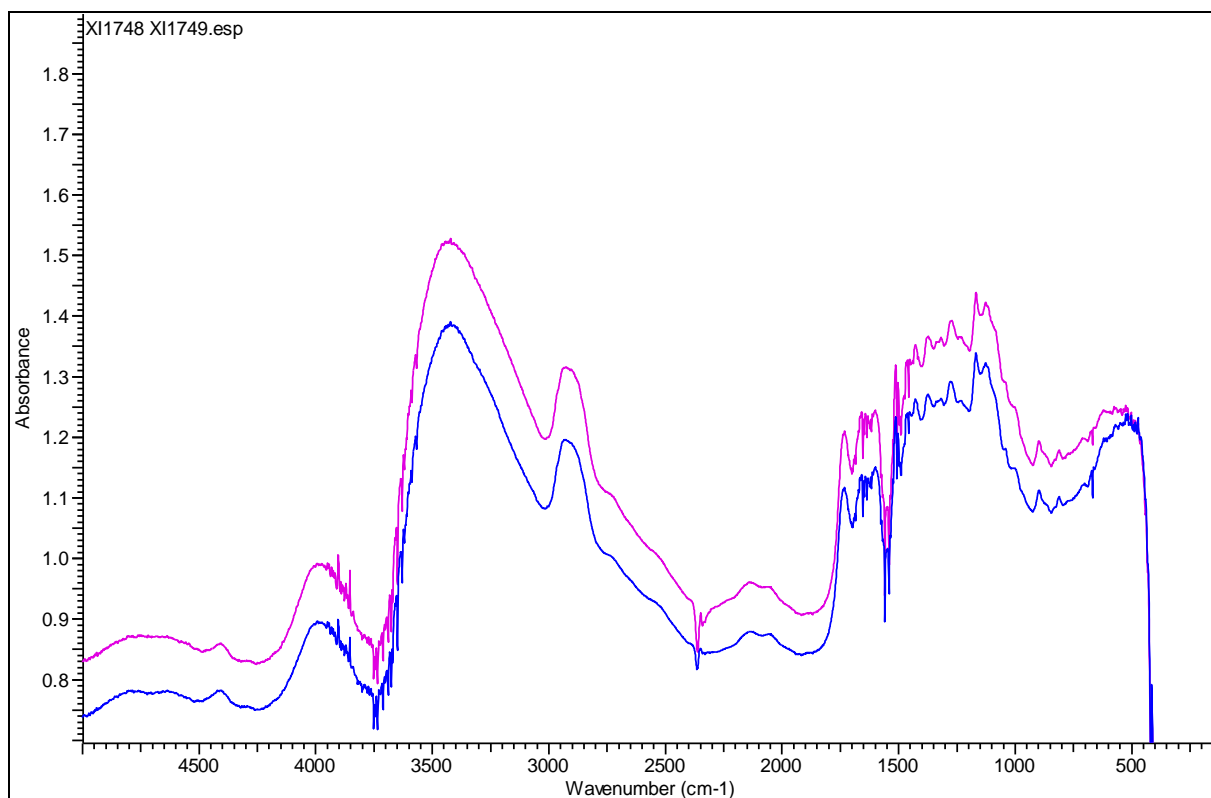


**Figure 3.12.** A DRIFT spectra of the untreated Scots Pine (*H*) (blue spectrum) and treated Scots Pine (*H*) (magenta spectrum) samples.

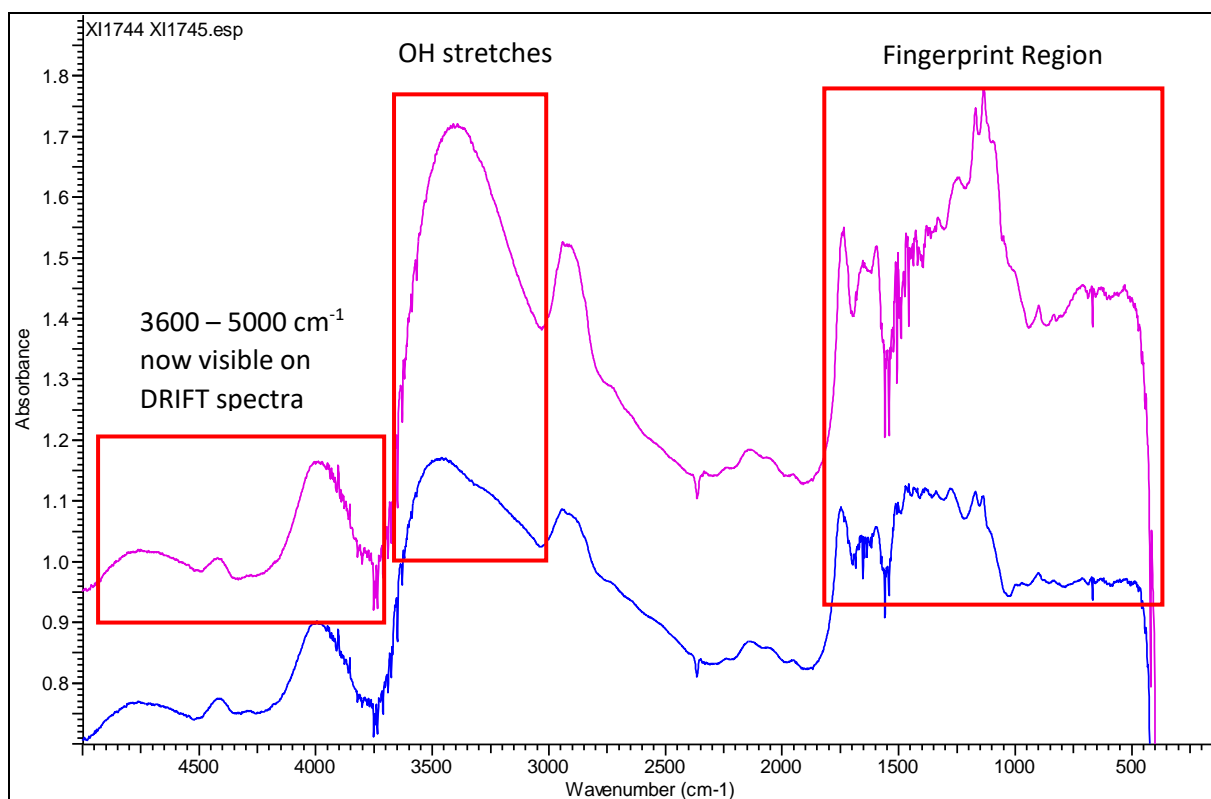


**Figure 3.13.** A DRIFT spectra of untreated Maple (*M*) (blue spectra) and treated Maple (*M*) (magenta spectra) samples.

### 3.2.3.3 FT-NIR Raman Spectroscopy

#### *Scots Pine (H)*

The Raman spectrum of treated and untreated Scots Pine (*H*) samples is shown in Figure 3.14 below. While characteristic signals are observed in the spectra, the signal-to-noise ratio is poorer than with FTIR, limiting the quantitative accuracy. Moreover, it is likely that the laser of the Raman instrument is partially drying the sample during measurement which could affect MC (Bumbrah and Sharma, 2016). However, it should be noted that Raman spectroscopy has been successfully used to characterise wood and pulp fibres (Agarwal, 2008).

#### *Maple (M)*

The Raman spectrum of treated and untreated Maple (*M*) samples is shown in Figure 3.15 below. Again, while characteristic signals are observed the signal-to-noise ratio is poorer than with FTIR, limiting the quantitative accuracy. Nonetheless, it is better than that for the Scots Pine (*H*) samples described above. Moreover, it should be remembered that it is likely that the laser of the Raman instrument is partially drying the sample during measurement.

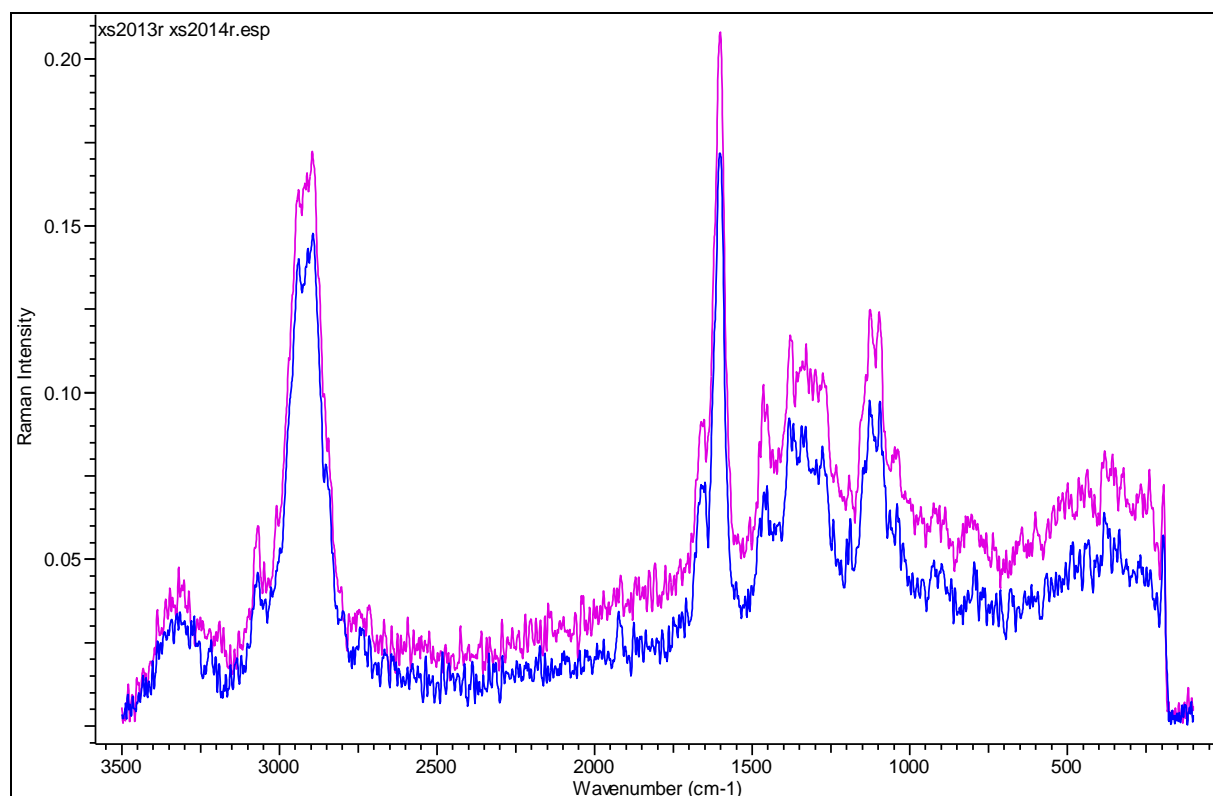


**Figure 3.14.** A Raman spectra to show the untreated Scots Pine (*H*) (blue spectrum) and treated Scots Pine (*H*) (magenta spectrum) samples.

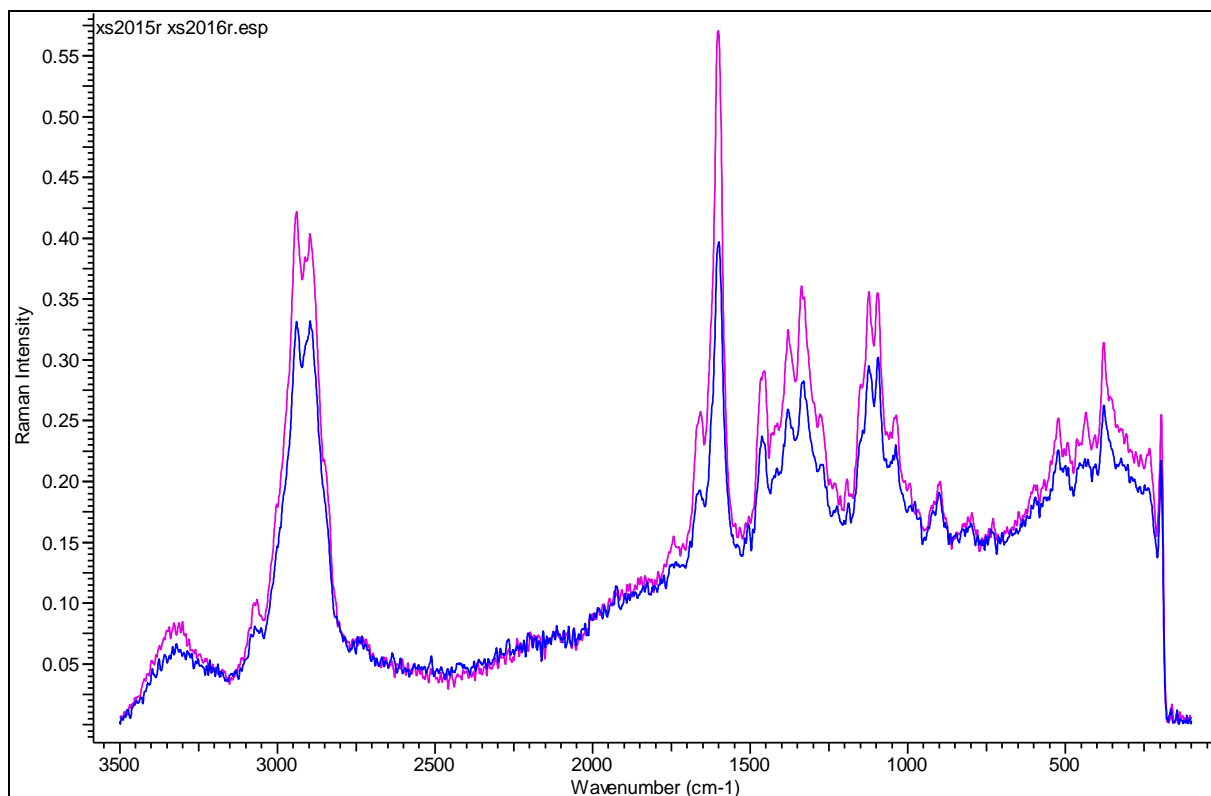


**Figure 3.15. A Raman spectra of the untreated Maple (*M*) (blue spectrum) and treated Maple (*M*) (magenta spectrum) samples.**

From the spectra observed it seems that the most promising vibrational spectroscopy method employed was infrared by diffuse reflectance (DRIFT) it gave the most information rich spectra for interpretation, with a low signal to noise ratio considering the natural variability of the wood sample surface. This technique can be applied to freshly sectioned portions of wood rather than powder, either with or across the grain, allowing the probing of internal levels of constituents compared to those on the established outer surfaces (Section 2.3.6.2, Chapter 2). The DRIFT spectra produced in this study indicated that, in theory, it may be possible to quantify the water present absorbed on the surface of the wood samples. This technique also highlighted differences in the fingerprint region, for hardwood and softwood samples that are interpreted correctly, the region may be able to provide further insight into how different wood species react to the supercritical treatment.

#### **3.2.3.4 DRIFT spectroscopy study**

Preliminary studies (Section 3.2.3) on untreated and treated wood samples with ATR-FTIR, DRIFT and Raman spectroscopy showed that in principle, it might be possible to quantify the



degree of water content and other constituents of the wood. This should at least be possible on a relative scale but with the caveat that these analyses were performed on the surface of each wood sample. It is certainly plausible that the interior constitution may vary from this. The most promising technique was found to be DRIFT spectroscopy (Figure 3.12, Figure 3.13). Therefore, an additional study using only DRIFT spectroscopy was carried out to see if any additional information could be gained from the modern wood samples White Oak (*M*), Red Oak (*M*), Maple (*M*) and Zebrano (*M*).

Four supercritical treatment types were chosen for the wood undergoing DRIFT analysis. These included  $\text{scCO}_2(\text{PURE})$ ,  $\text{scCO}_2(\text{MeOH})$  with MeOH at 2.5 mol% and 5.0 mol% as well as an additional treatment of  $\text{scCO}_2(\text{MeOH})$  with MeOH at 10.0 mol%. It should be noted here that the treatment with MeOH at 10.0 mol% requires a temperature of 51°C to reach supercritical conditions. However, because all the supercritical treatments were carried out at the higher pressure of 20 MPa, this will have ensured that the treatment with MeOH at 10.0 mol%, was well within the supercritical region even though the temperature remained at 50°C. Untreated oven-dried wood samples and wood samples soaked for 24 hours in distilled water were also analysed, these were termed ‘oven-dried’ and ‘soaked’ respectively. The same method for DRIFT spectroscopy was followed as outlined in Section 2.3.6.2.

For the all the wood samples that underwent DRIFT analysis the four-individual species all gave broadly similar spectra (Figure 3.16, Figure 3.17, Figure 3.18 and Figure 3.19). The annotated Figure 3.12 highlights the key features seen in the spectra that each modern wood sample produced. We can see that the broad band typically associated with OH stretches is observed at approximately  $3490\text{ cm}^{-1}$  for the oven-dried Red Oak (*M*) sample, as mentioned in Section 3.2.3.2. This band derives from a series of hydroxyl containing species, including water; variation in the proportions of these species will give apparent shift in the band maximum. In part, it may represent the nature of binding for water. It was assumed that the water absorbed into the wood during the supercritical treatment will be bound water (Section 2.4.1.5). Additionally, during soaking samples will initially absorb bound water and then once the cell walls become saturated, water will be absorbed into the cell cavities as free water. The soaked wood samples will then be saturated with water. The presence of free water is likely to cause a shift of the OH stretch observed towards the lower wavenumbers. A shift may also be observed for the samples treated with  $\text{scCO}_2$  that have absorbed higher levels of bound water, but no free water. For the soaked sample in Figure 3.19 the OH band is observed at around

3470  $\text{cm}^{-1}$ . As for all the wood spectra obtained in this study, the bands observed in the region around 2900  $\text{cm}^{-1}$  are associated with CH groups, as found in most of the organic molecular components. The bands in the region 2200-2300 $\text{cm}^{-1}$  are associated with atmospheric and absorbed  $\text{CO}_2$  (Lindon et al., 2016). The other bands in the spectra are associated with the principal constituents of wood, namely cellulose, hemicellulose and lignin. Chiefly the bands originating from cellulose are often partially hidden or limited in the fingerprint region (400 – 1800  $\text{cm}^{-1}$ ), this is due mainly to the physical arrangement of hemicellulose around the cellulose as described in Section 2.4.1.5. Comparisons between the fingerprint region of Figure 3.17 and Figure 3.19 for White Oak (*M*) and Red Oak (*M*) respectively, show many similarities in the vibrations. This is to be expected as the arrangement of hemicellulose and cellulose will be very similar in these two hardwood species.

It may be noted that the spectra have features at above 4000  $\text{cm}^{-1}$ , shoulders in the band at 3600  $\text{cm}^{-1}$  and features in the 1900 - 2200  $\text{cm}^{-1}$  region as well as a complex series of peaks in the fingerprint region. These are related to the detailed composition and physical state of the woods and would provide further information for the characterisation. Likewise, it can be seen that there is an apparent shift in the baseline level of the samples with treatment. This is associated with the general reflectivity and roughness of the surfaces and is again a characteristic of their nature. It is apparent that treatment of the woods affects the surface physically.

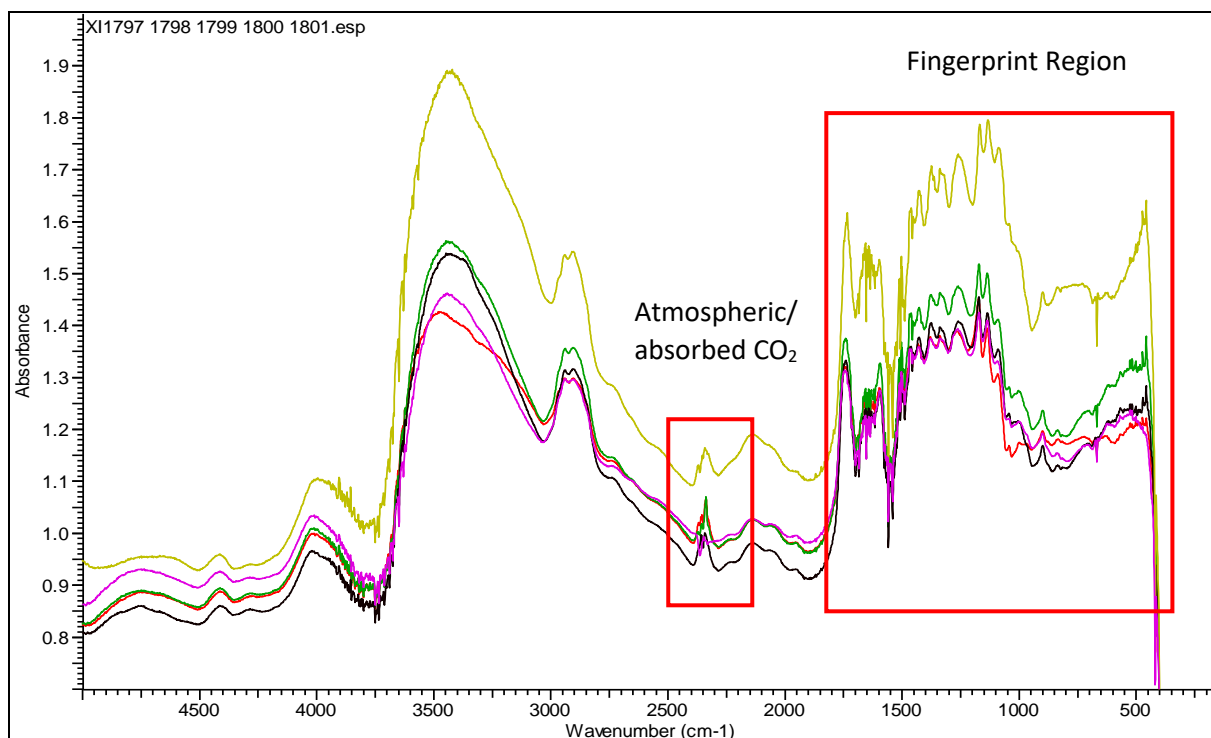


**Figure 3.16.** DRIFT spectra of the different treated Maple (*M*) samples; Oven-dried (magenta),  $\text{scCO}_2(\text{MeOH})$  with MeOH at 2.5 mol% (red),  $\text{scCO}_2(\text{MeOH})$  with MeOH 5.0 mol% (green),  $\text{scCO}_2(\text{MeOH})$  with MeOH at 10.0 mol% (black) and soaked (gold). The fingerprint region and atmospheric/absorbed  $\text{CO}_2$  peaks have been annotated.

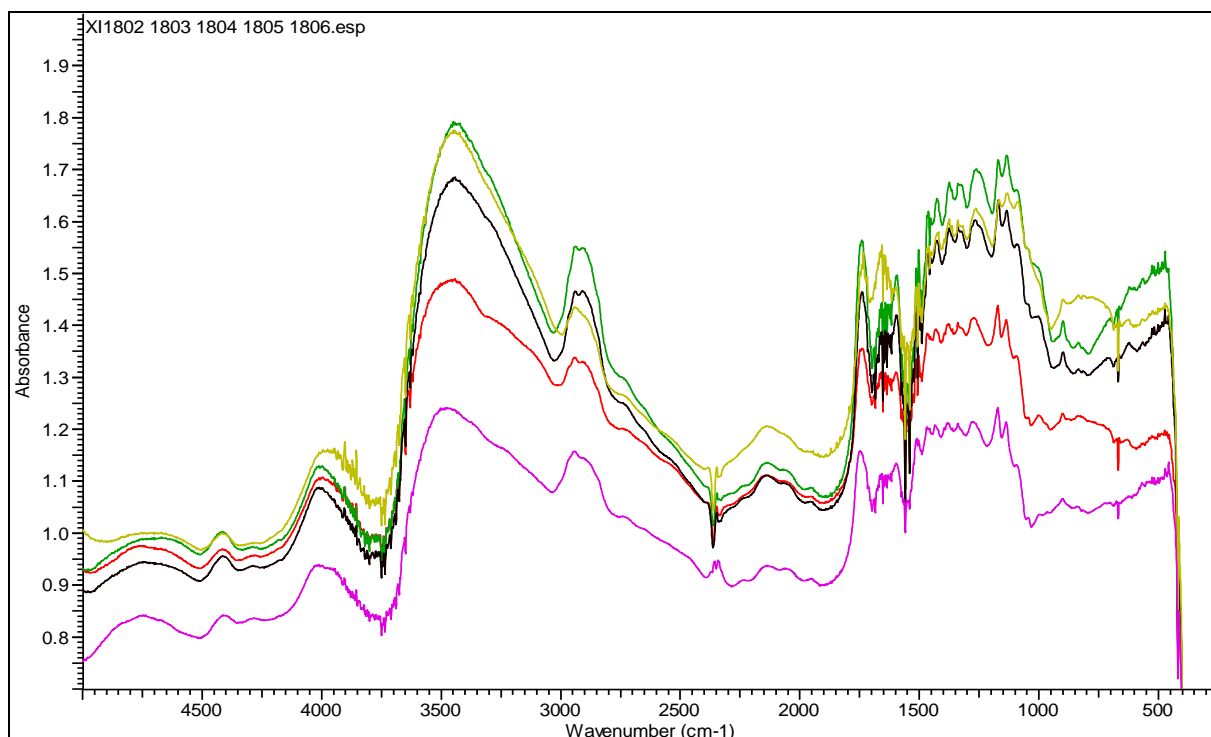


**Figure 3.17.** DRIFT spectra of the different treated White Oak (*M*) samples; Oven-dried (magenta),  $\text{scCO}_2(\text{MeOH})$  with MeOH at 2.5 mol% (red),  $\text{scCO}_2(\text{MeOH})$  with MeOH 5.0 mol% (green),  $\text{scCO}_2(\text{MeOH})$  with MeOH at 10.0 mol% (black) and soaked (gold).

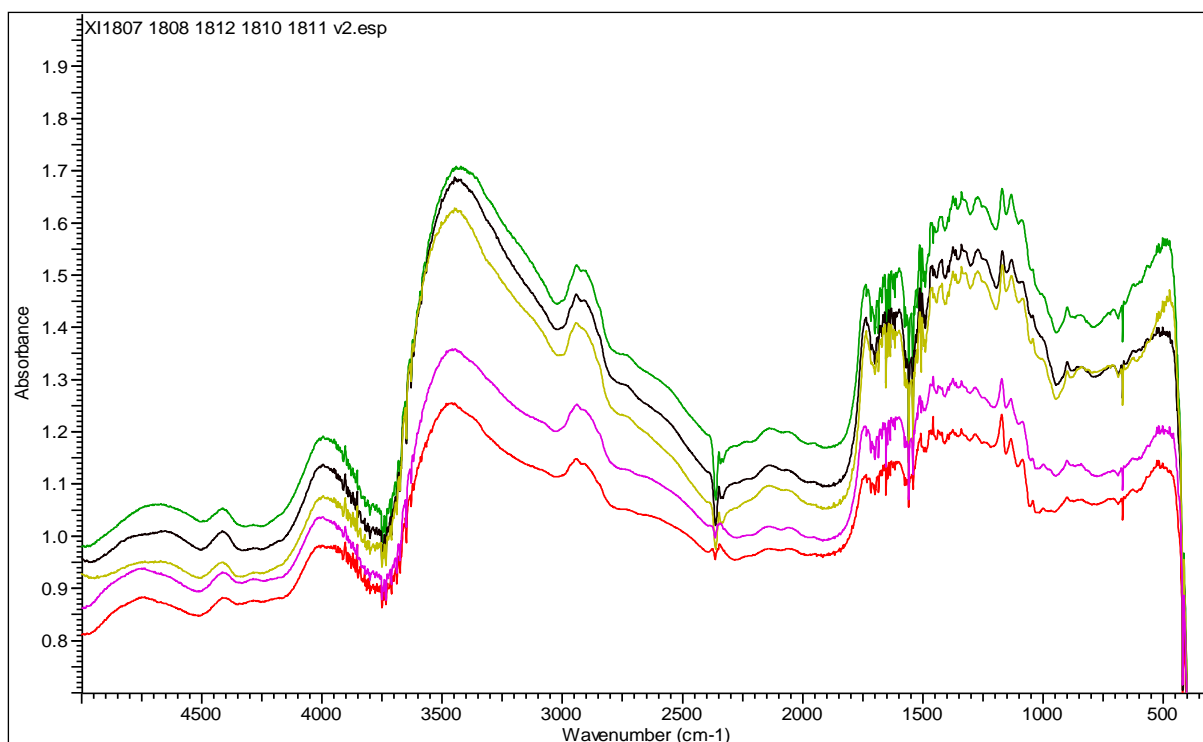


**Figure 3.18. DRIFT spectra of the different treated Zebrano (*M*) samples; Oven-dried (magenta), scCO<sub>2</sub>(MeOH) with MeOH at 2.5 mol% (red), scCO<sub>2</sub>(MeOH) with MeOH 5.0 mol% (green), scCO<sub>2</sub>(MeOH) with MeOH at 10.0 mol% (black) and soaked (gold).**

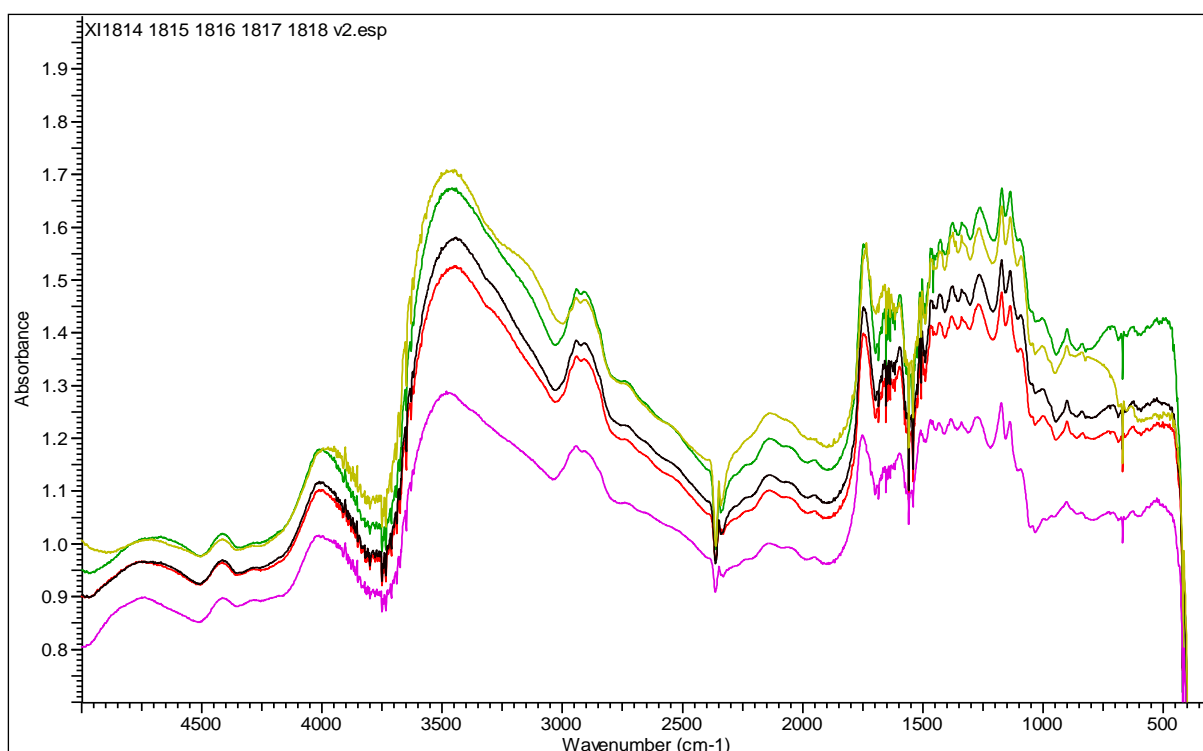


**Figure 3.19. DRIFT spectra of the different treated Red Oak (*M*) samples; Oven-dried (magenta), scCO<sub>2</sub>(MeOH) with MeOH at 2.5 mol% (red), scCO<sub>2</sub>(MeOH) with MeOH 5.0 mol% (green), scCO<sub>2</sub>(MeOH) with MeOH at 10.0 mol% (black) and soaked (gold).**

### ***O-H/C-H and O-H/“Cellulose” Ratios***

OH/CH and OH/“Cellulose” peak ratios were calculated using in-house software at Chiralabs Ltd (Oxford, UK) (Table 3.1). The areas of the peaks at about  $3460\text{ cm}^{-1}$  and  $2930\text{ cm}^{-1}$  can broadly be thought of as proportional to the amount of hydroxyl OH (i.e. including water) and CH groups respectively; the latter being a broad guide as to the “quantity” of fibrous wood. The ratios of these areas were calculated for each of the samples and are plotted in Figure 3.20, Figure 3.21, Figure 3.22 and Figure 3.23 versus treatment and wood type respectively. As expected the soaked samples were observed to have consistently a higher OH/CH ratio compared to the other samples; in contrast, the oven-dried samples have the lowest ratio of OH/CH for each wood. However, the type of water absorbed in the wood is not indicated here. The wood samples that have been soaked for 24 hours were saturated with water and will therefore comprise of free and bound water in the wood matrix. The oven-dried samples will contain very minimal water and would only be expected to have small amount of bound water left in the cell walls. It is therefore not unexpected that the ratios of the samples treated with  $\text{scCO}_2$  resemble more closely the ratios of the oven-dried samples, rather than the soaked samples. As discussed in Section 2.4.1.5 it has been assumed that, due to the relatively low levels of NMC achieved by the wood samples treated with  $\text{scCO}_2$  with and without a co-solvent, that only bound water will be present in the cell walls of these samples. Free water is only present once the fibre saturation point (FSP) is reached and MC levels of approximately 28% are achieved.

From a conservation viewpoint, a MC of 28% or greater would be harmful to the wood samples. Long term damage of the wood may be caused by the swelling of the structure and the loss of mechanical strength via the breakdown of microfibrils may also occur. Even though only low levels of hydration are achieved via  $\text{scCO}_2$  treatments, when considering an application with conservation departments this argument suggests that the supercritical hydration of the wood samples is preferential to soaking the wood samples in distilled water until they become saturated. Overtime saturated wood will start to deteriorate as hydrolysis causes the cellulose fibrils to breakdown and leave only lignin to support the wood structure (Section 1.3.2, Chapter 1).

Wood Type (Modern)	Wood Treatment Type	Peak Area Ratio 3460/2930 cm <sup>-1</sup> (OH/CH)	Peak Area Ratio 3460/4020 cm <sup>-1</sup> (OH/‘Cellulose’)
Maple	Oven-dried	9.36	7.94
White Oak		9.02	6.28
Zebrano		12.75	5.19
Red Oak		10.85	4.89
Maple	2.5 mol% co-solvent	10.46	8.12
White Oak		16.17	6.68
Zebrano		14.78	4.95
Red Oak		12.40	7.31
Maple	5.0 mol% co-solvent	9.42	9.00
White Oak		9.69	9.32
Zebrano		14.93	6.43
Red Oak		12.16	7.30
Maple	10.0 mol% co-solvent	9.64	1.14
White Oak		10.99	8.93
Zebrano		16.01	7.08
Red Oak		12.50	7.02
Maple	Soaked	15.92	11.08
White Oak		23.59	8.63
Zebrano		16.22	8.44
Red Oak		19.51	7.99

**Table 3.1.** Peak area ratios (OH/CH and OH/‘Cellulose’) for five different wood treatment types and four different modern wood types.

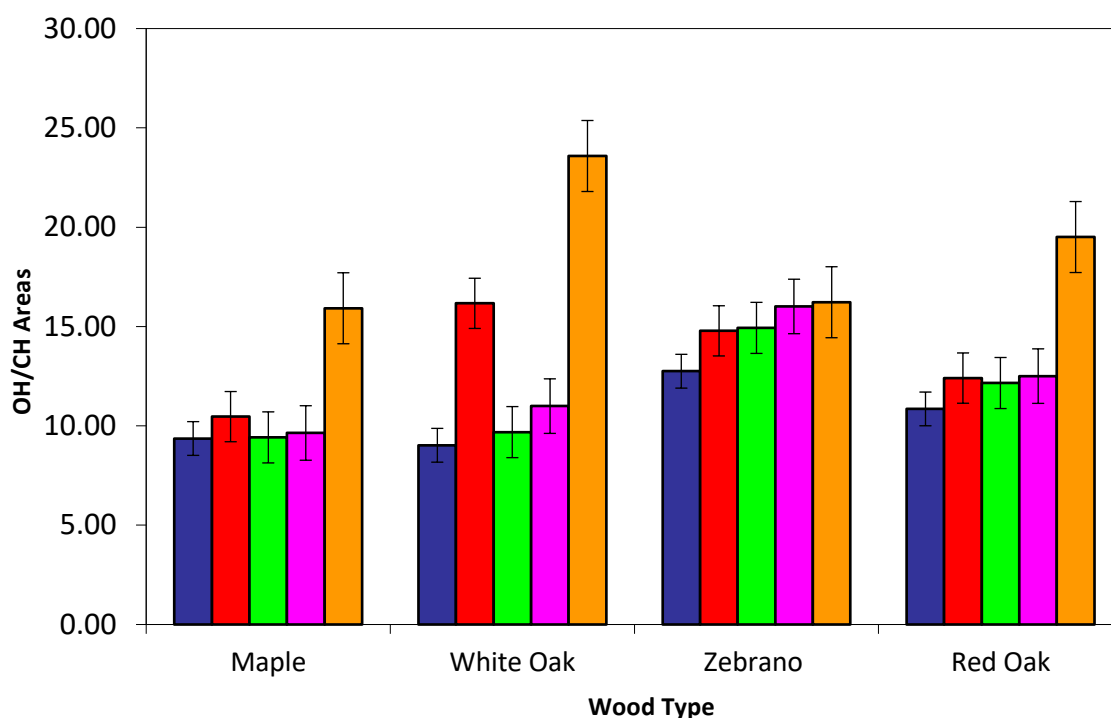


**Figure 3.20.** OH/CH peak areas (around 3460 & 2930  $\text{cm}^{-1}$  respectively) in DRIFT spectra obtained for Maple, White Oak, Zebrano and Red Oak having undergone the five different treatments: oven-dried (blue), 2.5 mol% MeOH (red), 5.0 mol% MeOH (green), 10.0 mol% MeOH (magenta) and soaked (orange). Each bar represents the overall mean from calculated ratio areas  $\pm$  one standard error of the mean.

Figure 3.20 seems to show a general trend for the treated wood samples that shows an increasing ratio with increasing co-solvent percentage, however some outliers are noticed; specifically, the ratio for sample of White Oak (*M*) treated with  $\text{scCO}_2(\text{MeOH})$ , with MeOH at 2.5 mol%, seems anomalously high. It is encouraging that the trend seen here supports the theory that by increasing MeOH concentration, there is an increased affinity in between  $\text{scCO}_2$  and water, which in turn increases the quantity of water absorbed by the wood samples. This theory is also supported by the NMC analysed in Section 2.4.1. It is interesting that in Figure 3.20 Zebrano (*M*) is shown to have consistently higher ratios of OH/CH from oven-dried all the way through to soaked. These ratios indicate higher levels of surface water absorption, in comparison to the three other wood species. However, the NMC data shows that Zebrano was the poorest wood species in the sample set at retaining water, and achieved no significant results. Therefore, these ratios suggest that although Zebrano (*M*) is able to absorb water into the surface level cells it seems unable to penetrate further into the wood matrix and retain water at a greater depth. This may also be due to the higher quantity of lignin known to be in tropical hardwood matrices in comparison to hardwood matrices. The lignin may form an arrangement

that makes it harder for the water molecules to hydrogen bond with the free hydroxyl sites on the cellulose polymer.

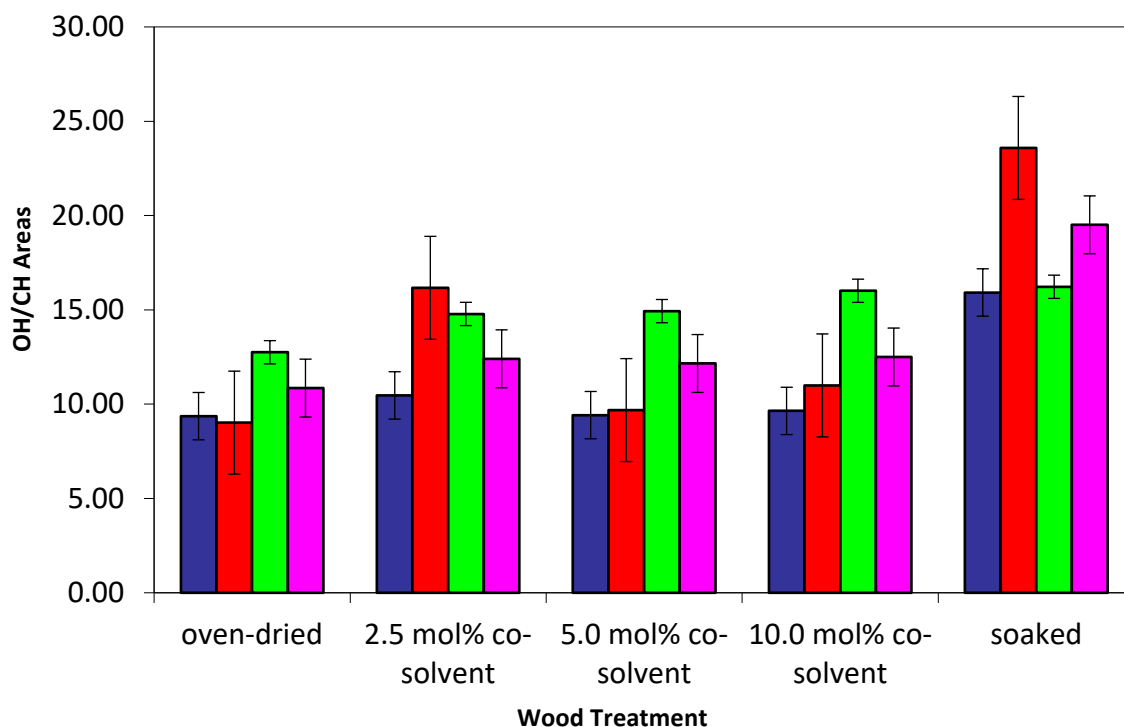


**Figure 3.21.** OH/CH peak areas (around 3460 & 2930  $\text{cm}^{-1}$  respectively) in DRIFT spectra obtained for Maple (blue), White Oak (red), Zebrano (green) and Red Oak (magenta) having undergone the five different treatments: oven-dried, 2.5 mol% MeOH, 5.0 mol% MeOH, 10.0 mol% MeOH and soaked. Each bar represents the overall mean from calculated ratio areas  $\pm$  one standard error of the mean.

An alternative approach is to consider the band at 4020  $\text{cm}^{-1}$  as representative of cellulose & hemicellulose levels and calculate the peak area ratio of hydroxyls (around 3460  $\text{cm}^{-1}$ ) relative to this, as shown in Figure 3.22 and Figure 3.23. As can be seen, there are some trends similar to those seen for the OH/CH ratio data. There is a general trend observed for each of the four woods the OH/“Cellulose” ratio increases with increasing levels of hydration, achieved either by increasing the concentration MeOH or by soaking the samples. The ratio increases as with increasing levels of water there is more chance that hydrogen bonds will be formed between the hydroxyls on the cellulose chain and the water molecules. Here Zebrano (*M*) consistently has the lowest OH/“Cellulose” ratios suggesting that minimal hydrogen bonds have been formed between OH and cellulose hydroxyls. Anomalous cases are seen in the White Oak (*M*) samples that have been soaked and undergone treatment with 2.5 mol% MeOH. It is known that White Oak (*M*) along with the other hardwood samples, responded well to the supercritical hydration treatment achieving some of the highest levels of NMC. However, it is certainly



surprising that the ratio of both OH/CH and OH/ “Cellulose” is so high for White Oak (*M*) treated with 2.5 mol% MeOH. This may be due to a combination of the White Oak (*M*) samples responding well the supercritical hydration treatment and some internal variability in the White Oak (*M*) samples tested in this DRIFT spectroscopy study that have allowed for unusual levels of hydration. Additional samples should be tested in future studies to fully understand the anomalies found here.

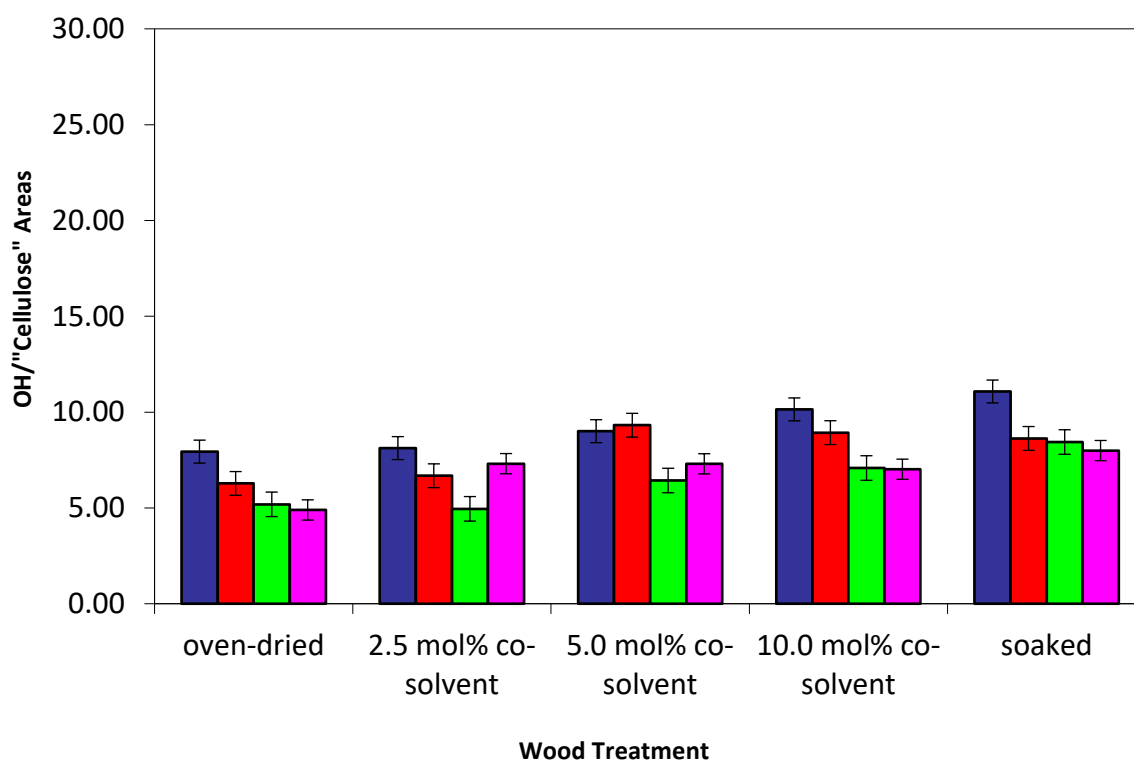


**Figure 3.22.** OH/'Cellulose' peak areas (around 3460 & 4020  $\text{cm}^{-1}$  respectively) in DRIFT spectra obtained for Maple (blue), White Oak (red), Zebrano (green) and Red Oak (magenta) having undergone the five different treatments: oven-dried, 2.5 mol% MeOH, 5.0 mol% MeOH, 10.0 mol% MeOH and soaked. Each bar represents the overall mean from calculated ratio areas  $\pm$  one standard error of the mean.

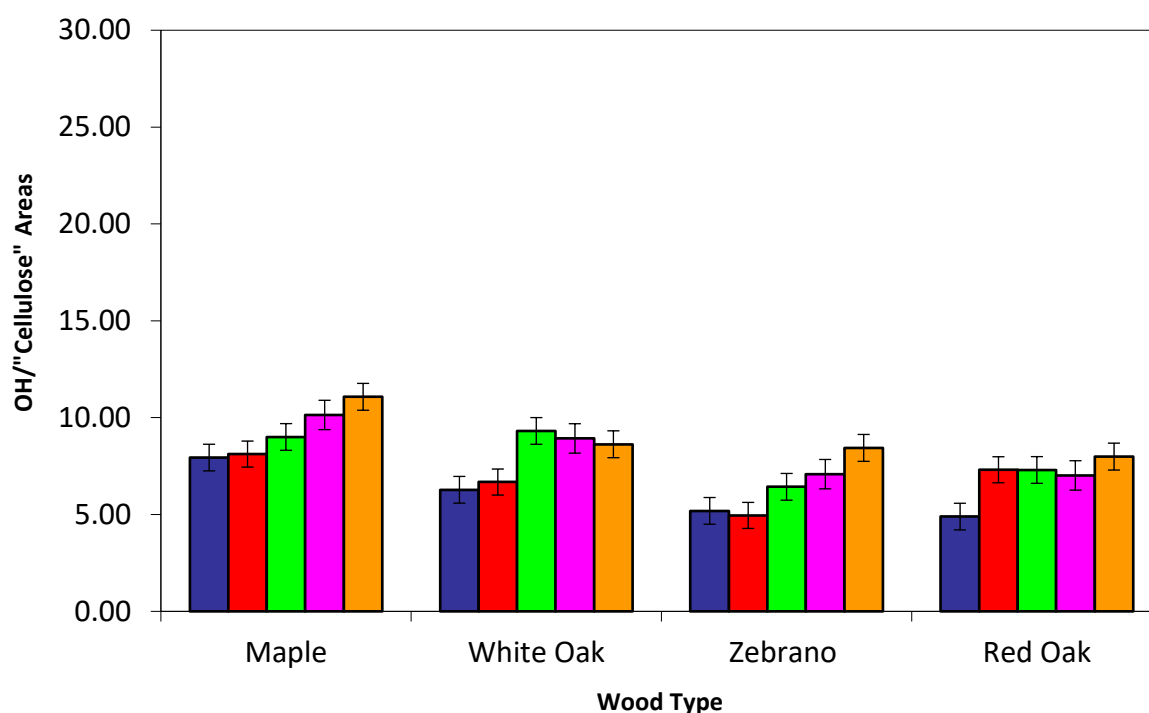


**Figure 3.23.** OH/'Cellulose' peak areas (around 3460 & 4020  $\text{cm}^{-1}$  respectively) in DRIFT spectra obtained for Maple, White Oak, Zebrano and Red Oak having undergone the five different treatments: oven-dried (blue), 2.5 mol% MeOH (red), 5.0 mol% MeOH (green), 10.0 mol% MeOH (magenta) and soaked (orange). Each bar represents the overall mean from calculated ratio areas  $\pm$  one standard error of the mean.

In summary, it can be said that this approach with DRIFT spectroscopy gave a reasonable degree of success. It is suggested that the likely chemical and physical processes of the treatments on the different wood species should be considered in relationship to the observed spectra. Additional features related to composition may be profitably considered in order to create an in-depth characterisation of the wood species in the sample set.

### 3.3 Macrostructural analysis

#### 3.3.1. Macrostructural hypotheses

The following hypotheses were made regarding the macrostructural properties of Maple (*H/M*), White Oak (*H/M*), Red Oak (*M*), Zebrano (*M*), Keruing (*H*) and Scots Pine (*H*):

- As per Section 1.5.4 (Chapter 1), the tropical hardwoods Keruing (*H*) and Zebrano (*M*), will be the strongest woods and Scots Pine (*H*) will be the weakest wood. The strengths of the hardwoods Maple (*H/M*), White Oak (*H/M*), and Red Oak (*M*) will lie in between the strongest and weakest strength values.
- The historic wood in the sample set is more than 100 years old. It is expected that all the historic wood samples will have been exposed to biodeterioration and/or abiotic deterioration at some point during that time. Consequently, historic wood samples will be less strong than modern wood samples.
- The hydration treatments with  $\text{scCO}_2(\text{PURE})$  and  $\text{scCO}_2(\text{MeOH})$  will maintain the strength of all of the wood samples, as demonstrated by previous studies carried out by Smith et al. (1992) and Morrell et al. (1996).

#### 3.3.2 Three-point bend test

To accurately assess the strength of wood, the terms of stress and strain must be understood. Stress is defined as the amount of force or load acting on a unit of area and strain is the deformation per unit of original length. Strength is often defined as the ability to resist applied stress and is also synonymous with the resistance of the material (Hoadley, 2000). The relationship between stress and strain is therefore of primary concern when considering the strength of wood. For each of the wood samples tested a stress/strain graph was plotted with load vs deformation (Figure 2.6, Figure 2.7), the proportional relationship depicted between stress and strain is defined in Hooke's Law. Hooke's Law is important as it states that wood is elastic up to a proportional limit, therefore strain is recoverable upon the removal of stress. The strength values for the wood sample set were all calculated from values within the wood species elastic limit (Figure 2.6). As Hooke's Law states, within the elastic limit stress and strain are directly proportional, here the relative gradient of the graph is equal to Young's Modulus or MOE. Therefore, the steeper the gradient, the higher the value of MOE and the stiffer the wood. Furthermore the higher the value of MOE, the lower the deformation under a given load. Values beyond the proportional limit were not used in the strength calculations

because as the wood is compacted more and more and resistance to the load increases, no useful maximum load is reached. The strength values calculated are therefore representative of the fibre strength at the proportional limit (FSPL).

The three-point bend test carried out is static and therefore representative of the bending that occurs on a centre-loaded, simple supported beam (Figure 2.5, Section 2.3.7). Here the bending caused by the load will shorten or compress the upper surface of the wood fibres through compression and lengthen or stretch the wood fibres on the lower surface through tension. These tension and compression stresses together are known as bending stresses or FSPL. The flexure formula calculation for maximum bending stress or MOR has been shown in Section 2.3.7, Equation 2.6 and Equation 2.7 respectively. Therefore the ‘strength’ values that are referred to for the rest of this Section are referring to the bending strength (MOR) of wood, and thus the woods ability to resist a load against axial tension and compression.

The main factors that affect the ability of wood to resist a load are as follows (Green, 2001):

- Type, direction, and duration of loading
- Moisture content and temperature
- Variability of the wood

By addressing each of these factors in turn, it may be possible to gain a greater understanding into the complex relationship between the impregnation of the different wood species using scCO<sub>2</sub>, and the resulting mechanical behaviours of the samples, which are discussed in the following Section 3.3.2.1.

#### ***Type, direction, and duration of loading***

The orthotropic nature of wood means that the resulting mechanical properties are independent in the direction of the three mutually perpendicular axis: radial, longitudinal and tangential axis. The tangential and radial directions are referred to as being perpendicular to, or against the grain, whilst the longitudinal direction is parallel or with the grain. Grain direction is important because the mechanical properties of the wood are more pronounced parallel to the grain (Greer, 2008). The strength values shown here are perpendicular to the grain, therefore they will be lower than values that would be calculated for compression parallel to the grain (Hoadley, 2000). The strength values obtained from the three-point bend test were only under load for 40 seconds, therefore only giving insight into the short-term load ability of the wood samples. The compressional tests performed will not take into consideration the time dependant

deformation that occurs in wood, called creep. However, the objects that may be subject to treatments with scCO<sub>2</sub> are limited by the maximum size of the pressurised cell. Therefore, larger items that are more likely to experience creep such as wooden furniture or architecture would never be considered for any of the suggested supercritical hydration treatments.

### ***Moisture content and temperature***

Pre-treatment, all the wood samples were tested after they had been oven-dried to a constant mass. Post-treatment the wood samples were tested at 504 hours, once all the samples had reached a constant NMC. As the MC of wood decreases below the FSP, the strength of wood will increase. FSPL in compression perpendicular to the grain is approximately tripled from the MC of green to the MC of oven-dried wood (Hoadley, 2000). All samples were oven-dried to a constant mass prior to treatment with scCO<sub>2</sub>. Therefore, any damage caused through high oven temperatures has been assumed constant for all the wood samples and is therefore negligible. During the compressional test the wood samples were exposed to no dramatic variations in temperature and lab conditions were monitored throughout the tests.

### ***Variability of wood***

Density and the average specific gravity of wood species provides the best indicator as to the woods strength. Within the wood sample set there is considerable variation in the values of specific gravity (Table 2.3). Within each individual wood sample there will also be considerable variation in specific gravity values due to density variation associated with the wood cell structure, these variations cannot be predicted. Density in softwoods and ring-porous hardwoods can in part be predicted by the growth rates of early and latewood. On the other hand there is no relationship between density and growth rates in diffuse-porous hardwoods (Section 2.4.1.4). In summary, the variability in individual clear wood samples is very difficult to predict.

It may be easier to predict differences in the wood densities of the historic and modern wood samples. Although all the wood samples were chosen for their uniformity and lack of defects, it is most likely that the historic wood samples have defects internally that may not be visible to the human eye and thus cause variations in the wood sample density. Previous research has shown that there are often structural changes that occur in wood that has been exposed to degradation over time (Christensen et al., 2006).

### 3.3.2.1 Bending strength of the wood samples pre-and post scCO<sub>2</sub> treatment

As described, the mechanics related to wood as an anisotropic, heterogenous material are very complex. However the pre-treatment strengths of the individual wood samples were as expected (Rowell, 2012) (Section 1.5.5, Chapter 1); the tropical hardwoods Zebrano (*M*) and Keruing (*H*) are shown to be the strongest samples, followed by the hardwoods Maple (*H/M*), White Oak (*H/M*) and Red Oak (*H*), and finally Scots Pine (*H*), the only softwood. Scots Pine (*H*) is by far the weakest at approximately 100 MPa, this Scots Pine (*H*) sample is also a historic wood thus making it even weaker than normal due to exposure to deteriorative processes over time. Zebrano (*M*) is the strongest wood of the samples, with a pre-treatment strength of about 800 MPa, it is also a modern wood sample and therefore has had little exposure to any deterioration processes. The difference in the strength values presented by Scots Pine (*H*) and Zebrano (*M*), can in the major part be attributed to the density of the species. Density is the single most important factor when predicting the strength of a specific wood. Zebrano (*M*) has a basic specific gravity of 0.67 and Scots Pine (*H*) has basic specific gravity of 0.39 (Rowell, 2012). Specific gravity, also known as the density index, is the ratio of the density of a substance to the standard density of a substance (e.g. water). In reality, both the specific gravity values of the Zebrano (*M*) and Scots Pine (*H*) samples will be lower than these because they have both been oven dried and now have a relatively low moisture content.

Of the hardwoods, Maple (*H/M*) is shown to be slightly stronger than White Oak (*H/M*) and Red Oak (*M*). The pre-treatment strength values show that the species of the wood is more of an influencing factor on strength than the age of the wood (Table 3.2). However, it can also be seen that of the species that have comparative historic and modern samples e.g. Maple (*M/H*), the modern sample is always stronger than the historic sample. As hypothesised, the historic wood samples have been adversely affected by degradation processes that have damaged the structural integrity of the wood samples (Gerhards, 1982).

Wood Species	MOR of samples/ MPa	Wood Type
Zebrano ( <i>M</i> )	791	Tropical Hardwood
Keruing ( <i>H</i> )	718	
Maple ( <i>M</i> )	640	Hardwood
Maple ( <i>H</i> )	634	
White Oak ( <i>M</i> )	528	
Red Oak ( <i>M</i> )	519	
White Oak ( <i>H</i> )	514	
Scots Pine ( <i>H</i> )	110	Softwood

**Table 3.2.** A table to show oven-dried wood samples in decreasing order of mean strength prior to treatment with  $\text{scCO}_2(\text{PURE})$  and  $\text{scCO}_2(\text{CH}_3\text{OH})$ . Strength values have been stated to an accuracy of 3 significant figures. N.B. MOR is defined here as the Modulus of Rupture.

Wood	MOR oven-dried/MPa	MOR $\text{scCO}_2(\text{PURE})/\text{MPa}$	MOR $\text{scCO}_2(\text{MeOH})$ 2.5mol%/MPa	MOR $\text{scCO}_2(\text{MeOH})$ 5.0mol%/MPa
Maple ( <i>M</i> )	640	738	684	675
White Oak ( <i>M</i> )	528	715	659	625
Red Oak ( <i>M</i> )	521	743	717	600
Zebrano ( <i>M</i> )	791	970	958	900
Maple ( <i>H</i> )	634	605	562	444
White Oak ( <i>H</i> )	514	633	574	524
Scots Pine ( <i>H</i> )	110	272	181	151
Keruing ( <i>H</i> )	718	845	776	767

**Table 3.3.** A table to show the calculated mean bending strength (MOR) values of wood species that have been treated with  $\text{scCO}_2(\text{PURE})$  and  $\text{scCO}_2(\text{MeOH})$  in comparison to the untreated oven-dried samples. Strength values have been stated to an accuracy of 3 significant figures. A plot to test whether there is a mathematical correlation between NMC and MOR is presented in Appendix 5, Figure 1.

The effect of SCF treatments on the bending strength and stiffness in Pine sapwood samples has been investigated by Smith, Demessie et al (1992). Mechanical tests indicated that the treated and untreated samples were not significantly different in MOE or MOR, therefore suggesting that SCF treatments are not damaging to the internal wood structure. Acda, Morrell et al (1996) have also previously reported that SCF treatments have had no negative effects on the MOR, MOE or dimensional stability of wood-based composites, SCF impregnation seemed not to adversely affect mechanical properties. Importantly, it should be noted that wood-based

composites are manmade and thus they are specially designed to be structurally different to naturally cut lumber to meet the demands of modern consumer. Therefore, the suggested property improvements may not be seen in wood species that have not been modified. Given the previous results for the mechanical testing of wood treated with SCF's (Morrell et al., 1993, Sahle-Demessie, 1994), it seems positive that the samples tested in this study either maintained or increased in MOR or bending strength post treatment both with  $\text{scCO}_2(\text{PURE})$  and  $\text{scCO}_2(\text{MeOH})$  (Table 3.3). The wood samples that maintained but did not improve in strength statistically gave no significant results in Student t Test (Section 2.3.8). Keruing (*H*) gave no significant results for any of the supercritical treatments, therefore maintaining its original strength pre-treatment. Maple (*M*) and White Oak (*H*) gave significant results with  $\text{scCO}_2(\text{PURE})$  but not with  $\text{scCO}_2(\text{MeOH})$ , Red Oak (*M*) gave all significant results except for the supercritical treatment with 5.0mol% MeOH. The remaining woods in the sample set all gave significant results.

A general trend was observed from the strength data which showed a negative correlation between the percentage concentration of the MeOH and the resulting strength of the wood samples (Figure 3.24, Figure 3.25, Figure 3.26, Figure 3.27, Figure 3.28, Figure 3.29, Figure 3.30, Figure 3.31). As the percentage concentration of MeOH was increased towards 5.0 mol%, the strength of the wood samples decreased. However, none of strength values for samples treated with 5.0 mol%  $\text{scCO}_2(\text{MeOH})$  decreased below the initial strength of the corresponding untreated wood sample; nonetheless it was lower than if the wood had just been treated with  $\text{scCO}_2(\text{PURE})$  (Table 3.3). As shown by hydration profile Figure 2.12, it is known that with increasing MeOH concentration, increasing levels of NMC are achieved by the treated wood samples. Increasing the overall moisture content of the wood decreases its stiffness, strength and brittleness (Greer, 2008) due to water forming hydrogen bonds with the cellulose hydroxyl sites, thereby increasing the surface area of the cell walls and altering its configuration. Hence, the decreasing strength of the samples positively affirms the assumption that  $\text{scCO}_2$  is successfully hydrating the wood sample structure to a certain degree.

This trend also raises an interesting point as to the correct selection of supercritical treatment for the wood samples, especially when considering the method for applications within conservation departments. The strength data suggests that a “happy medium” should be found between co-solvent addition and concentration, the levels of hydration achieved and the strength maintained or increased by the wood species, it also suggests that there may not be one supercritical treatment suitable for each wood species. The author had wanted to investigate the addition of 10.0 mol% MeOH to the  $\text{scCO}_2$  solvent stream. However, from a



conservation viewpoint, treating wood samples with  $\text{scCO}_2(\text{MeOH})$ , with MeOH at 10.0 mol%, does not seem sensible. If the same wood species that have been used in this study, are treated with 10.0 mol% MeOH then it can be assumed that the samples are likely to attain higher stabilised NMC than the mean NMC achieved in this study. It can therefore also be assumed that the samples are also likely to be weaker than their original, untreated state. Given that conservators seek to maintain or increase the strength and/or stability of an object, any one of the supercritical treatments investigated here would be more suitable than a treatment with 10.0 mol% MeOH.

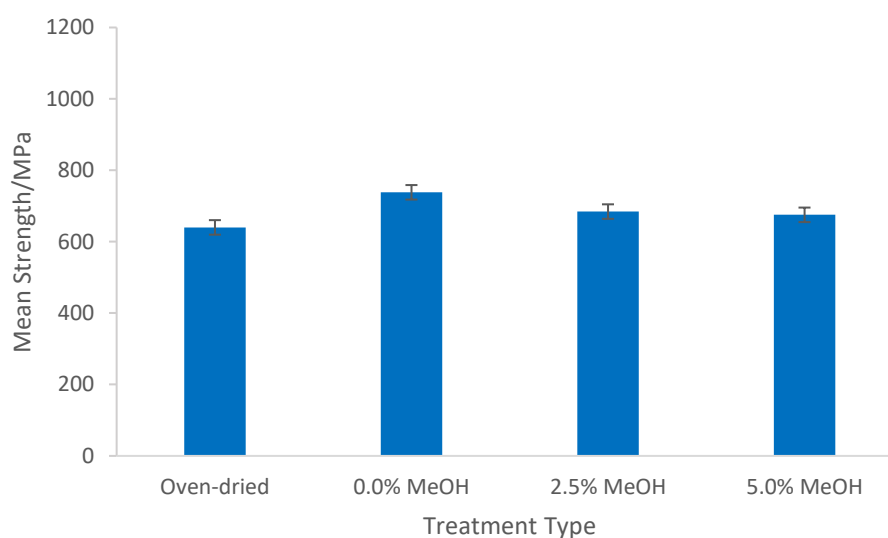


**Figure 3.24. A comparison of the mean strength values for Maple (*M*) pre and post treatment with  $\text{scCO}_2(\text{PURE})$  or  $\text{scCO}_2(\text{MeOH})$ . Each bar represents the overall mean from three independent sets of measurements  $\pm$  one standard error of the mean.**

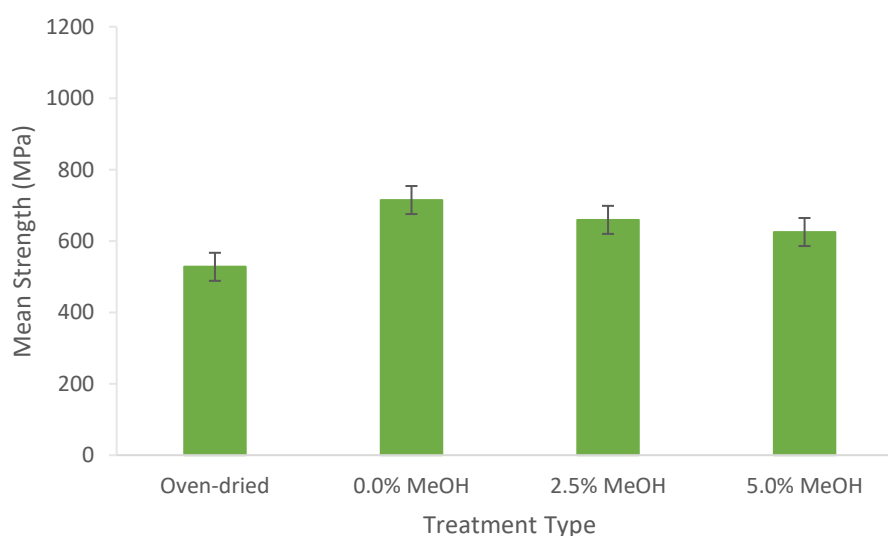


**Figure 3.25. A comparison of the mean strength values for White Oak (*M*) samples pre and post treatment with  $\text{scCO}_2(\text{PURE})$  or  $\text{scCO}_2(\text{MeOH})$ . Each bar represents the overall mean from three independent sets of measurements  $\pm$  one standard error of the mean.**

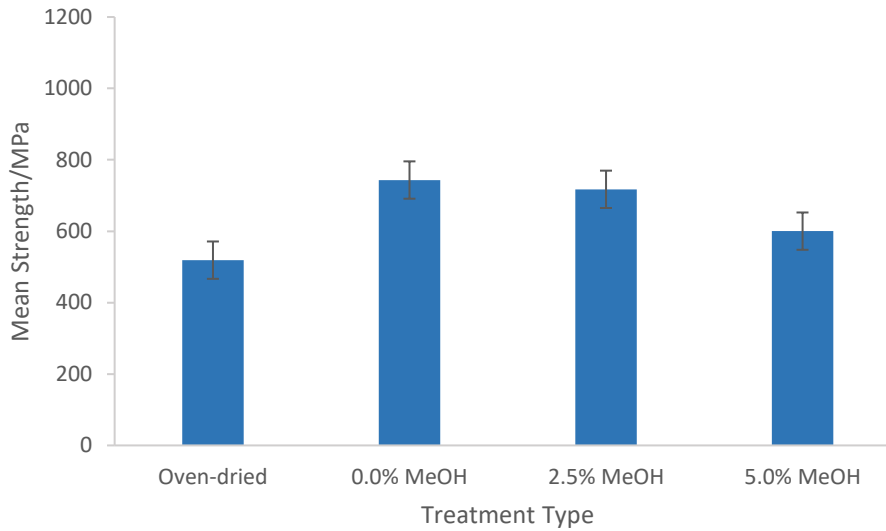


**Figure 3.26. A comparison of the mean strength values for Red Oak (*M*) pre and post treatment with  $\text{scCO}_2(\text{PURE})$  or  $\text{scCO}_2(\text{MeOH})$ . Each bar represents the overall mean from three independent sets of measurements  $\pm$  one standard error of the mean.**

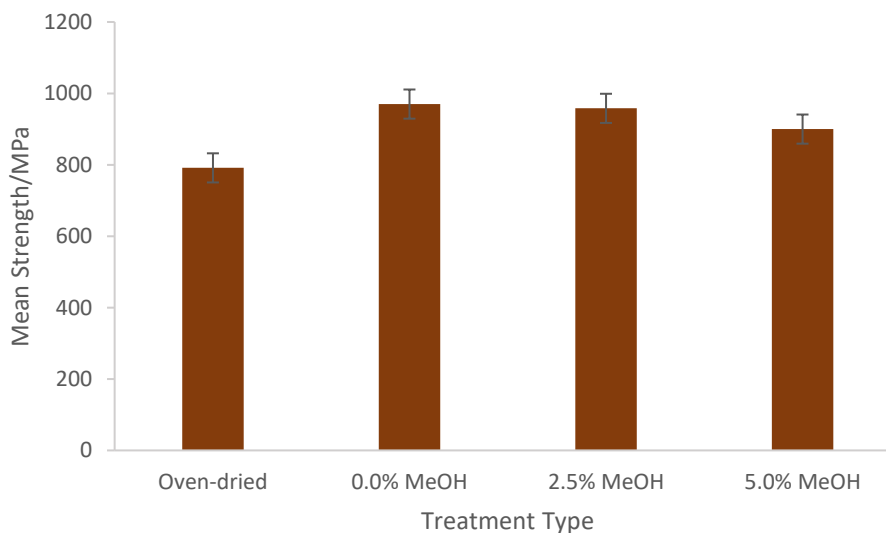


**Figure 3.27. A comparison of the mean strength values for Zebrano (*M*) pre and post treatment with  $\text{scCO}_2(\text{PURE})$  or  $\text{scCO}_2(\text{MeOH})$ . Each bar represents the overall mean from three independent sets of measurements  $\pm$  one standard error of the mean.**

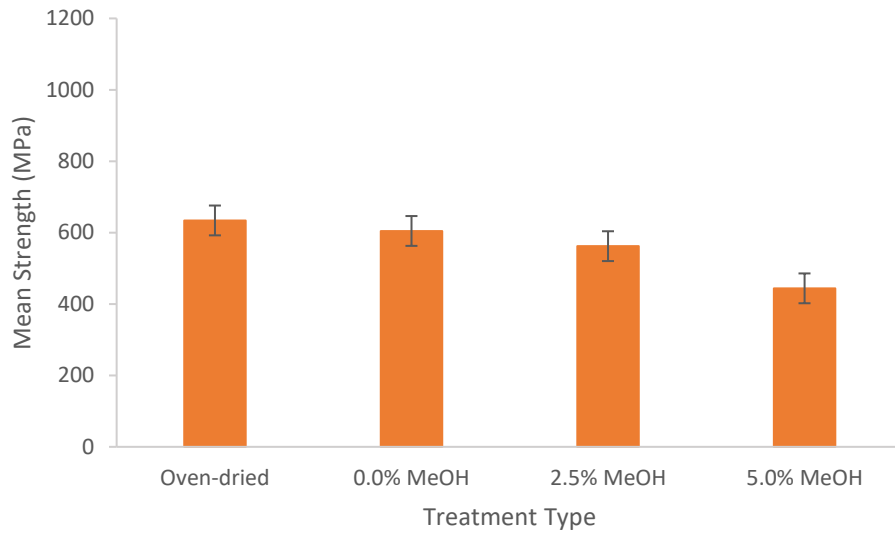


**Figure 3.28. A comparison of the mean strength values for Maple (*H*) samples pre and post treatment with  $\text{scCO}_2(\text{PURE})$  or  $\text{scCO}_2(\text{MeOH})$ . Each bar represents the overall mean from three independent sets of measurements  $\pm$  one standard error of the mean.**

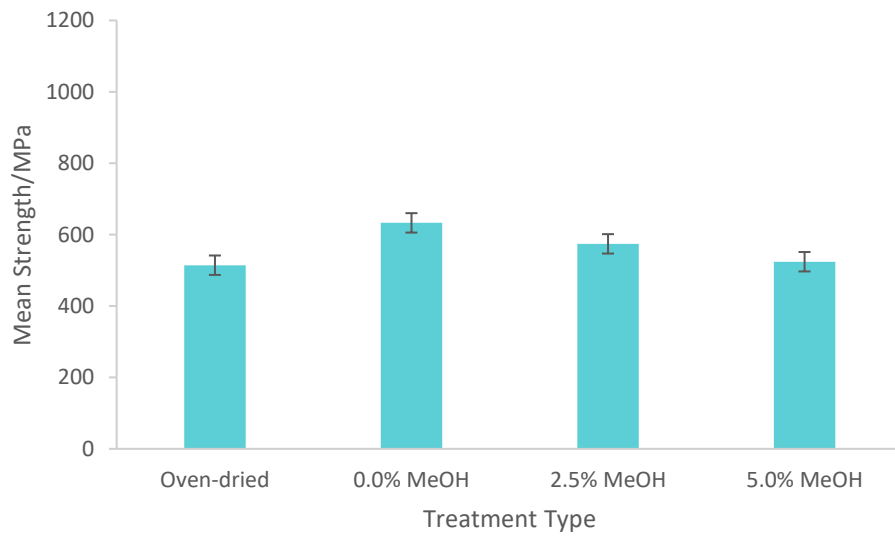


**Figure 3.29. A comparison of the mean strength values for White Oak (*H*) pre and post treatment with  $\text{scCO}_2(\text{PURE})$  or  $\text{scCO}_2(\text{MeOH})$ . Each bar represents the overall mean from three independent sets of measurements  $\pm$  one standard error of the mean.**

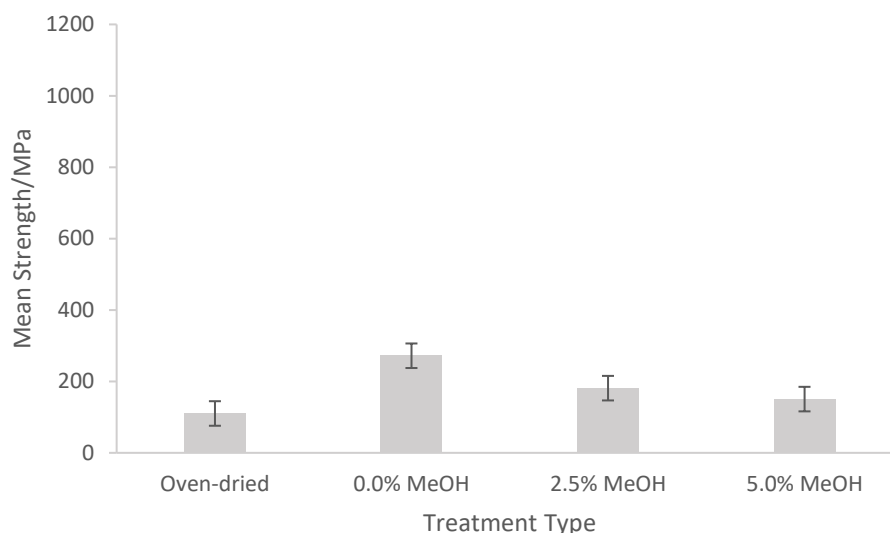


**Figure 3.30. A comparison of the mean strength values for Scots Pine (*H*) pre and post treatment with  $\text{scCO}_2(\text{PURE})$  or  $\text{scCO}_2(\text{MeOH})$ . Each bar represents the overall mean from three independent sets of measurements  $\pm$  one standard error of the mean.**

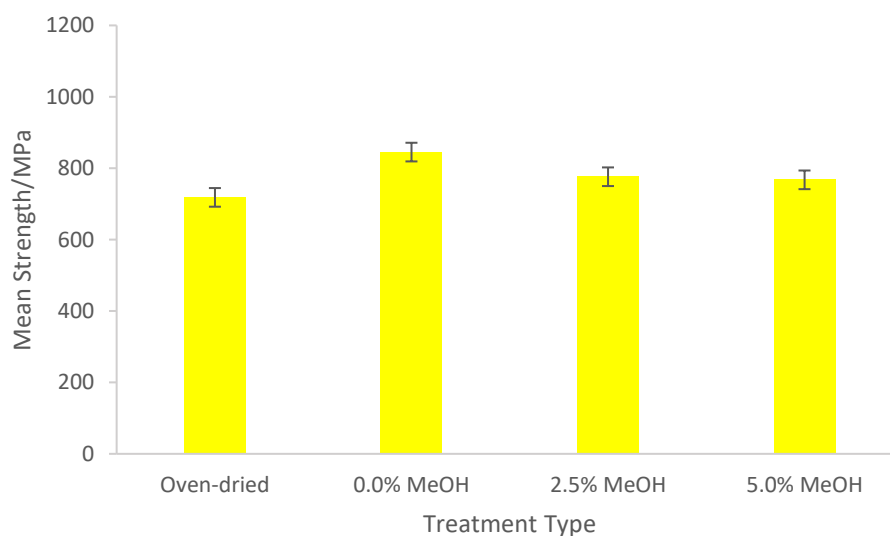


**Figure 3.31. A comparison of the mean strength values for Keruing (*H*) pre and post treatment with  $\text{scCO}_2(\text{PURE})$  or  $\text{scCO}_2(\text{MeOH})$ . Each bar represents the overall mean from three independent sets of measurements  $\pm$  one standard error of the mean.**

Figure 3.28 highlights Maple (*H*) as the only sample of both the historic and modern wood to show a decrease in strength, post  $\text{scCO}_2$  treatment. The addition of 5.0 mol% co-solvent is shown to decrease the strength of Maple (*H*) by the biggest margin, whilst  $\text{scCO}_2(\text{PURE})$  only decreases the strength by a small amount. It may be possible in the case of Maple (*H*) that an extraction has taken place via the supercritical solvent stream, alongside the supercritical hydration. The Maple (*H*) samples were collected as off-cuts from Oxford Violins, a violin

makers and dealer who specialise in restoration. Restorers at Oxford Violins had stated that the off-cuts may contain consolidants from prior restoration work and that these were likely to include low molecular weight organic waxes or resins. As mentioned in Section 1.1.3 (Chapter 1), scCO<sub>2</sub> has a very low solvating ability with highly polar compounds. However, it is generally accepted that if a compound dissolves in hexane, a short chain hydrocarbon, then it will dissolve in scCO<sub>2</sub>, due to their similar solvating abilities (Subramaniam et al., (1997)). This rule works well for low molar mass compounds such as organic waxes and resins. Increasing the concentration of MeOH will have increased the level of extraction experienced by the Maple (*H*), hence as the MeOH concentration increases, the strength of the maple decreases. For future work, it may be beneficial to carry out spectroscopic analyses of the Maple (*H*) samples pre and post treatment, to see if it is possible to identify the waxes and/or resins that are being extracted by scCO<sub>2</sub>. Natural deterioration over time could be an alternative explanation to the decrease in strength shown by Maple (*H*), however it does seem unusual that no other historic samples have shown the same trend. Nonetheless, natural degradation with age is an important factor to keep in mind when dealing with historic materials and high pressure supercritical systems, it is especially important when considering this mechanism for applications within conservation departments.

In general, the historic samples gave fewer significant results than the modern samples. However, the softwood Scots Pine (*H*) gave significant results for all the supercritical treatments. This is very encouraging because Scots Pine (*H*), had some of the lowest stabilised NMC of the whole sample set and gave no significant results for NMC (Section 2.4.1.2, Section 2.4.1.3). Given the low level NMC achieved by Scots Pine (*H*), it could be proposed that the scCO<sub>2</sub> is the responsible for the increased strength of the samples, rather than addition of water. scCO<sub>2</sub> is known to swell polymer chains (Section 1.2.2.1, Chapter 1). The low viscosity and very low surface tension of scCO<sub>2</sub> allows CO<sub>2</sub> to penetrate the amorphous regions of the polymer matrix easily, causing swelling and sorption of CO<sub>2</sub> (Üzer et al., 2006). Cellulose, hemicellulose and lignin form a series of complex matrix of organic polymers in wood. In the case of Scots Pine (*H*) it is feasible that penetration of scCO<sub>2</sub> into the organic amorphous polymer matrix in the wood samples occurred. This may cause the degraded cellulose, hemicellulose and lignin microfibril bundles to swell and expand, subsequently stabilising the wood sample structure and giving seemingly improved levels of strength.

Supercritical impregnation with CO<sub>2</sub> requires pressures above 7.2 MPa to reach the critical point. For the duration of the supercritical experiments the pressure was held at 20 MPa, to

ensure that the scCO<sub>2</sub> was at a high density. It is therefore important that particular attention was paid to the pressurisation and venting of a SCF system in order to minimise any damage that could be caused to the samples. Having studied the internal pressure development and deformation during SCF impregnation on wood-based materials, Oberdorfer et al (2004) state that for solid wood, pressure differences between the surface and the interior of the wood tended to be higher than for that of wood composites. Yet, unless flow directions were restricted and pressure was rapidly increased then the pressure differences weren't high enough to cause structural damage. As described in section 2.3.2 half the samples tested during this study were >100 years old. It is inevitable that the historic wood samples will have been subjected to chemical and physical degradation over time (Table 2.8), causing loss of structural integrity and the blocking of natural pathways including vessels, tyloses and pits. Due to the fragility of these samples a depressurisation study (Section 2.3.1.1) was carried out to make sure that the most suitable procedure was followed. Due to the care taken depressurising the cell and the conclusions made from the microstructural studies (Section 3.2), it can be assumed that in general no additional damage was caused internally to the wood samples via unsafe depressurisation. However, Maple (*H*) may again prove to be the exception to the rule here.

## **Chapter 4: A Feasibility Study for the Cleaning and Characterisation of Historic Leather Samples with Supercritical Carbon Dioxide**

### **ABSTRACT**

This chapter describes two feasibility studies for the treatment of historic leather samples with supercritical carbon dioxide ( $\text{scCO}_{2(\text{PURE})}$ ). In the first study six samples from three different leather sources were selected; three of the samples were treated with  $\text{scCO}_{2(\text{PURE})}$  in the presence of water for cleaning effects, the remaining three samples were left untreated. The comparative treated and untreated leather samples were analysed with Diffuse Reflectance Fourier Transform Infra-red Absorption Spectroscopy (DRIFT). The spectra obtained showed an inherent variance between the different leather pairs. The application of the method was shown to be descriptive of the different leather samples and the treatment type. It is suggested that this type of descriptive spectra may be useful within conservation departments for the characterisation of historic leather samples with unknown origins. Due to the reflective surfaces caused by coatings present on three of the leather samples, Reststrahlen band effects with DRIFT spectroscopy caused some of the spectra produced to be difficult to analyse.

In the second feasibility study a historic leather book spine was analysed using Scanning Electron Microscopy Energy Dispersive Spectroscopy (SEM-EDS) to look for any changes in elemental composition on the surface of the sample. The leather spine was subject to SEM-EDS pre-and post-treatment with  $\text{scCO}_{2(\text{PURE})}$ . Water was not added to the solvent stream to establish if  $\text{scCO}_{2(\text{PURE})}$  was an effective cleaning solvent by itself. Even though no substantial changes in elemental composition were observed, there was evidence to suggest that treatment via  $\text{scCO}_2$  with the addition of water may have more of a ‘cleaning’ effect on historic leather samples.

Finally, it was suggested that a collaborative approach using DRIFT spectroscopy and SEM/EDS may be useful for creating individual character profiles for materials of diverse origin, such as leather, which may then help conservators to create a viable action plan for suitable conservation methods.

*Keywords:* Supercritical Fluids, Supercritical Carbon Dioxide, Leather, DRIFT Spectroscopy, SEM-EDS, Leather Conservation

## 4.1 Introduction

. Detailed theory of supercritical fluids and their applications are found in Section 1.1,1.2, Chapter 1. Carbon dioxide (CO<sub>2</sub>) is the most commonly used solvent in SCF technologies and is the most applicable for uses within conservation as outlined in Section 1.1.2, Chapter 1.

There are several established technologies that use supercritical fluid extraction methods with scCO<sub>2</sub> as a solvent for cleaning. As a non-polar molecule, scCO<sub>2</sub> is particularly good at extracting non-polar, hydrophobic contaminants. As such scCO<sub>2</sub> behaves as a lipophilic solvent and will extract light oils and higher molecular weight materials e.g. waxes, paraffin's, lipids and resins (Reverchon, 1997). The addition of a co-solvent is needed to remove polar molecules effectively. The process is effective from a technical viewpoint and is superior to other methods when samples are composed of an intricate geometry, or when samples are water and or heat sensitive (Mchardy et al., 1993). Therefore, the process may be applicable for use within existing conservation practises.

Leather can be made from the skin of any animal and is often manufactured in a variety of ways (Section 1.6, Chapter 1). Cattle, sheep, pig and goat are the most commonly used animal skins. To make these skins into a flexible and durable leather product the dermis layer of the skin (Figure 1.15, Chapter 1) must be prepared and preserved via a tanning process, this layer of the skin consists mainly of collagen fibres. Each animal skin will be made up of a different collagen composition, therefore giving leather a unique appearance attributed to different animal species and even different individual animals from the same species (Dirksen, 1997). Historically, there have been a number methods for tanning leather to create a supple and durable product (Malea et al., 2010), the two main methods are vegetable and mineral tanning. Vegetable tanning is the most traditional method of the two, tanners use tannins derived from plant sources, such as oak bark, to produce a naturally coloured, strong leather. It is most likely that the historic leather samples used in this study were vegetable tanned. If the historic leather samples had been mineral tanned they would likely have gone through an alum tanning method rather than chromium tanning, which is a method that has only been used since the 1880's (Calnan and Haines, 1991).

Traditionally, tanning methods used a variety of harmful chemicals that can subsequently react with pollutants in the air and cause leather to degrade rapidly (Dirksen, 1997). In the most extreme cases the leather will be subject to acidic degradation by red rot. The complete removal



or reduction of these degradative constituents via a wet cleaning method is not commonly used within conservation practices. Instead, preventative conservation methods are preferred; by placing the degraded leather in a controlled environment conservators can minimise chemical disintegration without causing further damage via wet cleaning. Therefore, the development of a cleaning method that aims to stop, rather than halt, the degradation process and leaves the leather unharmed, may be of use within conservation departments. Previous work has shown that there may be a role for SCFs and more specifically  $\text{scCO}_2$ , within existing conservation practices. These have included the deacidification of books and paper and the removal of harmful pesticides from ethnographic objects and other fragile museum artefacts (Français et al., 1997, Tello, 2006). Therefore, it is feasible that the known cleaning properties of  $\text{scCO}_2$ , as stated above, may be harnessed to create a safe and effective cleaning method for historic materials.

It is the case that with many materials and objects found with museum collections there is also a wealth of information available to conservators that relates to the objects composition, age and origin. For these objects and/or materials there are a variety of established methods that are employed by conservation professionals to help clean, and preserve the objects for continued public enjoyment (Richmond, 2009). Although these approaches are usually very effective, sometimes conservators may require more tailor-made methods of conservation. A lack of information, especially for complex media such as leather and wood, may be problematic if the materials have been subject to degradation over time. Therefore, the ability to create an individual character profile for materials for such materials may be use to conservators, who are in most cases overwhelmed with a huge variety of problems to solve on a diverse range of media.

The main aim of the work presented in this chapter is to evaluate, via DRIFT spectroscopy, the treatment of historic leather samples with  $\text{scCO}_2$ , in the presence of water. Additionally, a twofold evaluation, via SEM/EDS, of a historic leather book spine that has been treated with  $\text{scCO}_{2(\text{PURE})}$ , is described. This work is carried out to examine whether it is feasible to ‘clean’ a book spine with the  $\text{scCO}_{2(\text{PURE})}$ , where the term clean is referring to the extraction or reduction of any chemical elements that may be accelerating degradation and limiting the long-term preservation historic leather. Secondly, it is anticipated that analysis with SEM-EDS may be able to provide information as to the type and abundance of chemical species present on the surface of the historic leather samples, which in turn can be interpreted by conservators to

deduce an optimal method for preservation. Furthermore, it may be used collaboratively with DRIFT to create material profiles for difficult to identify materials, conservators may then initiate effective action plans. Leather has been chosen as the test material because it is prolific within museum collections as a damaged and degraded material.

It should be noted that in Chapter 2 novelty was found in hydrating historic and modern wood samples with  $\text{scCO}_2(\text{PURE})/\text{scCO}_2(\text{MeOH})$  in the presence of water. In the feasibility studies carried out in this chapter novelty is found in the attempts to clean historic leather samples, of unknown origin, with  $\text{scCO}_2(\text{PURE})$  both in the presence of water and without water. It is not contradictory to suggest that a solvent stream of  $\text{scCO}_2(\text{PURE})$  in the presence of water may be able to clean a material in one instance and hydrate a material in another instance, it may even be possible for both processes to happen simultaneously. As such, the wood samples subject to treatment in Chapter 2 may have also been subject to cleaning via the  $\text{scCO}_2$  solvent stream, but this was not a property that was chosen to be analysed. Additionally, the leather samples treated in *this* chapter may have higher levels of hydration post treatment with  $\text{scCO}_2$ , but again this is not a property that will be analysed here.

## **4.2 Materials and Methods**

### **4.2.1 Materials**

The leather samples were selected and collected from the Leather Conservation Centre (Northampton, UK). All the leather samples were kept under ambient conditions until they were treated with  $\text{scCO}_2$ .  $\text{CO}_2$  (liquid withdrawal) was supplied by Air Liquide (Paris, France).

### **4.2.2 Leather preparation and characterisation**

The leather samples were taken from three larger leather pieces. Two samples were cut with scissors, or torn along existing fractures from each leather piece, so that treated and untreated samples were in a comparative pair. The origins of all the larger leather piece were unknown. However, they were all classed as ‘historic’ samples by a leather conservation professional, as they were deemed to be some 100 or more years old. It is also expected, but not certain, that these samples were vegetable tanned. The leather samples were kept in atmospheric conditions until they were treated, or underwent DRIFT analysis.

The leather book spine had become unattached from its original binding to the cover of a book. This sample was also classed as historic as it was known the book had been published in 1913, therefore the minimum age the leather is 104 years.

#### **4.2.3 Supercritical carbon dioxide treatment**

A schematic illustration of the supercritical treatment rig is shown in Figure 4.1, this is the same rig configuration as shown in Figure 2.1, Chapter 2 except that a 2 L pressure vessel has been used instead of a 25 mL pressure vessel. For treatment with  $\text{scCO}_{2(\text{PURE})}$ , the three leather samples were placed on a stainless-steel grate raised up from the base of the 2 L cell. Tissue saturated with distilled water was added into the hydration cell and sealed, the oven was then heated to 50°C. For the treatment with  $\text{scCO}_{2(\text{PURE})}$ , not in the presence of water, the leather book spine was placed vertically on the stainless-steel grate and the hydration cell was left empty.  $\text{CO}_2$  was pulled from the supply cylinder via a dessicator tube before it was cooled to a liquid state (to allow for efficient pumping) and compressed to the desired pressure by a Thar high pressure P-series pump. Once the desired temperature (50°C) and pressure (20 MPa) had been achieved the entry valve (MV1) into the oven was opened and the system was held at static pressure for 60 minutes. The pressure was controlled and monitored throughout the experiment using the computer (Thar Technologies Inc., Pittsburgh, PA, USA), whilst the oven temperature was monitored using a temperature probe (K Type thermocouple input probe) and digital monitor (TC305K Digital handheld thermometer). At the end of every experiment, the pump was turned off and the entry value into the oven (MV2) was closed whilst the exit value (MV2) was opened into a fume hood to allow for slow depressurisation over 60 minutes.

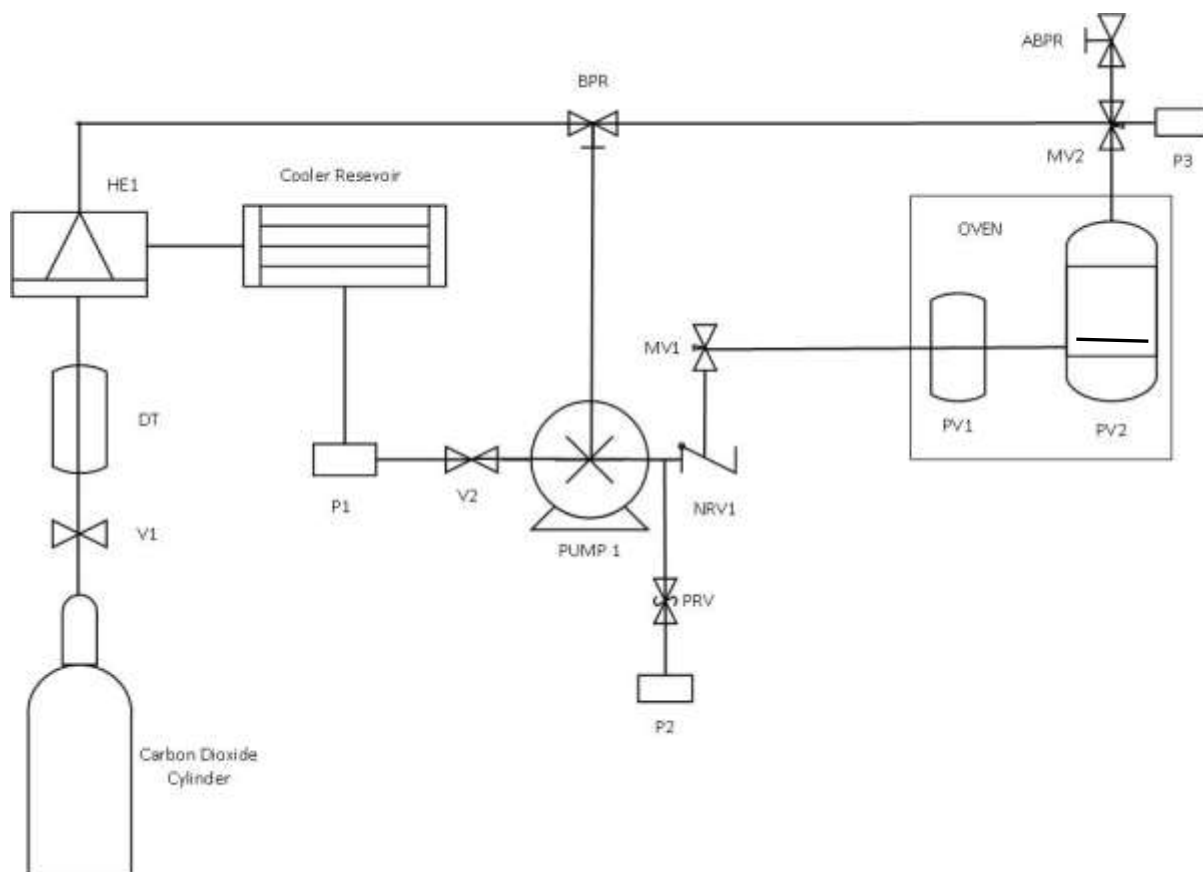


**Figure 4.1.** A schematic illustration of the supercritical hydration rig as constructed by the author. Key: V1 = CO<sub>2</sub> inlet valve; DT = dessicator tube; HE1 = refrigerated heat exchanger (cooling); P1,2,3 = pressure gauges; V2 = pump inlet valve; PUMP1 = pneumatic liquid CO<sub>2</sub> pump; PRV = safety pressure release valve; NRV1 = non-return valve; MV1,2 = micrometering valves, PV1 = hydration pressure vessel, PV2 = reaction pressure vessel (with additional stainless steel grate); ABPR = automated back pressure regulator; BPR = back pressure relief valve.

For the duration of the time post-SCF treatment the three treated leather samples (Figure 4.3, Figure 4.5, Figure 4.7) were kept in individual, nitrogen flushed containers until they underwent analysis with DRIFT spectroscopy. Post-SCF treatment the leather book spine (Figure 4.8) was kept in a sealed plastic bag, until it underwent analysis with SEM-EDS.

#### 4.2.4 DRIFT spectroscopy

The aim of the study was to investigate the sensitivity of the DRIFT spectroscopy technique to three pairs of treated and untreated leather samples. There are minimal prior investigations using DRIFT spectroscopy on either modern or historic leather samples presented in the literature (Section 1.7.3, Chapter 1). However, there are many feature rich DRIFT spectra produced from organic materials that deem leather a suitable material for this type of analysis

(Pandey and Theagarajan, 1997, Kaiser et al., 1997). All spectroscopic analysis was carried out at Chiralabs Limited (Oxford, UK).

Three untreated leather samples and the corresponding treated leather samples were analysed using DRIFT spectroscopy. The front and back of each leather samples were analysed, due to the presence of different coatings on the front side of the samples (Figure 4.2, Figure 4.3, Figure 4.4, Figure 4.5, Figure 4.6, Figure 4.7). It was anticipated that the coatings may interfere with the spectra and therefore each side was analysed and compared, with the need for some spectra to be disregarded. Each sample was placed on the holder of a Diffuse Reflectance (DRIFT) optics attachment and presented such that a rough flat face was illuminated.



**Figure 4.2. Two photographs showing the front (coated) and back of the untreated leather sample A.**



**Figure 4.3. Two photographs showing the front (coated) and back of the treated leather sample B.**



**Figure 4.4.** Two photographs showing the front (coated) and back of the untreated leather sample C.



**Figure 4.5.** Two photographs showing the front (coated) and back of the treated leather sample D.



**Figure 4.6.** Two photographs showing the front (coated) and back of the untreated leather sample E.



**Figure 4.7. Two photographs showing the front (coated) and back of the treated leather samples F.**

#### **4.2.5 SEM-EDS for elemental composition**

SEM-EDS analysis was used to provide evidence as to whether there were any changes in elemental composition, on the leather book spine caused by treatment with  $\text{scCO}_2(\text{PURE})$ . Therefore, the leather book spine was analysed by SEM-EDS, pre-and post-treatment, to give microscopic imaging with spatially delineated elemental composition. All spectroscopic analysis was carried out at Chiralabs Limited (Oxford, UK). The leather spine was analysed without processing, it was mounted atop an aluminium SEM stub via an adhesive carbon disc. The spine was then analysed at three different areas that could be returned to pre-and post-treatment, these areas are marked by red circles on Figure 4.8 below. The areas are taken to be representative of the dark leather, the damaged leather and the gold embossing that is found at various points on the leather book spine.

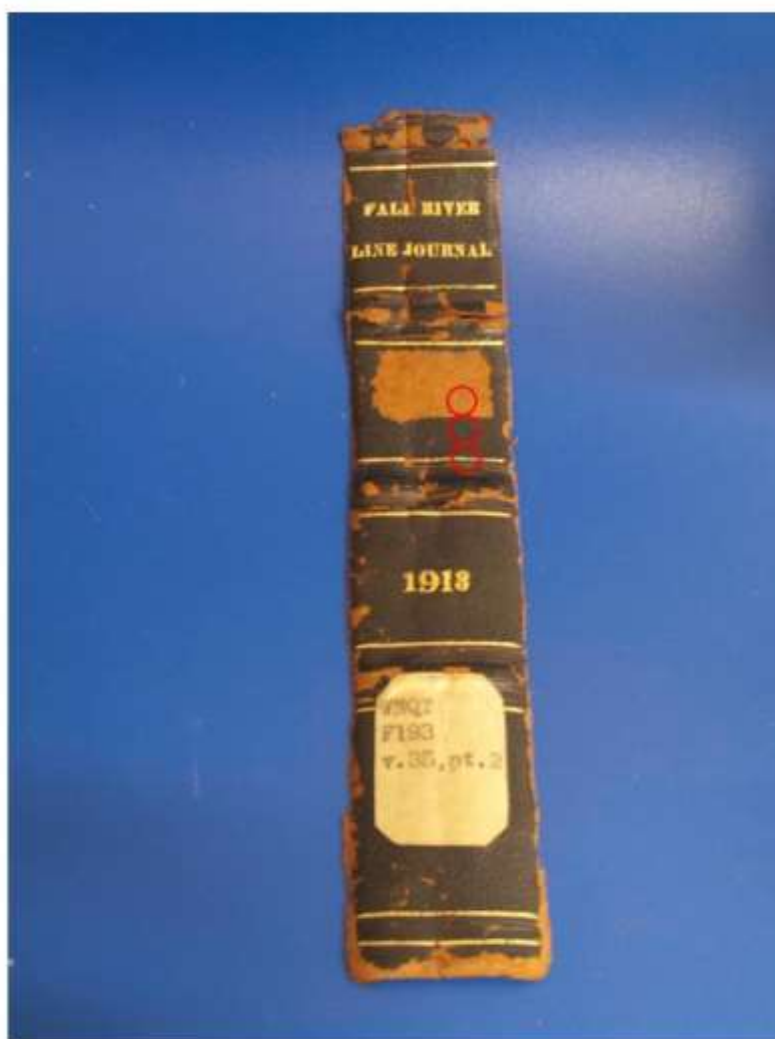


**Figure 4.8.** A photograph of the leather book spine treated with  $\text{scCO}_2(\text{PURE})$ . The areas analysed with SEM-EDS are marked with three red circles; dark leather, damaged leather and gold embossing.



## 4.3 Results and Discussion

### 4.3.1 Supercritical carbon dioxide treatment

The observations recorded in Table 4.1 were made following the  $\text{scCO}_2$  treatment of the three historic leather samples in Figure 4.3, Figure 4.5 and Figure 4.7. From these initial observations, it seems likely that the treatment of historic leather samples with  $\text{scCO}_2$  in the presence of water, is not damaging to the integrity of the leather. It may also be possible that the leather samples are being hydrated to a certain degree; indicated by the darker colour of the leather samples immediately after depressurisation of the system. However further studies of a higher number of treated leathers would need to be carried out to see if the hydration of the leather is viable. At this point it is difficult to assess whether the leather samples post-treatment are more clean than the leather samples post-treatment.

Leather Sample	Observations post $\text{scCO}_{2(\text{PURE})}$ treatment
Figure 4.3 <b>B</b>	The leather sample appeared darker in colour due to the presence of water and the possible hydration of the sample. There seems to be no loss of material. The coating on the front of the sample is more visible and has become lighter in colour, perhaps due to the cleaning effects of $\text{scCO}_2$ and/or the presence of water.
Figure 4.5 <b>D</b>	The sample appears mostly unchanged. The black coating remained intact and there has been no change of colour. The leather that is uncoated appears darker in colour due to the presence of water and the possible rehydration of the sample. There seems to be no loss of material.
Figure 4.7 <b>F</b>	The leather is darker in colour due to the presence of water and the possible hydration of the sample. There has been no loss of the delicate coating and the colours of the coating have been maintained.

**Table 4.1. Observations made by the author immediately after the leather samples had been treated with  $\text{scCO}_{2(\text{PURE})}$  in the presence of water.**

It is plausible that by comparing the DRIFT analysis of the treated and untreated leather samples, then suggestions may be made as to whether there have been significant changes in the leather composition post-treatment. These changes may be representative of the removal or reduction of a damaging extractive, thereby indicating that the leather has become more clean. In future work, it may also be helpful to use  $\text{scCO}_2$  with the addition of a co-solvent e.g. methanol (MeOH). Although  $\text{scCO}_{2(\text{PURE})}$  is good at removing non-polar molecules such as waxes and resins, the addition of a co-solvent would improve the effectiveness of treatment especially if polar molecules needed to be extracted. Conservators already apply a solution of

water and ethanol as a wet cleaning method for leather, thus  $\text{scCO}_2(\text{MeOH})$  may provide a more effective alternative.

#### 4.3.2 DRIFT spectroscopy

Three untreated leather samples and the corresponding treated leather samples were analysed with DRIFT spectroscopy. The spectra produced for the three pairs of treated and untreated leather samples were found to be different, as shown in the Figures 4.9 - 4.14. The variability was particularly noticeable for the band attributed to the OH group, which seemed to change position and intensity for samples from the same source. This may be due to different levels of hydration between the samples caused by the presence of water in the  $\text{scCO}_2(\text{PURE})$  solvent stream. The inherent variance between the sample pairs makes the application of the methodology descriptive of the nature of leather and its treatment, which may prove of value. There are also other additional features in the spectra that are related to the composition of the leather samples and may be profitably considered as a more detailed characterisation.

*Leather samples: A (Figure 4.2), B(Figure 4.3)*

As shown in Figure 4.9 the DRIFT spectra for the leather A shows some characteristic bands. The broad band observed at ca.  $3460\text{ cm}^{-1}$  is associated with OH stretches (Lindon et al., 2016). This band derives from a series of hydroxyl containing species, including water; variation in the proportions of these species will give apparent shift in the band maximum. In principle, it may represent the nature of binding for water. For leather B (Figure 4.10) this band is shifted slightly to the left at  $3475\text{ cm}^{-1}$ . The bands observed in the region around  $2900\text{ cm}^{-1}$  are associated with CH groups (Lindon et al., 2016), as found in most of the organic molecular components; these bands are less well defined for leather B in comparison to leather A. The bands in the region  $2200 - 2300\text{ cm}^{-1}$  are associated with atmospheric and absorbed  $\text{CO}_2$ , and are clear on both the spectra. The other bands in the spectra are associated with the principal constituents of leather.

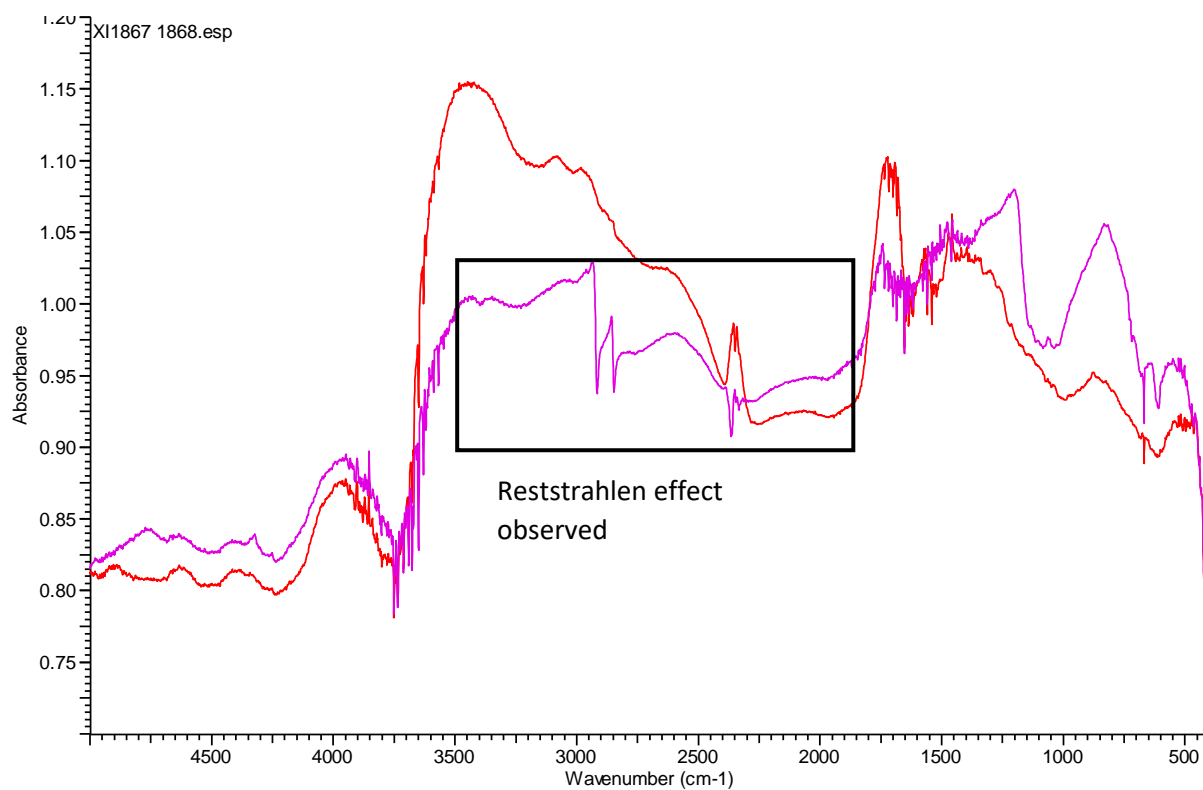


**Figure 4.9. DRIFT spectra for the untreated leather sample A: coated side (magenta), matt side (red). Annotated Reststrahlen effect.**

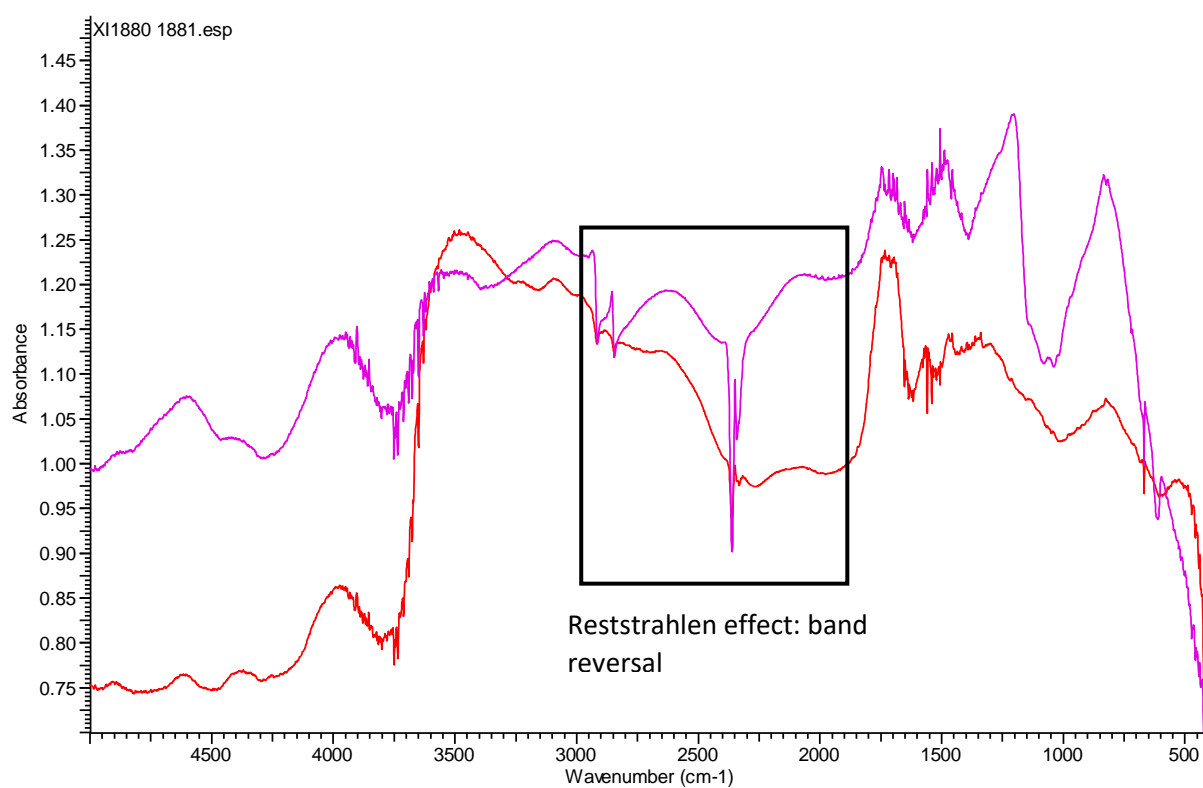


**Figure 4.10. DRIFT spectra for the treated leather sample B: coated side (magenta), matt side (red). Annotated Reststrahlen effect.**

The shiny coated surface present on the front of leather A and leather B has caused some Reststrahlen band effects, therefore some of the infrared bands are completely reversed (Figure 4.9, Figure 4.10). This phenomenon is often observed for reflective surfaces and is a sign of the occurrence of a different type of infrared reflectance called specular reflectance coupled with absorbance, which is undesirable when performing DRIFT. Consequently, it is best to analyse the DRIFT spectrum for the matt surface (red spectra) of both the leather samples.

*Leather samples: C (Figure 4.4), D (Figure 4.5)*

The DRIFT spectra produced for the untreated leather C are more consistent than the spectra for the untreated leather A as can be seen in Figure 4.11. Although both the leathers C and leather A present numerous characteristic bands, the big broad band from the OH region is now centred at  $3340\text{ cm}^{-1}$  for leather C. It is shifted towards lower wavenumber compared to the leather A. Spectra D (Figure 4.12), similarly to the spectra for B, shows signs of specular reflectance. It is therefore best to analyse the only matt surface spectra (red) of leather D. This spectrum, and both the spectra for leather C show less well defined bands in the region around which are  $2900\text{ cm}^{-1}$  associated with CH groups. The bands in the region  $2200 - 2300\text{ cm}^{-1}$  which are associated with atmospheric and absorbed  $\text{CO}_2$  and bands that are associated with the other constituents of leather are also observed for these spectra.

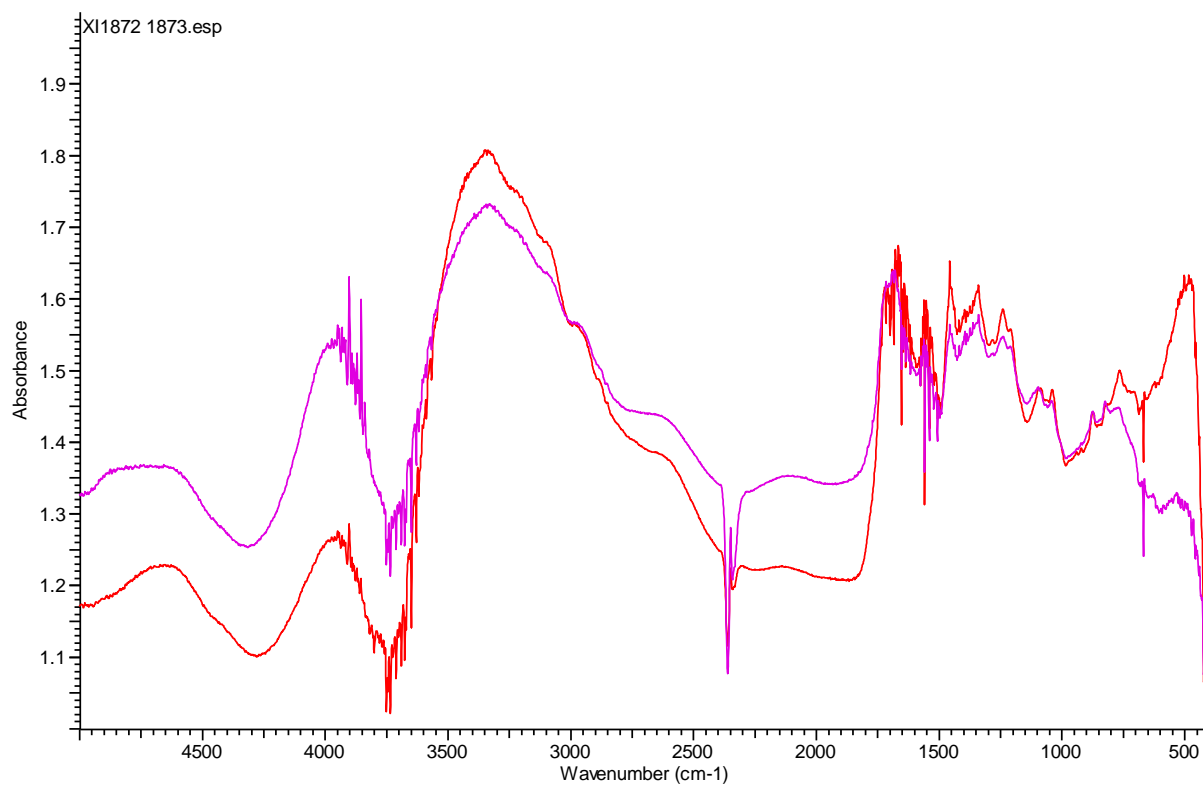


**Figure 4.11. DRIFT spectra for the treated leather sample C: coated side (magenta), matt side (red).**

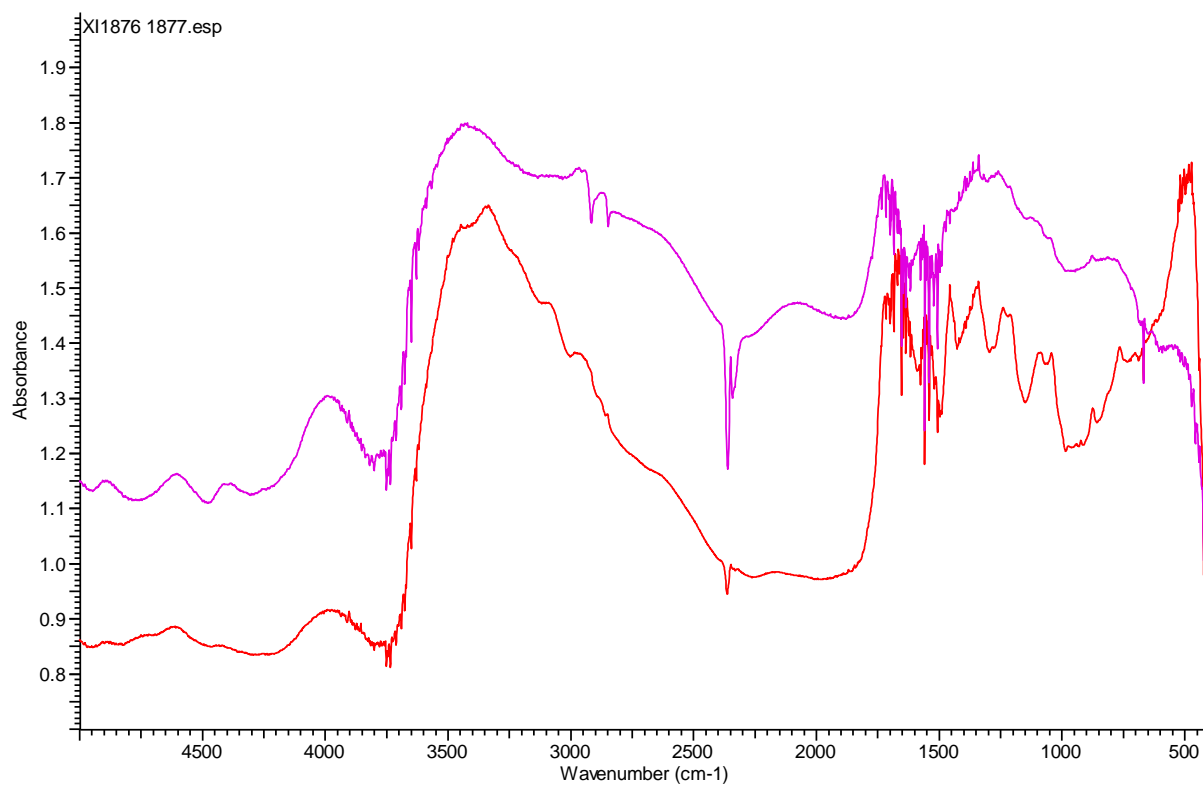


**Figure 4.12. DRIFT spectra for the treated leather sample D: coated side (magenta), matt side (red).**

*Leather samples: E (Figure 4.6), F(Figure 4.7)*

The two DRIFT spectra for sample E are consistent with each other, as shown in Figure 4.13. They both present numerous characteristic bands. The big broad band from the OH region seems to be made up by at least two bands: one centred at  $3440\text{ cm}^{-1}$  and another centred at  $3340\text{ cm}^{-1}$ . In contrast to leathers C and D the bands associated with CH groups that are observed in the region around  $2900\text{ cm}^{-1}$  are now well defined for leather E and leather F. The bands in the region  $2200 - 2300\text{ cm}^{-1}$  are associated with atmospheric and absorbed  $\text{CO}_2$ . The other bands in the spectra are associated with the principal constituents of leather e.g. collagen proteins. As seen in Figure 4.14, the DRIFT spectrum for leather F of the coated side (magenta) once again shows some signs of specular reflectance (complete inversion of some infrared bands apparent in the region  $2800 - 3000\text{ cm}^{-1}$ ). As a result, it is best to disregard this spectrum, and use the matt side (red) spectra as a fingerprint of the treated leather samples. For leather sample F the broad band associated with OH stretches has shifted to the slightly higher wave numbers at ca.  $3345\text{ cm}^{-1}$ , in comparison to leather E.

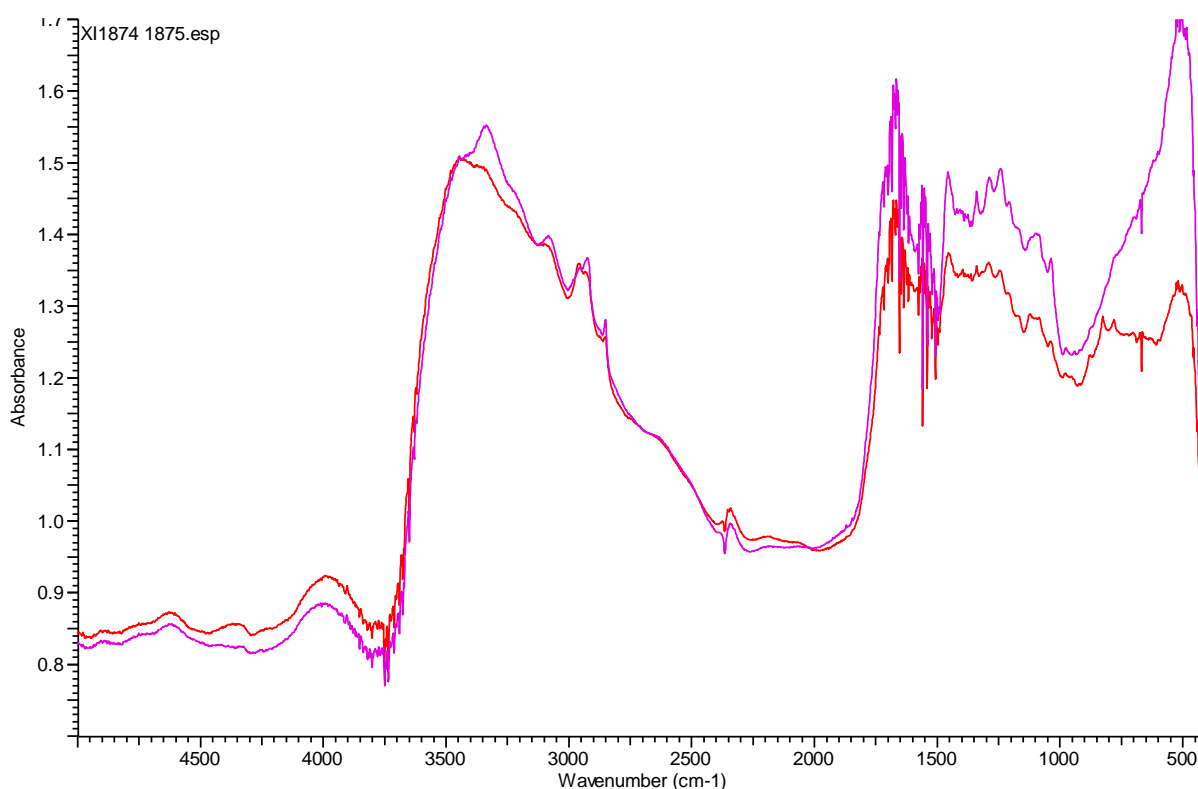


**Figure 4.13. DRIFT spectra for the treated leather sample E: coated side (magenta), matt side (red).**

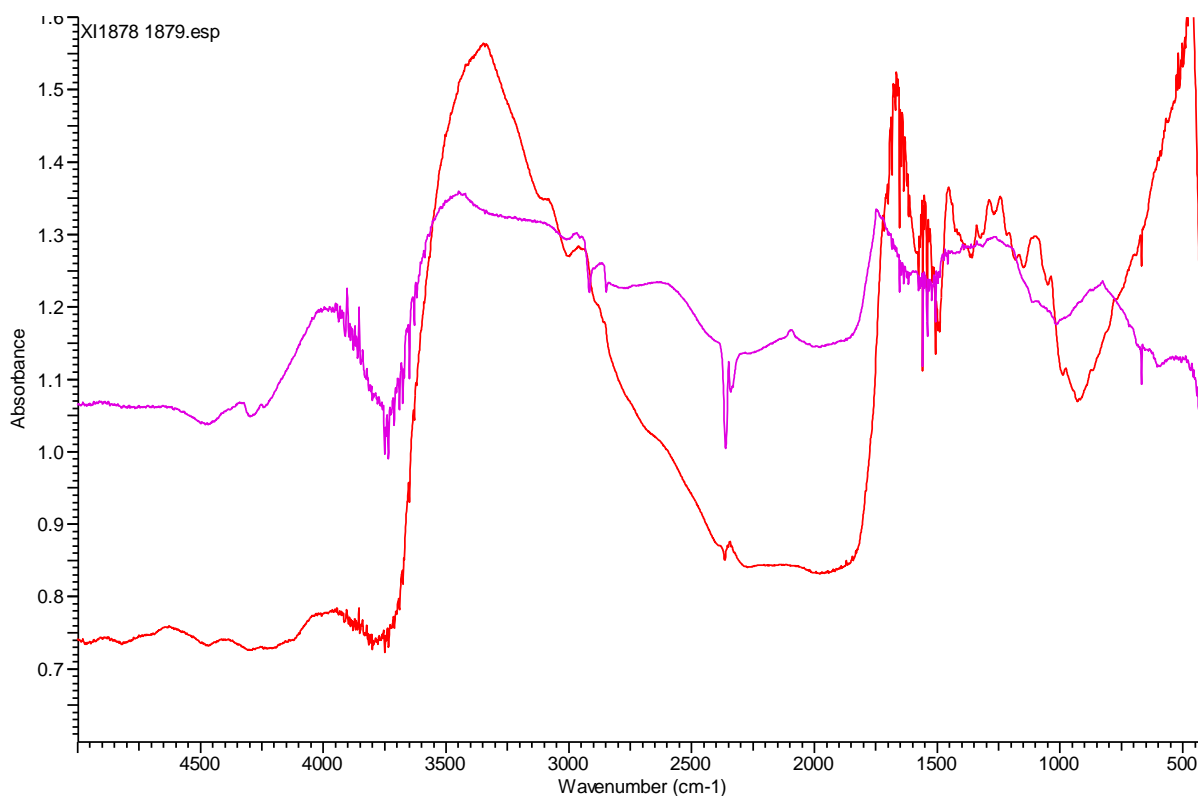


**Figure 4.14. DRIFT spectra for the treated leather sample F: coated side (magenta), matt side (red).**

*Comparison of untreated and treated leathers: A, B: C, D: E, F*

For both the untreated and treated leather samples the spectra show common features but are found to be not identical. Notably there is an inherent variation in the position of the broad band attributed usually to OH (and NH) groups above  $3000\text{ cm}^{-1}$ . This inherent variance between untreated samples makes the application of the methodology descriptive of the nature of the leather, which may prove of value. Direct comparisons in spectra can be made from the corresponding pairs of treated and untreated leathers shown in Figure 4.15.

It may be noted that the spectra have features at above  $4000\text{ cm}^{-1}$ , shoulders in the band at  $3600\text{ cm}^{-1}$  and features in the  $1900 - 2200\text{ cm}^{-1}$  region as well as a complex series of peaks in the fingerprint region. These are related to the detailed composition and physical state of the leathers and would provide further information for the characterisation. Likewise, there is an apparent shift in the baseline level of the samples independent of the sample being treated or not. This is associated with the general reflectivity and roughness of the surfaces and is again a characteristic of the nature of the samples.

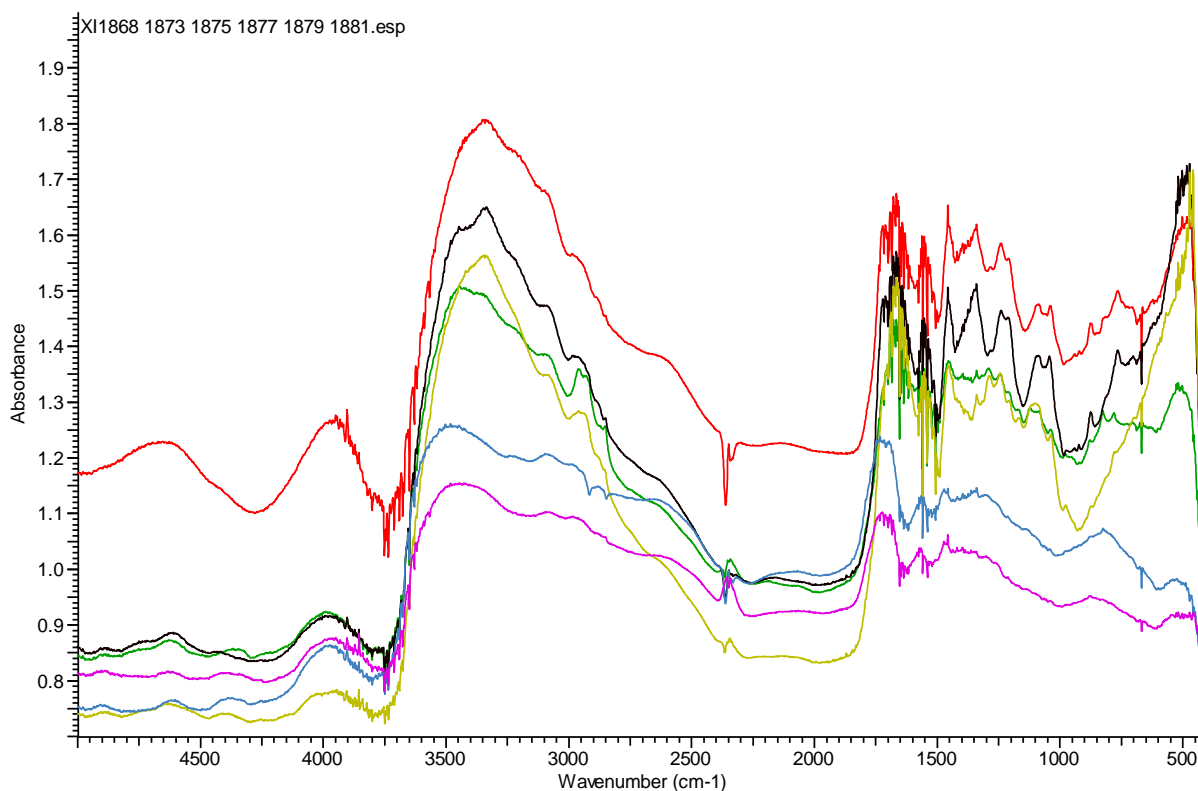


**Figure 4.15. DRIFT spectra of the matt brown sides of different untreated leathers [leather A (magenta), leather C (red) and leather E (green)] and treated leathers [leather B (blue), leather D (black), and leather F (gold)].**

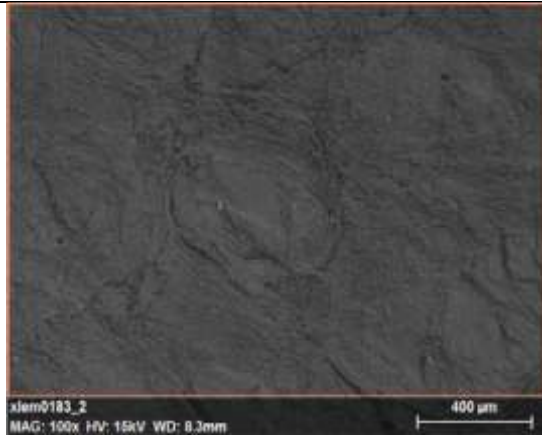
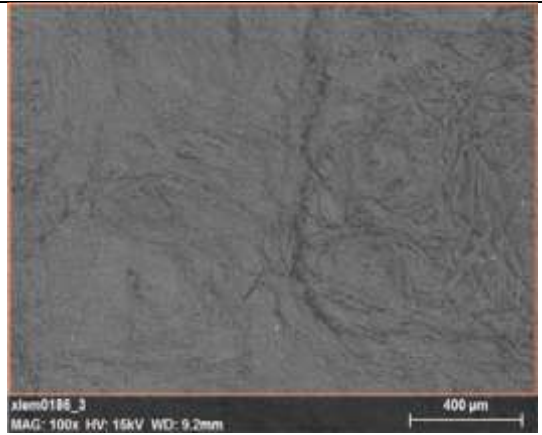
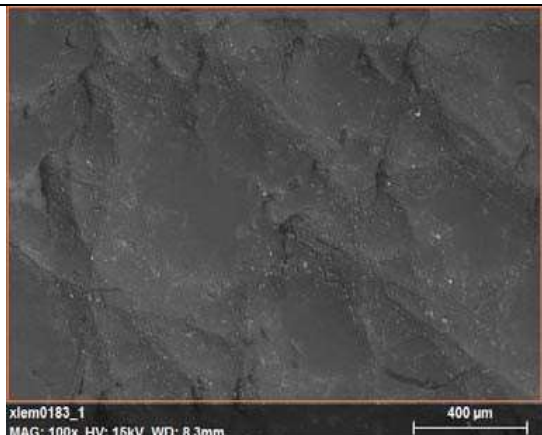
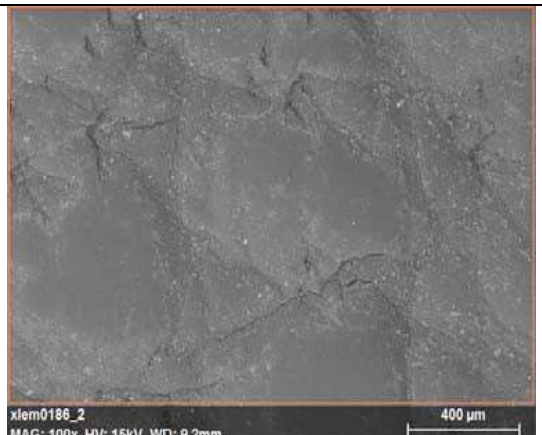
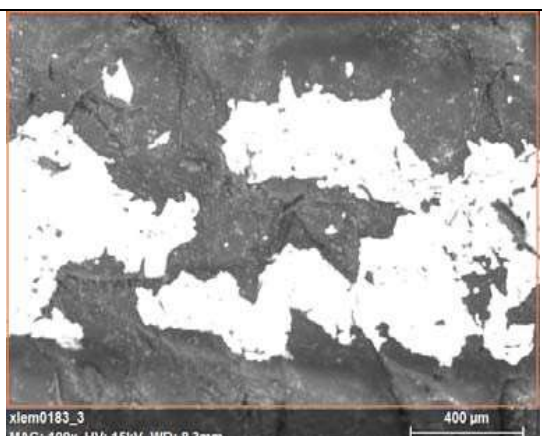
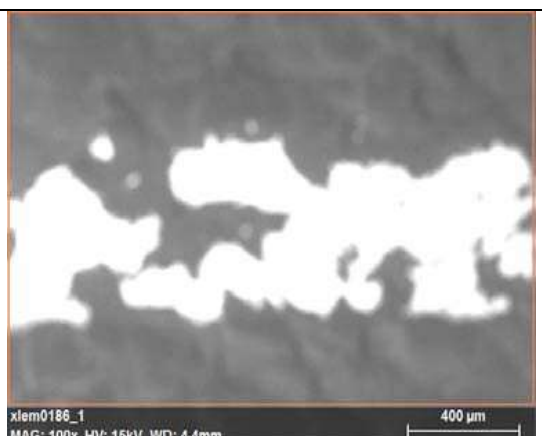
### 4.3.3 SEM-EDS

#### 4.3.3.1 SEM images

Figure 4.16 below depicts the SEM images of the book spine pre-and post-treatment for the areas marked in the Figure 4.8. It is not possible to compare individual features because the positioning of the image was not completely identical for each sample pre-and post-treatment. However, comments can be made about the general structure of the surfaces. The general physical structure of the three areas do not appear to have undergone any major changes pre-and post-treatment. This is not surprising as it is likely that the cleaning effect of  $\text{scCO}_2(\text{PURE})$  has been minimal; perhaps due to the short length of the treatment or the absence of water and/or a co-solvent. Although the  $\text{scCO}_2$  treatment has not caused any changes to the surface of the leather it has also not caused any damage to the sample. Given that that the  $\text{scCO}_2(\text{PURE})$  treatments seems not to be harming the historic leather, in future work it may be useful to carry SEM-EDS analysis on leather samples that have been treated with  $\text{scCO}_2(\text{co-solvent})$  in the presence of water. This modified supercritical treatment is likely to prove more effective.



In general, it can be seen that the dark leather areas appear more smooth than the damaged tan areas, which give a more fibrous appearance. It should also be noted that the gold embossing for the post-treatment SEM image is in poor focus, this may be due to movement or loss of gold during the scCO<sub>2</sub> treatment. However, the loss is not to a statistically definitive degree and is more likely to be caused from an instrumental issue regarding the inclusion of some leather in the analysis volume. Before it is possible to suggest these treatments for use within conservation departments, it would be necessary to prove to conservators that there is no loss of material during the supercritical treatment.

<u>Pre-treatment</u>	<u>Post-treatment</u>
	
Damaged tan leather	Damaged tan leather
	
Dark leather	Dark leather
	
Gold embossing	Gold embossing

**Figure 4.16. SEM images of the book spine pre-and post-treatment for three different areas of the spine: damaged tan leather, dark leather, gold embossing.**

#### 4.3.3.2 Elemental analysis

SEM-EDS is formally a semi-quantitative technique unless the methodology has been specifically calibrated for the sample under study. Nonetheless, it typically gives reproducible data of reasonable accuracy, especially in comparative investigations. Table 4.2 below summarises the elemental analysis of samples, averaged over the areas imaged; for the gold embossing, only the embossing was analysed and not the surrounding leather.

For the dark leather and the tan leather Table 4.2 shows that there are no significant changes in the elemental composition of either of those areas after the treatment with  $\text{scCO}_2(\text{PURE})$ . The gold is seen to contain copper and silver, consistent with typical gold impurities. The apparent reduction in the gold content in the gold embossing post-treatment may suggest a modicum of gold loss on treatment, but this is not statistically significant and would need to be repeated with other samples. It is plausible that is simply due to the vagaries of depth penetration of the analysis method and hence the amount of leather unavoidably included in the volume probed. This is consistent with the concomitant increase in carbon and oxygen content.

**Table 4.2 (next page). Comparison of SEM-EDS elemental analysis of pre-and post-treatment book spine (mean  $\pm$  standard deviation across imaged areas).<sup>a</sup>: With respect to total detected, values quoted to least significant figure; elements not listed are either not detectable (“N/D”) by the technique (*inc.* H, He, Li) or below detection limit (“<dl”); in the case here dl~0.01% in the area observed. <sup>b</sup>: Bromine levels may be confounded in the presence of Aluminium and *vice versa*.**

Element	Estimated Composition (%w/w) <sup>a</sup>					
	Tan Leather		Dark Leather		Gold Embossing	
	Pre-treatment [xlem183-2]	Post-treatment [xlem186-3]	Pre-treatment [xlem183-1]	Post-treatment [xlem186-2]	Pre-treatment [xlem183-3]	Post-treatment [xlem186-1]
H, He, Li, Be	N/D	N/D	N/D	N/D	N/D	N/D
Boron	<dl	<dl	<dl	<dl	<dl	<dl
Carbon	52 ±4	52 ±5	47 ±2	48 ±3	15 ±2	21 ±3
Nitrogen	10.8 ±0.2	11.2 ±0.1	7.5 ±0.2	8.0 ±0.04	3±1	4 ±1
Oxygen	34 ±1	34 ±1	38 ±1	38 ±1	14 ±2	16 ±2
Fluorine	0.03 ± 0.03	0.03 ± 0.04	<dl	<dl	<dl	<dl
Neon	<dl	<dl	<dl	<dl	<dl	<dl
Sodium	0.12 ± 0.01	0.09 ± 0.02	0.32 ± 0.01	0.43 ± 0.03	<dl	<dl
Magnesium	<dl	<dl	0.16 ± 0.01	0.21 ± 0.02	<dl	<dl
Aluminium <sup>b</sup>	<dl	<dl	0.29 ±0.03	0.30 ±0.02	0.2 ±0.1	0.07 ±0.08
Silicon	0.03 ±0.01	0.02 ±0.02	0.67 ±0.07	0.62 ±0.05	<dl	<dl
Phosphorus	<dl	<dl	0.02 ±0.01	0.05 ±0.01	<dl	<dl
Sulphur	2.3 ±0.2	2.0 ±0.2	2.2 ±0.2	1.9 ±0.1	<dl	<dl
Chlorine	0.05 ±0.01	0.04 ±0.01	0.05 ±0.01	0.06 ±0.01	<dl	<dl
Argon	<dl	<dl	<dl	<dl	<dl	<dl
Potassium	0.13 ±0.03	0.08 ±0.01	0.52 ±0.06	0.53 ±0.05	0.27 ±0.07	0.6 ±0.1
Calcium	0.19 ±0.02	0.17 ±0.01	1.03 ±0.04	0.97 ±0.02	0.41 ±0.08	0.8 ±0.3
Scandium	<dl	<dl	<dl	<dl	<dl	<dl
Titanium	<dl	<dl	<dl	<dl	<dl	<dl
Vanadium	<dl	<dl	<dl	<dl	<dl	<dl
Chromium	<dl	<dl	<dl	<dl	<dl	<dl
Manganese	<dl	<dl	<dl	<dl	<dl	<dl
Iron	0.15 ±0.02	0.13 ±0.01	1.1 ±0.2	0.83 ±0.06	<dl	<dl
Cobalt	<dl	<dl	<dl	<dl	<dl	<dl
Nickel	<dl	<dl	<dl	<dl	<dl	<dl
Copper	<dl	<dl	<dl	<dl	1.2 ±0.3	1.5 ±0.2
Zinc	<dl	<dl	<dl	<dl	<dl	<dl
Gallium	<dl	<dl	<dl	<dl	<dl	<dl
Germanium	<dl	<dl	<dl	<dl	<dl	<dl
Arsenic	<dl	<dl	<dl	<dl	<dl	<dl
Selenium	<dl	<dl	<dl	<dl	<dl	<dl
Bromine <sup>b</sup>	<dl	<dl	<dl	<dl	<dl	<dl
Krypton	<dl	<dl	<dl	<dl	<dl	<dl
....						
Silver	<dl	<dl	<dl	<dl	0.9 ±0.5	2 ±1
Tin	0.05 ±0.05	0.03 ±0.03	0.3 ±0.2	0.2 ±0.2	<dl	<dl
Barium	<dl	0.01 ±0.02	0.12 ±0.02	0.02 ±0.02	<dl	<dl
Gold	<dl	<dl	<dl	<dl	64 ±6	54 ±18

## Chapter 5: Overall Conclusions with Suggestions for Future Work

### 5.1 Overall conclusions

The main achievements and conclusions of this work have been discussed below, with reference to the aims outlined in Section 1.8, Chapter 1.

#### *Supercritical hydration*

- *Design, construct and optimise process equipment for supercritical hydration, using  $\text{scCO}_2$  as the fluid of choice, and additionally to investigate co-solvent addition and changes in experimental process parameters.*
- *Investigate supercritical hydration as a method for the addition of water to wood samples, including historic and modern, hardwood and softwood.*

From Figure 2.12 (Section 2.4.1.3, Chapter 2) a general trend is observed; increasing the concentration of MeOH (co-solvent) increases the levels of NMC achieved by all the wood species in the sample set. This trend had been predicted in the hypothesis outlined in Section 2.4.1.1. The hypothesis also stated that the modern wood samples would achieve higher stabilised NMC than the historic wood samples. This has been proved not to be the case with the historic and modern wood samples treated in this study. It was found here that both White Oak (*H*) and Maple (*H*) achieved some of the highest stabilised NMC of the sample set.

Evidence so far suggests that the temperate hardwoods are more consistent in their ability to retain water, additionally suggesting that wood type rather than wood age is more of an influencing factor on the absorbance levels of water. Even though the hardwoods may initially have a lower uptake of water molecules it seems they can retain a consistently higher NMC. Statistically this is supported by White Oak (*H*), Maple (*H*) and Red Oak (*M*) all giving significant results with 5.0 mol% MeOH, Maple (*H*) also gave significant results with 2.5 mol% MeOH. Due to the unpredictable nature of Scots Pine (*H*) and its reaction to the SCF treatments it would be interesting to investigate a greater number of softwood species undergoing  $\text{scCO}_2$  treatment. As discussed, it is most likely that the impregnation and subsequent absorption of water into the wood matrix is influenced by a combination of macrostructural and microstructural features, which can vary between individual the wood samples. Cell composition, pit and pore arrangement and age are the main factors that should be considered when selecting a wood species for treatment with  $\text{scCO}_2$  in the presence of water.

### ***Microstructural analysis***

- *Assess, via microstructural analytical techniques, the extent of any damage caused during the supercritical hydration treatments.*

In this instance, light microscopy has proved to be the most useful of the two imaging analyses. It has been suggested that SEM, in collaboration with the interior and exterior light microscopy images, may confirm or provide additional evidence on wood sample characterisation. However, SEM, as a standalone analysis cannot be used to assess whether the wood samples have been subject to any additional damage during the supercritical hydration treatment due to the erratic and damaging sample preparation method. The images produced by light microscopy of the untreated and treated wood samples suggest that no damage is being caused to the interior or the exterior of the samples. In comparison with the wood samples that were known to be heat damaged, the treated and untreated wood samples have undergone no colour changes and depict none of the characteristic features of damage.

The DRIFT spectroscopy studies were reasonably successful with significant trends being identified. All the DRIFT spectra for the four modern wood samples showed bands associated with OH groups (ca.  $3490\text{ cm}^{-1}$ ) and CH groups (ca.  $2900\text{ cm}^{-1}$ ). Bands associated with the principle constituents of wood, namely cellulose, hemicellulose and lignin were known to be partially hidden or limited to the fingerprint region of the spectra (ca.  $400 - 1800\text{ cm}^{-1}$ ) for DRIFT spectroscopy. The calculated OH/CH and OH/“cellulose” ratios gave insight as to the possible interactions associated with the hydroxyl groups and the fibrous wood constituents. The ratios also gave supporting evidence for relationship between co-solvent concentration and NMC.

### ***Macrostructural analysis***

- *Asses, via macrostructural analytical techniques, the extent of any damage caused during the supercritical hydration treatments.*
- *Investigate the potential of the supercritical hydration mechanism to maintain or increase the MOR of the wood samples.*

To draw conclusions from the significance of the bending strength (MOR) and Young's Modulus values, they must be looked at in conjunction with the NMC data highlighted in hydration profiles shown in Section 2.4.1.2 and Section 2.4.1.3. These have shown that increasing the co-solvent percentage in turn increases the stabilised NMC of all the wood

samples. Increasing the overall moisture content of the wood decreases its stiffness and strength (Greer, 2008) due to water forming cellulose-water bonds, thereby altering the cell wall structure and increasing its surface area. The decreasing strength values shown in Table 3.3 positively affirms the assumption that scCO<sub>2</sub> is successfully hydrating the oven dried wood samples to a certain degree.

Apart from Maple (*H*) (Figure 3.28) all the wood samples increased in MOR after treatment with scCO<sub>2</sub>. However, if these results are looked at in conjunction with the NMC data it seems that some woods are more suited to the supercritical treatments, than others. The supercritical treatment conditions of 20 MPa and 50°C for 45 minutes were constant throughout all the studies listed in this Chapter. Under these conditions, it was concluded in Section 2.4.1.4 and Section 2.4.1.5 that temperate hardwoods are the most suitable for treatment via scCO<sub>2</sub>(MeOH). The three-point bend tests carried out here have provided evidence that these temperate hardwoods have not only been stabilised but have also increased in MOR. In the case of Scots Pine (*H*), it is likely that the increase in MOR is due to the scCO<sub>2</sub> causing swelling of the amorphous cellulose polymers, rather than increased levels of NMC.

Maple (*H*) displays the possibility of SFE taking place alongside the supercritical hydration of the wood samples, which may be an area of concern for conservators. Having said that, the removal of waxy consolidants can be beneficial to conservators. The waxy residues can migrate towards the surface of the material attracting dirt and causing changes in colour. Therefore, stabilisation or at least the cleaning of a material, may be achieved by extracting the waxy residues and replacing them with a more suitable consolidant.

- *Present findings to conservation professionals at cultural heritage conferences and symposiums to assess the suitability of the supercritical hydration technique as a standalone, or collaborative method in art conservation. Compare this novel process with conventional methods of wood hydration used in conservation departments.*

Findings have been presented at conferences in both the UK and USA, as shown in the Publications section at the beginning of this thesis. It was found that some conservators had concerns regarding the methodology developed here. The main issues raised were associated with fragile materials being placed and sealed in a high pressure vessel, away from human contact. However, it was explained that several precautions had been taken to avoid the development of pressure differentials, which may cause damage to fragile materials. As such, conservators could see the benefit of an interventive methodology that stabilised and

strengthened dry wood via hydration. Currently, preventative methods are most commonly applied when dealing with dry wood. These mainly involve controlling the environment in which the wood samples are kept, thus appealing to their hygroscopic nature. However, the interventive methodology developed in this thesis may be used as a complimentary treatment to be used alongside these preventative methods, and not to replace them. The hydration levels achieved by the application of supercritical hydration may be maintained, and prolonged by the additional storage of the wood in a carefully controlled environment. Hence, wood samples may maintain an increased level of stabilisation for a longer period of time.

### ***Feasibility studies for historic leather***

- *In a feasibility study to investigate other historic media, assess the additional applications of scCO<sub>2</sub> technology for use in conservation departments.*

The feasibility studies described for the treatment of leather samples using scCO<sub>2(PURE)</sub> in the presence of water, have both shown positive results. It seems reasonable to suggest that the treatment was not harmful to the three historic leather samples and it was suggested that a degree of hydration may also be taking place. Further studies with a larger number of historic samples need to be carried out to establish the effectiveness of scCO<sub>2</sub> as a cleaning solvent for historic leather. The DRIFT analysis of the treated and untreated leather samples provided an insight into the characterisation of the three leather pairs of which the origins were unknown. It is also possible that the DRIFT spectroscopy showed the presence of water in the leather post-treatment. However, this was not conclusive and more samples would need to be analysed to see if this was statistically definitive. It should be noted that some spectra had to be disregarded due to the presence of Rastrahlen band effects caused by the reflective surfaces of the different coatings on the front of the leather samples. Therefore, in the future, care must be taken when selecting suitable leather samples for characterisation by DRIFT spectroscopy.

The scCO<sub>2(PURE)</sub> treatment and SEM-EDS analysis of the leather book spine provided beneficial evidence towards two areas of interest; cleaning and characterisation. The SEM images showed that there were no major physical changes to the surface of the spine post-treatment with scCO<sub>2(PURE)</sub>. Thus, it can also be suggested that the scCO<sub>2(PURE)</sub> caused no physical damage to the surface of the leather spine and could therefore be optimised in future studies as a non-toxic cleaning solvent in conservation techniques. Improvements may be made as to the efficiency of the scCO<sub>2</sub> solvent stream with the addition of a suitable co-solvent, thereby increasing the affinity of CO<sub>2</sub> with polar molecules. Alternatively, it may be possible



to create an analytical protocol using both DRIFT spectroscopy techniques and SEM-EDS techniques to create a character profile for deteriorated leather that can then be used by conservators to create an action plan for necessary to stabilisation of the material.

## 5.2 Suggestions for future work

Based on the experimental findings presented throughout this thesis, the following topics are suggested as the most promising areas for future work:

*Investigation of supercritical hydration with different co-solvents to aid the levels of hydration achieved by the wood samples, without causing damage to the structure*

The use of methanol as a co-solvent improved the levels of NMC achieved by the historic and modern wood samples. However, the increased hydration levels in turn compromised the maximum MOR that the wood samples achieved. Hence, increasing the co-solvent concentration, increased the stabilised NMC of the wood samples. However, a higher NMC decreases the overall MOR of the wood samples as water species weaken the wood cell walls. As such, it was suggested that a ‘happy medium’ should be found when choosing between co-solvent concentration, and the desired levels of MOR increase. Therefore, it would be interesting to investigate whether different co-solvents offer better levels of hydration with similar or improved responses in MOR. The varying affinities between different co-solvents and  $\text{scCO}_2$  may increase the hydration ability of the  $\text{scCO}_2$  solvent stream.

*Hydrating additional wood species, specifically softwood species.*

Scots Pine (*H*) was the only softwood in the sample set. However, it gave some interesting results that would have been better justified alongside additional softwood species. Instead, some assumptions were made as to why Scots Pine (*H*) achieved low levels of hydration in comparison to the temperate hardwoods. Incorporating additional softwood species for investigation via supercritical hydration, may give further evidence as to why softwood species were unable to achieve higher levels of hydration. Modern and historic softwood species should be investigated.

*Further DRIFT analysis to determine specific interactions.*

The DRIFT spectroscopy study was successful, however some questions remained and assumptions have been made. Further DRIFT analysis with a greater number of wood samples, could be used to confirm the presence of any specific interactions caused by the supercritical

hydration treatment. Specifically, OH/ “Cellulose” and OH/CH interactions may be determined, as well as additional features related to wood composition.

If evidence of specific interactions that occur during the supercritical hydration of wood can be collected and linked to the levels of hydration achieved, then there may be a potential to tune the existing mechanism for individual samples depending on the levels of hydration required, or for specific wood species and/or types. In addition to DRIFT techniques, there may be value in applying additional analytical techniques to the wood samples prior to treatment as this may further elucidate information about the sample. This approach would be particularly useful within a conservation setting where information about historic materials/media is often sparse.

*Comparative studies for the humidification of historic materials.*

It may be interesting to carry out studies that investigate modern conservation hydration techniques used on historic materials, in direct comparison to the supercritical hydration technique suggested here. Preventative conservation methods most commonly use humidity cabinets to maintain stable moisture levels in collections, therefore initial studies should primarily look at these such methods in detail.

*Expand on the feasibility studies with historic leather samples. Further studies may include the cleaning of historic leather and/or the removal of consolidant waxes and resins.*

The feasibility studies carried out in Chapter 4 show the potential for additional conservation treatments via scCO<sub>2</sub>. The studies have shown that the cleaning of historic leather with scCO<sub>2</sub> may provide greatest scope for success in the future. Certainly, investigations carried out by Sousa et al. (2007) on the cleaning of historic textiles suggest that scCO<sub>2</sub> may be harnessed as a very effective cleaning solvent for soiled leather samples. However, many modifications need to be made to the existing scCO<sub>2</sub> cleaning method already suggested. It will be necessary to investigate the addition of a co-solvent to scCO<sub>2</sub> solvent stream, as it is likely that this will increase the levels of cleaning achieved. It may also be more helpful to know the exact origin and use of the leather samples that are to undergo cleaning, thus allowing for precautions to be taken as regards material fragility and possible extractives.

Leather conservators are increasingly concerned with the damage caused by the application of waxy resins and oils to the surface of many leather objects and coverings in the past. These oils, or wax based consolidants were previously applied to leathers in an attempt to maintain

suppleness and avoid cracking. However, a number of problems faced by leather conservators are now associated with the application of these ‘projective’ consolidants e.g. migration of dirt and dust. It is well known that scCO<sub>2</sub> acts as lipophilic solvent and will extract light oils and higher molecular weight materials e.g. resins. Mechanical data for Maple (*H*) (Section 3.3.2.1, Chapter 3) has suggested that oil or wax based resins previously applied as a consolidant, have been extracted by the scCO<sub>2</sub>. It would be interesting to investigate the removal of previously applied waxes and oils from leather samples via a scCO<sub>2</sub> solvent stream, as a solution to a problem facing many leather conservators today. *Polymers and scCO<sub>2</sub> in contemporary conservation practices.*

Both Scots Pine (*H*) and Maple (*H*) samples investigated in this thesis have given examples of why it may be possible to apply scCO<sub>2</sub> treatments to problems facing contemporary art conservators. The increase in MOR for Scots Pine (*H*), suggested that scCO<sub>2</sub> may be swelling the natural wood polymer matrix and inducing a seemingly increased level of strength (Section 3.3.2.1, Chapter 3). Whilst Maple (*H*) provided an example of the scCO<sub>2</sub> ability to extract oil or wax based molecules.

scCO<sub>2</sub> is known to swell and expand several polymeric materials that are used in contemporary art, specifically polyurethane (PUR) foams. This property can be used to the advantage of conservators who are either looking to extract or impregnate degrading polymers as a means of increasing material stabilisation. Extraction of degradation materials and/or monomer residues, and the impregnation of organic UV absorbers, monomers and amino silanes or acrylates are all feasible via a scCO<sub>2</sub> solvent stream.

## 6.0 References

- Acda, M., Morrell, J. & Levien, K. (2001). **Supercritical fluid impregnation of selected wood species with tebuconazole**. Wood science and technology, 35, 127-136.
- Agarwal, U. P. (2008). **Raman spectroscopic characterization of wood and pulp fibers**. Characterization of lignocellulosic materials. Blackwell, Oxford, 17-35.
- Ahmed, S. A. & Chun, S. K. (2011). **Permeability of tectona grandis l. As affected by wood structure**. Wood Science and Technology, 45, 487-500.
- Alcántara, R. (2002). **Standards in preventive conservation: Meanings and applications**, ICCROM.
- Arney, J. S., Jacobs, A. J. & Newman, R. (1979). **The influence of deacidification on the deterioration of paper**. Journal of the American Institute for Conservation, 19, 34-41.
- Arshid, F., Giles, C. & Jain, S. (1956). **260. Studies in hydrogen-bond formation. Part v. Complex-forming properties of esters, and their relation to the adsorption properties of cellulose acetate and other polymers**. Journal of the Chemical Society (Resumed), 1272-1277.
- Baglioni, P., Chelazzi, D., Giorgi, R. & Poggi, G. (2013). **Colloid and materials science for the conservation of cultural heritage: Cleaning, consolidation, and deacidification**. Langmuir, 29, 5110-5122.
- Baiker, A. (1999). **Supercritical fluids in heterogeneous catalysis**. Chemical Reviews, 99, 453-474.
- Bao, F., Lu, J. & Avramidis, S. (1999). **On the permeability of main wood species in china**. Holzforschung, 53, 350-354.
- Baptista, A., Ferreira, I. & Borges, J. (2013). **Cellulose-based bioelectronic devices**. Cellulose-Medical, Pharmaceutical and Electronic Applications: InTech.
- Bardet, M., Foray, M. F., Maron, S., Goncalves, P. & Tr  n, Q. K. (2004). **Characterization of wood components of portuguese medieval dugout canoes with high-resolution solid-state nmr**. Carbohydrate Polymers, 57, 419-424.
- Barlee, R. (2001). **Aluminium tannages**. Skin deep, 16-18.
- Bastian, F., Jurado, V., Nov  kov  , A., Alabouvette, C. & Saiz-Jimenez, C. (2010). **The microbiology of lascaux cave**. Microbiology, 156, 644-652.
- Baty, J. (2010). **Deacidification for the conservation and preservation of paper-based works: A review**. BioResources, 5, 1955.
- Belouettar, S., Abbadi, A., Azari, Z., Belouettar, R. & Freres, P. (2009). **Experimental investigation of static and fatigue behaviour of composites honeycomb materials using four point bending tests**. Composite Structures, 87, 265-273.
- Benabid, F. Z. & Zouai, F. (2016). **Natural polymers: Cellulose, chitin, chitosan, gelatin, starch, carrageenan, xylan and dextran**. ALGERIAN JOURNAL OF NATURAL PRODUCTS, 4, 348-357.
- Berche, B., Henkel, M. & Kenna, R. (2009). **Critical phenomena: 150 years since cagniard de la tour**. Revista Brasileira de Ensino de F  sica, 31, 2602.2601-2602.2604.
- Bergman, R. C., Zhiyong; Carll, Charlie G.; Clausen, Carol A.; Dietenberger, Mark A.; Falk, Robert H.; Frihart, Charles R.; Glass, Samuel V.; Hunt, Christopher G.; Ibach, Rebecca E.; Kretschmann, David E.; Rammer, Douglas R.; Ross, Robert J.; Star (2010). **Forest products laboratory. Wood handbook - wood as an engineering material**. . General Technical Report FPL-GTR-190. Madison, WI: U.S. Department of Agriculture, Forest Service, Forest Products Laboratory, 508.
- Bj  rdal, C. G. & Nilsson, T. (2001). **Observations on microbial growth during conservation treatment of waterlogged archaeological wood**. Studies in Conservation, 46, 211-220.
- Blades, N., Cassar, M., Oreszczyn, T. & Croxford, B. (2000). **Preventive conservation strategies for sustainable urban pollution control in museums**. Studies in Conservation, 45, 24-28.
- Blanchette, R. A. (2000). **A review of microbial deterioration found in archaeological wood from different environments**. International Biodeterioration & Biodegradation, 46, 189-204.
- Blanchette, R. A., Cease, K. R., Abad, A., Koestler, R. J., Simpson, E. & Sams, G. K. (1991). **An evaluation of different forms of deterioration found in archaeological wood**. International Biodeterioration, 28, 3-22.

- Brancheriau, L., Bailleres, H. & Guitard, D. (2002). **Comparison between modulus of elasticity values calculated using 3 and 4 point bending tests on wooden samples.** Wood Science and Technology, 36, 367-383.
- Brown, J. & Rose, W. B. (1996). **Humidity and moisture in historic buildings: The origins of building and object conservation.** APT bulletin, 12-23.
- Brunet, J., Vouvé, J. & Malaurent, P. (2000). **Re-establishing an underground climate appropriate for the conservation of the prehistoric paintings and engravings at lascaux.** Conservation and Management of Archaeological Sites, 4, 33-45.
- Builes, S. & Vega, L. F. (2012). **Effect of immobilized amines on the sorption properties of solid materials: Impregnation versus grafting.** Langmuir, 29, 199-206.
- Bumbrah, G. S. & Sharma, R. M. (2016). **Raman spectroscopy – basic principle, instrumentation and selected applications for the characterization of drugs of abuse.** Egyptian Journal of Forensic Sciences, 6, 209-215.
- Burkhardt, K. (2012). **An evaluation of physico-chemical properties of the mobile phase in supercritical fluid chromatography when using sub-2 $\mu$ m particle columns.** Application Notes Jasco INC.
- Calnan, C. N. & Haines, B. (1991). **Leather: Its composition and changes with time,** Leather Conservation Centre.
- Camuffo, D., Van Grieken, R., Busse, H.-J., Sturaro, G., Valentino, A., Bernardi, A., Blades, N., Shooter, D., Gysels, K., Deutsch, F., Wieser, M., Kim, O. & Ulrych, U. (2001). **Environmental monitoring in four european museums.** Atmospheric Environment, 35, Supplement 1, S127-S140.
- Chaplin, T. D., Clark, R. J. H. & Martínón-Torres, M. (2010). **A combined raman microscopy, xrf and sem-edx study of three valuable objects – a large painted leather screen and two illuminated title pages in 17th century books of ordinances of the worshipful company of barbers, london.** Journal of Molecular Structure, 976, 350-359.
- Chen, H. (2014). "Chemical composition and structure of natural lignocellulose". **Biotechnology of lignocellulose.** Springer.
- Chen, H., Ferrari, C., Angiuli, M., Yao, J., Raspi, C. & Bramanti, E. (2010). **Qualitative and quantitative analysis of wood samples by fourier transform infrared spectroscopy and multivariate analysis.** Carbohydrate Polymers, 82, 772-778.
- Christensen, M., Frosch, M., Jensen, P., Schnell, U., Shashoua, Y. & Nielsen, O. F. (2006). **Waterlogged archaeological wood—chemical changes by conservation and degradation.** Journal of Raman Spectroscopy, 37, 1171-1178.
- Chueh, P. & Prausnitz, J. (1967). **Vapor-liquid equilibria at high pressures: Calculation of critical temperatures, volumes, and pressures of nonpolar mixtures.** AIChE Journal, 13, 1107-1113.
- Clifford, T. (1999). **Fundamentals of supercritical fluids,** Oxford University Press.
- Côté, W. A. (Year) Published. **Structural factors affecting the permeability of wood.** Journal of Polymer Science: Polymer Symposia, 1963. Wiley Online Library, 231-242.
- Čufar, K., Merela, M. & Erič, M. (2014). **A roman barge in the ljubljana river (slovenia): Wood identification, dendrochronological dating and wood preservation research.** Journal of Archaeological Science, 44, 128-135.
- Cussler, E. L. (2009). **Diffusion: Mass transfer in fluid systems,** Cambridge university press.
- Demeroukas, M. & Ritchie, F. (2015). **Skin and leather.** Basic Condition Reporting: A Handbook, 111.
- Dillow, A. K., Dehghani, F., Hrkach, J. S., Foster, N. R. & Langer, R. (1999). **Bacterial inactivation by using near-and supercritical carbon dioxide.** Proceedings of the National Academy of Sciences, 96, 10344-10348.
- Dirksen, V. (1997). **The degradation and conservation of leather.** Journal of Conservation and Museum Studies, 3.
- Domec, J. C. & Gartner, B. L. (2002). **How do water transport and water storage differ in coniferous earlywood and latewood?** Journal of Experimental Botany, 53, 2369-2379.

- Eckelman, C. A. (1994). **Wood moisture calculations**, Purdue University, Department of Forestry & Natural Resources.
- Ekart, M. P., Bennett, K. L., Ekart, S. M., Gurdial, G. S., Liotta, C. L. & Eckert, C. A. (1993). **Cosolvent interactions in supercritical fluid solutions**. *AIChE journal*, 39, 235-248.
- Elles, C. G. & Crim, F. F. (2006). **Connecting chemical dynamics in gases and liquids**. *Annu. Rev. Phys. Chem.*, 57, 273-302.
- Engelhardt, H. & Haas, P. (1993). **Possibilities and limitations of sfc in the extraction of aflatoxin b1 from food matrices**. *Journal of chromatographic science*, 31, 13-19.
- Eriksson, K.-E. L., Blanchette, R. A. & Ander, P. (1990). **Microbial and enzymatic degradation of wood and wood components**, Springer-verlag.
- Fandrich, R., Gu, Y., Burrows, D. & Moeller, K. (2007). **Modern sem-based mineral liberation analysis**. *International Journal of Mineral Processing*, 84, 310-320.
- Ferraz, A., Baeza, J., Rodriguez, J. & Freer, J. (2000). **Estimating the chemical composition of biodegraded pine and eucalyptus wood by drift spectroscopy and multivariate analysis**. *Bioresource Technology*, 74, 201-212.
- Foster, N. R., Singh, H., Yun, S. L. J., Tomasko, D. L. And Macnaughton, S. J. (2002). **Polar and nonpolar cosolvent effects on the solubility of cholesterol in supercritical fluids**. *Industrial & Engineering Chemistry Research*, 32(11), 2849-2853.
- Français, É., Perrut, M. & Brandt, A.-C. (1997). **Deacidification: Mass reinforcement of acidic and fragile papers with supercritical fluids**. *Conservation: A changing Science. Balance sheet and outlooks. Proceedings of the 3rd International ARSAG Study Days*. Paris: ARSAG.
- Ganitis, V., Pavlidou, E., Zorba, F., Paraskevopoulos, K. M. & Bikiaris, D. (2004). **A post-byzantine icon of st nicholas painted on a leather support. Microanalysis and characterisation of technique**. *Journal of Cultural Heritage*, 5, 349-360.
- Gerhards, C. C. (1982). **Effect of moisture content and temperature on the mechanical properties of wood: An analysis of immediate effects**. *Wood and Fibre*, 14 (1), 4 -36.
- Giorgi, R., Chelazzi, D. & Baglioni, P. (2005). **Nanoparticles of calcium hydroxide for wood conservation. The deacidification of the vasa warship**. *Langmuir*, 21, 10743-10748.
- Giorgi, R., Dei, L., Ceccato, M., Schettino, C. & Baglioni, P. (2002). **Nanotechnologies for conservation of cultural heritage: Paper and canvas deacidification**. *Langmuir*, 18, 8198-8203.
- Glastrup, J. (1987). **Insecticide analysis by gas chromatography in the stores of the danish national museum's ethnographic collection**. *Studies in Conservation*, 32, 59-64.
- Grattan, D. W. & Clarke, R. (1987). **Conservation of waterlogged wood**. *Conservation of marine archaeological objects*, 164-206.
- Green, D. (2001). **Wood: Strength and stiffness**. *Encyclopedia of Materials: Science and Technology*, 9732-9736.
- Greer, P., Chong Tan, (2008). **The structure and mechanical behaviour of wood**.
- Guldbeck, P. E. (1969). **Leather: Its understanding and care**. *History News*, 34, 12.
- Haake, L. (2014). **Waterlogged and dry wood: A comparison between conservation methods**. *Conservation and restoration of cultural heritage*. University of Amsterdam.
- Hacke, U. G., Sperry, J. S. & Pittermann, J. (2004). **Analysis of circular bordered pit function ii. Gymnosperm tracheids with torus-margo pit membranes**. *American Journal of Botany*, 91, 386-400.
- Haines, B. (1991a). "Skin structure and leather properties". **Leather: Its composition and changes with time**. Leather Conservation Centre.
- Haines, B. M. (1991b). "Natural ageing of leather in libraries". **Leather: Its composition and changes with time**. Leather Conservation Centre.
- Hamilton, D. L. (1999). **Methods of conserving archaeological material from underwater sites**. Texas A&M University.
- Hegg, T. (2010). **Supercritical fluid near the critical point: The piston effect**.
- Hoadley, R. B. (2000). **Understanding wood: A craftsman's guide to wood technology**, Taunton press.

- Howson, J. A. (1949). **Water sorption and the poly-phase structure of cellulose fibers**. Textile Research Journal, 19, 152-162.
- Huang, Y., Wang, L., Chao, Y., Nawawi, D. S., Akiyama, T., Yokoyama, T. & Matsumoto, Y. (2016). **Relationships between hemicellulose composition and lignin structure in woods**. Journal of Wood Chemistry and Technology, 36, 9-15.
- Icon. (2014). **The institute of conservation's professional standards** [Online]. Institute of Conservation Available from: <http://icon.org.uk/system/files/documents/professional-standards-2016.pdf> [Accessed November 2016].
- Illicka, A. & Lukaszewicz, J. P. (2015). **Discussion remarks on the role of wood and chitin constituents during carbonization**. Frontiers in Materials, 2.
- John, F. E. G., Montagna, W. (2015). **Human skin** [Online]. Encyclopaedia Britannica, Inc. Available from: <https://www.britannica.com/science/human-skin> [Accessed January 24 2017].
- Junior, S. a. R., Ferracane, J. L. & Della Bona, Á. (2008). **Flexural strength and weibull analysis of a microhybrid and a nanofill composite evaluated by 3-and 4-point bending tests**. Dental materials, 24, 426-431.
- Kaiser, K., Guggenberger, G., Haumaier, L. & Zech, W. (1997). **Dissolved organic matter sorption on sub soils and minerals studied by <sup>13</sup>C-NMR and drift spectroscopy**. European Journal of Soil Science, 48, 301-310.
- Kang, S. M., Unger, A. & Morrell, J. J. (2004). **The effect of supercritical carbon dioxide extraction on color retention and pesticide reduction of wooden artifacts**. Journal of the American Institute for Conservation, 43, 151-160.
- Kasturirangan, A. (2007). **Specific interactions in carbon dioxide and polymer systems**. Georgia Institute of Technology.
- Kaye, B. (1995). **Conservation of waterlogged archaeological wood**. Chemical Society Reviews, 24, 35-43.
- Kerr, A. & Goring, D. (1975). **Ultrastructural arrangement of the wood cell wall**. Cellulose chemistry and technology.
- Kerschner, R. L. (1992). **A practical approach to environmental requirements for collections in historic buildings**. Journal of the American Institute for Conservation, 31, 65-76.
- Kigawa, R., Strang, T., Hayakawa, N., Yoshida, N., Kimura, H. & Young, G. (2011). **Investigation of effects of fumigants on proteinaceous components of museum objects (muscle, animal glue and silk) in comparison with other non-chemical pest eradicating measures**. Studies in Conservation, 56, 191-215.
- Kjellow, A. W. & Henriksen, O. (2009). **Supercritical wood impregnation**. The Journal of Supercritical Fluids, 50, 297-304.
- Knapic, S., Tavares, F. & Pereira, H. (2006). **Heartwood and sapwood variation in acacia melanoxylon r. Br. Trees in portugal**. Forestry, 79, 371-380.
- Kodama, D., Nakajima, T., Tanaka, H. & Kato, M. (1998). **Partial molar volumes of methanol and ethanol at infinite dilution in supercritical carbon dioxide**. Netsu Bussei, 12, 186-190.
- Krishnamoorthy, G., Sadulla, S., Sehgal, P. & Mandal, A. B. (2012). **Green chemistry approaches to leather tanning process for making chrome-free leather by unnatural amino acids**. Journal of hazardous materials, 215, 173-182.
- Krug, S. & Hahn, O. (2013). **Portable x-ray fluorescence analysis of pesticides in the textile collection at the german historical museum, berlin**. Studies in Conservation, 0, null.
- Kumar, S. K., Chhabria, S. P., Reid, R. C. & Suter, U. W. (1987). **Solubility of polystyrene in supercritical fluids**. Macromolecules, 20, 2550-2557.
- Lalanne, P., Tassaing, T., Danten, Y., Cansell, F., Tucker, S. C. & Besnard, M. (2004). **CO<sub>2</sub>-ethanol interaction studied by vibrational spectroscopy in supercritical CO<sub>2</sub>**. The Journal of Physical Chemistry A, 108, 2617-2624.
- Lee, S. & Henthorn, K. H. (2012). **Particle technology and applications**, Taylor & Francis.

- Lenth, C. A. & Kamke, F. A. (2007). **Equilibrium moisture content of wood in high-temperature pressurized environments**. Wood and fiber science, 33, 104-118.
- Letellier, R. & Eppich, R. (2015). **Recording, documentation and information management for the conservation of heritage places**, Routledge.
- Liang, M.-T., Liang, R.-C., Huang, L.-R., Hsu, P.-H., Wu, Y.-H. & Yen, H.-E. (2012). **Separation of sesamin and sesamolin by a supercritical fluid-simulated moving bed**. American Journal of Analytical Chemistry, 3, 931.
- Lindon, J. C., Tranter, G. E. & Koppenaal, D. (2016). **Encyclopedia of spectroscopy and spectrometry**, Academic Press.
- Liu, Q., Wang, S., Zheng, Y., Luo, Z. & Cen, K. (2008). **Mechanism study of wood lignin pyrolysis by using tg-ftir analysis**. Journal of Analytical and Applied Pyrolysis, 82, 170-177.
- Lucas, S., Gonzalez, E., Calvo, M., Palencia, C., Alonso, E. & Cocero, M. (2007). **Supercritical co<sub>2</sub> impregnation of radiata pine with organic fungicides: Effect of operating conditions and two-parameters modeling**. The Journal of supercritical fluids, 40, 462-469.
- Łucejko, J. J., Modugno, F., Ribechini, E., Tamburini, D. & Colombini, M. P. (2015). **Analytical instrumental techniques to study archaeological wood degradation**. Applied Spectroscopy Reviews, 50, 584-625.
- Madden, O., Johnson, J. & Anderson, J. R. (2010). **Pesticide remediation in context: Toward standardization of detection and risk assessment**. A Chronology of Middle Missouri Plains Village Sites, 1.
- Malea, E., Boyatzis, S. C. & Kehagia, M. (Year) Published. **Cleaning of tanned leather: Testing with infra red spectroscopy and sem-edax**. Joint Interim-Meeting of Five ICOM. CC Working Groups, Rome 2010, 2010. 1.
- Mchardy, J., Stanford, T., Benjamin, L., Whiting, T. & Chao, S. (1993). **Progress in supercritical co<sub>2</sub> cleaning**. SAMPE Journal (Society of Aerospace Material and Process Engineers);(United States), 29.
- Meylan, B. A. & Butterfield, B. G. (1972). **Three-dimensional structure of wood: A scanning electron microscope study**, Syracuse University Press.
- Michell, A. J. (1994). **Vibrational spectroscopy: A rapid means of estimating plantation pulpwood quality?** Appita, 47, 29-37.
- Mizuno, S., Torizu, R. & Sugiyama, J. (2010). **Wood identification of a wooden mask using synchrotron x-ray microtomography**. Journal of Archaeological Science, 37, 2842-2845.
- Montanari, L., Fantozzi, P., Snyder, J. M. & King, J. W. (1999). **Selective extraction of phospholipids from soybeans with supercritical carbon dioxide and ethanol**. The Journal of supercritical fluids, 14, 87-93.
- Morrell, J., Levien, K., Sahle Demessie, E., Kumar, S., Smith, S. & Barnes, H. (1993). **Treatment of wood using supercritical fluid processes**. Proc. Can. Wood Preserv. Assoc, 14, 6-25.
- Motlagh, B., Gholipour, Y. & Ebrahimi, G. (2012). **Experimental investigation on mechanical properties of old wood members reinforced with frp composite**. WOOD RESEARCH, 57, 285-296.
- Muin, M. & Tsunoda, K. (2003). **Preservative treatment of wood-based composites with 3-iodo-2-propynyl butylcarbamate using supercritical carbon dioxide impregnation**. Journal of Wood Science, 49, 430-436.
- Mujika, F. (2006). **On the difference between flexural moduli obtained by three-point and four-point bending tests**. Polymer Testing, 25, 214-220.
- Novaes, E., Kirst, M., Chiang, V., Winter-Sederoff, H. & Sederoff, R. (2010). **Lignin and biomass: A negative correlation for wood formation and lignin content in trees**. Plant Physiology, 154, 555-561.
- Oakes, R. S., Clifford, A. A. & Rayner, C. M. (2001). **The use of supercritical fluids in synthetic organic chemistry**. Journal of the Chemical Society, Perkin Transactions 1, 917-941.



- Özcan, A. S. (1997). **Dyeing in supercritical carbon dioxide**. The University of Leeds, School of Chemistry.
- Pandey, K. K. & Pitman, A. J. (2003). **Ftir studies of the changes in wood chemistry following decay by brown-rot and white-rot fungi**. *International Biodeterioration & Biodegradation*, 52, 151-160.
- Pandey, K. K. & Theagarajan, K. S. (1997). **Analysis of wood surfaces and ground wood by diffuse reflectance (drift) and photoacoustic (pas) fourier transform infrared spectroscopic techniques**. *Holz als Roh- und Werkstoff*, 55, 383-390.
- Panshin, A. J. & Zeeuw, C. D. (1980). **Textbook of wood technology**, McGraw-Hill Book Co.
- Perrut, M. (2012). **Sterilization and virus inactivation by supercritical fluids (a review)**. *The Journal of Supercritical Fluids*, 66, 359-371.
- Pettersen, R. C. (1984). **The chemical composition of wood**. *The chemistry of solid wood*, 207, 57-126.
- Pizzo, B., Pecoraro, E., Alves, A., Macchioni, N. & Rodrigues, J. C. (2015). **Quantitative evaluation by attenuated total reflectance infrared (atr-ftir) spectroscopy of the chemical composition of decayed wood preserved in waterlogged conditions**. *Talanta*, 131, 14-20.
- Placet, V., Passard, J. & Perré, P. (2008). **Viscoelastic properties of wood across the grain measured under water-saturated conditions up to 135 c: Evidence of thermal degradation**. *Journal of Materials Science*, 43, 3210-3217.
- Porck, H. J. (1996). **Mass deacidification: An update on possibilities and limitations**, ERIC.
- Price, N. S., Talley, M. K. & Vaccaro, A. M. (1996). **Historical and philosophical issues in the conservation of cultural heritage**, Getty Publications.
- Purtell, R., Rothman, L., Eldridge, B. & Chess, C. (1993). **Precision parts cleaning using supercritical fluids**. *Journal of Vacuum Science & Technology A*, 11, 1696-1701.
- Reeb, J. E. (1995). **Wood and moisture relationships**, Oregon State University, Oregon State University Extension Service.
- Reverchon, E. (1997). **Supercritical fluid extraction and fractionation of essential oils and related products**. *The Journal of Supercritical Fluids*, 10, 1-37.
- Reverchon, E., Donsi, G. & Sesti Osseo, L. (1993). **Modeling of supercritical fluid extraction from herbaceous matrices**. *Industrial & engineering chemistry research*, 32, 2721-2726.
- Richmond, A. (2009). **Conservation: Principles, dilemmas and uncomfortable truths**, Taylor & Francis Ltd.
- Rowe, M. W., Phomakay, J., Lay, J. O., Guevara, O., Srinivas, K., Hollis, W. K., Steelman, K. L., Guilderson, T., Stafford Jr, T. W., Chapman, S. L. & King, J. W. (2013). **Application of supercritical carbon dioxide-co-solvent mixtures for removal of organic material from archeological artifacts for radiocarbon dating**. *The Journal of Supercritical Fluids*, 79, 314-323.
- Rowell, R. M. (2012). **Handbook of wood chemistry and wood composites**, CRC press.
- Sahle-Demessie, E. (1994). **Deposition of chemicals in semi-porous solids using supercritical fluid carriers**, UMI.
- Saito, M., Yamauchi, Y. & Okuyama, T. (1994). **Fractionation by packed-column sfc and sfe**, VCH.
- Sano, Y. & Jansen, S. (2006). **Perforated pit membranes in imperforate tracheary elements of some angiosperms**. *Annals of Botany*, 97, 1045-1053.
- Santos, R. B., Capanema, E. A., Balakshin, M. Y., Chang, H.-M. & Jameel, H. (2012). **Lignin structural variation in hardwood species**. *Journal of agricultural and food chemistry*, 60, 4923-4930.
- Saquin, C. D., Lucien, F. P. & Foster, N. R. (1998). **Steric effects and preferential interactions in supercritical carbon dioxide**. *Industrial & Engineering Chemistry Research*, 37, 4190-4197.
- Sawan, S. P. (1998). **Supercritical fluid cleaning: Fundamentals, technology and applications**, Elsevier.
- Schneider, P. F., Levien, K. L. & Morrell, J. J. (2006). **Effect of wood characteristics on pressure responses during supercritical carbon dioxide treatment**. *Wood and fiber science*, 38, 660-671.
- Selli, E., Langè, E., Mossa, A., Testa, G. & Seves, A. (2000). **Preservation treatments of aged papers by supercritical carbon dioxide**. *Macromolecular Materials and Engineering*, 280-281, 71-75.

- Sherman, R. (2007). **Carbon dioxide snow cleaning**. Particulate Science and Technology, 25, 37-57.
- Shieh, Y. T., Su, J. H., Manivannan, G., Lee, P. H., Sawan, S. P. & Dale Spall, W. (1996). **Interaction of supercritical carbon dioxide with polymers. II. Amorphous polymers**. Journal of applied polymer science, 59, 707-717.
- Shusheng, P., Langriah, T. & Keey, R. (1994). **Moisture movement in softwood timber at elevated temperatures**. Drying Technology, 12, 1897-1914.
- Siau, J. F. (1984). "Permeability". **Transport processes in wood**. Berlin, Heidelberg: Springer Berlin Heidelberg.
- Sihvonen, M., Järvenpää, E., Hietaniemi, V. & Huopalahti, R. (1999). **Advances in supercritical carbon dioxide technologies**. Trends in Food Science & Technology, 10, 217-222.
- Simpson, W. T. (1993). **Specific gravity, moisture content, and density relationship for wood**, US Department of Agriculture, Forest Service, Forest Products Laboratory Madison.
- Snyder, J. L., Grob, R. L., McNally, M. E. & Oostdyk, T. S. (1992). **Comparison of supercritical fluid extraction with classical sonication and soxhlet extractions for selected pesticides**. Analytical Chemistry, 64, 1940-1946.
- Sousa, M., Melo, M. J., Casimiro, T. & Aguiar-Ricardo, A. (2007). **The art of CO<sub>2</sub> for art conservation: A green approach to antique textile cleaning**. Green Chemistry, 9, 943-947.
- Sreeram, K. J. & Ramasami, T. (2003). **Sustaining tanning process through conservation, recovery and better utilization of chromium**. Resources, Conservation and Recycling, 38, 185-212.
- Srndovic, J. S. (2011). **Interactions between wood polymers in wood cell walls and cellulose/hemicellulose biocomposites**, Chalmers University of Technology.
- Stamm, A. J. (1964). **Wood and cellulose science**. Wood and cellulose science.
- Storch, P. S. (1987). **Curatorial care and handling of skin materials, part I: Tanned objects**. Conservation notes, 1-4.
- Subramaniam, B., Rajewski, R. A. & Snavely, K. ((1997)). **Pharmaceutical processing with supercritical carbon dioxide**. Journal of Pharmaceutical Sciences, 86, 885-890.
- Sundar, V. J., Raghava Rao, J. & Muralidharan, C. (2002). **Cleaner chrome tanning — emerging options**. Journal of Cleaner Production, 10, 69-74.
- Suresh, V., Kanthimathi, M., Thanikaivelan, P., Raghava Rao, J. & Unni Nair, B. (2001a). **An improved product-process for cleaner chrome tanning in leather processing**. Journal of Cleaner Production, 9, 483-491.
- Suresh, V., Kanthimathi, M., Thanikaivelan, P., Rao, J. R. & Nair, B. U. (2001b). **An improved product-process for cleaner chrome tanning in leather processing**. Journal of Cleaner Production, 9, 483-491.
- Taylor, L. T. (1996). **Supercritical fluid extraction**, Wiley Interscience Publishing, New York.
- Tello, H. (2006). **Investigations on super fluid extraction (sfe) with carbon dioxide on ethnological materials and objects contaminated with pesticides**.
- Tello, H. & Unger, A. (2010). **Liquid and supercritical carbon dioxide as a cleaning and decontamination agent for ethnographic materials and objects**. A Chronology of Middle Missouri Plains Village Sites, 35.
- Tomasko, D. L., Li, H., Liu, D., Han, X., Wingert, M. J., Lee, L. J. & Koelling, K. W. (2003). **A review of CO<sub>2</sub> applications in the processing of polymers**. Industrial & Engineering Chemistry Research, 42, 6431-6456.
- Tucker, S. C. & Maddox, M. W. (1998). **The effect of solvent density inhomogeneities on solute dynamics in supercritical fluids: A theoretical perspective**. The Journal of Physical Chemistry B, 102, 2437-2453.
- Turkulín, H. (Year) Published. **Sem methods in surface research on wood**. E18-High Performance Wood Coatings. Exterior and interior performance, 2004. Hrvatska znanstvena bibliografija i MZOS-Svibor.
- Unger, A., Schniewind, A. & Unger, W. (2001). **Conservation of wood artifacts: A handbook**, Springer Science & Business Media.

- Üzer, S., Akman, U. & Hortaçsu, Ö. (2006). **Polymer swelling and impregnation using supercritical co<sub>2</sub>: A model-component study towards producing controlled-release drugs.** The Journal of Supercritical Fluids, 38, 119-128.
- Van Soest, H. A., Stambolov, T. & Hallebeek, P. B. (1984). **Conservation of leather.** Studies in Conservation, 29, 21-31.
- Viñas, S. M. (2005). **Contemporary theory of conservation,** Routledge.
- Von Schnitzler, J. & Eggers, R. (1999). **Mass transfer in polymers in a supercritical co<sub>2</sub>-atmosphere.** The Journal of Supercritical Fluids, 16, 81-92.
- Walker, J. C. (2006). "Wood properties affecting treatment". **Primary wood processing: Principles and practice.** Springer Science & Business Media.
- Wallström, L. & Lindberg, K. a. H. (1999). **Measurement of cell wall penetration in wood of water-based chemicals using sem/eds and stem/eds technique.** Wood Science and Technology, 33, 111-122.
- Walsh, Z., Janeček, E.-R., Hodgkinson, J. T., Sedlmair, J., Koutsoubas, A., Spring, D. R., Welch, M., Hirschmugl, C. J., Toprakcioglu, C. & Nitschke, J. R. (2014). **Multifunctional supramolecular polymer networks as next-generation consolidants for archaeological wood conservation.** Proceedings of the National Academy of Sciences, 111, 17743-17748.
- Walters, C., Ballesteros, D. & Vertucci, V. A. (2010). **Structural mechanics of seed deterioration: Standing the test of time.** Plant Science, 179, 565-573.
- Waterer, J. W. (1971). **A guide to the conservation and restoration of objects made wholly or in part of leather.** New York: Drake Publishers Inc.
- Weidner, E. (Year) Published. **Impregnation via supercritical fluids principles and applications.** 10th International Symposium on Supercritical Fluids, San Francisco, CA, 2012.
- Woods, H. M., Silva, M. M., Nouvel, C., Shakesheff, K. M. & Howdle, S. M. (2004). **Materials processing in supercritical carbon dioxide: Surfactants, polymers and biomaterials.** Journal of Materials Chemistry, 14, 1663-1678.
- Yang, H., Yan, R., Chen, H., Lee, D. H. & Zheng, C. (2007). **Characteristics of hemicellulose, cellulose and lignin pyrolysis.** Fuel, 86, 1781-1788.
- Yang, H., Yan, R., Chen, H., Zheng, C., Lee, D. H. & Liang, D. T. (2006). **In-depth investigation of biomass pyrolysis based on three major components: Hemicellulose, cellulose and lignin.** Energy & Fuels, 20, 388-393.
- Zabel, R. & Morrell, J. (1992). **Wood stains and discolorations.** Wood Microbiology: decay and its prevention, 326-343.
- Zimmt, W. S., Odegaard, N., Moreno, T. K., Turner, R. A., Riley, M. R., Xie, B. & Muscat, A. J. (2010). **Pesticide extraction studies using supercritical carbon dioxide.** A Chronology of Middle Missouri Plains Village Sites, 51.

## Appendix

### Appendix 1

Wood sample	Mass (g)						
	Week 1	Week 2	Week 4	Week 8	Week 12	Week 16	Week 20
Oven-dried	1.699	1.724	1.731	1.738	1.742	1.745	1.752
Treated 1	2.109	2.100	2.087	2.076	2.070	2.068	2.066
Treated 2	1.993	1.981	1.963	1.959	1.955	1.951	1.951
Treated 3	2.006	1.988	1.976	1.951	1.943	1.939	1.938

**Figure 1a.** Table showing the mass data for control wood samples that were kept in a low humidity desiccator with silica gel for 48 weeks. Data from week 1 to week 20.

Wood sample	Mass (g)						
	Week 24	Week 28	Week 32	Week 36	Week 40	Week 44	Week 48
Oven-dried	1.752	1.752	1.752	1.752	1.753	1.753	1.753
Treated 1	2.065	2.065	2.065	2.064	2.064	2.065	2.065
Treated 2	1.951	1.951	1.954	1.952	1.952	1.952	1.953
Treated 3	1.935	1.935	1.936	1.936	1.936	1.936	1.936

**Figure 1b.** Table showing the mass data for the control wood samples that were kept in a low humidity desiccator with silica gel for 48 weeks. Data from week 24 to week 48.

### Appendix 2

Experiment Number	Temperature 15 minute intervals (°C)		
	15 minutes	30 minutes	45 minutes
1	50.77	50.59	50.23
2	50.96	50.45	40.42
3	50.74	51.02	50.85
4	50.63	50.60	50.42
5	50.89	50.76	50.71
6	50.22	50.22	50.21
7	50.65	50.45	50.54
8	50.99	51.00	50.92
9	51.02	50.86	5.79
10	50.67	50.52	50.55

**Figure 2a.** Table to show typical temperature recordings in the oven for a supercritical hydration experiment. Experiments were 45 minutes long and recordings were taken every 15 minutes.

### Appendix 3

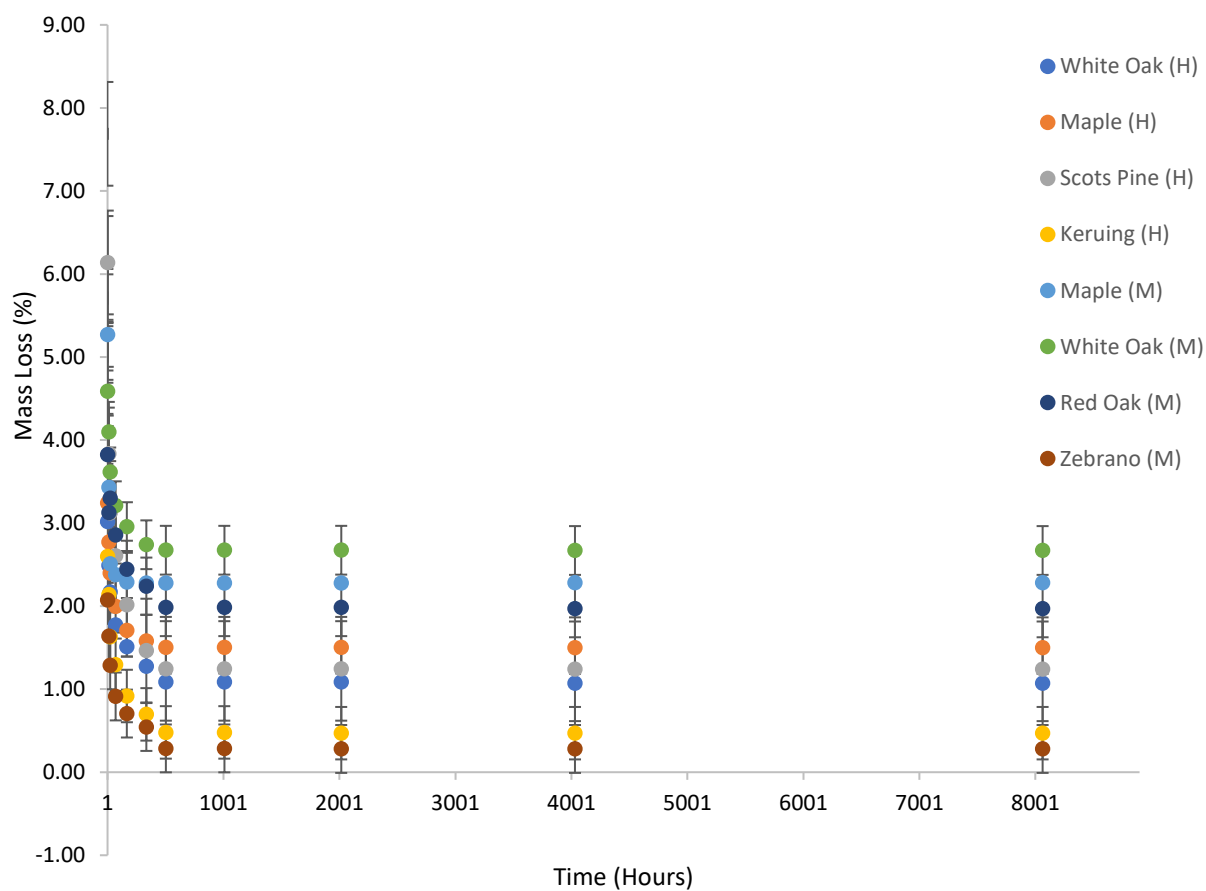


**Figure 1. A mass loss profile for wood samples weighed over 8,064 hours (48 weeks). The wood samples have been treated with  $\text{scCO}_2(\text{PURE})$  in the presence of water for 45 minutes. Each point represents the overall mean from five independent sets of measurements  $\pm$  one standard error of the mean.**

## Appendix 4

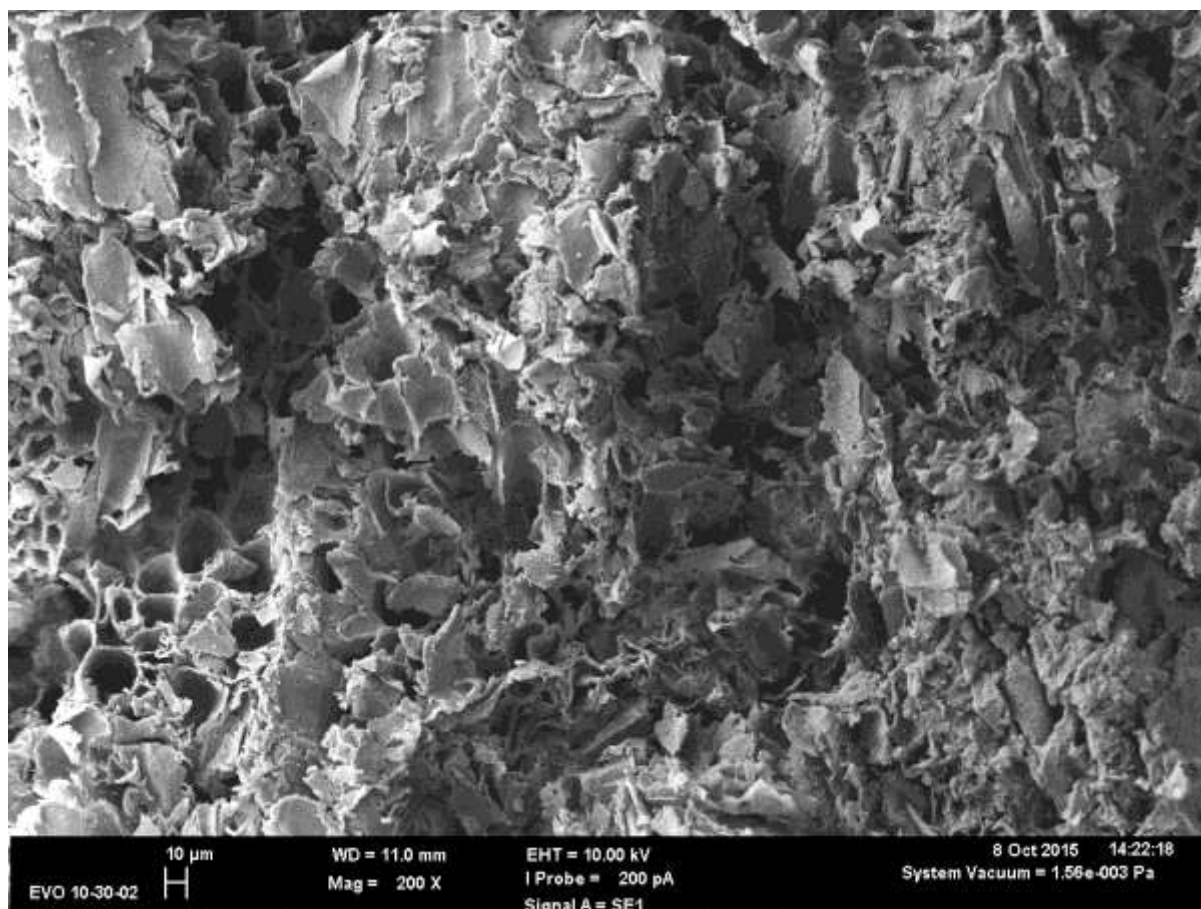


**Figure 3a.** A SEM image at a magnification of 200 x and resolution 10 μm, Zebrano (*M*) treated with scCO<sub>2</sub>(PURE).

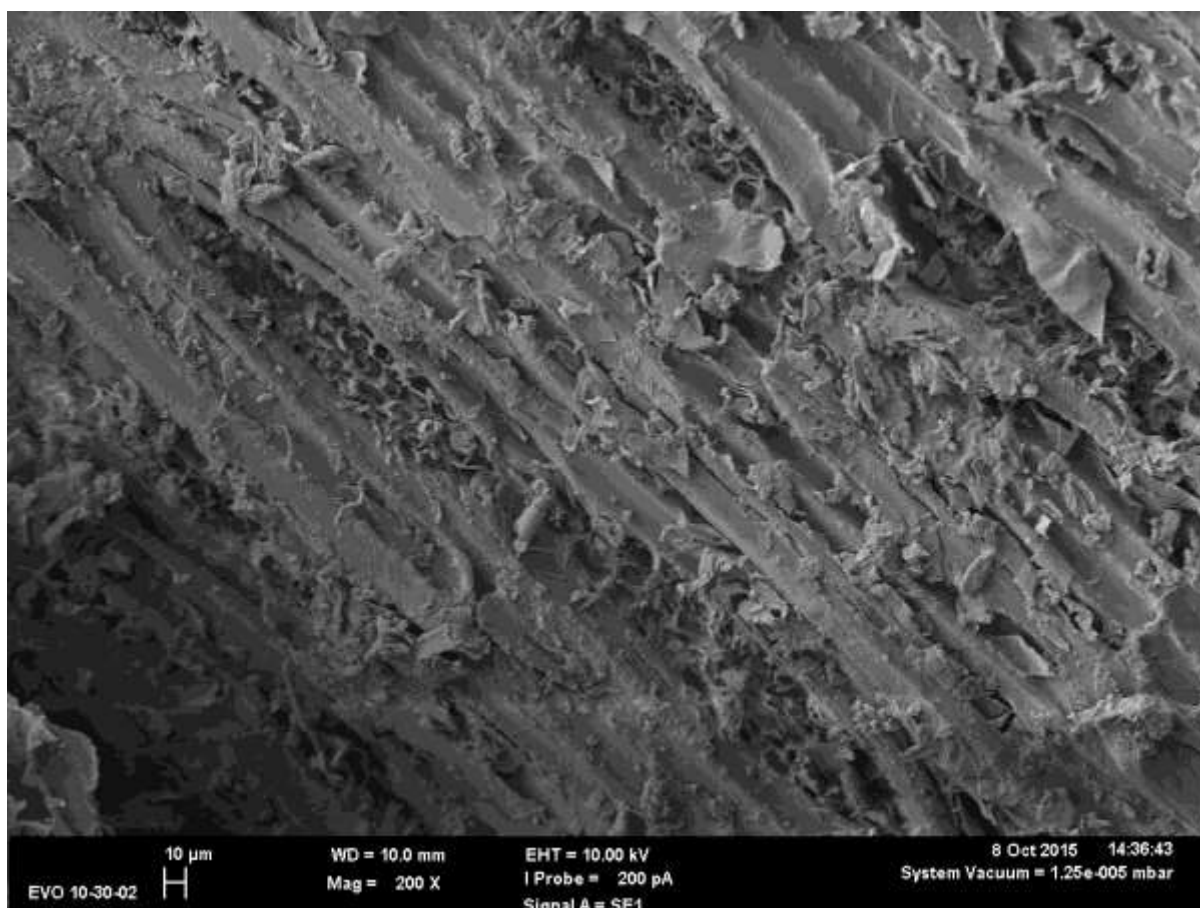


**Figure 3b.** A SEM image at a magnification of 200 x and resolution 10 μm, Zebrano (*M*) treated with scCO<sub>2</sub>(PURE).

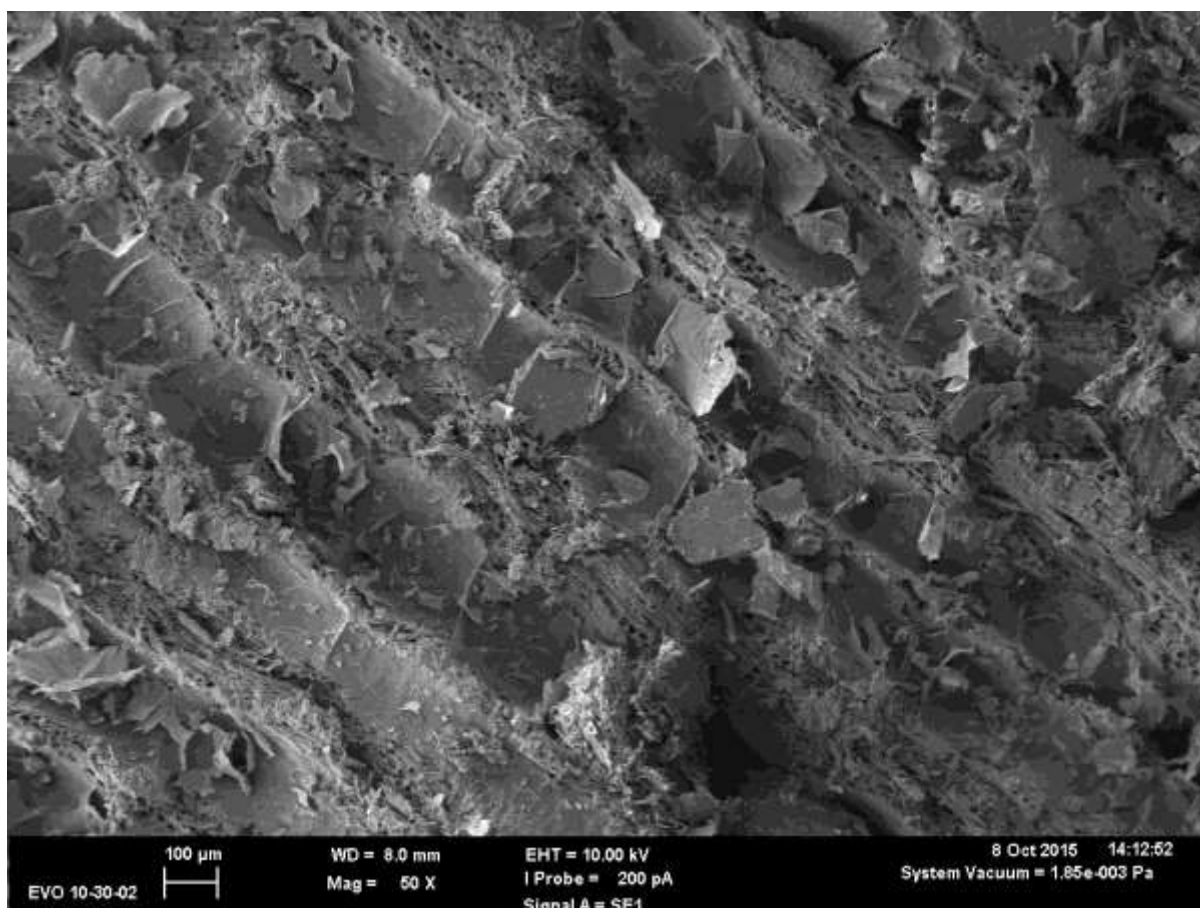


**Figure 3c.** A SEM image at a magnification of 50 x and resolution 100 μm, White Oak (*M*) treated with scCO<sub>2</sub>(PURE).



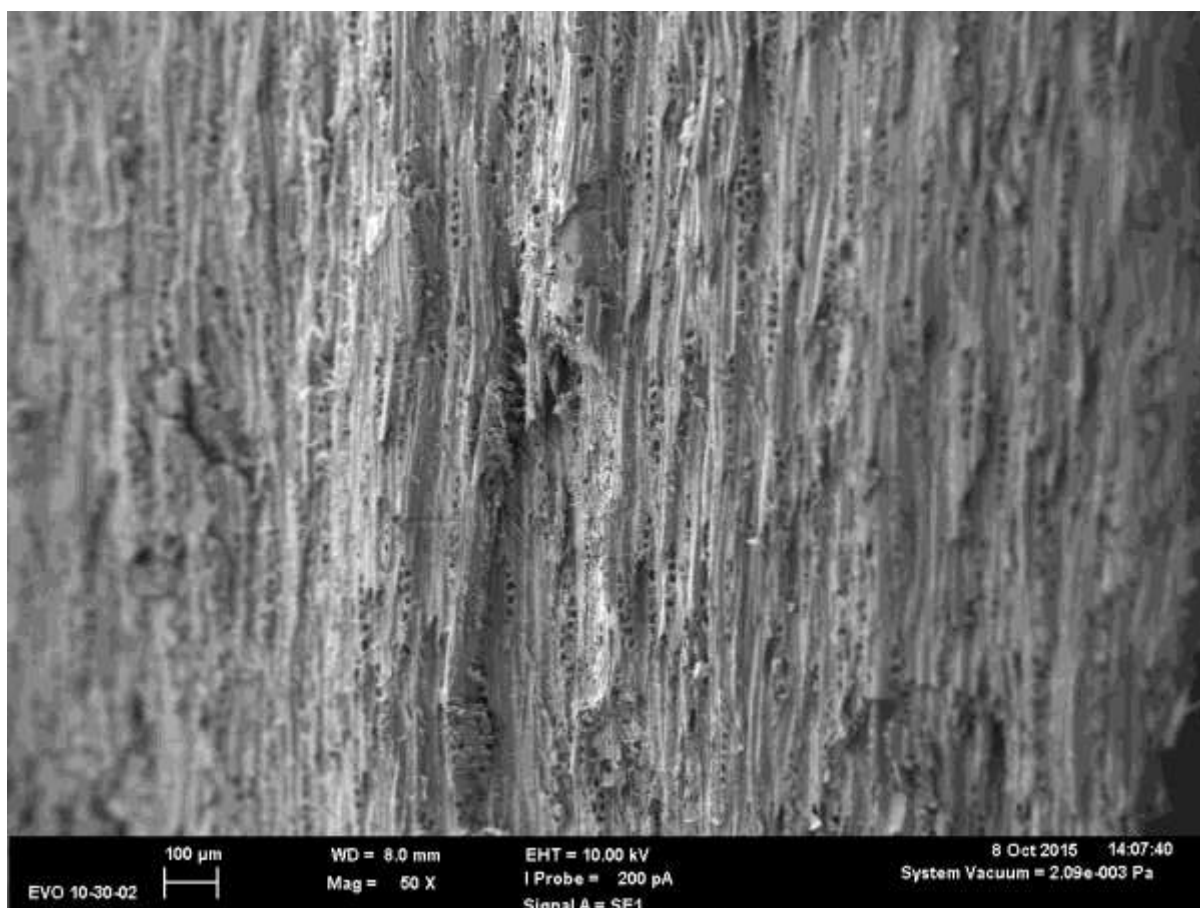


**Figure 3d.** A SEM image at a magnification of 50 x and resolution 100 μm, Red Oak (*M*) treated with scCO<sub>2</sub>(PURE).

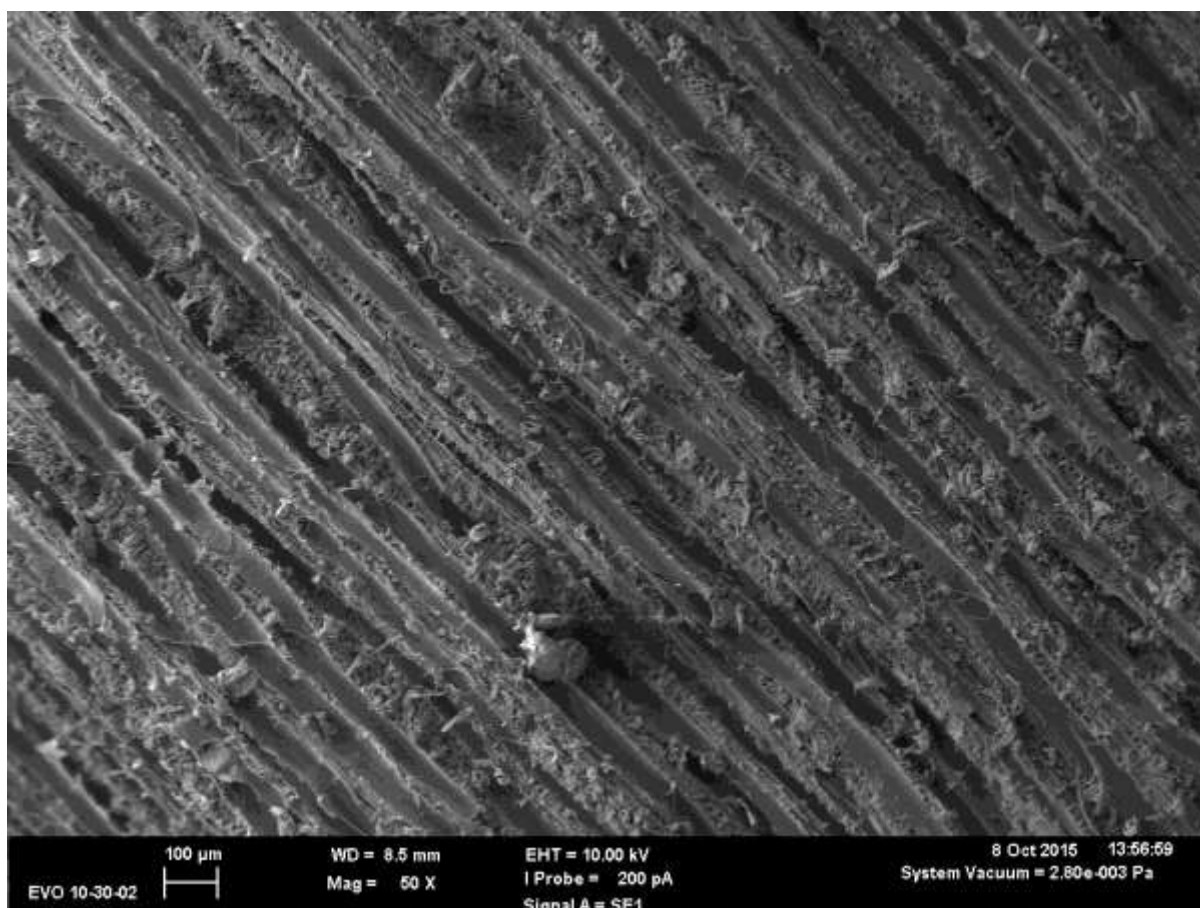


**Figure 3e.** A SEM image at a magnification of 50 x and resolution 100  $\mu\text{m}$ , White Oak (*M*) treated with  $\text{scCO}_2(\text{PURE})$ .

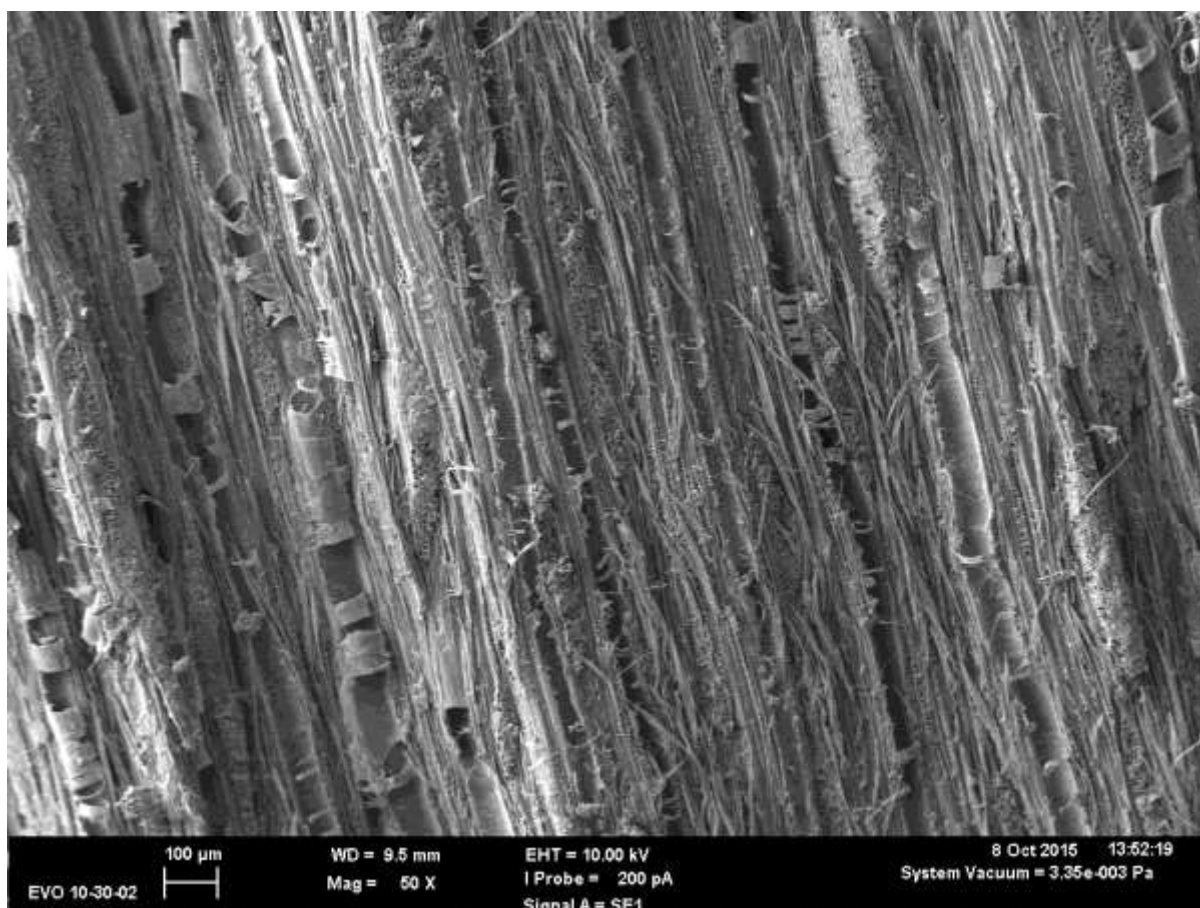


**Figure 3f.** A SEM image at a magnification of 50 x and resolution 100 μm, White Oak (*M*) treated with scCO<sub>2</sub>(PURE).

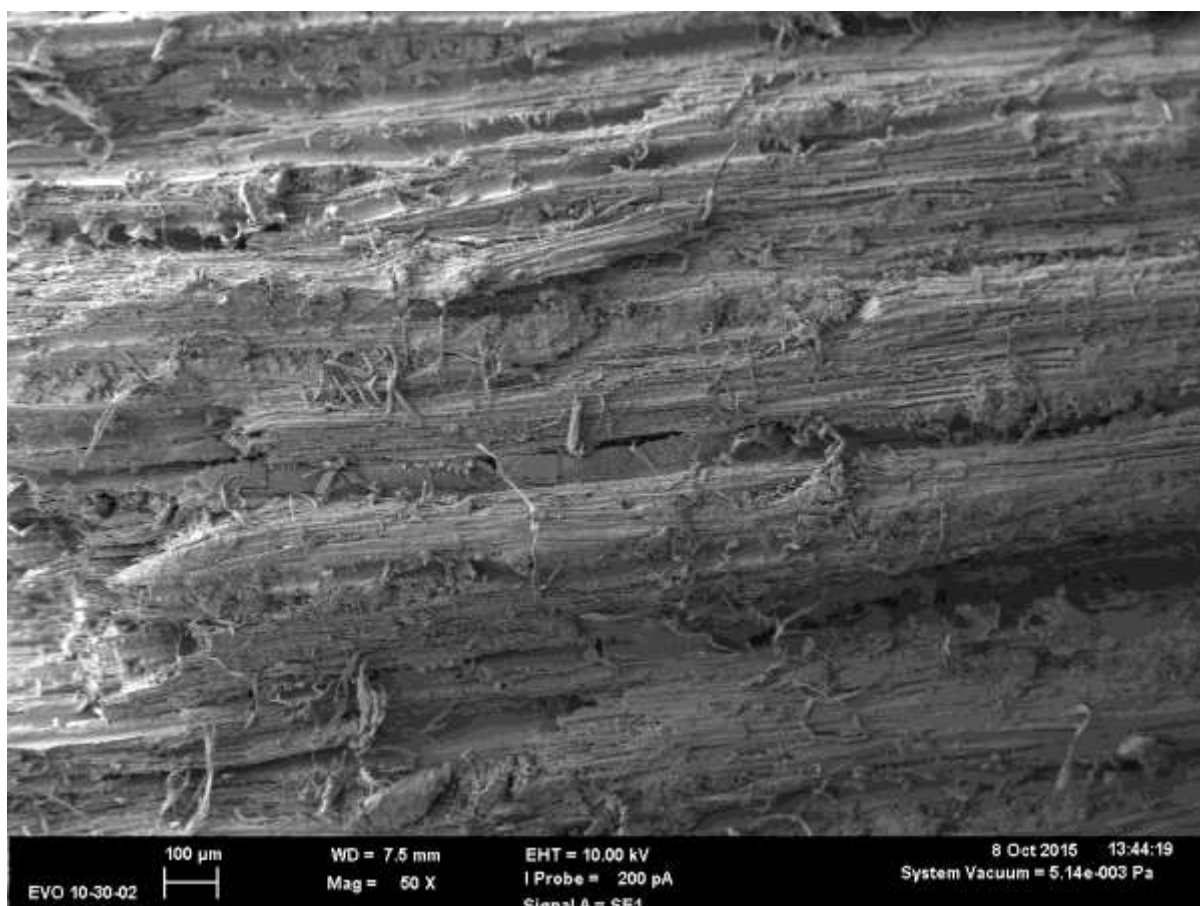


**Figure 3g.** A SEM image at a magnification of 50 x and resolution 100 μm, Maple (*M*) treated with scCO<sub>2</sub>(PURE).

#### Appendix 4

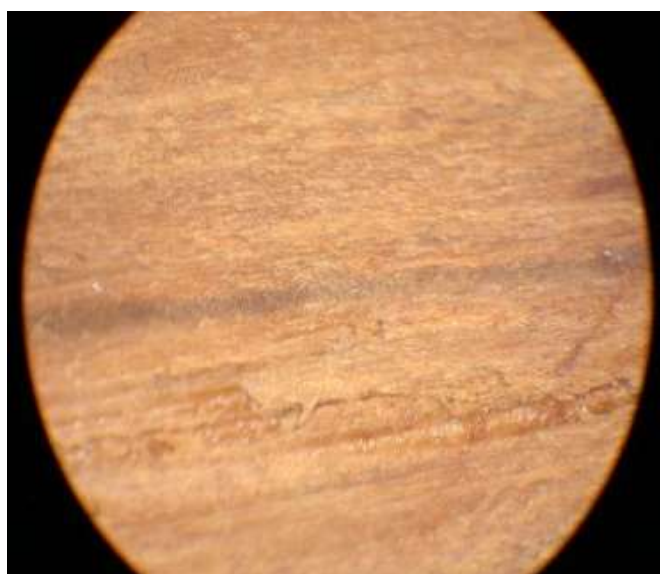


**Figure 4a.** Original size light microscopy image at a 40 x magnification of a White Oak (*H*) untreated exterior

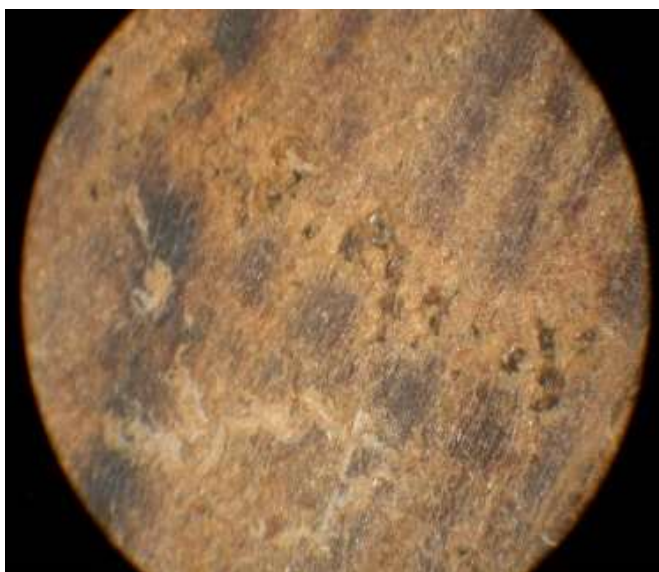


**Figure 4b. Original size light microscopy image at a 40 x magnification of a White Oak (*H*) untreated interior**

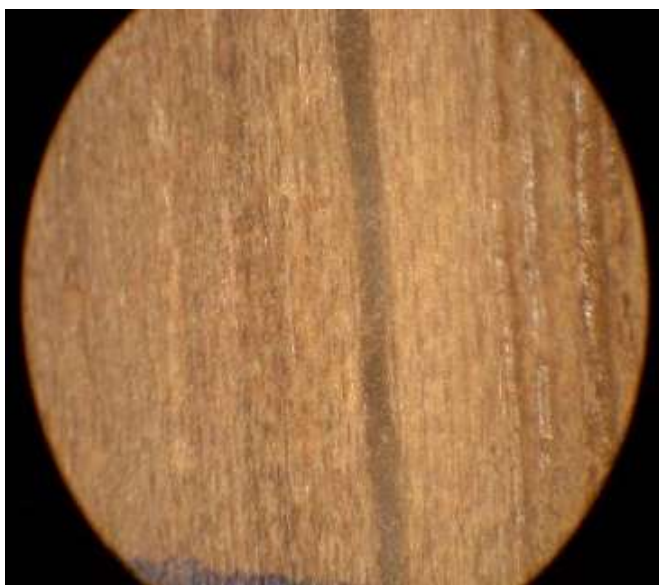


**Figure 4c. Original size light microscopy image at a 40 x magnification of a White Oak (*H*) treated exterior**





**Figure 4d. Original size light microscopy image at a 40 x magnification of a White Oak (*H*) treated interior**

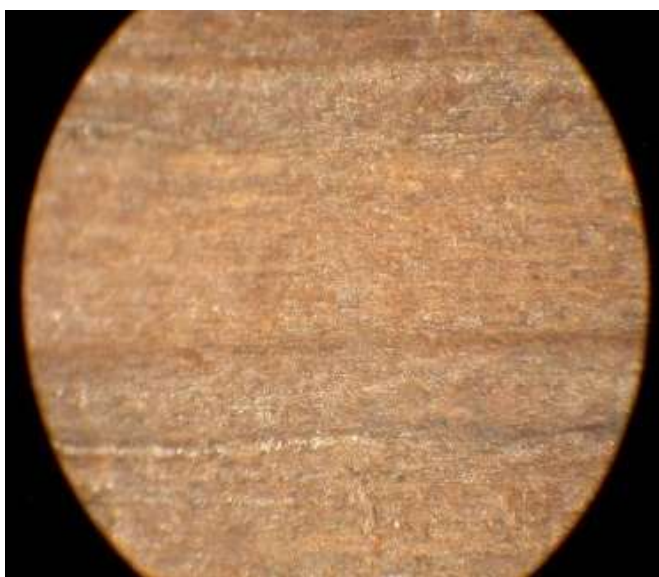


**Figure 4e. Original size light microscopy image at a 40 x magnification of a White Oak (*H*) damaged exterior**

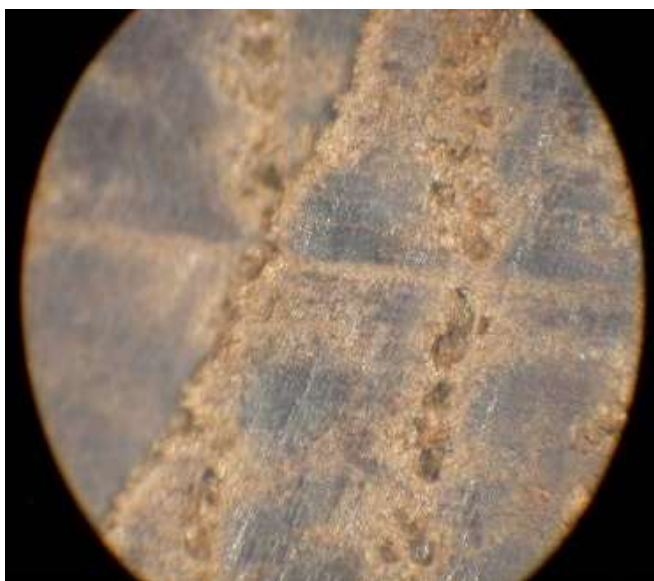


**Figure 4f. Original size light microscopy image at a 40 x magnification of a White Oak (*H*) damaged interior.**

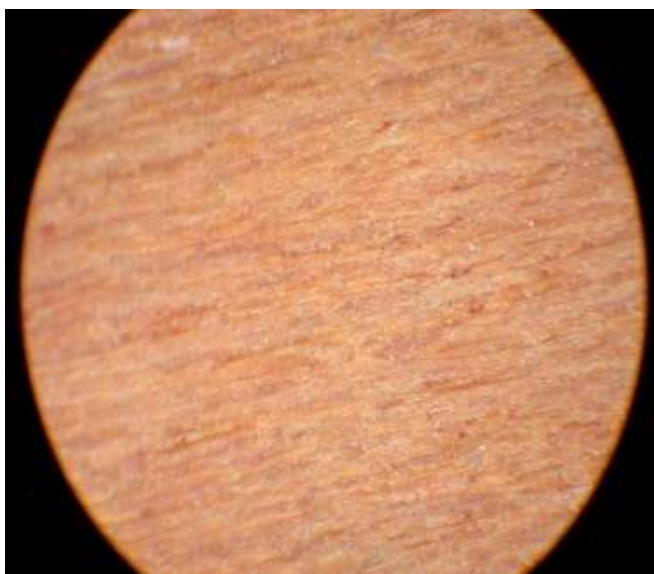


**Figure 4g. Original size light microscopy image at a 40 x magnification of a Maple (*H*) untreated exterior.**

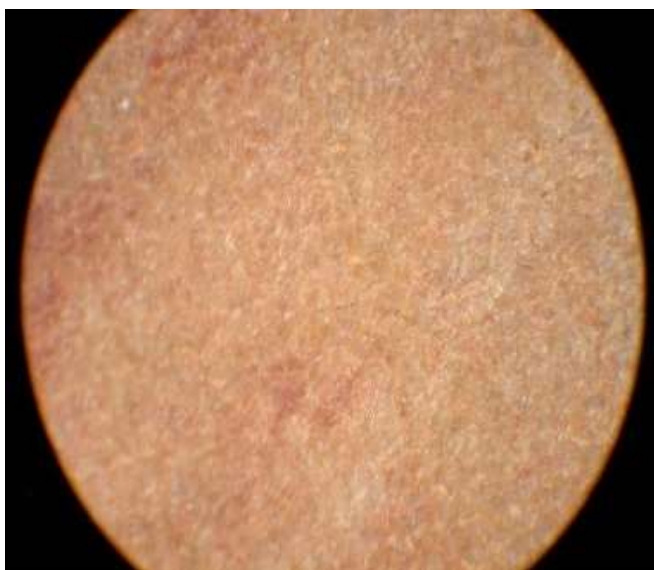


**Figure 4h. Original size light microscopy image at a 40 x magnification of a Maple (*H*) treated interior.**

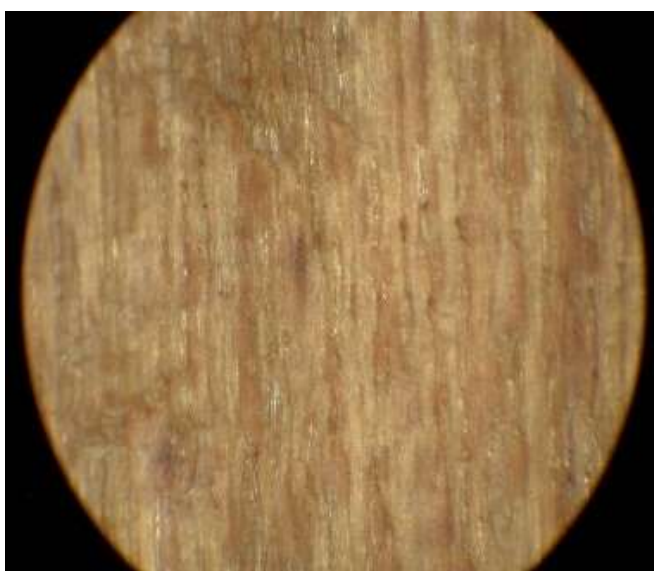


**Figure 4i. Original size light microscopy image at a 40 x magnification of a Maple (*H*) treated exterior**



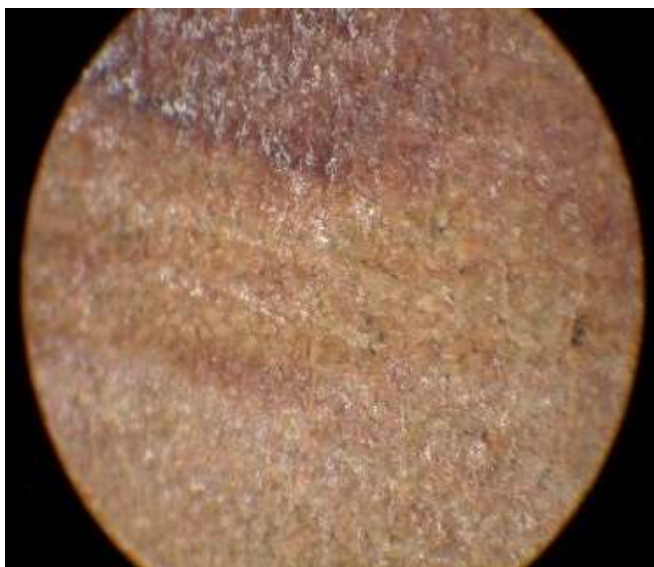


**Figure 4j.** Original size light microscopy image at a 40 x magnification of a Maple (*H*) treated interior.

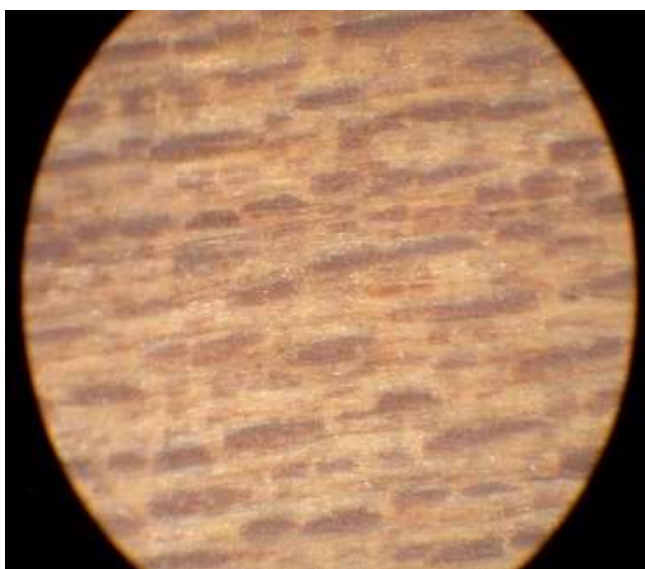


**Figure 4k.** Original size light microscopy image at a 40 x magnification of a Maple (*H*) damaged exterior.

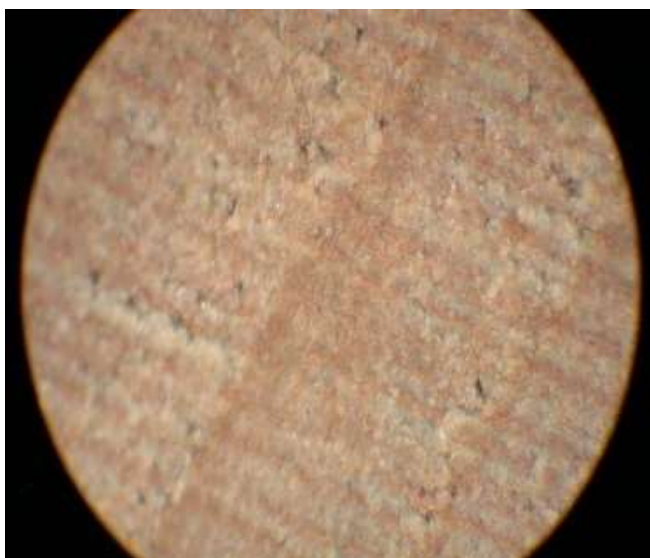


**Figure 4l. Original size light microscopy image at a 40 x magnification of a Maple (*H*) damaged interior.**

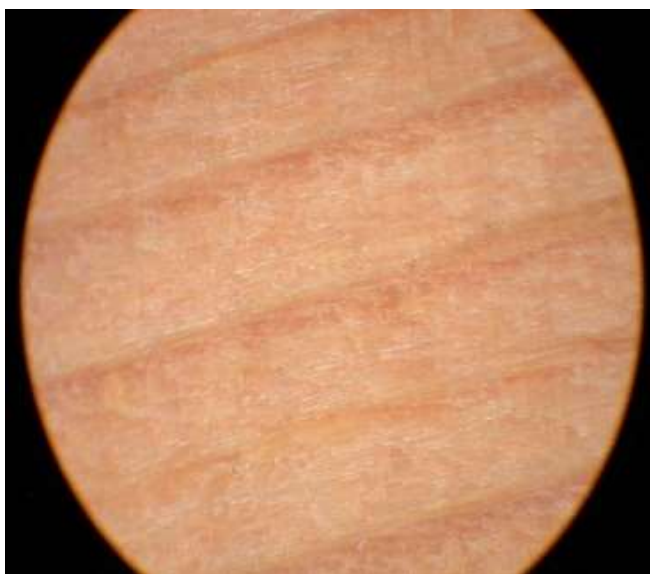


**Figure 4m. Original size light microscopy image at a 40 x magnification of a Scots Pine (*H*) untreated exterior.**

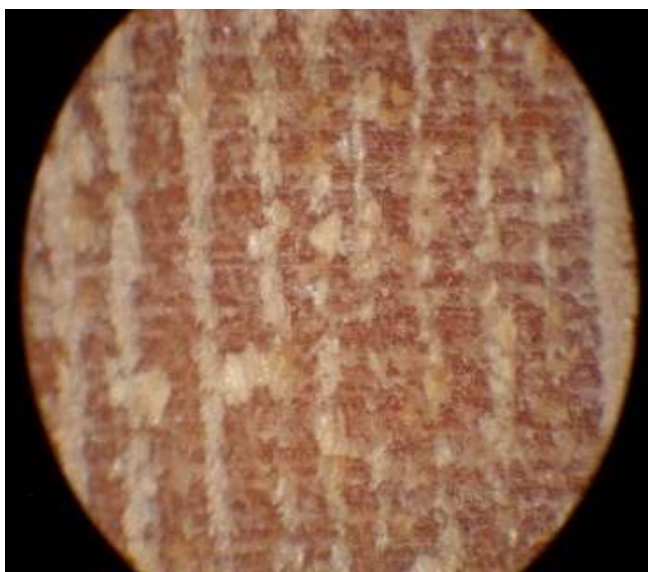


**Figure 4n. Original size light microscopy image at a 40 x magnification of a Scots Pine (H) untreated interior.**

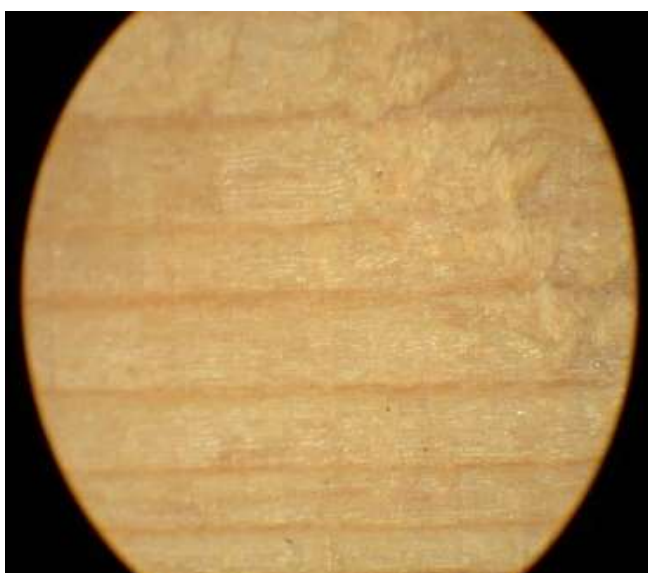


**Figure 4n. Original size light microscopy image at a 40 x magnification of a Scots Pine (H) treated exterior.**

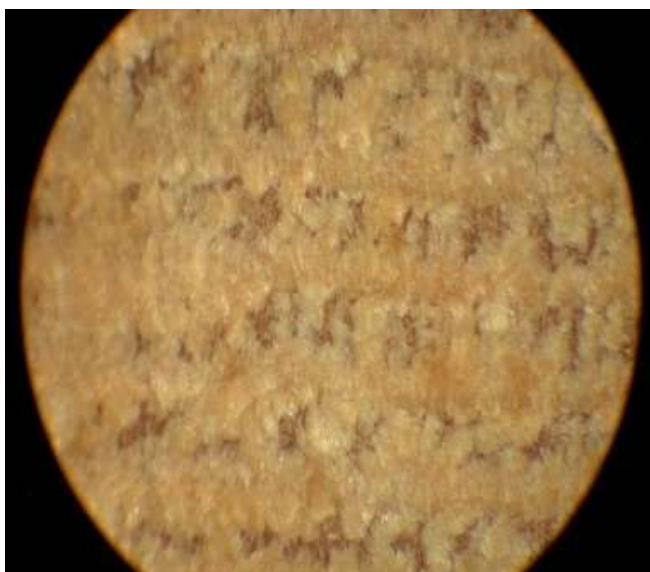


**Figure 4o.** Original size light microscopy image at a 40 x magnification of a Scots Pine (*H*) treated interior.

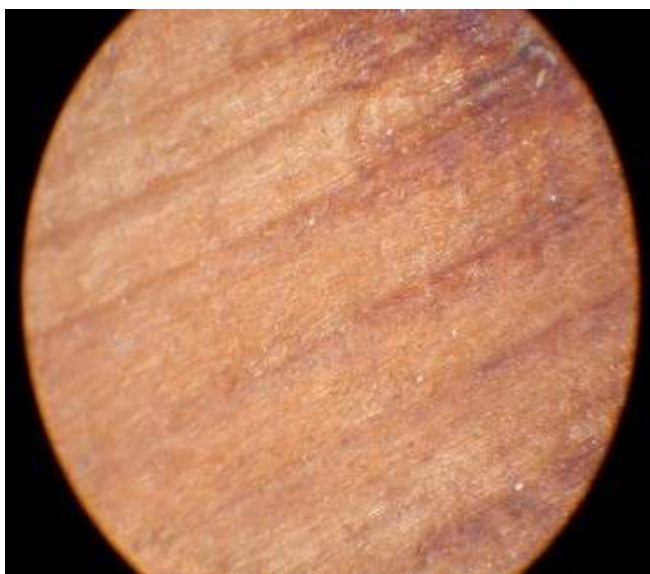


**Figure 4p.** Original size light microscopy image at a 40 x magnification of a Scots Pine (*H*) damaged exterior.

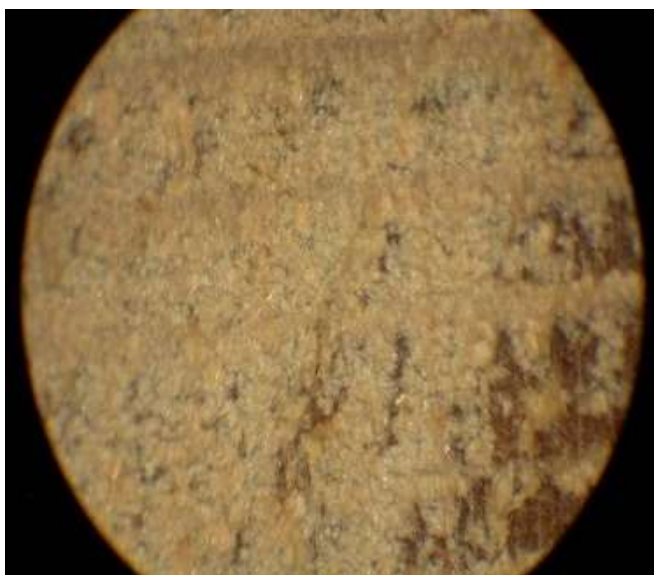


**Figure 4p.** Original size light microscopy image at a 40 x magnification of a Scots Pine (*H*) damaged interior.

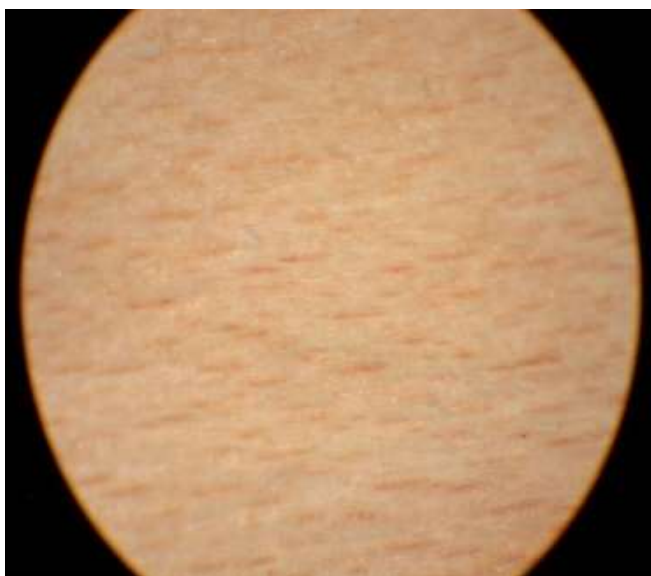


**Figure 4q.** Original size light microscopy image at a 40 x magnification of a Maple (*M*) untreated exterior.



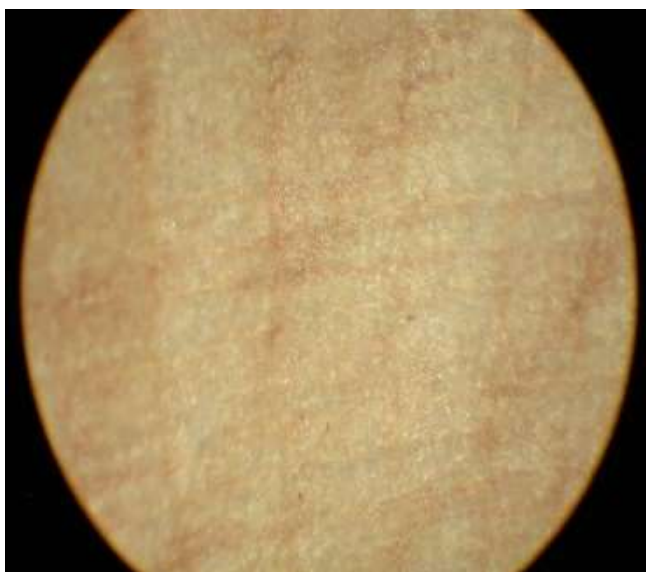


**Figure 4r. Original size light microscopy image at a 40 x magnification of a Maple (*M*) untreated interior.**

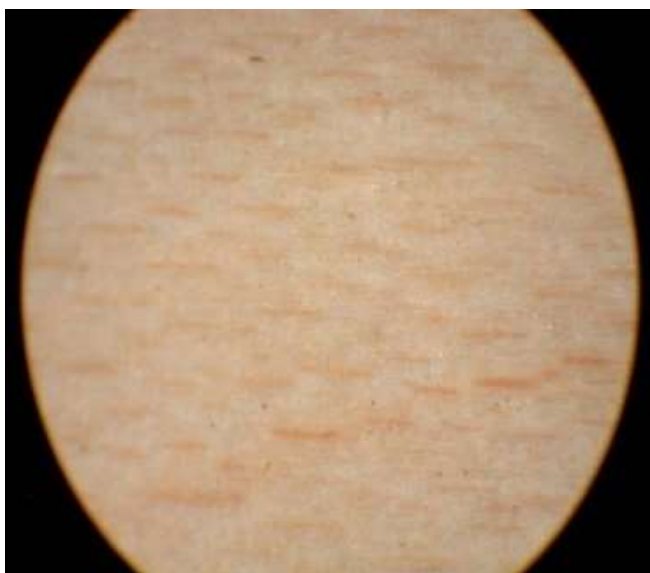


**Figure 4s. Original size light microscopy image at a 40 x magnification of a Maple (*M*) treated exterior.**

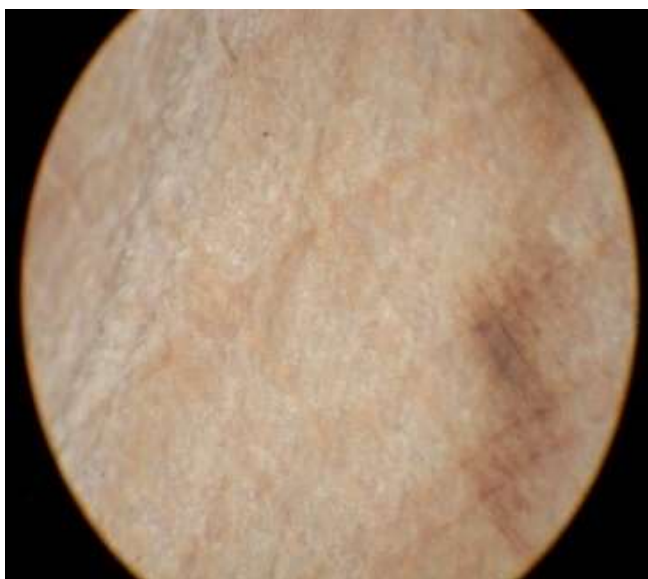


**Figure 4t. Original size light microscopy image at a 40 x magnification of a Maple (*M*) treated interior.**

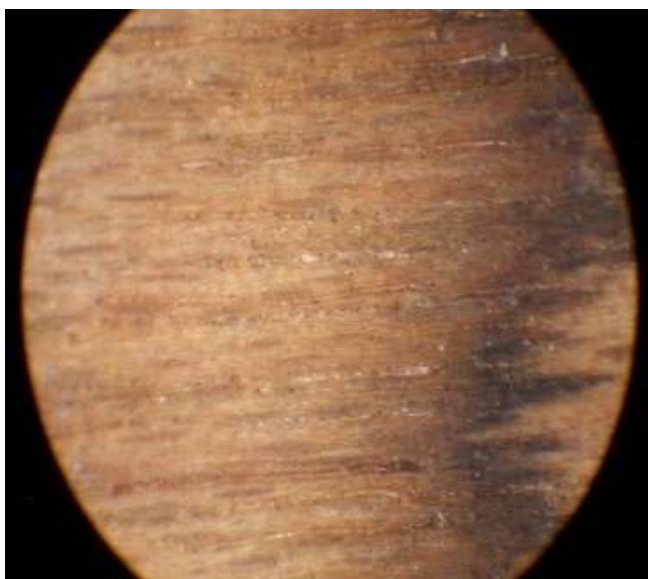


**Figure 4u. Original size light microscopy image at a 40 x magnification of a Maple (*M*) damaged exterior.**

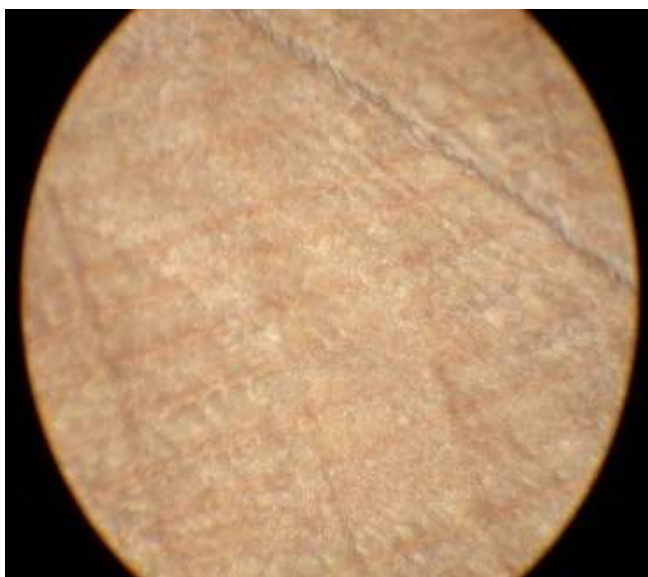


**Figure 4v. Original size light microscopy image at a 40 x magnification of a Maple (*M*) damaged interior.**





**Figure 4w.** Original size light microscopy image at a 40 x magnification of a Zebrano (*M*) untreated exterior.



**Figure 4x.** Original size light microscopy image at a 40 x magnification of a Zebrano (*M*) untreated interior.

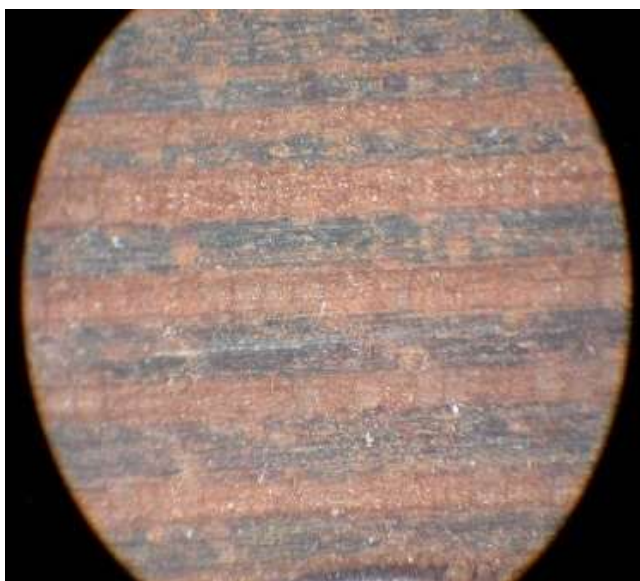


**Figure 4y. Original size light microscopy image at a 40 x magnification of a Zebrano (*M*) treated exterior.**

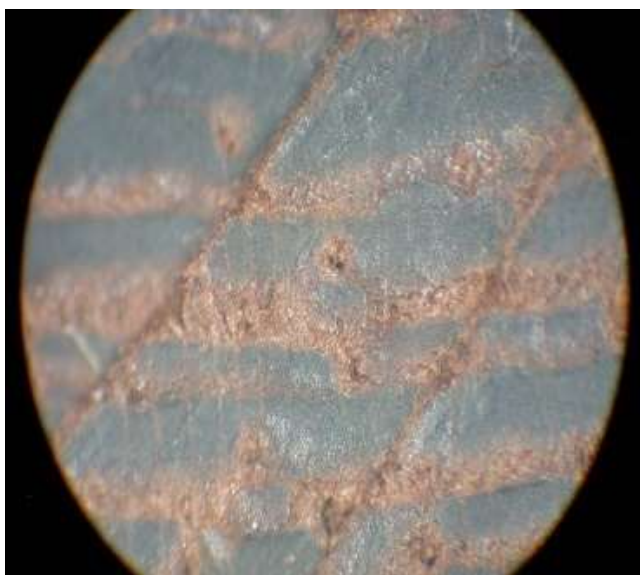


**Figure 4z. Original size light microscopy image at a 40 x magnification of a Zebrano (*M*) treated interior.**

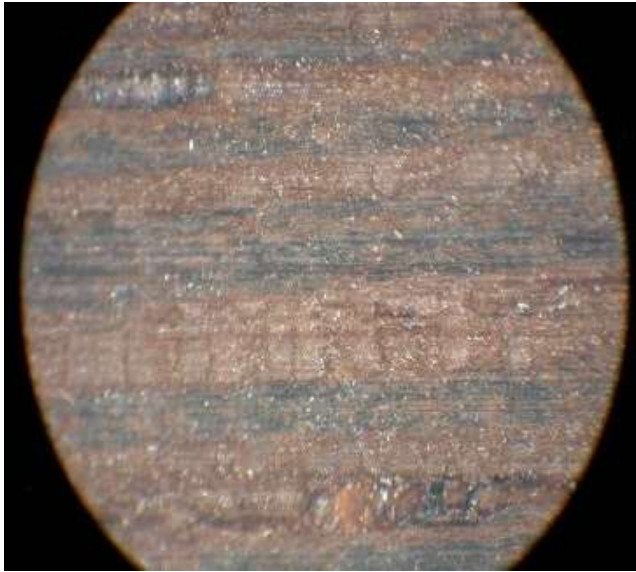


**Figure 4aa.** Original size light microscopy image at a 40 x magnification of a Zebrano (*M*) damaged exterior.



**Figure 4ab.** Original size light microscopy image at a 40 x magnification of a Zebrano (*M*) damaged interior.

## Appendix 5

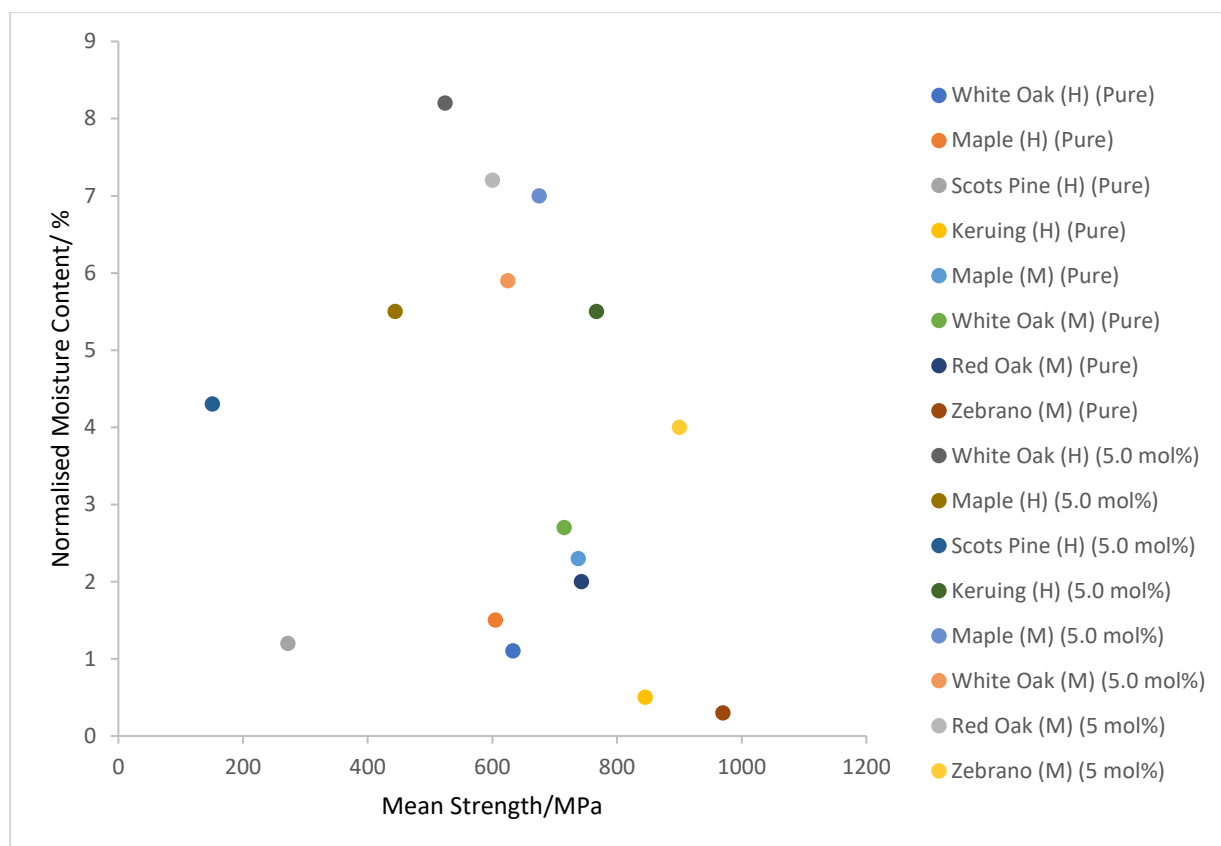


**Figure 1. A plot to test if there is a mathematical correlation between the normalised moisture content (NMC) and the mean strength (MOR) of the wood samples treated with  $\text{scCO}_2(\text{PURE})$  and  $\text{scCO}_2(\text{MeOH})$  with MeOH at 5.0 mol% Values of NMC and MOR were measured at 504 hours.**

